เคมีแร่ของมลทินในแซปไฟร์หินบะซอลต์จากเอเชียตะวันออกเฉียงใต้

นางพรมณี ขำเลิศ

วิทยานิพนธ์นี้เป็นส่วนหนึ่งของการศึกษาตามหลักสูตรปริญญาวิทยาศาสตรดุษฎีบัณฑิต
สาขาวิชาธรณีวิทยา ภาควิชาธรณีวิทยา
คณะวิทยาศาสตร์ จุฬาลงกรณ์มหาวิทยาลัย
ปีการศึกษา 2554

MINERAL CHEMISTRY OF INCLUSIONS IN BASALTIC SAPPHIRES FROM SOUTHEAST ASIA

Ms. Pornmanee Khamloet

A Dissertation Submitted in Partial Fulfillment of the Requirements
for the Degree of Doctor of Philosophy Program in Geology
Department of Geology
Faculty of Science
Chulalongkorn University
Academic Year 2011

Thesis Title	MINERAL CHEMISTRY OF INCLUSIONS IN BASALTIC SAPPHIRES FROM SOUTHEAST ASIA
By	Ms. Pornmanee Khamloet
Field of Study	Geology
Thesis Advisor	Associate Professor Visut Pisutha-Arnond, Ph. D.
Thesis Co-advisor	Assistant Professor Chakkaphan Sutthirat, Ph. D.

Accepted by the Faculty of Science, Chulalongkorn University in Partial Fulfillment of the Requirements for the Doctoral Degree

…… Dean of the Faculty of Science
(Professor Supot Hannongbua, Dr. rer. nat.)

THESIS COMMITTEE

…… Chairman
(Associate Professor Montri Choowong, Ph. D.)

…… Thesis Advisor
(Associate Professor Visut Pisutha-Arnond, Ph. D.)

…… Thesis Co-advisor
(Assistant Professor Chakkaphan Sutthirat, Ph. D.)

…… Examiner
(Vichai Chutakositkanon, Ph. D.)

…… External Examiner
(Assistant Professor Phisit Limtrakun, Ph. D.)

…… External Examiner
(Bhuwadol Wanthanachaisaeng, Dr. rer. nat.)

…… External Examiner
(Somruedee Satitkune, Dr. rer. nat.)

พรมณี ขำเลิศ : เคมีแร่ของมลทินในแซปไฟร์หินบะซอลต์จากเอเชียตะวันออกเฉียงใต้ (MINERAL CHEMISTRY OF INCLUSIONS IN BASALTIC SAPPHIRES FROM SOUTHEAST ASIA) อ. ที่ปรึกษาวิทยานิพนธ์หลัก: รศ.ดร.วิสุทธิ์ พิสุทธอานนท์, อ. ที่ปรึกษาวิทยานิพนธ์ร่วม: ผศ.ดร.จักรพันธ์ สุทธิรัตน์, 185 หน้า.

มลทินแร่ในพลอยแซปไฟร์ โดยเฉพาะอย่างยิ่งจากแหล่งบ่อพลอย กาญจนบุรี และบางส่วนจาก จันทบุรี และแพร่ ในประเทศไทย จากแหล่งห้วยทราย ในประเทศลาว แหล่งไพลิน ในประเทศกัมพูชา และแหล่งเกียเงีย ในประเทศเวียดนาม ได้ถูกคัดเลือกสำหรับการศึกษาในครั้งนี้ พบว่ามลทินแร่ในพลอยแซปไฟร์จากแหล่งบ่อพลอยประกอบด้วย แอลคาไลน์เฟลด์สปาร์ เนฟิลีน เฮอร์ซินีติก-สปิเนล เซอร์คอน แมงกานิเฟอร์รัส-อิลเมไนต์ เอนสทาไทท์ที่มีปริมาณซิลิกาสูง การ์เนตชนิดไพโรป-แอลมันดีนที่มีองค์ประกอบไปทางไพโรป โมนาไซต์ แคลไซต์ แซฟฟิรีน ไบโอไทต์-โฟลโกไปต์ และสตอโรไลท์ จากความหลากหลายของมลทินแร่สามารถจำแนกได้เป็น 2 กลุ่ม คือ กลุ่มเฟลสิกที่มีแอลคาไลสูง และกลุ่มที่ได้จากกระบวนการแปรสัมผัส ซึ่งบ่งบอกถึงกำเนิดในสภาพแวดล้อมที่ต่างกัน ข้อมูลที่ได้ถือเป็นหลักฐานใหม่ที่ยืนยันว่าพลอยแซปไฟร์จากแหล่งบ่อพลอยน่าจะกำเนิดมาจาก 2 รูปแบบ คือ รูปแบบที่หนึ่งมีความสัมพันธ์กับการตกผลึกในสภาพแวดล้อมที่สัมพันธ์กับแมกม่าชนิดเฟลสิกที่มีแอลคาไลสูง ในบริเวณเปลือกโลกตอนล่าง ซึ่งมีหลักฐานปรากฏจากการพบมลทินแร่กลุ่มเฟลสิกที่มีแอลคาไลและจากธรณีเคมีของธาตุร่องรอยและธาตุหายากในแร่เซอร์คอนที่เกิดร่วมกับแซปไฟร์ ส่วนรูปแบบที่สองกำเนิดมาจากแมกม่าผสมของหินเปลือกโลกที่ถูกแปรสัมผัสกับหินหลอมเหลวปนเปื้อนที่เกิดจากการดันตัวของบะซอลต์ในบริเวณชั้นเนื้อโลกส่วนบนหรือชั้นเปลือกโลกส่วนล่าง ซึ่งมีหลักฐานปรากฏจากการพบมลทินแร่ที่ได้จากกระบวนการแปรสัมผัส

นอกจากนี้ ชนิดของมลทินแร่ที่พบในพลอยแซปไฟร์จากเอเชียตะวันออกเฉียงใต้ในพื้นที่อื่นๆ ส่วนใหญ่ยังคล้ายกับที่พบในพลอยแซปไฟร์จากแหล่งบ่อพลอย ยกเว้นมลทินแร่อิลเมไนต์ โมนาไซต์ แคลไซต์ และไบโอไทต์-โฟลโกไปต์ ที่ไม่พบ แต่พบมลทินแร่เฟอโรโคลัมไบต์ ไพโรคลอร์ และอะพาไทต์ เพิ่มเติมในพลอยแซปไฟร์จากเอเชียตะวันออกเฉียงใต้ ด้วยเหตุผลนี้ จึงสรุปได้ว่าพลอยแซปไฟร์ในภูมิภาคเอเชียตะวันออกเฉียงใต้กำเนิดมาจาก 2 รูปแบบ คือ พลอยแซปไฟร์ที่กำเนิดมาจากการตกผลึกจากไซอีไนต์ที่มีแอลคาไลด์สูง และพลอยแซปไฟร์ที่กำเนิดมาจากแมกม่าผสมจากขบวนการแปรสัมผัส

จากข้อมูลการหาอายุโดยวิธียูเรเนียม-ตะกั่ว ของมลทินแร่เซอร์คอนจากแหล่งบ่อพลอยให้อายุ 24±0.9 ล้านปี และจากข้อมูลอายุโดยวิธีทอเรียม-ยูเรเนียม-ตะกั่วของมลทินแร่โมนาไซต์จากแหล่งบ่อพลอยให้อายุช่วง 25-30 ล้านปี และ 42-45 ล้านปี ซึ่งข้อมูลอายุของมลทินแร่ที่ได้ มีค่าใกล้เคียงกันอย่างมากกับอายุช่วงเริ่มต้นของกระบวนการประทุของหินภูเขาไฟบะซอลต์ ในมหายุคซิโนโซอิกของประเทศไทย ซึ่งเป็นเหตุผลสนับสนุนว่าการกำเนิดพลอยแซปไฟร์น่าจะเกิดขึ้นในช่วงประวัติความร้อนเดียวกันตั้งแต่ช่วงเริ่มต้นของการกำเนิดบะซอลต์มหายุคซิโนโซอิกในประเทศไทยรวมถึงในภูมิภาคเอเชียตะวันออกเฉียงใต้

ภาควิชา ธรณีวิทยา ..... ลายมือชื่อนิสิต .....

สาขาวิชา ธรณีวิทยา ..... ลายมือชื่อ อ.ที่ปรึกษาวิทยานิพนธ์หลัก .....

ปีการศึกษา 2554 ..... ลายมือชื่อ อ.ที่ปรึกษาวิทยานิพนธ์ร่วม .....

5073849023: MAJOR GEOLOGY

KEYWORDS: BASALTIC SAPPHIRE / MINERAL INCLUSION / ZIRCON DATING

PORNMANEE KHAMLOET: MINERAL CHEMISTRY OF INCLUSIONS IN BASALTIC SAPPHIRES FROM SOUTHEAST ASIA. ADVISOR: ASSOC. PROF. VISUT PISUTHA-ARNOND, Ph. D., CO-ADVISOR: ASST. PROF. CHAKKAPHAN SUTTHIRAT, Ph. D., 185 pp.

Mineral inclusions in sapphires from Bo Phloi, Kanchanaburi, in particular, and some from Chanthaburi and Phrae in Thailand; Huai Sai in Laos; Pailin in Cambodia and Gia Nghia in Vietnam were selected for this study. Mineral inclusions discovered in Bo Phloi sapphires include alkali feldspar, nepheline, hercynitic spinel, zircon, manganiferous-ilmenite, silica-rich enstatite, pyrope-almandine garnet richer towards pyrope component, monazite, calcite, sapphirine, biotite-phlogopite and staurolite. These mineral inclusions can be categorized into two groups namely felsic alkaline suite and contact metamorphic suite, which appear to have originated from different environments. These inclusion suits has provided new evidences to propose a bimodal genetic model of Bo Phloi sapphire. Firstly, the felsic alkaline-related origin is based on the occurrence of felsic alkaline inclusion suite together with trace elements and REE's geochemistry of sapphire-associated zircons indicating that majority of the sapphires appear to have crystallized in an environment related to high alkali felsic melt at lower crust. Secondly, the contact metamorphic-related origin is based on the finding of contact metamorphic inclusion suite, suggesting that some of these sapphires could also originate from the metasomatised crustal rocks and contaminated melt at contact zone of basaltic intrusion at upper mantle or lower crust.

Furthermore, most mineral inclusions found in Southeast Asia sapphires also are similar to those inclusions observed in Bo Phloi sapphires, except ilmenite, monazite, calcite and biotite-phlogopite have not so far been found in Southeast Asia sapphires, while ferrocolumbite, pyrochlore and apatite inclusions appear in these sapphires. Therefore, the mineral inclusions found in Southeast Asia sapphires are also divided into two groups namely 'syenitic melt-related' and 'contact metamorphic-related' suites. It can be proposed that sapphires in Southeast Asia region also originated from the bimodal genetic model similar to those occur in Bo Phloi sapphires.

U-Pb dating data of Bo Phloi zircon inclusion yield an age of 24±0.9 Ma including Th-U-Pb age of monazite inclusions at ~25-30 and ~42-45 Ma that are very close to the volcanism of Cenozoic basalts in Thailand. Therefore, the sapphire formation may have the same thermal history as partial melting in the upper mantle leading to early state of Cenozoic basaltic eruption of Thailand as well as Southeast Asia region.

Department : Geology	Student's Signature .....
Field of Study : Geology	Advisor's Signature .....
Academic Year : 2011	Co-advisor's Signature .....

ACKNOWLEDGEMENTS

The author would like to express deeply sincere gratitude to her thesis advisor, Associate Professor Visut Pisutha-Arnond, Ph.D. and co-advisor, Assistant Professor Chakkaphan Sutthirat, Ph.D. for their suggestion, supervisions, encouragements and contributions, providing samples, and help throughout the completion of this thesis. Without their kindly help this study would not have been possible. Thanks are also extended to Associate Professor Montri Choowong, Ph. D., Vichai Chutakositkanon, Ph. D., Assistant Professor Phisit Limtrakun, Ph. D., Bhuwadol Wanthanachaisaeng, Dr. rer. nat. and Somruedee Satitkune, Dr. rer. nat. for being members of the thesis committee whose comments are especially helpful.

The author sincerely appreciates the Department of Geology, Faculty of Science, Chulalongkorn University for providing her knowledge and support the laboratory experiments. The author would like to thank the Gem and Jewelry Institute of Thailand (GIT) for permission to use basic equipment and advanced laboratory instruments, i.e. gemological microscope, Laser Raman Spectroscopy. Many thanks are also due to Miss Sopit Poompeang for assistance on EPMA analysis. A special thank has to be expressed also to Dr. Elena Belousova, Department of Earth and Planetary Sciences, Macquarie University, Sydney for helping on the study of trace element analysis and U-Pb dating of zircon inclusion.

The author owes all my life to my parents Mr. Sompoch and Mrs. Laead Khamloet; I could not have come this far without their enormous sacrifice and encouragement. Finally, several persons, whose names cannot be entirely listed, are also deeply thanked.

CONTENTS

Page

LIST OF TABLES

LIST OF FIGURES

CHAPTER 1
INTRODUCTION

1.1 General Statement

The early works related to basaltic corundums in Southeast Asain region were initially focused on basaltic rocks, xenoliths and xenocrysts embedded in basaltic hosts (e.g., Yaemniyom and Pongsapich,1982; Vichit, *et al.*, 1978; Coenraads *et al.*, 1995; Sutherland, 1996), hence the origin of basaltic corundum was not really well understood at the beginning. Later some studies on the sapphire surface features and rarely on corundum-bearing assemblages and corundum megacrysts in host basalts revealed that basaltic sapphires were carried from their initial provenances by basaltic magma rising up to the earth surface (e.g., Coenraads, 1992a,b; Krzemnicki *et al.*, 1996; Pisutha-Arnond *et al.*, 1999; Sutherland and Schwarz, 2001). Because corundum-bearing xenoliths, which could unravel the corundum origin directly, were rarely ever found in those gem fields, the information obtained from such important pieces of evidence were therefore rather limited. Hence to resolve their mysterious origin at depth, one needs to resort to the study of inclusions trapped in their host corundum. Even though the study of inclusions in basaltic corundum has become more concern during the last decade, only some information of their mineral chemistry has been published prior to starting of this study.

One of the most interesting aspects in geology and gemology is the study of inclusions observed in samples. The mineral inclusions, in particular, presented in corundum may preserve the valuable information about the chemical environment, physical conditions and geological processes that relate to the host corundum formation. For the last two decades, many previous researchers studied the mineral inclusions in corundum by using the optical microscope and Raman spectroscope (e.g., Dao and Delaigue, 2000; Singbamroong and Thanasuthipitak, 2004; Palenza *et al.*, 2008). Nevertheless, the application of the Electron Probe Micro Analyzer (EPMA) has become an important technique for identifying the phase of mineral inclusions and, on the quantitative analysis mode, providing elemental compositions of samples. Nowadays, more attentions have been paid on mineral chemistry of inclusions in corundum (e.g., Sutherland *et al.*, 2002; Saminpanya and Sutherland, 2011) because they can be used to decipher the geological environment in which the

crystal was formed, and thereby to distinguish corundums according to their geological and geographical origin.

Some workers reported various mineral inclusions found in basaltic sapphires particularly located within Southeast Asia and Australia (e.g., Guo *et al.*, 1994; Pisutha-Arnond *et al.*, 1999; Sutthirat *et al.*, 2001; Sutherland *et al.*, 2002; 2003). The information of such mineral inclusions was applied for reconstruction of the genetic model of the basaltic sapphires. Several genetic models have consequently been proposed (e.g., Coenraads *et al.*, 1990; Levinson and Cook, 1994; Guo *et al.*, 1996a; Sutherland and Coenraads, 1996; Sutherland *et al.*, 1998b; Pisutha-Arnond *et al.*, 1999). However, data of mineral chemistry of inclusions that are the most important data leading to more precise genetic model of sapphire are rare and ambiguously reported. Therefore, the main objective of this work is to carry out more detail on this matter. Accurate mineral chemistry of inclusion in sapphire from Southeast Asia localities, especially from Bo Phloi deposit in Kanchanaburi, Thailand, which is the well-known “basaltic” gem corundum occurrence, is the main interest for this study.

1.2 Objectives

The main objectives of this thesis are the detailed study on mineral chemistry of inclusions in sapphires from basaltic deposits in Southeast Asia, with particular emphasis on Bo Phloi area, Kanchanaburi, Thailand. The results from this study will be used to construct the relation between their mineral inclusions and host sapphires leading to local genetic model of Bo Phloi deposit in comparison with regional genetic model of Southeast Asia sapphires.

1.3 Theoretical Background and Relevant Researches

1.3.1 Importance of Inclusions in Corundum

In 1991, John Koivula has provided probably the best definition of the word of inclusion in corundum:

“Broadly defined, an inclusion is any irregularity observable in a gem – by the unaided eye or [using] some tool such as a hand lens or microscope. The 'irregularity' may be a substance, such as a solid mineral crystal or a fluid filling a cavity, or it may be an unfilled cavity, a fracture, or a growth pattern that produces some optical effect.”

Inclusions in corundum can be classified according to the scheme proposed by Gübelin and Koivula (2005), which are based upon their ages with respect to that of the host crystal that were classified into 3 groups as follows:

1. ***Protogenetic inclusion:*** inclusions that are formed before the host. These are strictly of a solid nature (pre-existing liquids and gases do not count). They are always typically mineral crystals more or less corroded.
2. ***Syngenetic inclusion:*** inclusions that are formed at the same time as the host. They are imprisoned inside it during its formation or have appeared during its cooling as rutile needles in rubies.
3. ***Epigenetic inclusion:*** inclusions that are formed immediately, or even millions of years, after the host stopped growing. Typical from of this type are limonite, iron staining or oil that can fill the natural fissures of the gemstones.

The detailed study of inclusion in corundum is one of the best methods to provide the valuable information for geology and gemology. A variety of inclusions present in sapphire should be related to geologic setting of their formation. In some cases, typical inclusions may in turn indicate specific type of deposit. Inclusions provide an important tool for constraining the geological history of sapphire because they provide a direct indicator to assemblage during and after the formation of sapphire that affected the host mineral at the time of its formation. Moreover, mineral chemistry will also indicate chemical potential of the crystallization environment of sapphire and its inclusion. This investigation is therefore focused on chemical quantitative analysis of mineral inclusions embedded in sapphires which are assumed to have originated during crystallization of sapphire.

1.3.2 Inclusion Study in Corundum

Several previous researchers reported on the inclusion studies in corundum by using various instrumental techniques such as optical microscope, Raman spectroscope, Electron Probe Micro Analyzer (EPMA), Sensitive High Resolution Ion Microprobe (SHRIMP) and Laser Ablation Inductively Coupled Plasma Mass Spectrometry (LA-ICP-MS) technique (e.g., Maesschalck and Oen, 1989; Dao, and Delaigue, 2000; Abduriyim and Kitawaki, 2006; Pakhomova *et al.,* 2006).

The application of optical microscope and Raman spectroscope on mineral inclusion in Ban Huai Sai sapphire in Laos was reported by Singbamroong and Thanasuthipitak (2004). They found inclusions of feldspar, zircon, monazite, ferrocolumbite and pyrochlore in such sapphire which provided the important evidence to distinguish Lao sapphire from neighbouring Thailand and Cambodia localities. Nevertheless, a later work (Pumpang, 2007) by Raman technique reported that such inclusions found in Ban Huai Sai sapphires also generally presented in the other basaltic sapphires in Southeast Asia such as Thailand, Vietnam and Cambodia. In addition, Palenza *et al.* (2008) reported the application of Micro-Raman spectroscopy for characterizing mineral inclusions within corundum from different origins. This study importantly correlated inclusion varieties and geographic origins through the discrimination between magmatic and metamorphic environments. The study of Raman spectrograph presented that the appearance of hematite (Fe_2O_3) inclusion containing high Fe and Ti contents found specific in corundum from igneous rocks and alkali basaltic terrains consistent with documented by Sutherland *et al. (*1998b). On the other hand, corundums contain the inclusions of diaspore, calcite, CO_2, and sulfur phases were proposed to be typical metamorphic deposit. Calcite inclusion was suggested to have originated from marble-hosted deposit. However, the ambiguous information of some mineral inclusions such as anatase and graphite were also found in this study which has pointed out the imperfections of the results obtained from Raman study. Although Raman spectroscopic technique is the most efficient way to study inclusion and has been used by many researchers, this technique has a certain limitation for study on mineral phase identification. For example, Raman method is unable to identify a specifical inclusion with extensive solid-solution or complex chemical composition. In fact, the accurate mineral chemistry of inclusion, that may yield the constraint on geological condition of corundum formation, impossible to be obtained from this method.

Alternative EPMA technique, which can provide the accurate chemical analysis of micro-phase including inclusion in corundum, has been applied for this aspect by some researchers (e.g., Guo *et al.*, 1994; Sutherland *et al.*, 2002). Guo *et al.* (1994) firstly reported the occurrence of a cobalt-rich spinel inclusion in a gem-quality blue sapphire from Bo Phloi in Thailand. The result from EPMA technique illustrated that its composition was analogous to the composition of Co-chromite

((Co, Ni, Fe^{2+}) (Cr, $Al)_2O_4$). This study demonstrated the application of EPMA method to obtain an important evidence of the new inclusion present in Bo Phloi sapphire. Sutherland *et al.* (2002) published the effectiveness of EPMA technique to obtain the mineral chemistry of inclusion in sapphires from Huai Sai, Laos. They reported that alkali-feldspar inlusions in Huai Sai sapphire gave its end-member proportion as $Ab_{81.7}An_{9.5}K_{8.8}$ which closed to the albite-anorthoclase-oligoclase meeting point. The presence of this alkali-feldspar end-member led them to conclude that the formation of Huai Sai sapphire was related to strongly alkaline melts.

In addition, the application of the SHRIMP method on trace element study of mineral inclusion, particular in zircon inclusion, within corundum are able to imply the crystallization environment as well as geochronological information of corundum (e.g. Coenraads, 1990; Guo *et al*, 1996b). The SHRIMP U-Pb isotopic dating of zircon inclusions in sapphire from New South Wales, Australia studied by Coenraads *et al.* (1990) gave the age at 35±1.9 Ma and 33.7±2.1 Ma which match with the New South Wales basalt having a K-Ar age of 19 to 38 Ma and zircon fission track ages of 2 to 49 Ma. In addition, the SHRIMP analysis of zircon inclusion found in Huai Sai in Laos sapphire by Sutherland *et al.* (2002) displayed enrichment in Hf, Y and REE, suggesting the sapphire crystallized from highly evloved alkaline melt. The U-Pb isotopic (SHRIMP) dating of such zircon inclusion gave ages of 1.2-1.3±0.3 Ma.

1.3.3 Mineral Inclusion in Basaltic Corundum

Corundum is found in certain alkali basalt fields and their associated alluvial deposits. This occurrence is significant due to the large number of associated economic gem corundum deposits. Corundums related to the Late Mesozoic to Late Cenozoic basalts, such as those occur in Tasmania, Australia, Southeast Asia and China; particular in Southeast Asia deposit, are important gemfields in the world. Mineral inclusions in basaltic corundum have become more concern during the last decade. Many previous publications interested to study on inclusion and corundum formation whether sampled from Thailand areas comprise of the Bo Phloi, Chanthaburi-Trat and Phrae localities (Guo *et al.,* 1994; Pisutha-Arnond *et al.,* 1999; 2005; Srithai and Rankin, 1999; Sutthirat *et al.,* 2001; Limtrakun *et al.,* 2001; Saminpanya, 2001; Saminpanya *et al.,* 2003; Chualaowanich *et al.,* 2005; Yui *et al.,* 2003; 2006), from Huai Sai, Laos (Bosshart, 1995; Sutherland *et al.,* 2002), from

Vietnam (Pham Van *et al.*, 2004; Garnier *et al*., 2005) and from Australia (Guo *et al.*, 1996a; Oaks *et al.*, 1996; Sutheraland *et al.*, 1998a, 1998b).

Bosshart (1995) reported zircon, cheralite (a thorium-rich monazite group mineral) inclusions found in Ban Huai Sai sapphire from Laos, while a columbite-like mineral, probably euxenite-(Y) and albite inclusions additionally encounterd in these sapphires by Sutherland *et al.* (2002). In addition, Intasopa *et al.* (1999) studied alkaline basalt and corundum in Chanthaburi-Trat, Thailand. They presented various mineral inclusions analysed by optical microscope and Raman method in Chanthaburi-Trat corundum including spinel, gahnite, hercynite, pleonaste, biotite mica, diopside, ferrocolumbite, zircon, monazite, garnet, rutite, boehmite, feldspar, bismuth and thorite. Subsequently, they proposed that these corundums possibly crystallized from peraluminous alkaline felsic magma which was formed by partial melting of metasomatized lithospheric rock at the crustal level shallower than 80 km. Moreover, preliminary report by Somwangsombat and Sutthirat (2009) presented the common mineral inclusions consisting of feldspar and zircon found in sapphire from Gia Nghia, Vietnam.

Guo *et al.* (1996a) reported two distinctive suites of mineral inclusions contain in basaltic sapphires namely alkali feldspar suite (feldspar, zircon, uraninite, ilmenite, Fe-Cu sulphides inclusions) and carbonatitic suite (titaniferius columbite, uranopyrochlore, fersmite inclusions) from basaltic terrains including from Australia, China and Thailand. Furthermore, Hughes (1997) reported a wide range of inclusion found in corundum from major occurrences including alkali basalts such as Kanchanaburi, Chanthaburi-Trat and Phrae provinces in Thailand, Pailin in Cambodia, Queensland and New South Wales in Australia. The most common inclusions occurred in basaltic sapphire were Nb_2Ta oxides (such as titaniferous columbite and uranpyrochlore), alkali feldspar, low-Ca plagioclase (albite-oligoclase) and zircon, whereas uncommon inclusions such as Fe Cu-sulphide (low Ni), cobalt-rich spinel, Th Ce-rich phosphate and uraninite were rarely observed.

Moreover, Sutherland *et al.* (1998a) presented interesting information of chemical and geological characteristics of gem corundum from the basaltic fields in Barrington, Australia, and in Pailin, Cambodia. Both gem fields had similar gem suites from two distinct geologic origins namely “magmatic” and “metamorphic” suites. Both origins of these basaltic corundums could be distinguished by the

different types of mineral inclusions and trace/minor elements. Metamorphic origin was characterized by mineral inclusions of magnesium spinel (Mg-rich) and sapphirine whereas magmatic formation contained inclusions of ferrian spinel (Fe-rich), zircon, Nb-Ta-U- and/or Th-rich oxide minerals such as pyrochlore. Moreover, chemical differentiation between both origins was also possible using the elemental ratios (e.g., Cr_2O_3/Ga_2O_3 and Fe_2O_3/TiO_2) of host corundum.

Concerning the inclusion study of Bo Phloi sapphire in Thailand, many researchers reported a number of inclusion observed in this sapphire. Saminpanya (2000) reported nepheline ($Ne_{68.3}Ks_{28.6}Q_3$) inclusion in Bo Phloi sapphire; subsequently, he proposed a nepheline syenite origin of this sapphire based on the presence of nepheline inclusion. In addition, the study of fluid inclusion in Bo Phloi sapphires by Srithai and Rankin (1999) and the finding of hercynitic spinel inclusion from the same deposit by Rankin and Edwards (2003) indicated a magmatic source of its host sapphire. Moreover, the cobalt-rich spinel inclusion reported by Guo *et al.* (1994) suggested as a result of a complex magma mixing process in the lower crust. This process was probably involving an alkali-rich felsic melt and a silica-deficient carbonatite type melt. Furthermore, Pisutha-Arnond *et al.* (1999; 2005) discovered more mineral inclusions in Bo Phloi sapphires including alkali feldspar, zircon, monazite, hercynitic spinel, Nb-oxide, maganoan ilmenite, nepheline, pyrochlore (?), thorite (?), biotite (?) and calcite.

Based on the previous study above, the diversity of mineral inclusion in basaltic sapphire was displayed; however, most of those inclusion phases were identified by Raman technique, only some chemical data of such mineral inclusions were analyzed by EPMA. As a result, the detailed study of inclusion in basaltic sapphire is still needed to be done, in particular on the mineral chemistry of inclusion in Southeast Asia. It is expected that the accurate information of mineral chemistry of inclusion will be able to give a better constraint on the genetic model of the sapphires.

1.4 Scope of Study

The main focus of this research is to study the mineral chemistry of inclusions in sapphires from various deposits in Southeast Asia with a special emphasis on sapphire from Bo Phloi deposit, Kanchanaburi in Thailand. Characteristic of internal features in these samples are investigated under an optical microscope before being

identified using a Raman Spectroscope. Subsequently, major and minor compositions of these inclusions are obtained by EPMA technique. In addition, other basaltic sapphire elsewhere in Southeast Asia is also investigated using the same procedures for comparison with the result earned from Bo Phloi sapphire. Finally, reconstruction of sapphire formations in Southeast Asia based on mineral chemistry of inclusion from Chanthaburi and Phrae in Thailand, Huai Sai in Laos, Pailin in Cambodia and Gia Nghia in Vietnam, particularly from Bo Phloi sapphire, are carried out, Moreover, the age dating of representative zircon inclusion is performed by using U-Pb dating. In addition, the preliminary study of Th-U-Pb dating on zircon and monazite inclusions by EPMA techniques is also studied.

It should be emphasized here again that the scope of this study is focused mainly on the inclusion study of Bo Phloi sapphires and extended to basaltic sapphires in the Southeast Asian region. The formation of basaltic ruby such as those occurred at Thai-Cambodia border (i.e., in Trat area of Thailand and extended to Pailin area of Cambodia) is beyond the scope of this study. This is because the basaltic ruby could have been formed under a different source provenance and condition (Sutthirat *et al.*, 2001; Saminpanya and Sutherland, 2011).

1.5 Methodology

The procedure of this study can be divided into several steps as summarized in the flow chart (Figure 1-1). The detail of each step is described below.

Literature review was the first step carried out on previous literatures related to this study such as inclusions in basaltic sapphires worldwide. Laboratory work started with sample collections from the basaltic localities in Southeast Asia, including Bo Phloi, Chanthaburi and Phrae in Thailand, Huai Sai in Laos, Pailin in Cambodia and Gia Nghia in Vietnam. The Bo Phloi sapphires in Thailand are the main focus of this study, whereas samples from the other Southeast Asia localities are also studied to gain more information of the region. The samples of each locality were grouped based on the color appearance then they were sorted out for inclusions under a binocular microscope. Inclusions observed in those samples range from some micrometers to hundreds of micrometers in size. The samples that contain large enough mineral inclusions were selected for Raman spectroscopic study and chemical analyses. The selected samples were then weighted, photographed, measured the

specific gravity (in order to cross-check whether each sample was really sapphire) and finally labeled wherever appropriate. After that the samples were mounted in epoxy resin and then carefully cut and polished on 600 and 1000 μm polishing powders until the mineral inclusions were exposed on the surface. Subsequent polishing utilized 6, 3 and 1 μm diamond pastes to give a good quality polished surface for further analyses.

After sample preparation steps, the sapphire samples were investigated by both optical and chemical techniques. All polished samples from each group of sapphire from different localities were examined the internal features and then photographed using a standard gem stereoscope. Subsequently, mineral inclusions exposed at or near surface were preliminarily examined their phase identities by using a Laser Raman Spectroscope at the Gem and Jewelry Institute of Thailand (Public Organization) (GIT). Then the samples were carbon-coated and the exposed inclusions were analyzed their major and minor element compositions by using EPMA method at Department of Geology, Faculty of Science, Chulalongkorn University. The EPMA technique was mainly employed in this work because it had relatively low detection limits and provided accurate chemical composition data. The EPMA machine was also equipped with mapping facilities enabling mapping of element distributions (Pownceby *et al.*, 2007). Even though the EPMA analysis can be accomplished at a micro-scale, and not only able to identify the elements present but also can measure them with a small degree of error, it still has the limitation; for example, the EPMA technique is not sensitive to many elements below 100 ppm. As such, some trace element composition of inclusions had to be obtained by LA-ICP-MS technique. In this work, the trace elements study and U-Pb dating of representative zircon inclusion were analysed by using LA-ICP-MS technique in collaboration with Dr. Elena Belousova, Macquarie University, Australia. The results of trace element analyses were used to interpret the mineral chemistry of inclusions and understand the environment of sapphire formation. Moreover, a preliminary study of Th-U-Pb dating of some monazite and zircon inclusions was also studied by using EPMA method at Department of Geology, Faculty of Science, Chulalongkorn University. The results are useful for studying the geochronology thus provides likely age and constraints on the zircon/sapphire crystallization.

Thereafter, data compilation, interpretation, thesis writing and defense were carried out at the end.

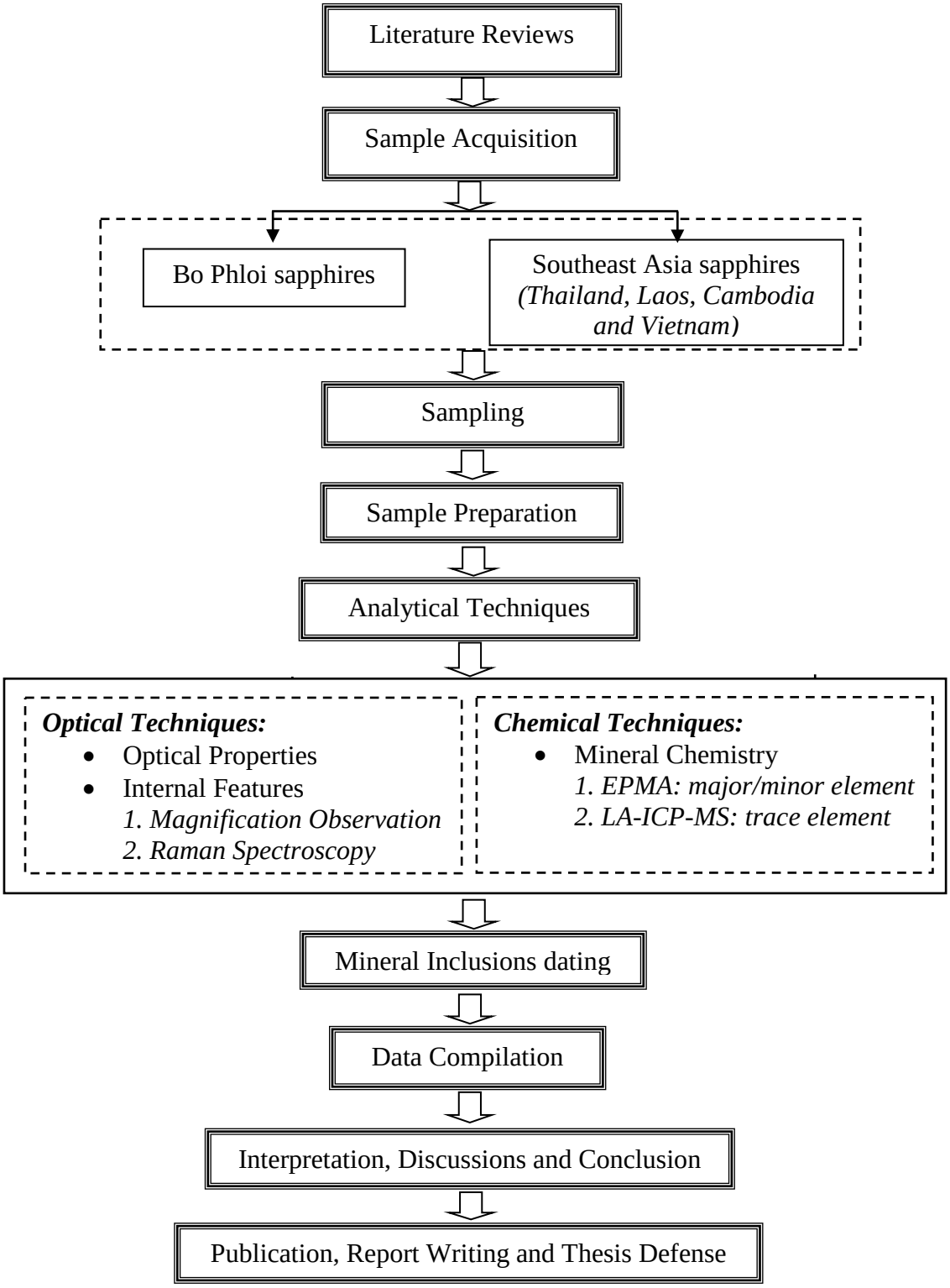

Figure 1-1 Schematic diagrams show the methodology framework of this study.

1.6 Analytical Techniques

1.6.1 Electron Probe Micro-Analyzer

The Electron Probe Micro Analyzer (EPMA) (Model JXA-8100), based at Department of Geology, Chulalongkorn University (Figure 1-2) was mainly technique used for chemical analysis of mineral inclusions within sapphires in this study. This method is a non-destructive analytical technique; therefore it has been conventionally used to investigate the chemical compositions of minerals in geology and gemstones.

The electron beam was focused on the surface of sample, and produced characteristic X-ray of the samples. The characteristic X-rays were detected at wavelengths, and their intensities were measured to determine concentrations. In this work, the EPMA was applied to examine mineral inclusions in three different aspects including qualitative analyses, quantitative analyses and qualitative X-ray mapping.

For quantitative analyses, most of the standards used for calibration were pure oxide and mineral standards including corundum for Al, wollastonite for Si and Ca, periclase for Mg, fayalite for Fe, potassium titanium phosphate for K, Ti and P, jadeite for Na, barite for Ba, manganosite for Mn, eskolite for Cr, zinc oxide for Zn, strontium barium niobate for Nb, Hafnium for Hf, Zirconium for Zr. The other elements (i.e., Pb) were calibrated using internal standards. In addition, the standards of Rare Earth Element (REE), thorium and uranium are prepared by Miss Sopit Pumpang and then used for calibration. Appropriate crystals in all five spectrometers were fully engaged for analyses of these elements. Operating condition was set at an accelerating voltage of 15.0 kV, about 23.8 nA sample current, with focused beam (smaller than 1 μm). Measuring times were set at 30 seconds and 10 seconds for peak counts and background counts, respectively, for each element using suitable analytical crystals. The analytical results were then taken automatic ZAF correction before reported in form of percent oxides. Fe^{2+} and Fe^{3+} ratios of some particular minerals were recalculated using equation of Droop (1987).

Figure 1-2 Electron Probe Micro Analyzer (EPMA), Model JXA-8100 based at Department of Geology, Faculty of Sciences, Chulalongkorn University.

1.6.2 Laser Raman Spectroscopy

The Laser Raman spectroscopy (Model 1000, Ranishaw) based at GIT (Figure 1-3) was used to identify the phase of mineral inclusions in sapphire samples in this work. In generally, Raman spectroscopy is a spectroscopic technique used to study vibrational, rotational, and other low-frequency modes in a system. It relies on inelastic scattering, or Raman scattering, of monochromatic light, usually from a laser in the visible, near infrared, or near ultraviolet range. The laser light interacts with molecular vibrations, phonons or other excitations in the system, resulting in the energy of the laser photons being shifted up or down. The shift in energy gives information about the vibrational modes in the system. Infrared spectroscopy yields similar, but complementary, information. Raman spectroscopy is commonly used in chemistry, since vibrational information is specific to the chemical bonds and symmetry of molecules. Therefore, it provides a fingerprint by which the molecule can be identified. In addition, Raman spectroscopy is a non-destructive method which provides a quick identification of mineral, gemstones and other materials. However, this method has some limitation such as only inclusions lying close to the surface of the samples/sapphires and unable to clearly distinguish some mineral inclusions that set deep into the sapphire samples. The good analytical results are obtained from mineral inclusions that are exposed or very close to the sample surface with a maximum depth of 5 mm provide the best result.

Raman machine was calibrated with silicon plate and its center about 520 nm before using the Raman spectroscope for the characterization of mineral inclusions. The laser source used for this study was 514.5 nm. Raman spectrum wavelength and was set between 200 to 2000 cm^{-1} and the data acquisition times of 10 seconds with the accumulations for three times.

Figure 1-3 Laser Raman spectroscope (Model 1000, Ranishaw) based at the GIT.

1.7 Organization of Thesis

This report is composed of five chapters which including introduction sections, followed by the main body of work of this study, and ending up with conclusion and recommendations for further work. An introduction to the research project (e.g., general statement, aims, objectives, and methodology) has already been presented in this chapter. In addition, a review of the literature on theoretical background and relevant researches is also presented in chapter 1. Sample collection from Bo Phloi sapphires are described in Chapter 2, and this is followed by a detailed study of mineral inclusions and their mineral chemistry. The compositional chemistry of inclusions from Southeast Asia sapphires (e.g., some deposits in Thailand, Laos, Cambodia and Vietnam) is reported and correlated between different deposits in Chapter 3; in addition, some data of mineral chemistry from Bo Phloi sapphires are also presented for comparison with those deposits in some Southeast Asia sapphires. Trace elements of representative zircon inclusion and the data of U-Pb dating of zircon inclusion from Bo Phloi sapphire are reported in Chapter 4. In addition, the preliminary study of *in-situ* Th-U-Pb dating of zircon and monazite inclusions by using EPMA method is reported in this chapter. In Chapter 5, all results from the

previous chapters are discussed, and genetic model of Bo Phloi sapphire formation and the generalized model of Southeast Asia sapphire formation are proposed. Finnally, the conclusions and some recommendations for further works are also included in this chapter.

CHAPTER 2
BO PHLOI SAPPHIRE

2.1 Introduction

Bo Phloi gem field of Kanchanaburi province, western Thailand, (Figure 2-1) is a well-known "basaltic" gem corundum deposit that has supplied large quantities of a good quality sapphire to the world market. It used to be the biggest alluvial sapphire mining in Southeast Asia. In general, Bo Phloi sapphires are found in secondary deposits derived from weathered alkali basalt that outcrops at Khao Lantom, near Bo Phloi city, and at Huai Maka of Ban Chong Dan. Opencast mining in Bo Phloi area is generally confined to a paystreak, a sapphire-bearing gravel bed normally about 3 meters thick and lying at 13 to 15 meters depth (Hansawek and Pattamalai, 1997).

The gem-related Bo Phloi basalt is characterized by dark, dense, fine-grained and porphyritic rocks. Megacrysts of clinopyroxene, black spinel, sanidine, olivine, anorthoclase were often observed; besides, ultramafic nodules (especially spinel lherzolite) and gneissic xenoliths were also reported (e.g., Sutthirat *et al.,* 1999; Sutthirat, 2001; Srithai, 2005). In addition, the megacrysts in Bo Phloi basalt comprise nepheline, Al-Ti magnetite, and mostly important corundum (Pisutha-Arnond *et al.,* 1999). These basalts were geochemically classified as basanitoid by Vichit *et al.* (1978) and as nepheline hawaiite by Barr and Macdonald (1978) and Yaemniyom and Pongsapich (1982). Geochronologically, the Bo Phloi basalt was reported to have a K/Ar age of 3.14±0.17 Ma (Barr and Macdonald, 1981) and a $^{40}Ar/^{39}Ar$ age of 4.17±0.11 Ma (Sutthirat *et al.,* 1994).

In-depth studies of mineral inclusions in Bo Phloi sapphires have been published by a few researchers. Saminpanya (2000) reported nepheline inclusion ($Ne_{68.3}Ks_{28.6}Q_3$) and proposed a genesis model related to nepheline syenite. Cobalt-rich spinel inclusion was presented by Guo *et al.* (1994); consequently, they suggested a complex magma mixing process involving an alkali-rich felsic melt and a silica-deficient carbonatite melt in the lower crust for the formation of spinel and sapphire in this area. In addition, Pisutha-Arnond *et al.* (1999, 2005) proposed a genesis model of Bo Phloi sapphire, based on information of "*corsilzirspite*" (a corundum+silimanite +zircon+spinel xenolith) pebble found in gem-bearing layer and inclusion suites (including alkali feldspar, zircon, monazite, hercynitic spinel, Nb-oxide, maganoan

ilmenite, nepheline, pyrochlore (?), thorite (?), biotite (?) and calcite), that might be occurred by contact metamorphic/metasomatic/contamination processes caused by interaction between gabbroic melt and Al-rich crustal rocks. Although more mineral types of inclusion were mentioned in the last report, their mineral chemistries were not fully analyzed by EPMA.

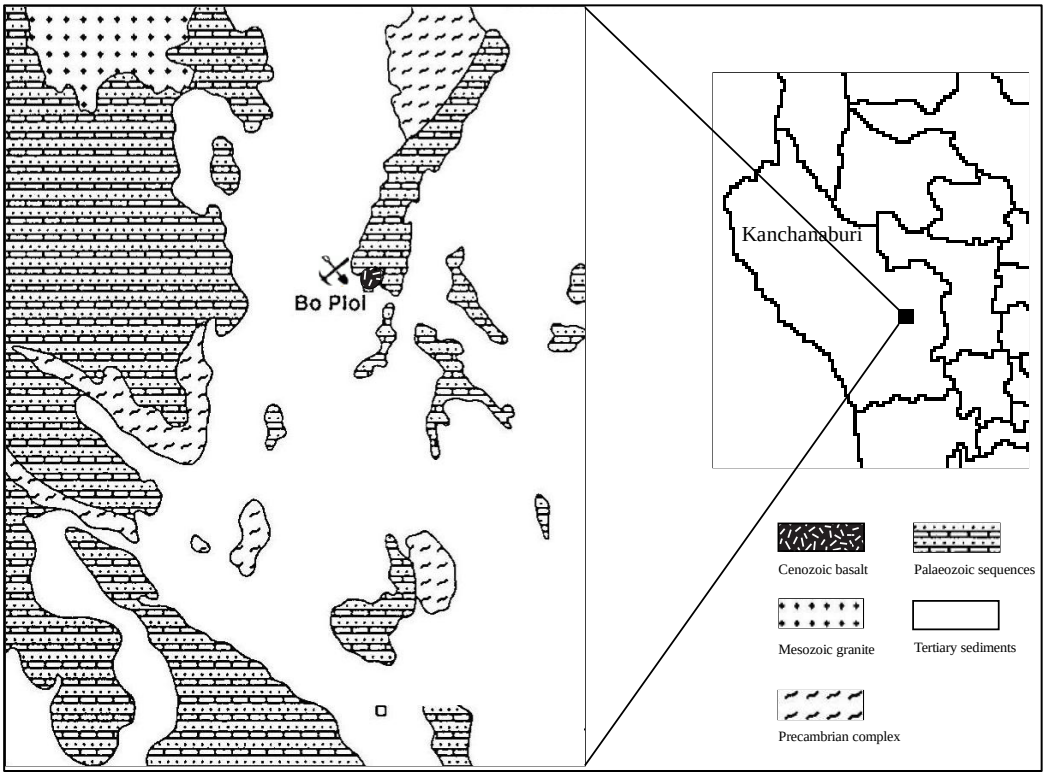

Figure 2-1 Geologic map of Bo Phloi area, Kanchanaburi province, western Thailand (modified after Vichit *et al.*, 1978).

2.2 Methodology

After sampling step, the rough Bo Phloi sapphires were examined optically under a binocular microscope to pick up suitable samples containing more inclusions before they were mounted in epoxy resin. The samples containing larger mineral inclusions were carefully polished until the inclusions were exposed on the surface. Because of most mineral inclusions observed in these sapphires are small in size (<50 μm). It is certainly necessary to use microscope with high magnification to observe their inclusion morphology.

The most practical technique used for mineral inclusion identification in any transparent mineral is an optical microscopic observation in combination with Raman spectroscopic technique (Dao and Delaigue, 2000; Palenza *et al.*, 2008). In addition,

the use of the confocal laser system of this method allows the subsurface of the crystal to be sampled with a high spatial resolution. However, this method has a certain limitation to examine the samples; for example, the technique is unable to identify specifically inclusion with extensive solid-solution or complex chemical composition and with large sample size (approximately ≥ 50 μm). Moreover, inclusion samples need to be exposed or very close to the sample surface with a maximum depth of 5 mm. In fact, the mineral inclusions found in these sapphires are small in size and rather difficult for sample preparation. In addition, this technique cannot provide quantitatively chemical composition of mineral inclusions which may yield the constraint on geological condition of their host sapphire formation. Therefore, only dark grayish brown sapphires were selected for initial identification of mineral inclusions using Raman technique in this study.

Subsequently, the selected samples of each group of Bo Phloi sapphires were carbon-coated for analysis of major components of mineral inclusions using EPMA technique, a JEOL model JXA-8100, based at the Department of Geology, Faculty of Science, Chulalongkorn University. Operating condition was set at an accelerating voltage of 15.0 kV, about 24 nA beam current, with a focused beam (smaller than 1 μm). Mineral and pure oxide standards were selected for calibration. Measuring times were set at 30 seconds for each element using suitable analytical crystals before ZAF correction was automatically carried and results were reported in form of percent oxides. Fe^{2+} and Fe^{3+} ratios of some particular iron-containing minerals were recalculated using equation of Droop (1987).

2.3 Sample Characteristics

Bo Phloi sapphire samples used in this study were received directly from local mines in the Bo Phloi gem field. More than 170 grains of Bo Phloi sapphires, obviously contain lots of mineral inclusions, were selected for this study. These sapphires are about 2 mm in size and represent the majority of stones from this gem field (Figure 2-2). They were subdivided, based on color appearances, into two main varieties; i.e., grayish brown and blue groups. Moreover, grayish brown sapphires have two color shades including dark grayish brown (45 samples) and light grayish brown (48 samples) whereas blue samples also contain blue (50 samples) and light blue (30 samples) shades (see Figure 2-2). The internal features of these sapphires

were investigated under a gemological microscope as displayed in the Figures below. Moreover, summary of mineral inclusions analyzed by Raman and mostly by EPMA techniques are also shown below.

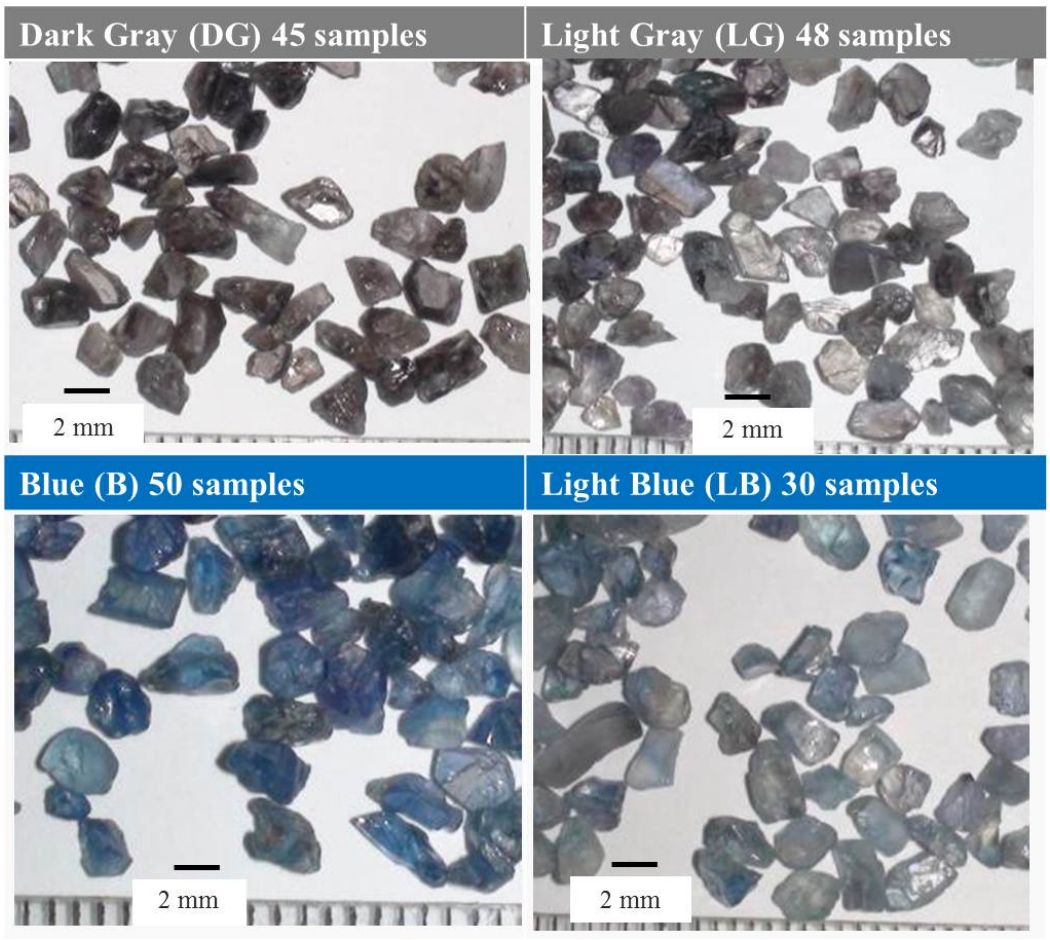

Figure 2-2 Sample collections of Bo Phloi sapphires including grayish brown (upper photos) and blue varieties (lower photos), which individually present different shades.

2.3.1 Internal Features

Most sapphire samples selected in this study are transparent to translucent specimens (Figure 2-3) which needle-like inclusions are generally found in most grains, particularly in the dark grayish brown samples (Figure 2-4). Moreover, the muti-phase inclusions and hexagonal brown colored zoning are also appeared in some grains as displayed in Figures 2-5 and 2-6, respectively.

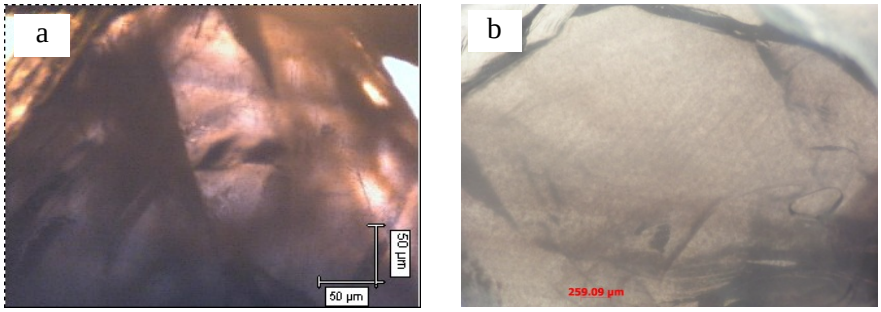

Figure 2-3 Dark brown color zones (a) and needle-like inclusions (b) found in the dark grayish brown sapphires.

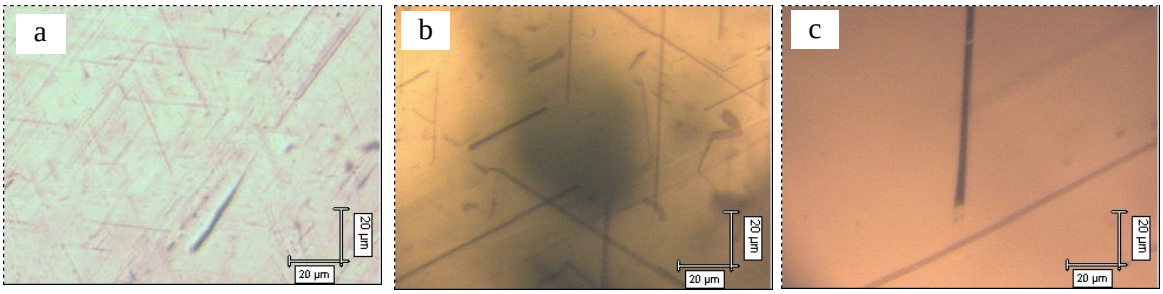

Figure 2-4 Needle-like inclusions intersecting at 60°/120° along dark color zones of the dark grayish brown sapphires.

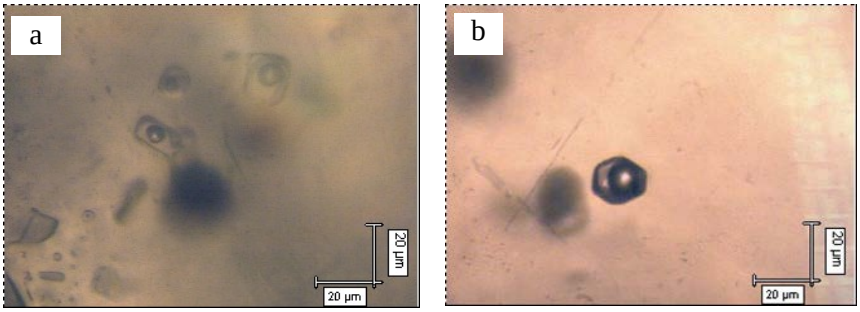

Figure 2-5 Muti-phase inclusions in the dark grayish brown sapphires.

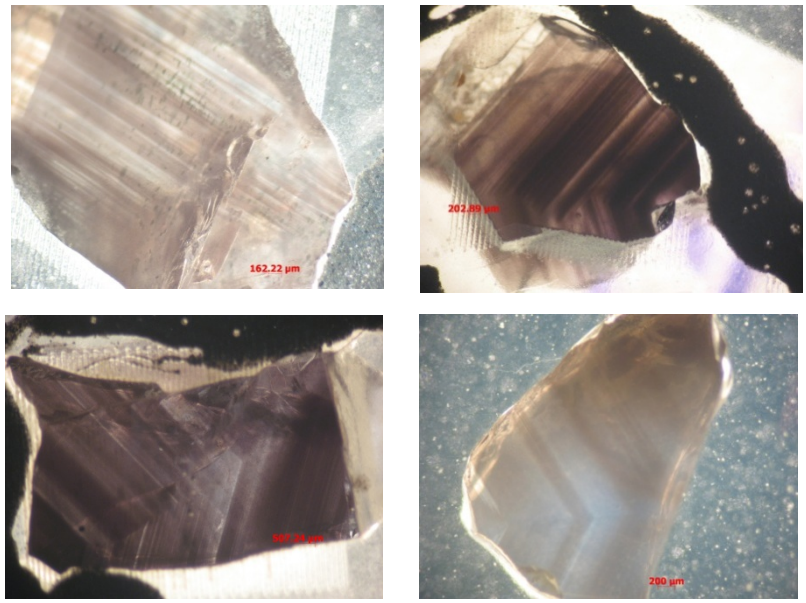

Figure 2-6 Parts of the hexagonal brown colored zoning found in the dark grayish brown sapphires.

2.3.2 Types of Mineral Inclusion

In this study, there are some mineral inclusions in Bo Phloi sapphires that are able to cut open or stay very close to sample surface and identified by the Raman technique. There are parts of mineral inclusions namely feldspar, spinel, mica and monazite could be analyzed using this method. Among those inclusions, feldspar is the most common mineral inclusion found in these sapphires. Due to the limitation of Raman technique as previously described, the EPMA technique was the main instrument used for phase identification and investigation of mineral chemistry of these mineral inclusions. Types of mineral inclusions in Bo Phloi sapphires analyzed by both Raman and EPMA methods are present in Table 2-1.

Table 2-1 Summary of mineral inclusions in the Bo Phloi sapphires mostly analyzed by EPMA as well as Raman techniques.

Mineral group	Mineral inclusions	Grayish brown sapphires		Blue sapphires	
		Dark gray *(45 samples)*	Light gray *(48 samples)*	Blue *(50 samples)*	Light blue *(30 samples)*
Silicates	Zircon	***	**	**	**
	Feldspar	**	**	***	***
	Nepheline	**	***	**	-
	Enstatite	**	***	**	-
	Garnet	**	*	-	-
	Sapphirine	-	*	*	-
	Mica	**	-	-	-
	Staurolite	-	*	-	-
Oxides	Spinel	***	***	-	-
	Ilmenite	**	-	-	**
Carbonates	Calcite	*	-	-	-
Phosphates	Monazite	***	-	-	-

**** often found*
*** found*
** rarely found*
- not found

2.4 Characteristics of Mineral Inclusions

The details of each mineral inclusion found in these sapphires including the morphology of crystal under a microscope and back scattered electron images (BSI) are illustrated in this section. In addition, some Raman spectra are also displayed. Moreover, the representative EPMA data of each mineral inclusion are also reported and described in detail.

Feldspar: is the most common mineral inclusions found in all color varieties of Bo Phloi sapphires; however, it is more often found in blue varieties both blue and light blue sapphires. Some photomicrographs and BSI images of feldspar inclusions observed in these sapphires are illustrated in Figures 2-7 and 2-8, respectively. More photomicrographs and BSI images of feldspar inclusions are collected in Appendix A.

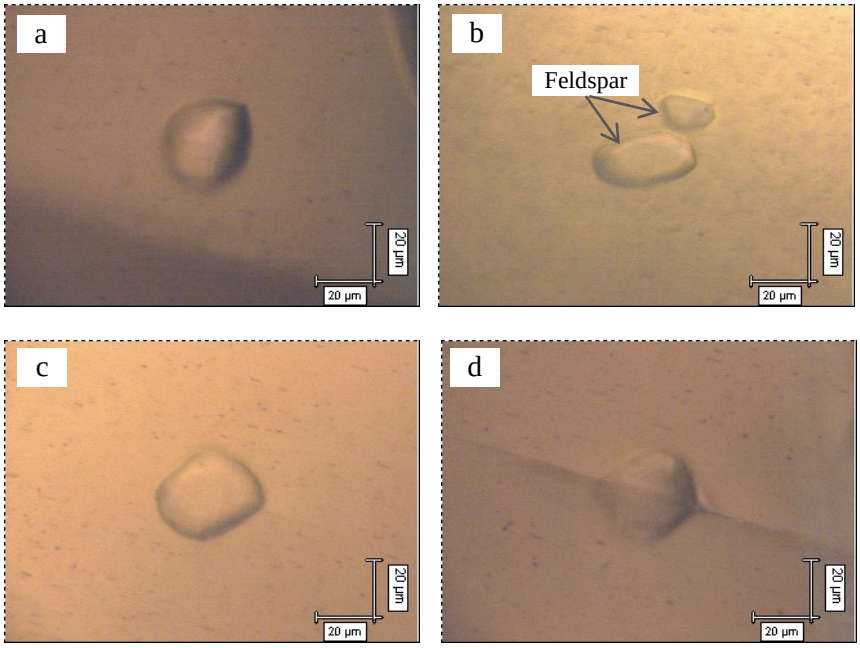

Figure 2-7 Photomicrographs of feldspar inclusions (a-d) observed in the dark grayish brown sapphires.

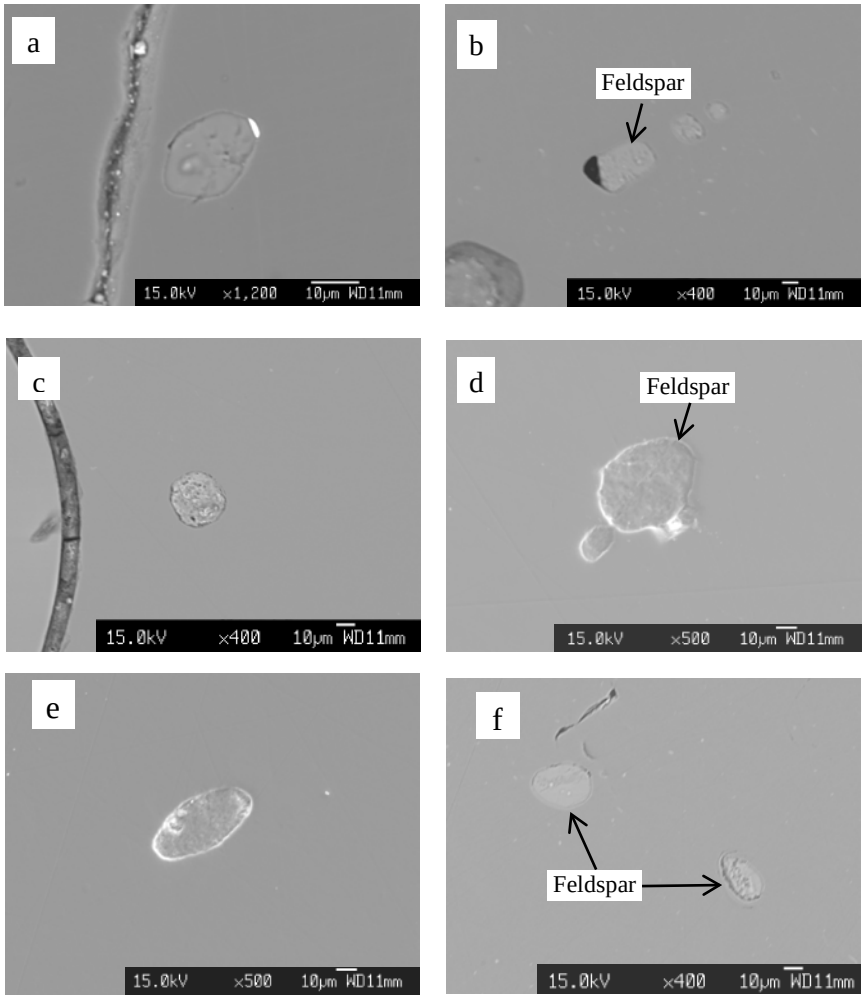

Figure 2-8 Back scattered electron images (BSI) of feldspar inclusions in Bo Phloi sapphires: (a) dark grayish brown sapphire; (b, c) light grayish brown sapphires; (d, e) blue sapphires; (f) light blue sapphire.

In addition, the Raman spectra of feldspar inclusions were also selected and displayed in Figures 2-9. More spectrums of these inclusions are reported in Appendix B.

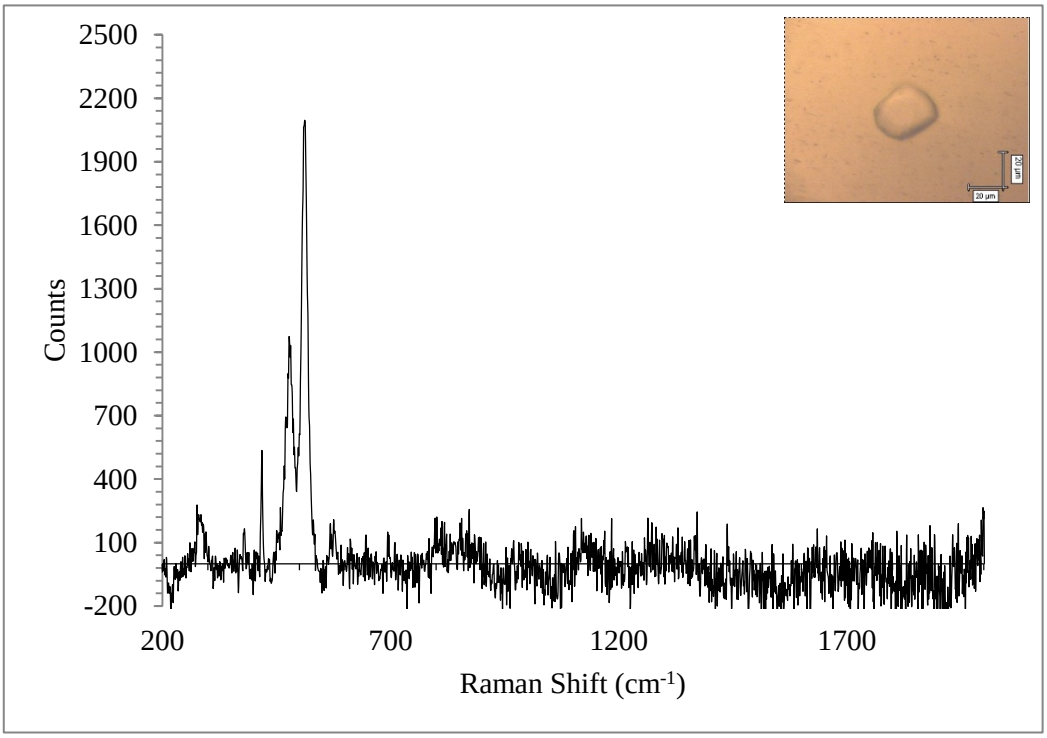

Figure 2-9 Raman spectrum of feldspar inclusion observed in the sample *1C4a2-1* of the dark grayish brown sapphire.

Representative EPMA analyses of feldspar inclusions obtained from all color varieties of Bo Phloi sapphires are summarised in Table 2-2 for comparison and more analyses are reported in Appendix C. The compositions of feldspar inclusions in the dark grayish brown sapphire are relatively more sodic than those of the light grayish brown and light blue sapphires whereas those in the blue sapphires appear to have K-rich composition. Ternary diagram of atomic Ca-K-Na proportion (Figure 2-10) show that compositions of all feldspar inclusions found in these Bo Phloi sapphires fall toward the area of Na-rich or albite component with low to moderate potash and low Ca contents. Based on these compositions all of these feldspars are clearly classified as alkali feldspar; however, here different groups can be distinguished in the ternary diagram. The first group ranges within compositions of $Ab_{70-77}Or_{9-23}An_{6-14}$ which are composed all analyses in dark grayish brown sapphires and one sample in light blue sapphire. The second group ($Ab_{52-63}Or_{28-35}An_{3-14}$) is characterized by inclusions found in all light grayish brown sapphires, some light blue and some blue sapphires. The last group ($Ab_{42-45}Or_{42-49}An_{7-14}$) clearly belongs to blue sapphires only. It may indicate that blue sapphire formation is related to K-richer environment whereas

grayish brown sapphires formation is associated to Na-rich one. Light blue and light brown sapphires appear to be transitional formation between those formation enviroments. Na-rich alkaline feldspar or albite inclusions of similar chemical composition were also detected in blue and brown varieties of Bo Phloi sapphire by Pisutha-Arnond *et al.* (1999) and also reported by Guo *et al.* (1994).

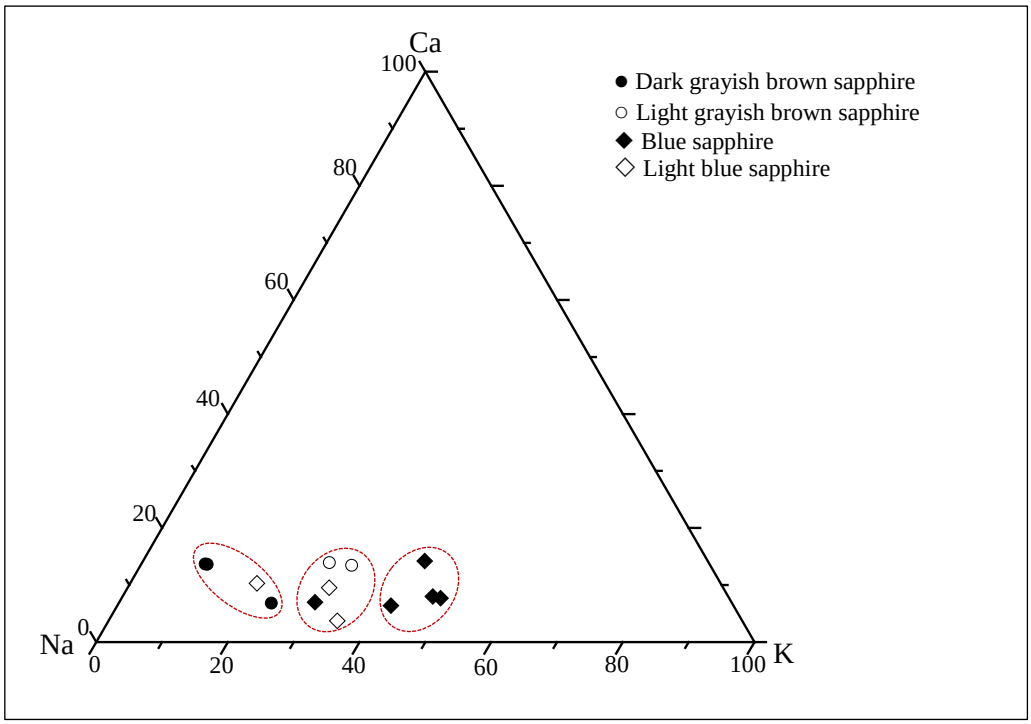

Figure 2-10 Ternary Ca-Na-K plots of alkali feldspar inclusions found in Bo Phloi sapphires.

Nepheline: nepheline inclusions are found in most colors of Bo Phloi sapphires except light blue sapphires. Some BSI images of nepheline inclusions are shown in Figures 2-11 and more images are displayed in Appendix A. Representative EPMA analyses of nepheline inclusions are summarised in Table 2-3, and more analyses are reported in Appendix C. Based on 32 oxygens, recalculated formula of most analyses show slightly high Si (>8) and slightly low Al (<8) atoms with total cations less than 24 atoms per 32 oxygens. This may be caused by lower potassium and/or sodium contents than the ideal composition. As such, vacancies in cation sites appear to have occurred within these nephelines structure. For example, the chemical formula of sample *LGC12e-1* can be expressed as $Na_{7.027}K_{0.797}\square_{0.058}Al_{7.485}Si_{8.375}O_{32}$. However, atomic proportions of all analyses are usual for the nepheline chemistry that is rich in sodium contents (Na_2O ~ 14-18 %). In addition, a nepheline inclusion in a

blue sappire sample *(3BA3g)* gives quite different composition from the other nepheline inclusions; it is potassic richer composition ($Na_{5.238}K_{1.969}\square_{0.581}Al_{8.073}Si_{8.044}O_{32}$). Nepheline inclusions of similar chemical composition were also detected in Bo Phloi sapphires by previous investigators (Pisutha-Arnond *et al.*, 1999; Saminpanya, 2000).

In general, nepheline inclusions in Bo Phloi sapphire contain chemical composition similar to that of nepheline from nepheline syenite (Deer *et al.*, 1992) which is associated with low-temperature feldspars of albite-microcline series. Moreover, nepheline is the most typical mineral in alkaline rocks. Therefore, this evidence implies that the nepheline inclusions within Bo Phloi sapphires may be related to a silica-undersaturation and high alkali (Na and K) environment.

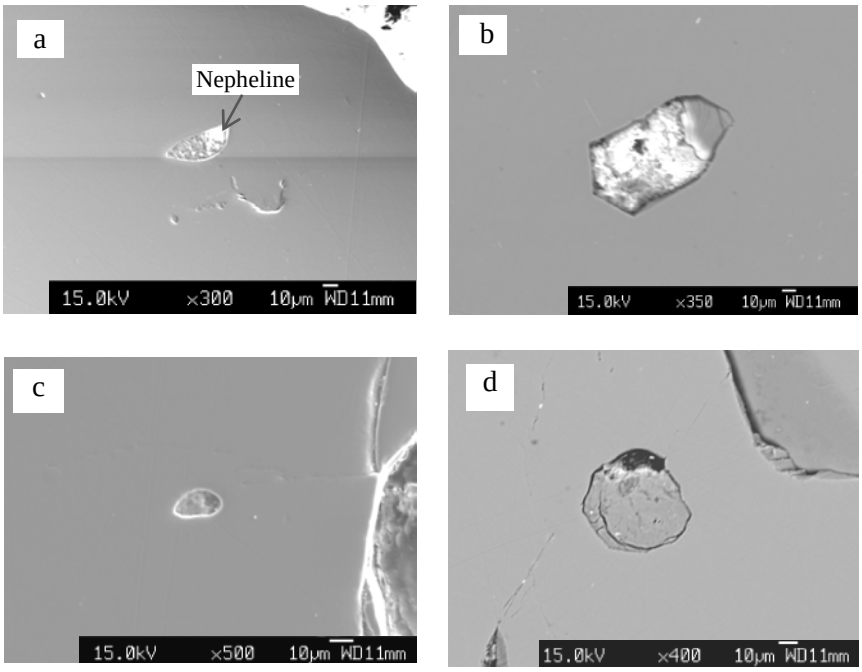

Figure 2-11 Back scattered electron images (BSI) of nepheline inclusions in Bo Phloi sapphires: (a) dark grayish brown sapphire; (b) light grayish brown sapphire; (c, d) blue sapphires.

Table 2-2 Representative EPMA analyses of **feldspar inclusions** in Bo Phloi sapphires *(n.a. = not analyzed).*

Mineral phase	Grayish brown sapphire					Blue sapphire							
Analysis (wt%)	Dark Gray			Light Gray		Blue					Light Blue		
	1C4ia2-1	1C4ib2	2B3idl-4	3LGC1g-3	3LGC3c	3BBn1a-11	3BBn3a-11	3BD1a	3BD1a-1	3BD3a	3LBA2g	3LBA2f	3LBB6a
SiO_2	63.84	63.69	65.72	64.81	64.00	65.61	65.17	63.55	64.83	65.60	63.09	65.62	65.88
TiO_2	0.05	0.05	0.00	0.06	0.01	0.03	0.00	0.02	0.00	0.01	0.03	0.02	0.04
Al_2O_3	22.14	22.18	20.25	26.30	26.20	19.98	22.12	20.50	19.94	21.50	21.80	19.86	19.56
FeO	0.05	0.05	0.04	0.38	0.10	0.06	0.01	0.05	0.11	0.04	0.06	0.04	0.07
MnO	0.03	0.02	0.01	0.09	0.03	0.00	0.00	0.00	0.00	0.00	0.03	0.02	0.01
MgO	0.01	0.00	0.00	0.05	0.00	0.01	0.00	0.01	0.03	0.05	0.00	0.00	0.01
BaO	0.03	0.02	0.00	n.a.	n.a.	0.06	0.00	n.a.	n.a.	n.a	0.07	0.00	0.00
CaO	2.69	2.71	1.39	1.96	2.01	1.37	1.45	1.62	1.69	2.59	2.07	2.13	0.83
Na_2O	8.32	8.38	7.95	4.39	4.59	6.19	7.27	5.11	5.26	4.31	7.20	8.04	7.57
K_2O	1.66	1.61	4.01	3.93	3.45	7.53	5.19	8.59	8.39	6.52	5.60	3.34	6.50
Total	98.82	98.71	99.37	101.97	100.39	100.84	101.21	99.45	100.25	100.62	99.95	99.07	100.45
8 (O)													
Si	2.853	2.850	2.937	2.794	2.794	2.933	2.875	2.895	2.925	2.908	2.841	2.939	2.947
Ti	0.002	0.002	0.000	0.002	0.000	0.001	0.000	0.001	0.000	0.000	0.001	0.001	0.001
Al	1.166	1.170	1.066	1.337	1.348	1.053	1.150	1.101	1.060	1.124	1.157	1.048	1.031
Fe	0.002	0.002	0.001	0.014	0.004	0.002	0.000	0.002	0.004	0.002	0.002	0.002	0.003
Mn	0.001	0.001	0.000	0.003	0.001	0.000	0.000	0.000	0.000	0.000	0.001	0.001	0.000
Mg	0.000	0.000	0.000	0.003	0.000	0.001	0.000	0.001	0.002	0.003	0.000	0.000	0.001
Ba	0.001	0.000	0.000	-	-	0.001	0.000	-	-	-	0.001	0.000	0.000
Ca	0.129	0.130	0.067	0.091	0.094	0.066	0.068	0.079	0.082	0.123	0.100	0.102	0.040
Na	0.721	0.727	0.689	0.367	0.388	0.537	0.622	0.451	0.460	0.371	0.628	0.698	0.656
K	0.095	0.092	0.228	0.216	0.192	0.429	0.292	0.499	0.483	0.369	0.321	0.191	0.371
Total*	4.970	4.973	4.989	4.827	4.822	5.022	5.007	5.029	5.017	4.899	5.054	4.981	5.050
Atomic%													
Na	76.34	76.62	70.00	54.46	57.58	52.02	63.29	43.84	44.90	42.99	59.85	70.46	61.52
Ca	13.61	13.67	6.78	13.47	13.94	6.38	6.97	7.67	7.98	14.24	9.52	10.31	3.71
K	10.04	9.71	23.21	32.07	28.48	41.60	29.74	48.50	47.12	42.77	30.63	19.23	34.77
Total**	100.00	100.00	100.00	100.00	100.00	100.00	100.00	100.00	100.00	100.00	100.00	100.00	100.00

Table 2-3 Representative EPMA analyses of **nepheline inclusions** in Bo Phloi sapphires *(n.a. = not analyzed).*

Mineral phase	Grayish brown sapphire							Blue sapphire		Nepheline (anal.1)
Analysis (wt%)	Dark Gray		Light Gray					Blue		
	2A7ia	1A3ia	3LGC4c-2	3LGC5c-2	3LGC12e-1	3LGC12e-2	3LGC12f	3BA3g	3BC3a-2	(Deer *et al.*, 1992)
SiO_2	42.43	42.54	43.44	44.62	43.90	43.58	42.86	42.20	40.49	44.65
TiO_2	n.a.	n.a.	0.03	0.03	0.02	0.02	0.08	0.05	n.a.	0.00
Al_2O_3	35.80	35.32	34.36	33.90	33.29	32.95	36.06	35.94	34.48	32.03
FeO	0.00	1.33	0.35	0.74	0.28	0.25	0.15	0.43	4.39	0.59
MnO	0.04	0.02	0.03	0.15	0.00	0.02	0.00	0.00	0.49	n.a.
MgO	0.02	0.02	0.00	0.02	0.00	0.00	0.00	0.04	0.05	0.00
CaO	2.58	2.56	0.31	0.58	0.29	0.27	0.30	0.52	0.53	0.71
Na_2O	15.66	15.17	15.53	19.28	19.00	19.05	17.88	14.17	14.68	17.25
K2O	4.54	4.52	5.61	1.69	3.28	3.15	3.54	8.10	5.48	3.66
Total	101.06	101.49	99.65	101.01	100.06	99.29	100.88	101.44	100.57	98.89
32 (O)										
Si	8.032	8.055	8.326	8.381	8.375	8.379	8.085	8.044	7.883	8.595
Ti	-	-	0.004	0.004	0.003	0.003	0.011	0.007	-	0.000
Al	7.987	7.881	7.762	7.503	7.485	7.467	8.018	8.073	7.911	7.267
Fe^{2+}	0.000	0.211	0.056	0.117	0.045	0.040	0.024	0.068	0.715	0.095
Mn	0.006	0.003	0.006	0.024	0.000	0.003	0.000	0.001	0.080	-
Mg	0.006	0.006	0.000	0.005	0.000	0.000	0.000	0.011	0.013	0.000
Ca	0.523	0.519	0.063	0.117	0.059	0.056	0.060	0.106	0.111	0.146
Na	5.746	5.568	5.771	7.020	7.027	7.102	6.541	5.238	5.539	6.438
K	1.096	1.091	1.371	0.405	0.797	0.772	0.852	1.969	1.360	0.899
Total*	23.396	23.334	23.359	23.576	23.791	23.822	23.591	23.516	23.611	23.440
∑R	7.888	7.697	7.268	7.658	7.942	7.987	7.512	7.419	7.120	7.629
Vacancy (□)	0.112	0.303	0.732	0.342	0.058	0.013	0.488	0.581	0.880	0.371

Spinel: is a common inclusion observed in only grayish brown sapphires. Some micro-sized spinel octahedra crystals are also recognized (Figure 2-12). Moreover, some BSI images obtained from both dark grayish brown and light grayish brown sapphires are illustrated in Figure 2-13. More photomicrographs and BSI images of feldspar inclusions are reported in Appendix A.

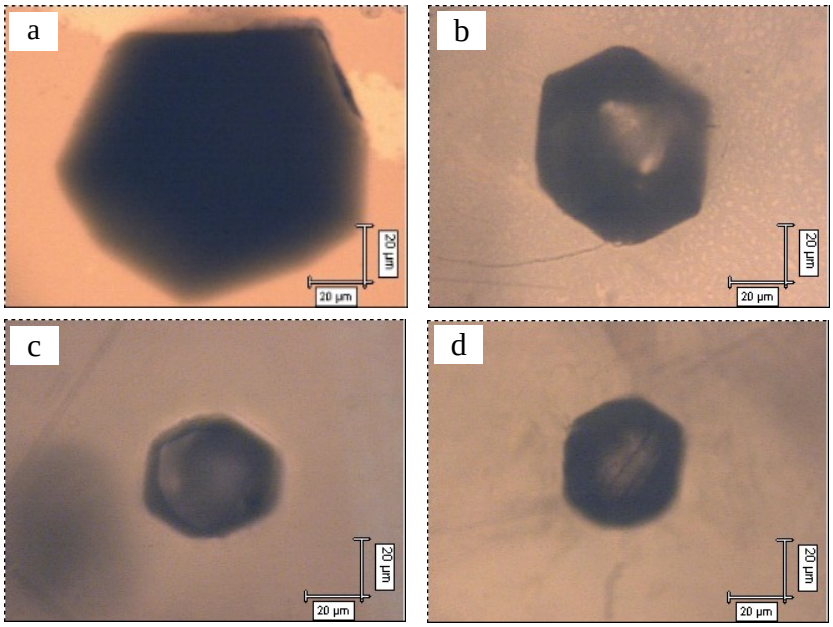

Figure 2-12 Octahedral spinel inclusions (a-d) under microscope found in the dark grayish brown sapphires.

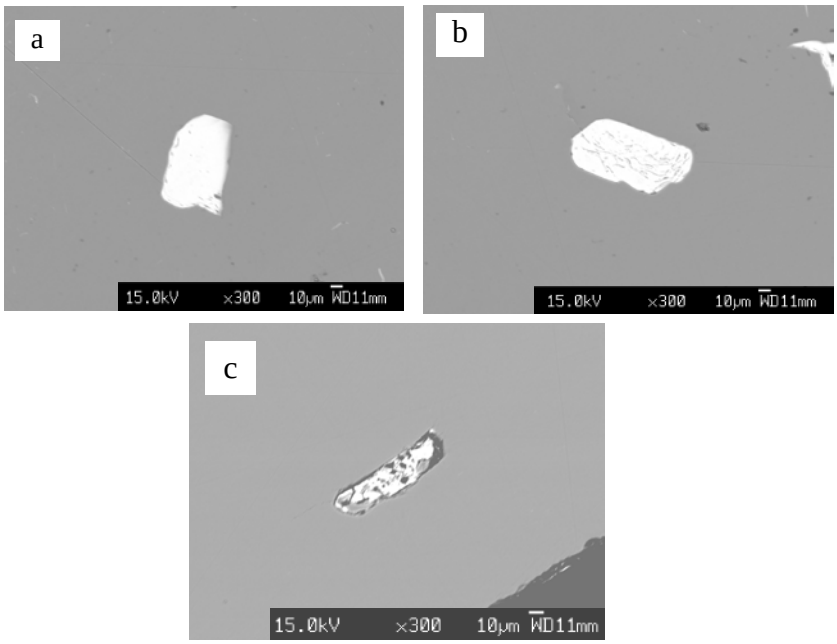

Figure 2-13 Back scattered electron images (BSI) of spinel inclusions in Bo Phloi sapphires: (a, b) dark grayish brown sapphires; (c) light grayish brown sapphire.

In addition, Raman spectra of spinel inclusions are representatively shown in Figures 2-14 and more spectrums are collected in Appendix B.

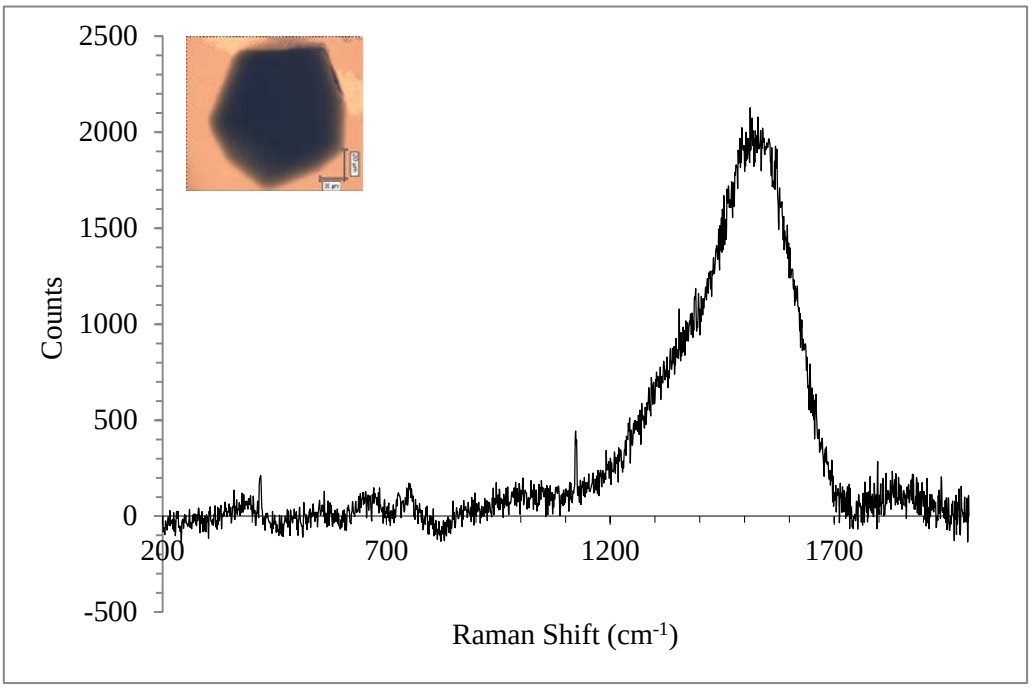

Figure 2-14 Raman spectrum of a spinel inclusion found in sample *1B3ia2* of the dark grayish brown sapphire.

Chemical compositions of spinel inclusions observed only in grayish brown sapphires are shown in Table 2-4. All analyses of spinel inclusion vary in a narrow range of composition mainly composed of 56-60% Al_2O_3, 34-38% FeO and 3-6% MgO whereas the other components are negligible. Based on these chemical analyses, all spinel inclusions fall within the spinel-hercynite series (see Figure 2-15). The hercynitic spinel inclusions of similar composition were also detected in Bo Phloi sapphires by previous investigators (Pisutha-Arnond *et al.*, unpublished data; and Saminpanya and Sutherland, 2011).

The Chemical composition of spinel inclusion under this study are Cr poor (0.00-0.03 p.f.u.) similar to those (Cr = 0.142 p.f.u.) in Bo Phloi sapphire reported earlier by Saminpanya and Sutherland (2011) and those (Cr = 0.00 p.f.u.) of spinel inclusions in sapphire from New England, Australia (Sutherland *et al.*, 1998b). The spinel inclusions in the Bo Phloi sapphires (studied here) however contain slightly Fe richer and Mg poorer than alluvial spinel (belonging to pleonastic composition of

spinel-hercynite series) that is associated with Bo Phloi sapphire (Saminpanya and Sutherland, 2008; and Pisutha-Arnond *et al.*, 1999).

The detailed composition of these hercynitic spinel inclusions however differ from those of a cobalt-rich spinel inclusion in Bo Phloi sapphires previously reported by Guo *et al.* (1994, 1996a), as the latter suggested the origin of Bo Phloi sapphires probably involving a complex mixing of silicic melt with carbonatitic melt. In fact, the hercynitic spinel generally relates to both metamorphic and igneous sources (Deer *et al.*, 1992) and found in magmatic blue sapphires elsewhere (Sutherland and Coenraads, 1996).

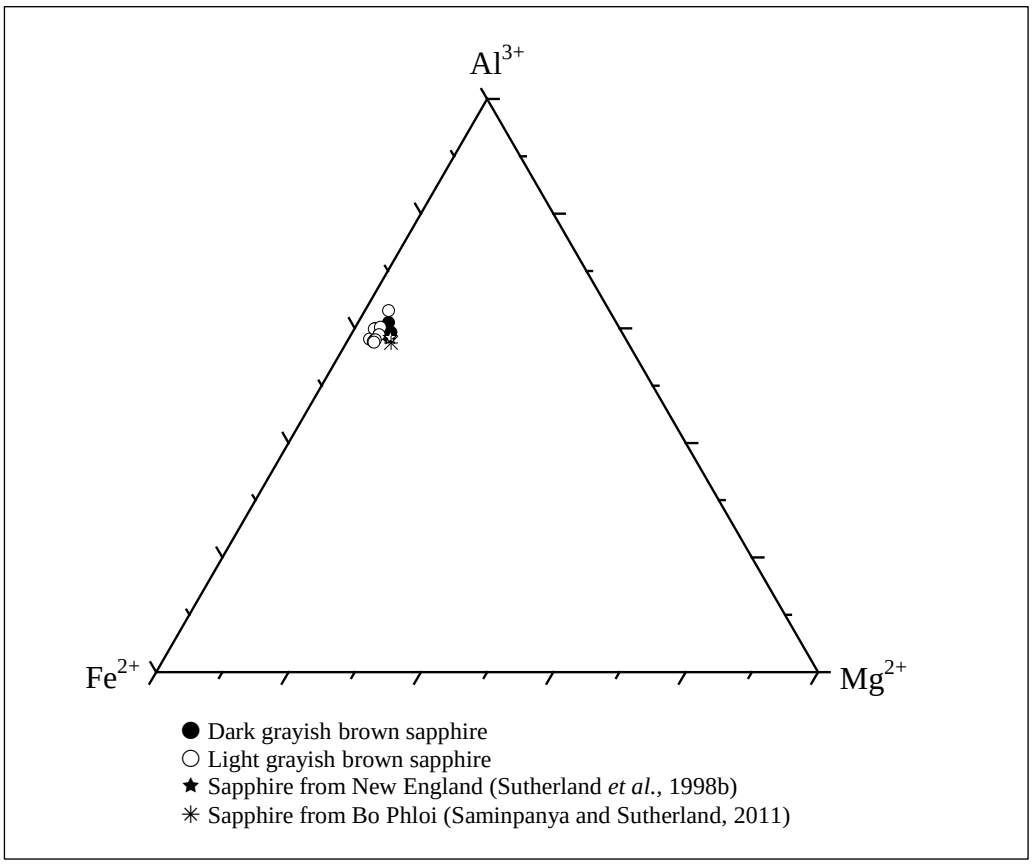

Figure 2-15 Ternary Al-Fe^{2+}-Mg plots of compositions of spinel inclusions found in Bo Phloi sapphires compared to spinel inclusion in sapphire from New England, Australia and Bo Phloi, Thailand.

Table 2-4 Representative EPMA analyses of **spinel inclusions** in Bo Phloi sapphires *(n.a. = not analyzed).*

Mineral phase Analysis (wt%)	Grayish brown sapphire										New England inclusion	Bo Phloi inclusion	alluvial Bo Phloi
	Dark Gray				Light Gray						(Sutherland *et al*., 1998b)	(Saminpanya and Sutherland, 2011)	(Saminpanya and Sutherland, 2008)
	1B3ia2-1	1B3ia2	1B3ia1	2DGB5b-1	3LGD4a-2	3LGD4b	3LGD4c	3LGD4c-1	3LGD4d	3LGD4d-1			
SiO_2	0.03	0.02	0.01	0.09	0.01	0.00	0.00	0.00	0.00	0.00	0.00	0.40	0.30
TiO_2	0.07	0.11	0.15	0.09	0.18	0.17	0.18	0.19	0.16	0.20	0.13	n.a.	0.56
Al_2O_3	59.52	59.64	59.25	60.08	59.02	58.34	58.78	56.68	57.34	56.87	57.04	56.70	59.10
Cr_2O_3	0.16	0.16	0.00	0.00	0.05	0.02	0.07	0.03	0.00	0.00	0.00	0.80	0.00
FeO	35.39	35.52	35.98	33.88	36.58	36.14	35.19	37.68	35.92	37.16	34.66	35.30	19.87
MnO	0.22	0.22	0.24	1.39	0.85	0.98	0.88	0.92	0.99	0.96	0.48	0.90	n.a.
MgO	5.85	5.89	5.90	4.56	3.01	4.19	3.76	3.89	4.18	4.07	6.09	6.70	18.95
ZnO	0.14	0.12	0.00	0.18	0.03	0.02	0.03	0.04	0.03	0.03	0.69	n.a.	0.00
CaO	0.00	0.00	0.00	0.01	0.00	0.00	0.00	0.00	0.00	0.00	0.00	n.a.	n.a.
Total	101.36	101.69	101.53	100.28	99.74	99.85	98.89	99.44	98.62	99.29	99.09	100.80	98.78
32 (O)													
Si	0.007	0.003	0.001	0.020	0.003	0.000	0.000	0.000	0.000	0.000	0.000	0.090	0.064
Ti	0.011	0.018	0.026	0.016	0.031	0.029	0.032	0.033	0.027	0.035	0.022	-	0.089
Al	15.570	15.557	15.510	15.848	15.840	15.635	15.825	15.418	15.588	15.451	15.364	15.032	14.781
Cr	0.028	0.029	0.000	0.000	0.010	0.004	0.013	0.006	0.000	0.000	0.000	0.142	0.000
Fe^{2+}	6.157	6.159	6.106	6.233	6.881	6.482	6.627	6.615	6.453	6.530	5.846	6.162	2.332
Fe^{3+}	0.412	0.415	0.577	0.107	0.086	0.391	0.097	0.658	0.474	0.634	0.778	0.478	1.194
Mn	0.041	0.041	0.045	0.264	0.164	0.189	0.169	0.180	0.193	0.187	0.093	0.171	-
Mg	1.934	1.942	1.953	1.522	1.023	1.419	1.282	1.340	1.439	1.399	2.075	2.247	5.996
Zn	0.023	0.020	0.000	0.029	0.005	0.003	0.004	0.007	0.006	0.005	0.116	-	0.000
Ca	0.000	0.000	0.000	0.001	0.000	0.000	0.000	0.000	0.000	0.000	0.000	-	-
Total*	24.183	24.185	24.218	24.040	24.042	24.151	24.049	24.255	24.179	24.240	24.295	24.323	24.456
$\sum R^{2+}$	8.155	8.163	8.105	8.050	8.073	8.093	8.083	8.141	8.090	8.121	8.130	8.581	8.328
$\sum R^{3+}$	16.028	16.022	16.113	15.991	15.969	16.059	15.966	16.114	16.089	16.119	16.165	15.742	16.128

$\sum R^{2+} = Fe^{2+}+Mn+Mg+Zn+Ca$, $\sum R^{3+} = Si+Ti+Al+Cr+Fe^{3+}$

Ilmenite: ilmenite inclusions are relatively rare in all sample varieties of Bo Phloi sapphires. However, some micro-sized ilmenites are found in these sapphires as presented by BSI images in Figure 2-16.

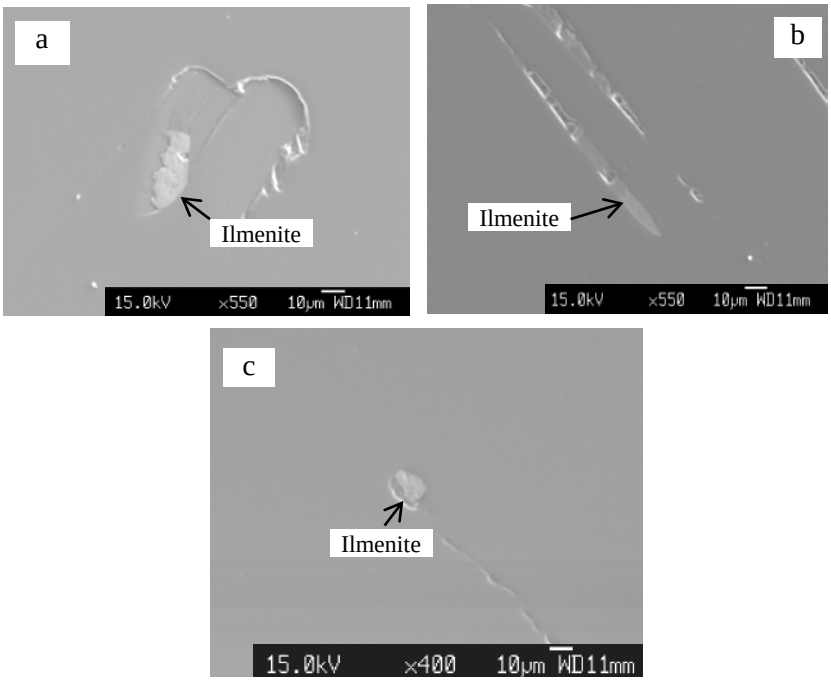

Figure 2-16 Back scattered electron images (BSI) of micro-sized ilmenite inclusions in Bo Phloi sapphires: (a, b) dark grayish brown sapphires; (c) light blue sapphire.

Although, EPMA analyses of ilmenite inclusions are rather poor qulity due to their very small sizes. Some selected EPMA analyses of ilmenite inclusion are exhibited in Table 2-5. Ilmenite inclusions show a similar composition in both dark grayish brown and light blue sapphires. Their compositions vary in narrow ranges of 49-50% TiO_2, 35-41% FeO and 6-10% MnO with traces of MgO; except one ilmenite inclusion in a blue Bo Phloi sapphire *(3LBA2d)* sample shows relatively low TiO_2 (45.73%), low FeO (27.64%) and higher MnO (17.59%). Chemical formular of these ilmenite inclusions could be expressed as $(Fe, Mn, Mg)^{2+}$ $(Ti, Fe)^{3+}O_3$ with a certain amount of Mn and lesser amount of Mg substitution in octahedral site. It therefore should be classified as manganiferous ilmenite (see Figure 2-17). A mangeniferous ilmenite inclusion of similar composition was also found in grayish brown Bo Phloi sapphire by Pisutha-Arnond *et al.* (1999). Manganiferous ilmenite commonly occurs in granitic rocks, and also in carbonatites which may contain anomalous niobium (Deer *et al.*, 1992). Furthermore, most ilmenite inclusions in Bo Phloi sapphires

exhibit slightly Fe-richer than those found in the BGY sapphires (~32% FeO) of inclusion in sapphire from New England, Australia (Sutherland *et al.*, 1998b).

Table 2-5 Representative EPMA analyses of **ilmenite inclusions** in Bo Phloi sapphires *(n.a. = not analyzed)*.

Mineral phase Analysis (wt%)	Grayish brown sapphire		Blue sapphire		New England
	Dark Gray		Light Blue		(Sutherland *et al.*, 1998b)
	2DGA3c-2	2DGA4a-1	3LBA2a-1	3LBA2d	
SiO_2	0.02	0.00	0.05	0.00	0.70
TiO_2	49.45	50.29	49.63	45.73	59.04
Al_2O_3	1.30	0.32	0.76	6.90	0.45
FeO	41.02	39.02	35.79	27.64	32.05
MnO	6.88	8.46	10.80	17.59	0.40
MgO	0.69	0.24	0.53	0.98	1.85
ZnO	0.04	0.01	n.a.	n.a.	0.00
CaO	0.00	0.00	0.00	0.00	0.00
Total	99.40	98.34	97.56	98.84	94.49
6 (O)					
Si	0.001	0.000	0.003	0.000	0.035
Ti	1.893	1.950	1.931	1.713	2.204
Al	0.078	0.020	0.047	0.405	0.026
Fe^{2+}	1.547	1.563	1.422	0.904	2.135
Fe^{3+}	0.199	0.119	0.127	0.248	-
Mn	0.297	0.369	0.473	0.742	0.017
Mg	0.052	0.019	0.041	0.073	0.137
Zn	0.002	0.000	-	-	0.000
Ca	0.000	0.000	0.000	0.000	0.000
Total*	4.067	4.040	4.043	4.084	3.748
ΣR^{2+}	1.897	1.951	1.935	1.718	2.289
ΣR^{3+}	2.169	2.089	2.105	2.366	1.425

$\Sigma R^{2+} = Fe^{2+}+Mn+Mg+Zn+Ca$,
$\Sigma R^{3+} = Si+Ti+Al+Fe^{3+}$

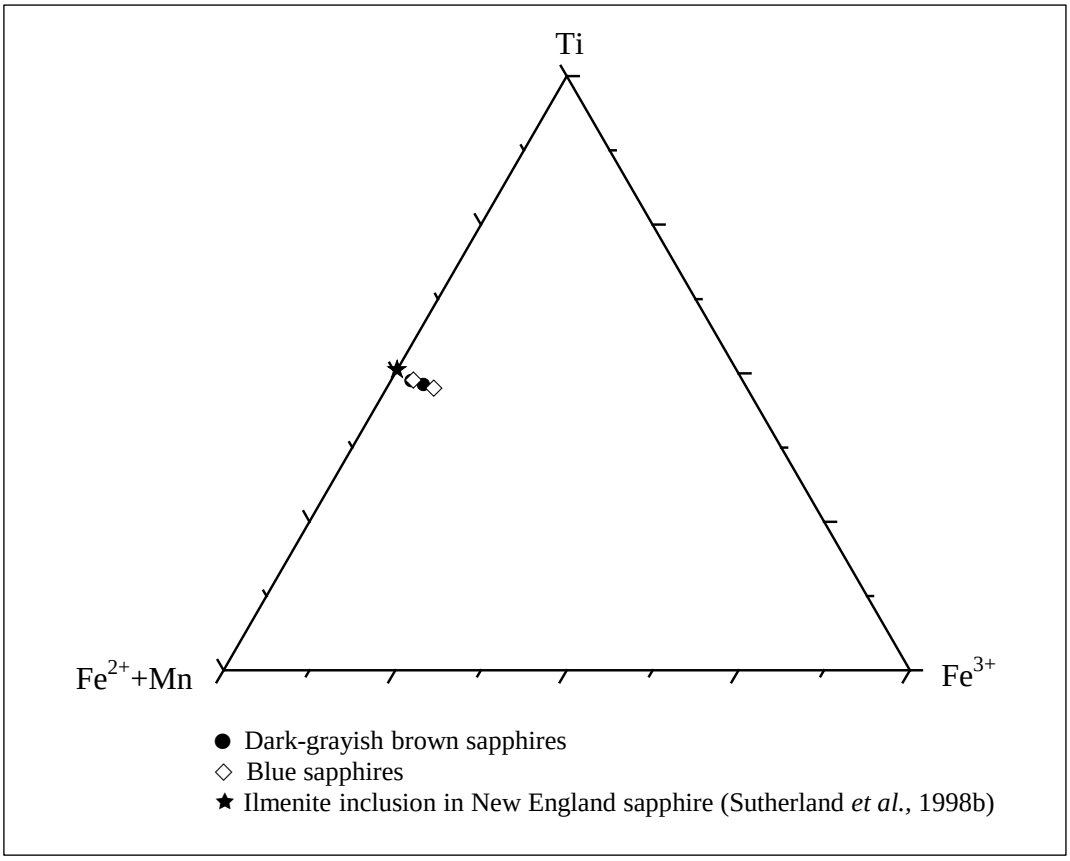

Figure 2-17 Ternary Ti-(Fe^{2+}+Mn)-Fe^{3+} plots of compositions of ilmenite inclusions found in Bo Phloi sapphires.

Pyroxene: pyroxene inclusions are found in both grayish brown and blue sapphires. These minerals are rather small in sizes, a micro-sized pyroxene inclusion found in dark grayish brown sapphire is displayed as BSI image (Figures 2-18) and more images are listed in Appendix A.

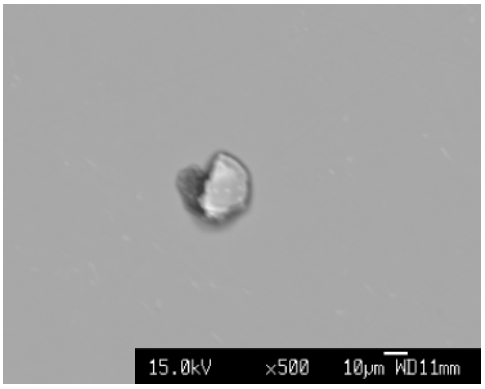

Figure 2-18 Back scattered electron image (BSI) of pyroxene inclusion in the dark grayish brown sapphire.

In general, the chemical compositions of these pyroxene inclusions are fairly similar in both varieties; they are composed significantly of 60-65% SiO_2, 30-35% MgO. However, the variation of Al_2O_3 contents (up to about 7%) may be detected in these analyses. Based on the Al_2O_3 contents can divide these pyroxene analyses into two groups. The first group consists of lower Al_2O_3 content (less than 1 wt%, see Table 2-6) whereas the second one contains higher Al_2O_3 (see Table 2-7). The calculated formulae of both pyroxene groups contain significantly high Si and slightly low Mg, although they fit quite well with enstatite composition (see Figure 2-19). Moreover, total cations calculated on basic of 6 oxygen atoms, of all analyses are lower than 4. This may suggest presence of vacancies in the cation sites. Excess of Si^{4+} and the substitution of Mg^{2+} by Al^{3+} may lead to charge compensation in cation sites by such vacancy. Considering the chemical compositions in Table 2-6, the amount of Si_{excess} are almost equal to the nearby vacancy occurred in the enstatite structure. This study demonstrates that Si_{excess} incorporation into M site in the enstatite structure is charge-balanced by Mg^{2+} vacancies. In contrast, the relationship of the Si_{excess} and vacancy are ambiguous when the higher Al_2O_3 contents detected in enstatite analyses. The higher Al_2O_3 contents may obtain from the host of sapphires during analytical process because the small grains of these inclusions. Nevertheless, both compositions of Si-rich enstatite inclusions seem to be derived from contaminated melts of mafic and felsic contents which imply origined from contact reaction zone of crustral materials; richer in both Si and Al, and mantle-derived basaltic magma.

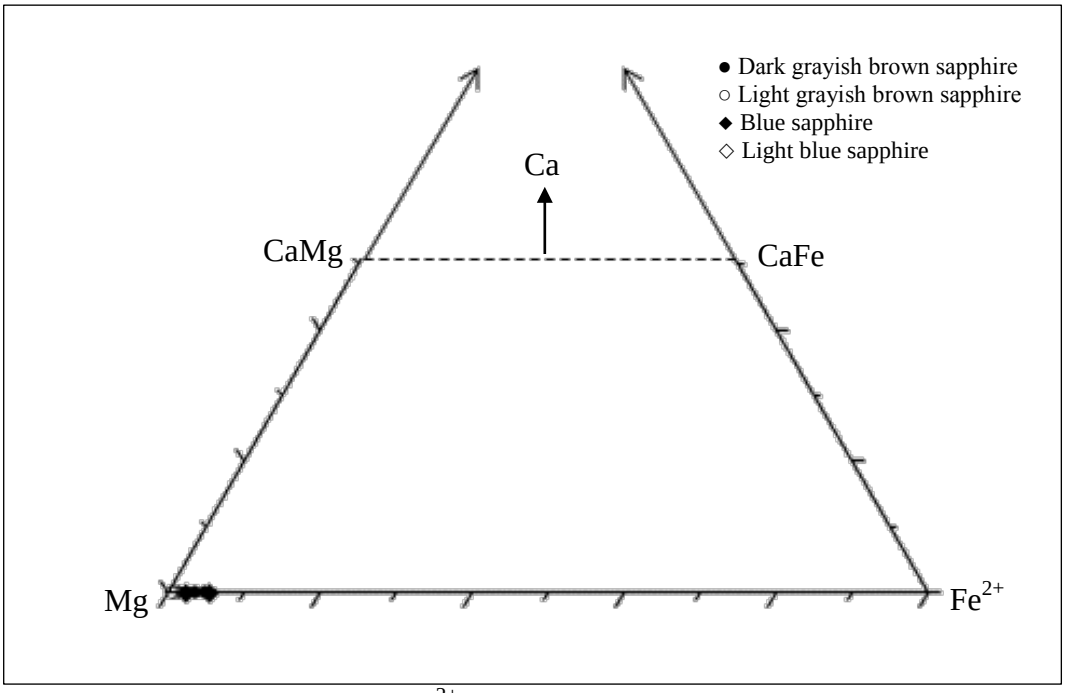

Figure 2-19 Quadrilateral Ca-Mg-Fe^{2+} plots of pyroxene inclusions found in Bo Phloi sapphires (modified after Lindsley, 1983).

Table 2-6 Representative EPMA analyses of **pyroxene inclusions** in Bo Phloi sapphires *(n.a. = not analyzed).*

Mineral phase	Grayish brown sapphire							Blue sapphire
Analysis (wt%)	Dark Gray					Light Gray		Blue
	2DGA7 c-2	2DGA7 c-3	2DGB2 a-2	2DGB9 c-2	2DGB10 e-1	3LGC8b -1	3LGC8 b-2	3BC2a
SiO_2	63.28	65.23	60.30	61.43	61.30	64.53	64.77	64.73
TiO_2	0.06	0.00	0.03	0.03	0.02	0.02	0.02	0.02
Al_2O_3	0.35	0.21	0.09	0.20	0.62	0.31	0.40	0.15
Cr_2O_3	0.05	0.00	0.04	0.00	0.07	0.04	0.01	0.00
FeO	3.95	0.86	3.26	6.36	5.93	1.46	0.50	1.30
MnO	0.00	0.01	0.00	0.00	0.01	0.00	0.02	0.03
MgO	31.21	33.13	35.69	30.93	31.21	32.58	33.01	31.75
NiO	0.04	0.00	0.01	0.00	0.00	n.a.	n.a.	0.05
CaO	0.02	0.01	0.02	0.00	0.03	0.01	0.02	0.00
Na_2O	0.04	0.00	0.02	0.00	0.01	0.03	0.06	0.01
K_2O	0.03	0.01	0.01	0.01	0.02	0.01	0.03	0.00
Total	99.02	99.45	99.47	98.97	99.22	98.99	98.84	98.05
6 (O)								
Si	2.142	2.163	2.046	2.110	2.098	2.157	2.159	2.179
Ti	0.001	0.000	0.001	0.001	0.000	0.001	0.000	0.000
Al	0.014	0.008	0.003	0.008	0.025	0.012	0.016	0.006
Cr	0.001	0.000	0.001	0.000	0.002	0.001	0.000	0.000
Fe	0.112	0.024	0.092	0.183	0.170	0.041	0.014	0.037
Mn	0.000	0.000	0.000	0.000	0.000	0.000	0.001	0.001
Mg	1.575	1.638	1.805	1.584	1.592	1.624	1.640	1.593
Ni	0.001	0.000	0.000	0.000	0.000	-	-	0.001
Ca	0.001	0.000	0.001	0.000	0.001	0.000	0.001	0.000
Na	0.002	0.000	0.001	0.000	0.001	0.002	0.004	0.000
K	0.001	0.000	0.001	0.000	0.001	0.000	0.001	0.000
Total*	3.851	3.833	3.952	3.886	3.889	3.837	3.835	3.818
ΣVacancy (□)	0.149	0.167	0.048	0.114	0.111	0.163	0.165	0.182
Si_{excess}	0.142	0.163	0.046	0.110	0.098	0.157	0.159	0.179
Charge balanced	3.982	3.998	3.990	3.997	3.989	3.992	3.990	3.993

Enstatite formula = $(Mg, Fe, Al, Si_{excess})_2Si_2O_6 = (M2)_2Si_2O_6$
*Charge balanced = (Mg*2+Fe*2+Al*3+Si_{excess}*4)*

Table 2-7 Representative EPMA analyses of **pyroxene inclusions** in Bo Phloi sapphires *(n.a. = not analyzed).*

Mineral phase Analysis (wt%)	Grayish brown sapphire									Blue sapphire
	Dark Gray			Light Gray						Blue
	2DGA 7b-1	2DGA 7a-2	2DG B8d	3LGC 4b-1	3LGC 3c-1	3LGC 6c-1	3LGD 10a	3LG D6c	3LGD 6d-3	3BA9b
SiO_2	60.69	60.64	62.07	61.85	60.04	62.55	62.47	60.10	61.85	60.28
TiO_2	0.00	0.03	0.01	0.01	0.02	0.05	0.00	0.00	0.01	0.04
Al_2O_3	2.15	4.08	5.98	2.75	5.76	5.57	4.76	3.86	6.97	2.92
Cr_2O_3	0.02	0.02	0.01	0.03	0.05	0.00	0.00	0.00	0.07	0.15
FeO	2.39	4.90	3.41	4.10	4.42	0.41	1.42	1.47	0.30	3.50
MnO	0.00	0.02	0.00	0.04	0.00	0.00	0.00	0.01	0.00	0.00
MgO	35.20	29.37	28.16	30.59	28.96	30.43	30.27	33.73	30.27	33.69
NiO	n.a.	n.a.	n.a.	n.a.	n.a.	n.a.	n.a.	n.a.	n.a.	0.00
CaO	0.03	0.01	0.02	0.02	0.00	0.02	0.01	0.01	0.01	0.00
Na_2O	0.02	0.01	0.03	0.01	0.01	0.00	0.01	0.02	0.02	0.03
K_2O	0.03	0.02	0.00	0.00	0.00	0.00	0.00	0.00	0.03	0.06
Total	100.53	99.10	99.69	99.39	99.25	99.03	98.95	99.21	99.53	100.66
6 (O)										
Si	2.026	2.061	2.073	2.088	2.033	2.076	2.086	2.019	2.044	2.019
Ti	0.000	0.001	0.000	0.000	0.000	0.001	0.000	0.000	0.000	0.001
Al	0.085	0.164	0.235	0.110	0.230	0.218	0.187	0.153	0.272	0.115
Cr	0.000	0.001	0.000	0.001	0.001	0.000	0.000	0.000	0.002	0.004
Fe	0.067	0.139	0.095	0.116	0.125	0.011	0.040	0.041	0.008	0.098
Mn	0.000	0.001	0.000	0.001	0.000	0.000	0.000	0.000	0.000	0.000
Mg	1.751	1.488	1.402	1.540	1.462	1.506	1.507	1.689	1.491	1.682
Ni	-	-	-	-	-	-	-	-	0.000	0.000
Ca	0.001	0.001	0.001	0.001	0.000	0.001	0.000	0.000	0.000	0.000
Na	0.001	0.001	0.002	0.001	0.001	0.000	0.001	0.001	0.001	0.002
K	0.001	0.001	0.000	0.000	0.000	0.000	0.000	0.000	0.001	0.002
Total*	3.933	3.857	3.809	3.857	3.852	3.814	3.821	3.905	3.820	3.923
ΣVacancy (□)	0.067	0.143	0.191	0.143	0.148	0.186	0.179	0.095	0.180	0.077
Si_{excess}	0.026	0.061	0.073	0.088	0.033	0.076	0.086	0.019	0.044	0.019
Charge balanced	3.994	3.992	3.994	3.993	3.994	3.994	3.998	3.997	3.990	3.980

Enstatite formula = (Mg, Fe, Al, Si_{excess})$_2Si_2O_6$ = (M2)$_2Si_2O_6$
*Charge balanced = (Mg*2+Fe*2+Al*3+Si_{excess}*4)*

Garnet: garnet inclusions are mainly observed in grayish brown sapphire. Representative EPMA analyses of these minerals are summarized in Table 2-8 and an extended set of acceptable analyses is listed in Appendix C. Their oxide compositions fall in narrow ranges of 42-43% SiO_2, 23-25% Al_2O_3, 20-21% MgO and 12-14% FeO. Chemical compositions of all inclusions fall within the range of almandine-pyrope series with high $Mg/(Mg+Fe^{2+})$ ratios ranging between 0.72-0.75 Mg# that are similar to those of garnet xenocrysts found in Nong Bon basalt of Trat ruby deposit reported by Sutthirat *et al.* (2001) and garnet inclusion in Bo Rai ruby (0.81 Mg#) (Saminpanya and Sutherland, 2011). Both ruby deposits are situated in the eastern Thailand.

Although, garnet inclusions in Bo Phloi sapphies have high Mg proportion in their formula similar to those of garnet xenocryst in Nong Bon basalt and garnet inclusion in Bo Rai ruby, inclusions in Bo Phloi sapphires appear to lack Ca component (see Figure 2-20). These garnet inclusions are characterized by $Py_{72.30\text{-}75.45}Alm_{24.50\text{-}27.53}Gro_{0.05\text{-}0.17}$. These compositions indicate rather mafic composition. Hence they are pyrope-almandine solid solution in which the composition is richer towards pyrope end member (or abbreviated as pyr>alm garnet).

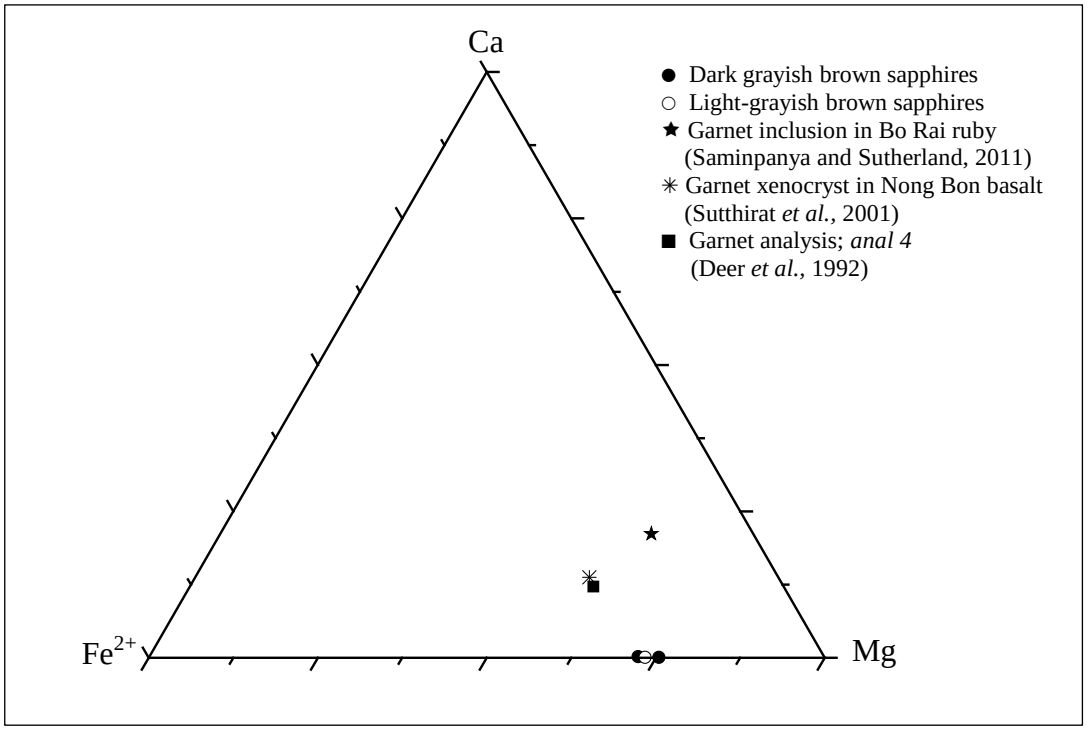

Figure 2-20 Ternary Ca-Fe^{2+}-Mg plots of compositions of garnet inclusions found in Bo Phloi sapphires.

Table 2-8 Representative EPMA analyses of **garnet inclusions** in Bo Phloi sapphires *(n.a. = not analyzed).*

Mineral phase Analysis (wt%)	Grayish brown sapphire			Bo Rai inclusion (Saminpanya and Sutherland, 2011)	Nong Bon xenocryst (Sutthirat *et al.*, 2001)	Pyrope (anal.4) (Deer *et al.*, 1992)
	Dark Gray		Light Gray			
	2DGA8g	2DGB1a	3LGD6c-3	BREP1-GRT1	NB-5A	
SiO_2	42.12	42.07	42.80	41.90	40.62	41.52
TiO_2	0.06	0.01	0.01	n.a.	0.52	n.a.
Al_2O_3	24.43	25.14	23.88	23.40	22.48	23.01
Cr_2O_3	0.03	0.04	0.04	n.a	0.05	0.22
FeO	12.27	13.58	13.32	7.70	14.08	14.08
MnO	0.00	0.01	0.02	0.20	0.37	0.33
MgO	21.21	20.00	20.68	18.20	16.34	16.64
CaO	0.02	0.07	0.03	8.40	5.35	4.71
Na_2O	n.a.	n.a.	n.a.	0.40	n.a.	n.a.
Total	100.13	100.94	100.78	100.20	99.81	100.51
24 (O)						
Si	5.966	5.942	6.046	5.975	5.944	6.007
Ti	0.006	0.001	0.001	-	0.057	-
Al	4.079	4.185	3.975	3.933	3.877	3.923
Cr	0.003	0.005	0.004	-	0.006	0.025
Fe	1.454	1.604	1.573	0.918	1.723	1.703
Mn	0.000	0.002	0.003	0.024	0.046	0.040
Mg	4.478	4.212	4.356	3.869	3.565	3.589
Ca	0.003	0.010	0.005	1.283	0.839	0.730
Na	-	-	-	0.111	-	-
Total*	15.988	15.962	15.963	16.003	16.057	16.019
$\sum R^{2+}$	5.935	5.828	5.936	6.095	6.172	6.063
$\sum R^{3+}$	4.087	4.191	3.980	3.933	3.940	3.949
$Mg/(Mg+Fe^{2+})$	0.75	0.72	0.73	0.81	0.67	0.68

$\sum R^{2+} = Fe^{2+}+Mn+Mg+Ni+Ca$, $\sum R^{3+} = Ti+Al+Cr$

Sapphirine: is comparatively rare inclusion in Bo Phloi sapphire. A few sapphirine inclusions with acceptable compositions are obtained in this study (Table 2-9). Table 2-9 also displays compositions of sapphirine inclusions occurred in Bo Na Wong ruby sample *NWEP9-SPR3* reported by Saminpanya and Sutherland (2011) and sample *NWEP-9* reported by Sutthirat *et al.* (2001). Bo Na Wong ruby deposit is situated in basaltic terrain of eastern Thailand. Sapphirine inclusions in the Bo Phloi sapphire contain 2.07-2.41 Si p.f.u. and 7.68-9.04 Al p.f.u., with a narrow range of $Mg/(Mg+Fe^{2+})$ ratios (0.98-0.99). Their $Mg/(Mg+Fe^{2+})$ values are slightly higher than those of sapphirine inclusions in Bo Na Wong ruby (Sutthirat *et al.*, 2001; Saminpanya and Sutherland 2011).

Sapphirine is a comparatively rare mineral, and occurs characteristically in high grade, aluminium-rich, silica-poor, regional and contact metamorphic rocks (Deer *et al.,* 1992). Sapphirine is a known inclusion in a ruby from Bo Rai (Koivula, 1987). In addition, Sutherland and Coenraads (1996) and Sutherland *et al.* (1998b) reported sapphirine co-existing with spinel in pink sapphire and ruby from basaltic terrains from Australia. These authors suggested a crystallization temperature of 780–940 ºC for the aggregates and reactions with the host magma at over 1000 ºC. Therefore, the presence of sapphirine inclusions reported in this study may indicate that the Bo Phloi sapphires crystallized probably in high temperature condition of regional or contact metamorphism.

Table 2-9 Representative EPMA analyses of **sapphirine inclusions** in Bo Phloi sapphires *(n.a. = not analyzed).*

Mineral phase	Grayish brown sapphire	Blue sapphire	Bo Na Wong inclusion (Saminpanya and Sutherland, 2011)	Bo Na Wong inclusion (Sutthirat *et al.*, 2001)
Analysis (wt%)	Light Gray	Blue		
	3LGD6d-2	3BB8b-1	NWEP9-SPR3	NWEP-9
SiO_2	20.87	18.32	13.80	13.79
TiO_2	0.06	0.04	n.a.	0.00
Al_2O_3	56.50	67.94	62.90	62.91
Cr_2O_3	0.00	0.00	0.20	0.24
FeO	0.38	0.47	3.10	3.07
MnO	0.01	0.00	0.20	0.21
MgO	20.95	13.30	19.00	18.99
CaO	0.02	0.05	0.10	0.11
Na_2O	0.06	0.00	n.a.	n.a.
K_2O	0.04	0.00	n.a.	n.a.
Total	98.89	100.12	99.30	99.32
20 (O)				
Si	2.407	2.069	1.621	1.620
Ti	0.005	0.004	-	0.000
Al	7.682	9.043	8.709	8.710
Cr	0.000	0.000	0.019	0.022
Fe	0.036	0.044	0.305	0.302
Mn	0.001	0.000	0.020	0.021
Mg	3.604	2.239	3.328	3.326
Ca	0.003	0.006	0.013	0.014
Na	0.012	0.000	-	-
K	0.006	0.000	-	-
Total*	13.757	13.406	14.015	14.014
$\sum R^{2+}$	3.644	2.289	3.665	3.662
$Mg/(Mg+Fe^{2+})$	0.99	0.98	0.92	0.92

$\sum R^{2+} = Fe^{2+}+Mn+Mg+Ni+Ca$

Mica: mica inclusions are present in only dark grayish brown sapphire varieties; however, its softness and perfect cleavage cause poor polished surface. Only a few analyses from particularly dark grayish sapphire are acceptable and shown in Table 2-10. In addition, the Raman spectrum of this inclusion is displayed in Figure 2-21.

Table 2-10 Representative EPMA analyses of **mica and staurolite inclusions** in Bo Phloi sapphires *(n.a. = not analyzed).*

Mineral phase	Mica			Staurolite	
Analysis (wt%)	Grayish brown sapphire			Grayish brown sapphire	Deer
	Dark Gray			Light Gray	*et al.*, (1992)
	1A3ia2-1	1A3ia3-3		3LGC9b-1	anal. 1
SiO_2	36.21	38.02		28.67	27.22
TiO_2	2.83	2.93		0.00	0.56
Al_2O_3	28.28	25.64		58.92	54.16
Cr_2O_3	n.a.	n.a.		0.03	n.a.
FeO	10.18	9.77		0.31	13.78
MnO	0.07	0.05		0.00	0.23
MgO	13.38	13.40		12.04	2.34
CaO	0.00	0.00		n.a.	n.a.
Na_2O	0.07	0.07		n.a.	n.a.
K_2O	6.34	7.48		n.a.	n.a.
Total	97.35	97.37		99.97	98.29
24 (O)			48 (O)		
Si	5.456	5.745		7.657	7.860
Ti	0.320	0.333		0.000	0.122
Al	5.021	4.567		18.544	18.431
Cr	-	-		0.005	-
Fe^{2+}	0.309	0.153		0.069	3.327
Fe^{3+}	0.974	1.082		0.000	0.000
Mn	0.009	0.007		0.000	0.056
Mg	3.005	3.019		4.793	1.007
Ca	0.000	0.000		-	-
Na	0.019	0.021		-	-
K	1.218	1.441		-	-
Sum	16.331	16.369		31.068	30.803
∑Si+Al	8.000	8.000	$\sum R^{2+}$	4.862	4.391
∑R	7.094	6.907	$\sum R^{3+}$	18.550	18.552
∑Alkali	1.237	1.462			

$\Sigma R = Ti+Al_{excess}+Fe^{2+}+Fe^{3+}+Mn+Mg$, $\Sigma Alkali = Ca+Na+K$

$\Sigma R^{2+} = Fe^{2+}+Mn+Mg+Ca$, $\Sigma R^{3+} = Ti+Al+Cr+ Fe^{3+}$

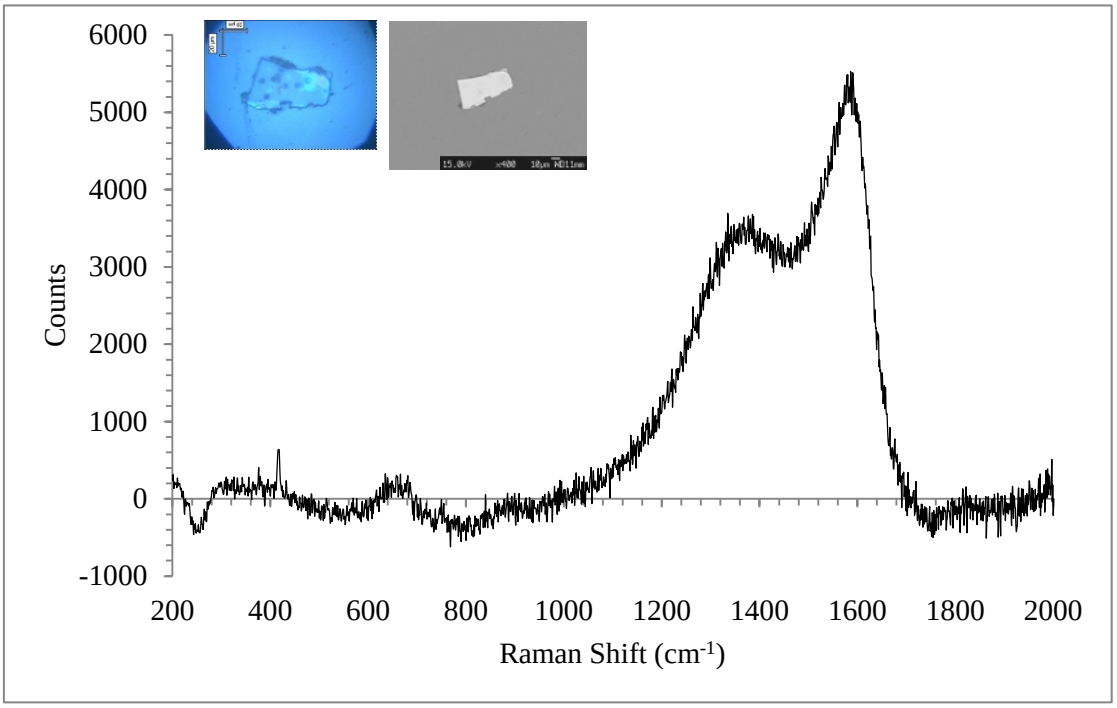

Figure 2-21 Raman spectrum of a mica inclusion found in the sample *1A3ia2-1* of the dark grayish brown sapphire.

As shown in Table 2-10, major compositions of both analyses are about 36-38% SiO_2, 29-30% Al_2O_3, 9-10% FeO, ~13% MgO, 6-7% K_2O and ~3% TiO_2. They fall within the ranges of mica compositions reported by Deer *et al.* (1992), although these samples show relatively lower MgO contents. However, the chemical compositions of these mica inclusions seem to be in the biotite-phlogospite range rather than in the muscovite range. In general, biotite-phlogospite is formed under a wide range of temperature and pressure conditions, besides, it occurs abundantly in many contact and regionally metamorphosed sediments. Among the intrusive igneous rocks, it occurs especially common in granites, granite pegmatites and nepheline-syenites (Deer *et al.*, 1992).

Staurolite: in this study, only one small staurolite inclusion is recognized in a light grayish brown sample. The analytical data of this mineral inclusion (Table 2-10) however do not fit precisely the typical formula, $(Fe, Mg)_2Al_9(Si, Al)_4O_{20}(O, OH)_4$, of staurolite. However, this is the first time that staurolite has been identified as a mineral inclusion in the Bo Phloi sapphire.

In general, staurolite is a crucial assemblage of intermediate-high grade metamorphic rocks. It is also a common constituent of medium grade regionally metamorphosed argillaceous sediments, typically developed in rocks rich in alumina (Deer *et al.,* 1992). In addition, occurrence of staurolite was also reported as intergrowth with orthopyroxene and spinel in an ultra-high-temperature Al-Mg granulite (Belyanin *et al.*, 2010). Therefore, the presence of staurolite inclusion in this study may indicate that Bo Phloi sapphires possibly crystallized under a high temperature metamorphic condition.

Zircon: is also a common inclusion found in all color varieties of Bo Phloi sapphire. Among the micro-sized mineral inclusions found in Bo Phloi sapphires, zircon inclusions show the largest size of up to 200 μm across. Some BSI images of zircon inclusions are illustrated in Figure 2-22 and more images are reported in Appendix A.

Representative EPMA analyses of these inclusions are summarized in Table 2-11 and more analyses are reported in Appendix C. Their chemical compositions vary within a narrow range of 32.16-34.44% SiO_2, 60.79-66.18% ZrO_2 and slightly more variable range of 1.37-3.50% HfO_2. Zircon inclusions in blue sapphires contain slightly higher Hf than those of zircon inclusions in the grayish brown sapphires, particularly zircon inclusions in sample *3BC9a-1* (up to 3.50% HfO_2). However, they show rather uniform chemical compostions as plotted in the Si-Zr-Hf ternary diagram (Figure 2-23). In addition, zircon inclusions in Bo Phloi sapphire also shown somewhat higher HfO_2 content than that of alluvial zircon (0.81 wt% HfO_2) in Bo Phloi gem field reported by Sutthirat (2001), but similar to that of zircon inclusion (3.58 wt% HfO_2) from Ban Huai Sai sapphire, Laos (Sutherland *et al.*, 2002) (see Table 2-11). Ternary Si-Zr-Hf plots (Figure 2-23), show clearly variation of Hf contents increasing from alluvial Bo Phloi zircon toward zircon inclusions in grayish brown sapphire and blue sapphire, respectively; besides, high Hf content also present in zircon inclusion of blue sapphire from Laos.

The Bo Phloi Zircon inclusions in this study are compositionally higher HfO_2 content than those in alluvial Bo Phloi zircon reported by Sutthirat (2001) which indicating both zircons may be originated from a different origin. Chemical compositions of Bo Phloi zircon inclusions fall within the Hf-rich end for the zircon-

corundum co-crystallization series, which ranges HfO_2 1.30-3.50 wt%. The Hf contents of Bo Phloi zircons consistent with the amount of HfO_2 found in zircon inclusions within sapphire from other basaltic areas (*e.g.*,1.5 wt% HfO_2 from Lava Plains, Australia; Khao Wua, Thailand, through 2.6-3.2 wt% HfO_2 from New England, Austraria; Loch Roag, Scotland, to 3.6-3.8 wt% HfO_2 from Huai Sai, Laos; Wenchang, China) (Aspen *et al.*, 1990; Coenraads *et al.*, 1990; 1995; Guo *et al.*, 1996a, b; Sutherland *et al.*, 1998a; 2002). Wark and Miller (1993) reported that the Hf content in the zircon can roughly reflect degree of differentiation of parental melt. The high abundances of Hf of the Bo Phloi zircon inclusion suggest that the sapphire source was a highly evolved material. Moreover, trace and isotope analyses of zircon inclusions of Bo Phloi sapphires are reported in Chapter 4.

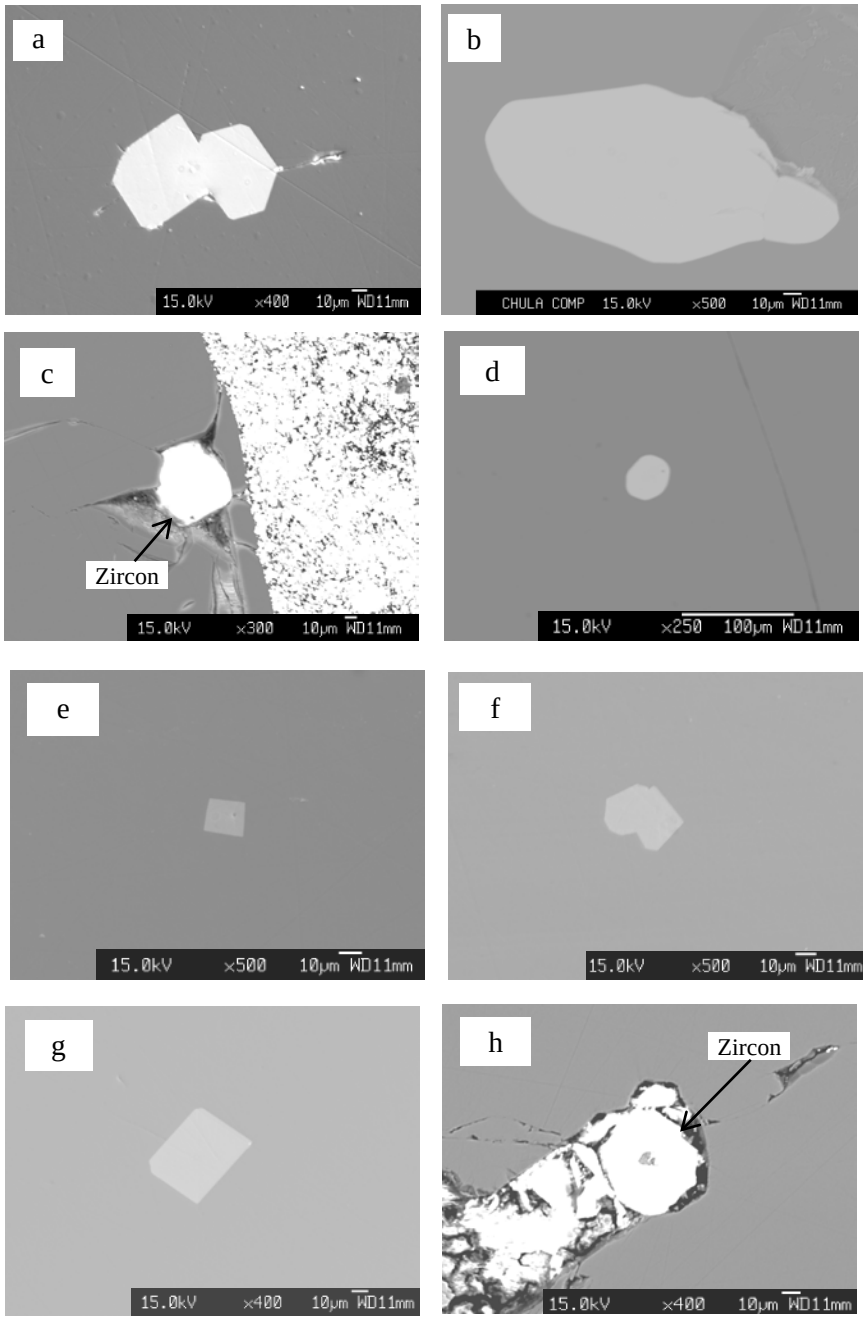

Figure 2-22 Back scattered electron images (BSI) of zircon inclusions in Bo Phloi sapphires: (a, b) dark grayish brown sapphires; (c, d) light grayish brown sapphires; (e, f) blue sapphires; (g, h) light blue sapphires.

Table 2-11 Representative EPMA analyses of **zircon inclusions** in Bo Phloi sapphires *(n.a. = not analyzed).*

Mineral phase	Zircon inclusion								Alluvial Bo Phloi zircon	Ban Huai Sai Zircon inclusion
Analysis (wt%)	Grayish brown sapphire				Blue sapphire					
	Dark Gray		Light Gray		Blue		Light Blue		(Sutthirat, 2001)	(Sutherland *et al*., 2002)
	1B3ib2	2DGC6a-REE2	3LGC1c-1	3LGC1d	3BC9a-1	3BC13a	3LBA7a	3LBC9a	KBPZ1-1	85N
SiO_2	33.08	32.49	34.22	33.08	34.14	34.44	34.10	33.83	31.57	31.23
ZrO_2	64.65	65.57	64.04	66.18	62.40	63.36	64.91	65.13	68.42	64.02
HfO_2	1.62	1.75	1.37	1.59	3.50	2.40	2.39	2.33	0.81	3.58
Al_2O_3	0.12	0.01	0.00	0.02	0.17	0.05	0.10	0.02	0.00	0.01
CaO	0.01	0.00	0.02	0.01	0.00	0.02	0.02	0.00	0.00	n.a.
FeO	0.06	0.06	0.03	0.00	0.04	0.06	0.02	0.05	0.00	0.06
Total	99.54	99.87	99.68	100.87	100.25	100.33	101.54	101.35	100.80	98.90
4 (O)										
Si	1.013	0.998	1.038	1.004	1.036	1.040	1.023	1.019	0.968	0.981
Zr	0.966	0.982	0.947	0.979	0.923	0.933	0.949	0.956	1.023	0.980
Hf	0.017	0.018	0.014	0.016	0.036	0.025	0.024	0.024	0.008	0.038
Al	0.004	0.000	0.000	0.001	0.006	0.002	0.004	0.001	0.000	-
Ca	0.000	0.000	0.001	0.000	0.000	0.001	0.001	0.000	0.000	0.000
Fe	0.002	0.001	0.001	0.000	0.001	0.002	0.001	0.001	0.000	0.002
Total*	2.002	2.001	2.001	2.000	2.002	2.002	2.001	2.001	2.000	2.001
Atomic%										
Si	50.8	49.9	51.9	50.2	51.9	52.1	51.2	51.0	48.4	49.1
Zr	48.4	49.1	47.4	49.0	46.3	46.7	47.6	47.8	51.2	49.0
Hf	0.8	0.9	0.7	0.8	1.8	1.2	1.2	1.2	0.4	1.9
Total**	100.0	100.0	100.0	100.0	100.0	100.0	100.0	100.0	100.0	100.0

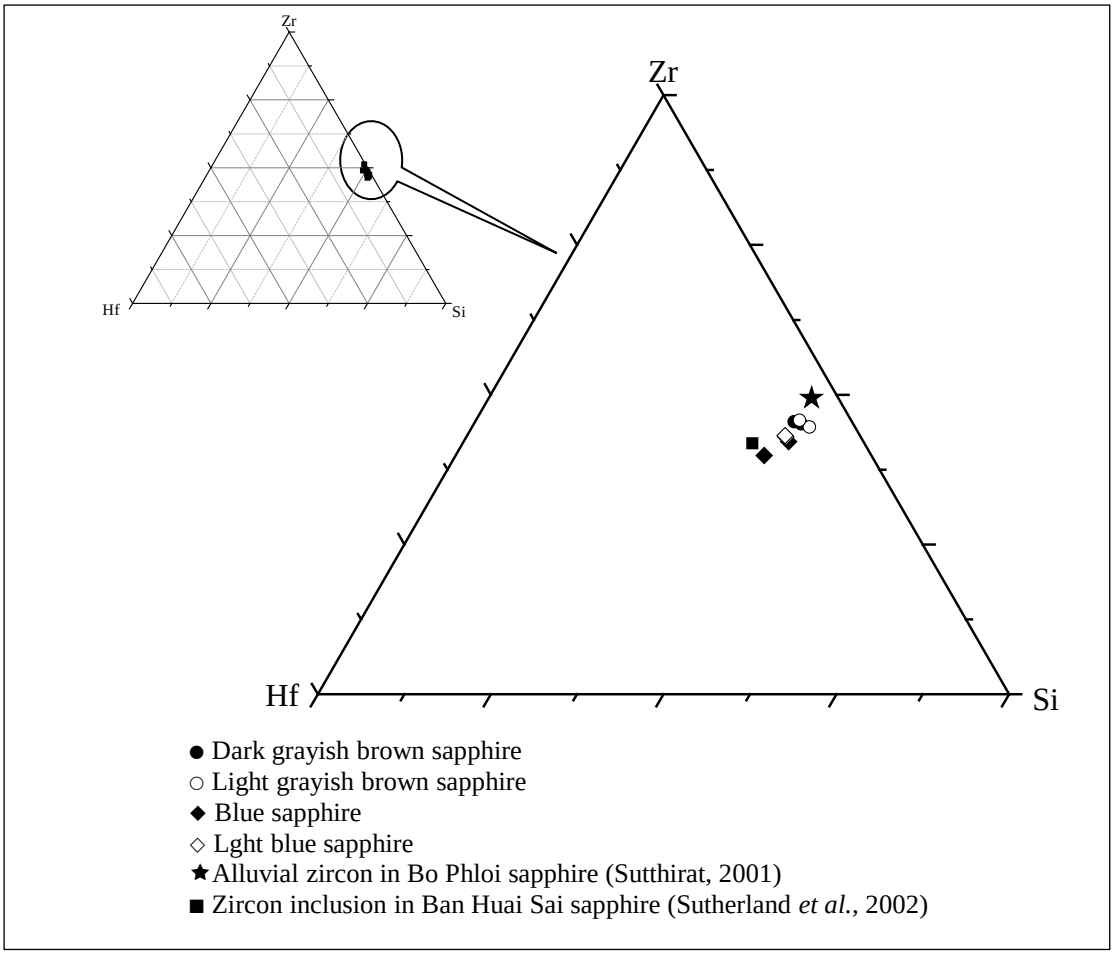

Figure 2-23 Ternary Si-Zr-Hf plots of zircon inclusions, and also additional analyses of alluvial zircon in Bo Phloi sapphire (Sutthirat, 2001) and zircon inclusion from Ban Huai Sai sapphire, Laos (Sutherland *et al.*, 2002).

Other Mineral Inclusions: because the occurrences of monazite inclusion in Bo Phloi sapphire were identified by Raman spectroscopic technique in this study (see Figure 2-25 and Appendix B) and also presented in previous reports (Intasopa *et al.*, 1998; Pisutha-Arnond *et al.*, unpublished data). EPMA method had been applied for these inclusions under this study but due to a certain limitation, the partial chemical analyses give unsatisfied results are displayed in Appendix C. However, the qualitative analyses of monazite inclusions were also analysed as the data tablulated in Table 2-12. As shown in the table, all analyses illustrate the similar elemental compositions which contain up to ~ 45 wt% Th along with Ce and La. Actually, their formula should be constrained by light rare earth phosphate [(LREE)PO_4]. These monazite inclusions are characterized about ($Th_{0.45-0.51}Ce_{0.24-0.28}La_{0.11-0.13}Pr_{0.07}Nd_{0.07}$)$PO_4$. These compositions suggest rather a Th-rich monazite phase. Monazite inclusion was also reported from basaltic sapphires such as Cyangugu District in SW Rwanda (Krzemnicki *et al*., 1996), Thailand and Combodia (Intasopa *et al.*, 1998) and Huai Sai in Laos (Singbamroong and Thanasuthipitak, 2004); however, all of these previous works were identified by the Raman technique. Monazite usually occurs as rare accessory mineral in granitic rocks, syenitic rocks and granitic pegmatites with greatly enrichment of Ce, La and Nd (Deer *et al.*, 1992). Moreover, the study of monazite geochronology will be reported in Chapter 4.

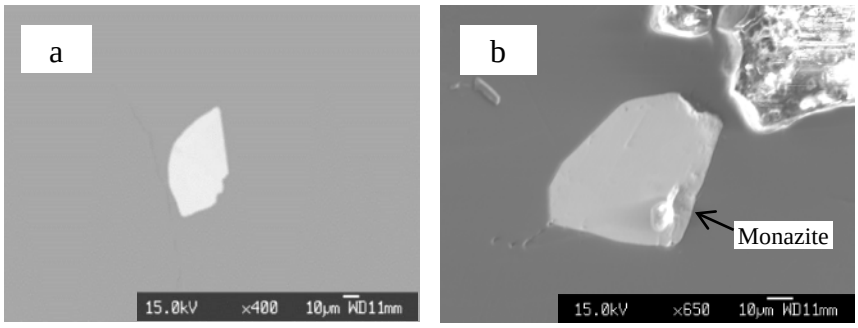

Figure 2-24 Back scattered electron images (BSI) of monazite inclusions in the dark grayish brown sapphires.

Table 2-12 Qualitative EPMA analyses of **monazite inclusions** in Bo Phloi sapphires.

Mineral phase	Grayish brown sapphire		
Analysis (wt%)	Dark Gray		
	2C9ia2	1C21b	1C22b
Si	3.51	4.39	3.88
P	10.56	8.63	10.07
Ca	0.54	-	0.55
La	10.68	9.57	11.29
Ce	22.52	20.59	23.97
Pr	5.41	6.16	6.99
Nd	6.25	5.91	6.63
Th	40.55	44.75	36.63
Total	100.00	100.00	100.00
Cation calculation			
P*	1.00	1.00	1.00
La	0.13	0.11	0.13
Ce	0.26	0.24	0.28
Pr	0.06	0.07	0.08
Nd	0.07	0.07	0.08
Th	0.47	0.51	0.43
Total*	2.00	2.00	2.00

P; when fix = 1 P p.f.u.*

Calcite is also recognized as inclusion in Bo Phloi sapphires. Because of the softness of calcite inclusions that makes it difficult to take a good polish on the host sapphire surface, reliable chemical compositions of this inclusion could not be obtained in this study. However, some analyses gave very high CaO content (up to 50% CaO; Appendix C) in some inclusions confirming the presence of calcite inclusions in the Bo Phloi sapphire. As stated earlier, calcite inclusion has been reported in Bo Phloi sapphire by Pisutha-Arnond *et al.* (unpublished data). Calcite may occur in certain alkaline igneous rocks, notably some nepheline-syenites (Deer *et al.*, 1992). Therefore, the finding of calcite inclusions in this study may support the evidence of nepheline-syenite origin of Bo Phloi sapphire.

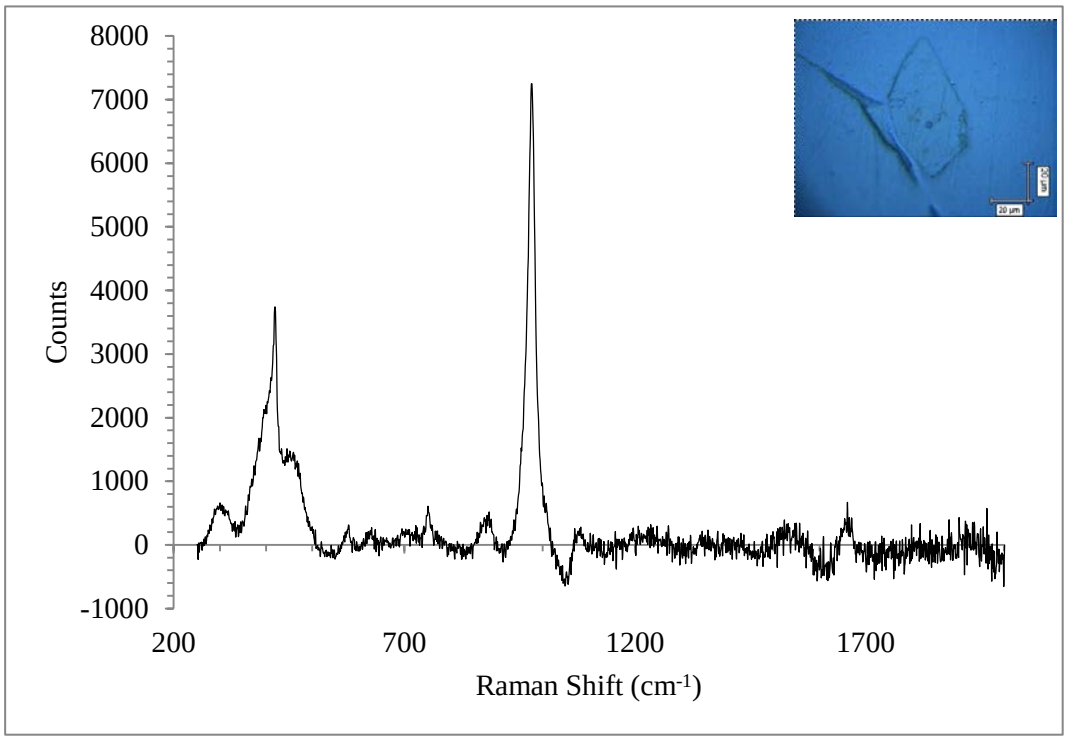

Figure 2-25 Raman spectrum of a monazite inclusion observed in sample *2C9ia2* of the dark grayish brown sapphire.

CHAPTER 3
SOUTHEAST ASIA SAPPHIRES

3.1 Introduction

Cenozoic basaltic volcanism is a notable feature of the Southeast Asia. Many gem corundum deposits are associated with these alkali basalts where sapphires and rubies have been mined in several parts of the region. However, sapphire mines, particularly for blue, yellow and green sapphires, have been extensively operated rather than ruby mines in these basaltic fields. Even though these basaltic sapphires have derived from a similar kind of magma, their initial formations could be different in details. It is therefore interesting to compare mineral inclusions in basaltic sapphires of the region with those of the Bo Phloi in Thailand in which it was the biggest mining operation in this region. The basaltic sapphires selected for this study are from Chanthaburi and Phrae in Thailand, from Huai Sai in Laos, from Pailin in Cambodia, and from Gia Nghia in Vietnam (Figure 3-1). The general information from each locality is summarized below.

Chanthaburi and Phrae Deposits in Thailand:

Significant gem corundum (ruby and sapphire) deposits in Thailand occur in three areas; Chanthaburi and Trat provinces in the east, Bo Phloi in Kanchanaburi province in the west, and Phrae province in the north, although some occurrences have been reported in the provinces of Lampang, Chiang Rai, Ubon Ratchathani and Sri Sa Ket provinces (Sutthirat, 2001). All Thai corundum deposits are exclusively associated with Cenozoic basalts in which they can be subdivided into basanitoids and hawaiite (Barr and Macdonald, 1978; 1981). It was expected that corundum is typically associated with basanitoids (Jungyusuk and Khositanont, 1992; Vichit, 1992; Sutthirat *et al.,* 1994). Since Kanchanaburi sapphire is the main focus in this study, sapphires from Chanthaburi and Phrae are additional Thai stones that are selected for comparative study.

The Chanthaburi-Trat gem field can be categorized on the basis of the gem character and geographic location into three zones (Vichit, 1992), namely, the western, the central and the eastern zones. The main deposits of sapphire have been mined in the western zone where is mostly located in Chanthaburi. Age of basaltic

volcanism in Chanthaburi area ranges between 0.44±0.11 Ma (K-Ar dating at Khao Ploi Waen; Barr and Mccdonald, 1981) and 3.0±0.19 Ma (Ar-Ar dating at Khao Wua; Sutthirat *et al.*, 1994). The gem varieties found in the western zone, Chanthaburi, are mainly blue, green, and yellow sapphires together with accessory minerals including zircon and spinel with rare garnet (Vichit, 1992; Sutthirat, 2001).

Corundum-related basaltic lavas in Phrae province cover a large area in the north of Thailand. Age of this basalt is about 5.64±0.28 Ma (K-Ar dating at Denchai; Barr and Macdonald, 1981). Most of gem deposits in this area occur in alluvial and terrace deposits along streams on both sides of Nam Yom river bank; the most important occurrences located at Ban Bo Kaeo and Huai Mae Sung in Den Chai district. Sapphires in various shades of blue are the main variety, although green, yellow and star sapphires can also be found, while ruby is very rare. Blue and green sapphires have been found associated with black spinel, sanidine, augite, olivine and zircon as alluvial deposits in the streams (Vichit, 1992).

Huai Sai Deposit in Laos:

Huai Sai sapphire deposit is scattered around the Laos-Thailand border, located near the town of Bo Keo province. The Huai Sai basalt exposures in the area include dykes and plugs of alkali basalt and basanite having a K-Ar age of 1.74±0.18 Ma (Barr and Macdonald, 1981; Whitford-Strak, 1987). Xenolith- and xenocryst-rich alkali basalts, some containing sapphire and zircon, may typically indicate the later pulses in the basaltic cycles.

Pailin Deposit in Cambodia:

The most famous corundum deposits in Cambodia were discovered at Pailin area, western region close to the border of Thailand. Geologic setting in this area is similar to the eastern part of Chanthaburi-Trat gem deposits in Thailand in which corundum deposits are mostly related to Cenozoic volcanism. Pailin basalt extruded onto Pre-Cambrian metamorphic basement and Triassic greywacke. Characteristics of these basalts are similar to those of Chanthaburi-Trat area in Thailand (Sutherland *et al.*, 1998a). Pailin basalt was reported to have a K/Ar age of 1.09±0.13 Ma (Barr and Macdonald, 1981).

Gia Nghia Deposit in Vietnam:

The areas of Central and Southern Vietnam are extensively covered by basaltic plateaus of several hundred meters in thickness covering an area larger than 23,000 km^2 (Hoang and Flower, 1998). Sapphires have been found in basaltic alluvial within four provinces of southern Vietnam, i.e., Binh Thuan, Lam Dong, Dong Nai, and Dac Lac. Basaltic volcanism in the southern Vietnam appears to have taken place during Tertiary to Quaternary with age ranging from about 0.4-8 Ma (Garnier *et al.*, 2005). Among these basalts, various compositions have been recognized from tholeiite to strong alkali basalts. Sapphire deposits of Southern Vietnam are mainly characterized by placers derived from eroded alkali-basalt flows (Smith *et al.*, 1995).

3.2 Sample Characteristics

Sapphire samples used in this study were obtained from several field surveys to Kanchanaburi, Chanthaburi and Phrae in Thailand, Huai Sai in Laos, Pailin in Cambodia and Gia Nghia in Vietnam. Details of selected samples in each locality are described below.

Chanthaburi Sapphires in Thailand:

The Chanthaburi sapphires used in this study contain five trapiche specimens. These trapiche sapphires contain several mineral inclusions. Previous works focused on these trapiche samples have never been reported before. They vary in size from 5 to 10 mm (Figure 3-2,❶). Their color appearances are mainly blue; combination of yellow shade is also observed in some samples.

Phrae Sapphires in Thailand:

Thirteen samples from Phrae sapphire collection (Figure 3-2,❷) are composed of one traphiche sample and twelve blue sapphires that contain some mineral inclusions. Their sizes vary from 3 to 5 mm, and their colors are mainly blue while the trapiche is yellowish blue.

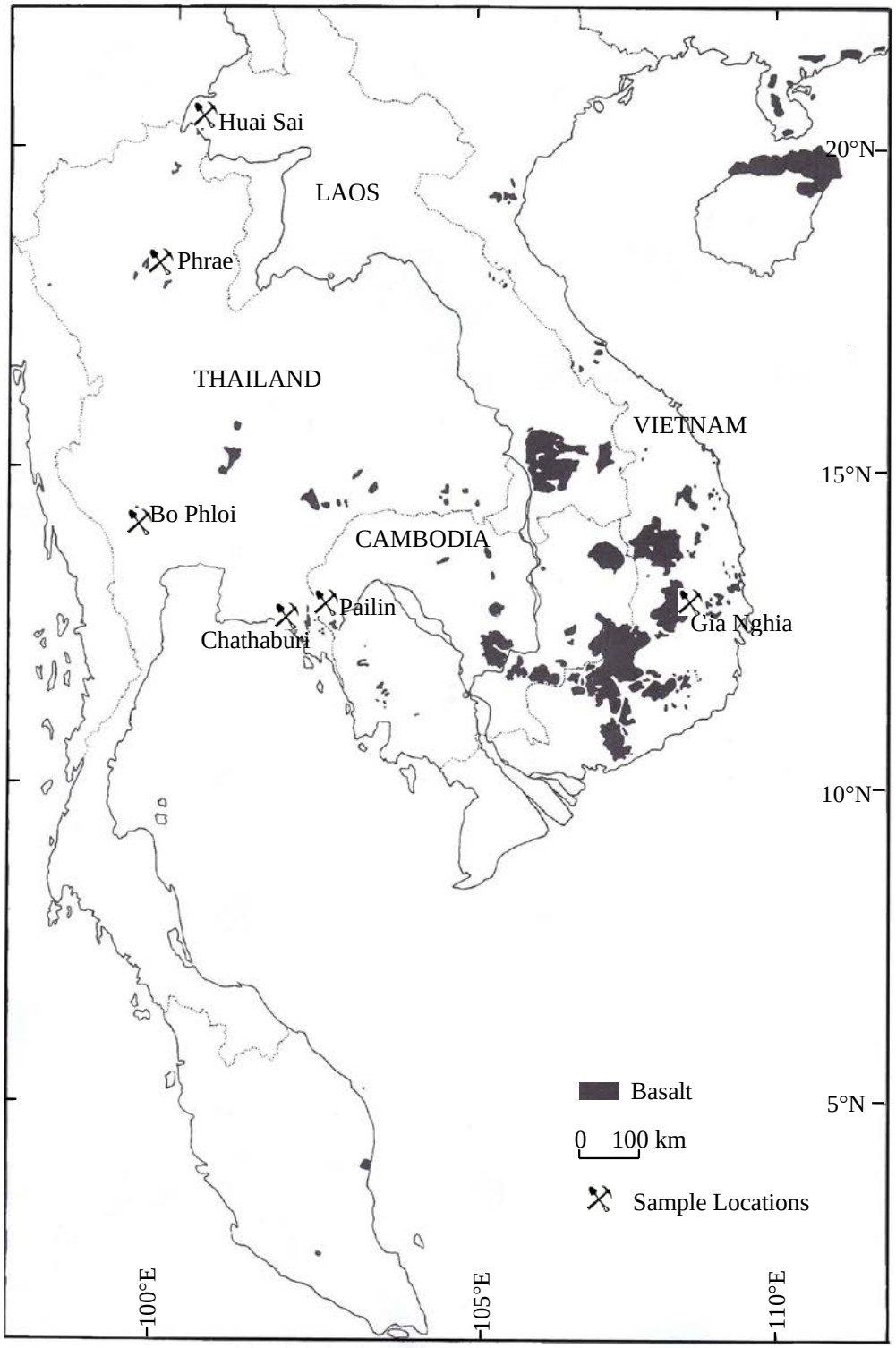

Figure 3-1 Map showing the distribution of Cenozoic basalts in Southeast Asia. The locations where sapphires were selected for this study are Bo Phloi, Chanthaburi and Phrae in Thailand, Huai Sai in Laos, Pailin in Cambodia and Gia Nghia in Vietnam (modified after Barr and Macdonald, 1981).

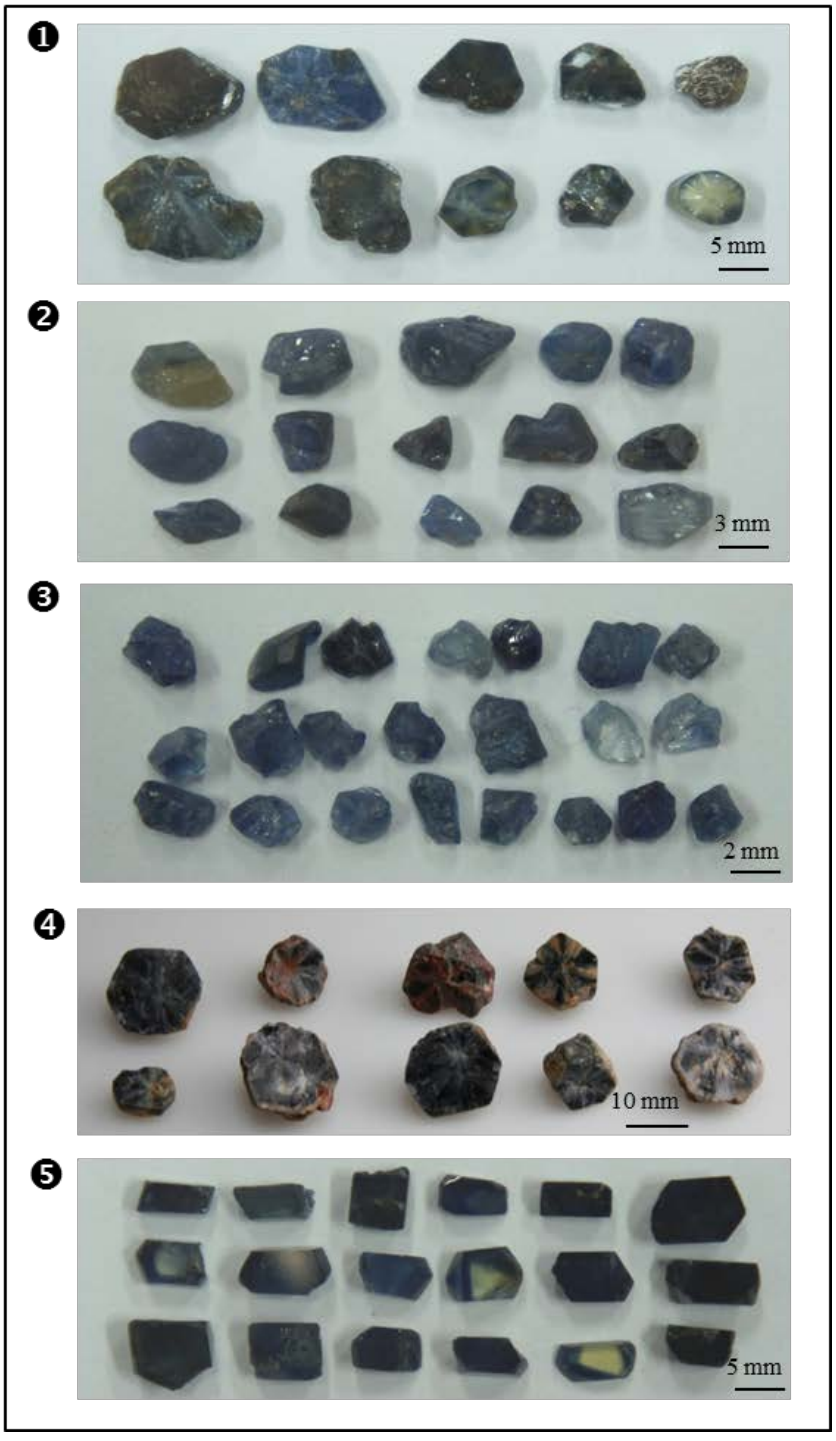

Figure 3-2 Representative sample specimens selected to this study including ❶ trapiche sapphires from Chanthaburi in Thailand; ❷ Phrae sapphires in Thailand; ❸ Huai Sai sapphires in Laos; ❹ trapiche sapphires from Pailin in Cambodia and ❺ Gia Nghia sapphires in Vietnam.

Huai Sai Sapphires in Laos:

Twenty samples of Huai Sai sapphire collection obtained from local prospectors (Figure 3-2,❸) vary in size from 2 to 3 mm and contain some mineral inclusions. Their colors are mainly blue.

Pailin Sapphires in Cambodia:

Seven samples of Pailin trapiche sapphires vary from 5 to 15 mm, and their colors are mainly grayish black but some grains are brownish black (Figure 3-2,❹).

Gia Nghia Sapphires in Vietnam:

Seventeen sapphires and one trapiche specimen from Gia Nghia, Southern Vietnam were selected for this study (Figure 3-2,❺). Their sizes vary from ~ 3 to 5 mm except the trapiche (~10 mm), and their colors are dark-blue with some yellow shade.

3.3 Mineral Inclusions

Many mineral inclusions were found in basaltic sapphires from Southeast Asia under this study. However, due to the nature of materials and the complex chemistry of some mineral inclusions, some mineral inclusions were unable to be identified by Raman technique. Consequently, only Pailin sapphires in Cambodia were selected for phase identification using the Raman method. However, the study of mineral inclusions in sapphires from Southeast Asia was mainly carried out using EPMA technique. Types of mineral inclusions found in each locality identified by both Raman and mainly EPMA techniques are summarized in Table 3-1.

Table 3-1 Summary of mineral inclusions found in sapphires from Southeast Asia.

Mineral group	Mineral inclusions	Thailand			Laos	Cambodia	Vietnam
		Kancha-naburi *(1 samples)*	Chantha-buri *(5 samples)*	Phrae *(13 samples)*	Huai Sai *(20 samples)*	Pailin *(7 samples)*	Gia Nghia *(18 samples)*
Silicates	Zircon	*	-	*	-	-	-
	Feldspar	-	-	*	***	*	*
	Nepheline	-	*	*	*	-	-
	Enstatite	*	*	*	*	*	*
	Garnet	-	-	*	**	*	-
	Sapphirine	-	-	-	**	-	-
	Staurolite	-	-	-	-	-	*
Oxides	Spinel	-	-	*	*	-	-
	Columbite	-	*	-	-	***	-
	Pyrochlore	-	-	-	-	**	-
	Apatite	-	*	-	-	-	-

**** often found*
*** found*
** rarely found*
- not found

Representatives of photomicrograph and back scattered electron images (BSI) of these inclusions are displayed below; more data are listed in Appendix A. In addition, some Raman spectra of inclusions are also reported here. Details of elemental compositions of each mineral inclusion found in each gem deposit are also illustrated below.

Feldspar: is a common type of inclusion found in most localities studied here except in Chanthaburi sapphires. Representative micro-sized feldspar inclusions exhibited as BSI images in these sapphires are exhibited in Figures 3-3.

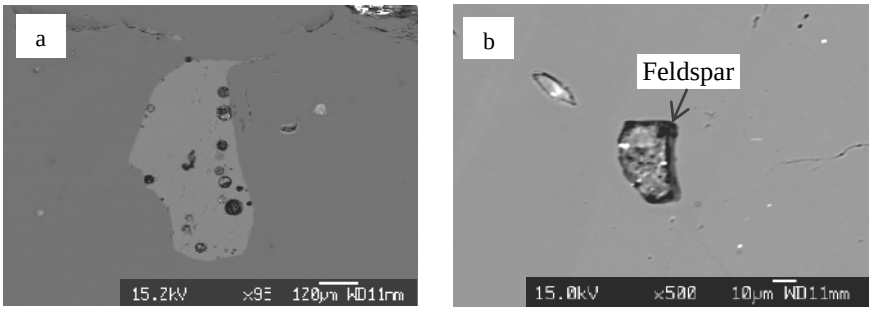

Figure 3-3 Back scattered electron images (BSI) of feldspar inclusions found in (a) Pailin sapphire in Cambodia and (b) Huai Sai sapphire in Laos.

The representative EPMA analyses of feldspar inclusions are presented in Table 3-2, and more analyses are listed in Appendix C. All feldspar inclusions contain rather low CaO contents (0.30 to 3.24 wt%) by which those from Pailin in Cambodia and Gia Nghia in Vietnam give somewhat higher CaO content (~2.4-3.2 wt%). In the ternary atomic Ca-Na-K plot, most of them fall in the area of alkali feldspar (Figure 3-4). The Gia Nghia feldspar inclusions ($Or_{11-12}Ab_{73-78}An_{10-14}$) and some Bo Phloi's ($Or_{10-31}Ab_{60-76}An_{9-14}$) are slightly more sodic while the Huai Sai feldspar inclusions ($Or_{38-45}Ab_{50-55}An_{3-8}$) are relatively more potassic. Although all Southeast Asia sapphires seem to occur widely separated geographically, most feldspar inclusions are a very coherent geochemical group. Such similarity of feldspar inclusions composition implies that the sapphire formation of Southeast Asia sapphires could be originated from a similar provenance of alkali-rich environment. In general, the alkali feldspars are essential constitutions of alkali and acid igneous rocks. They are particularly abundant in syenites, granites, granodiorites and their volcanic equivalents (Deer *et al.,* 1992).

Table 3-2 Representative EPMA analyses of **feldspar inclusions** in basaltic sapphires of Southeast Asia *(n.a. = not analyzed)*.

Mineral phase	Thailand			Laos			Cambodia		Vietnam	
Analysis (wt%)	Bo Phloi		Phrea	Huai Sai			Pailin		Gia Nghia	
	1C4ia 2-1	3LBA2g	TP2b-1	HSA1c3	HSA7b4	HSA7g5	TPA6f3	TPA7f	GNB 2c-3	GNB 2d-6
SiO_2	63.84	63.09	63.30	65.06	65.97	63.64	63.60	64.85	63.19	63.24
TiO_2	0.05	0.03	0.16	0.37	0.15	0.12	0.02	0.08	0.04	0.04
Al_2O_3	22.14	21.80	22.00	20.66	20.68	20.90	21.31	22.60	22.26	21.63
FeO	0.05	0.06	0.48	1.22	0.36	0.32	0.10	0.11	0.18	0.22
MnO	0.03	0.03	0.18	0.23	0.02	0.02	0.00	0.00	0.02	0.00
MgO	0.01	0.00	0.11	0.08	0.01	0.03	0.02	0.01	0.06	0.00
BaO	0.03	0.07	n.a.	0.00	0.09	0.04	0.05	0.00	0.06	0.04
CaO	2.69	2.07	0.30	0.56	1.47	1.45	3.07	3.24	2.95	2.42
Na_2O	8.32	7.20	4.43	5.24	5.50	6.34	4.99	5.90	8.23	9.76
K2O	1.66	5.60	3.32	6.99	7.10	6.68	8.18	4.17	2.10	2.23
Total	98.82	99.95	94.27	100.40	101.34	99.53	101.34	100.96	99.07	99.56
8 (O)										
Si	2.853	2.841	2.924	2.913	2.924	2.881	2.852	2.855	2.832	2.835
Ti	0.002	0.001	0.006	0.012	0.005	0.004	0.001	0.003	0.001	0.001
Al	1.166	1.157	1.198	1.090	1.080	1.115	1.126	1.172	1.176	1.143
Fe	0.002	0.002	0.019	0.046	0.013	0.012	0.004	0.004	0.007	0.008
Mn	0.001	0.001	0.007	0.009	0.001	0.001	0.000	0.000	0.001	0.000
Mg	0.000	0.000	0.007	0.005	0.001	0.002	0.002	0.001	0.004	0.000
Ba	0.001	0.001	-	0.000	0.002	0.001	0.001	0.000	0.001	0.001
Ca	0.129	0.100	0.015	0.027	0.070	0.070	0.147	0.153	0.141	0.116
Na	0.721	0.628	0.397	0.455	0.473	0.556	0.434	0.504	0.715	0.848
K	0.095	0.321	0.196	0.399	0.401	0.385	0.468	0.234	0.120	0.127
Total*	4.970	5.054	4.768	4.956	4.968	5.028	5.035	4.925	4.997	5.080
Atomic%										
Na	76.34	59.85	65.34	51.63	50.11	54.96	41.36	56.55	73.22	77.71
Ca	13.61	9.52	2.46	3.06	7.38	6.94	14.03	17.18	14.49	10.64
K	10.04	30.63	32.19	45.32	42.51	38.09	44.61	26.27	12.29	11.66
Total**	100.00	100.00	100.00	100.00	100.00	100.00	100.00	100.00	100.00	100.00

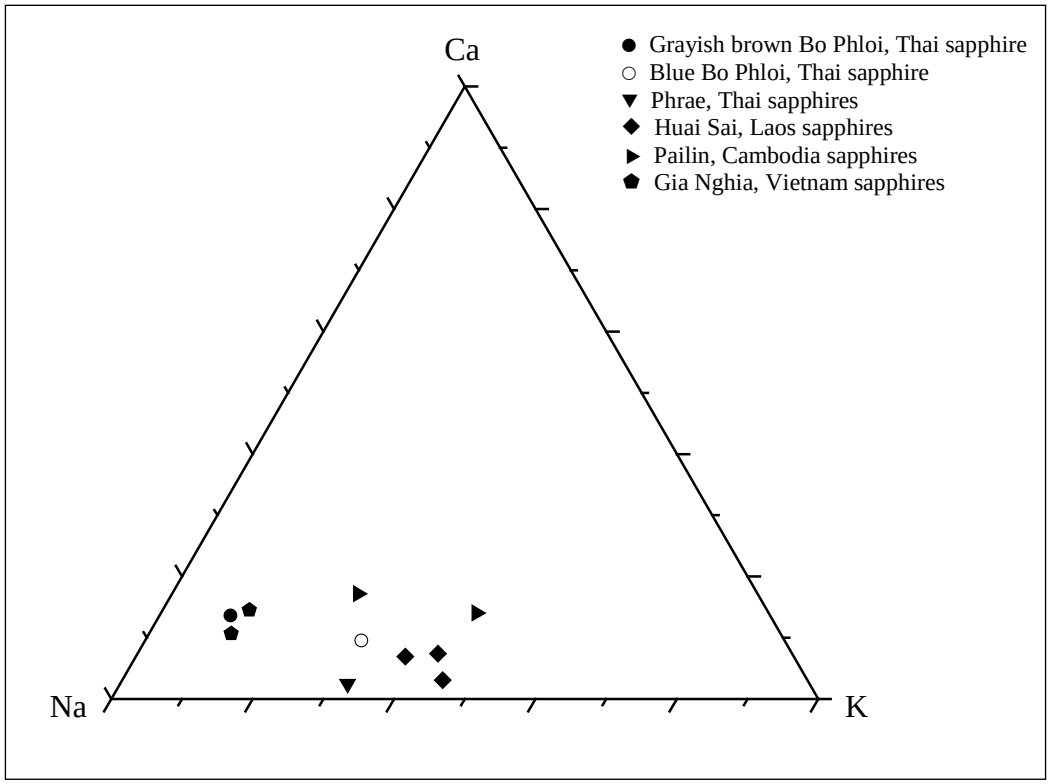

Figure 3-4 Ternary Ca-Na-K plots of feldspar inclusions found in basaltic sapphires of Southeast Asia.

Nepheline: Nepheline inclusions were observed in Thai sapphires from Bo Phloi, Chanthaburi and Phrae), and in Huai Sai sapphires from Laos. Representative BSI images of nepheline inclusion are illustrated in Figures 3-5. Chemical compositions of these inclusions are summarized in Table 3-3, and additional analyses are listed in Appendix C.

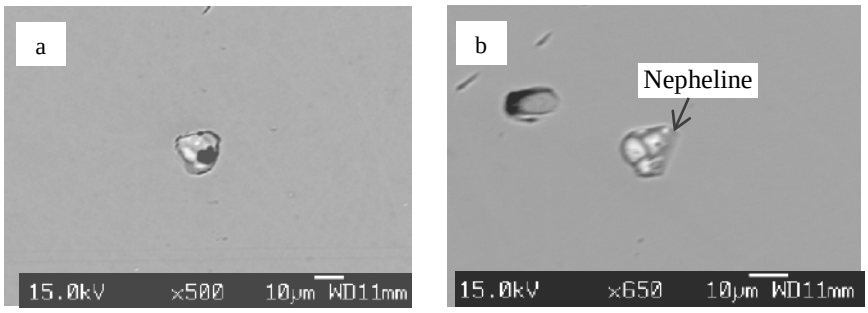

Figure 3-5 Back scattered electron images (BSI) of nepheline inclusions found in (a) Phrae sapphire in Thailand and (b) Huai Sai sapphire in Laos.

All nepheline inclusions are clearly sodium-rich (Na_2O ~ 15-19 wt %). Many of them contain about 40-44% SiO_2, 32-36% Al_2O_3, 14-18% Na_2O, 4-8% K_2O, 0-3% CaO. Two Huai Sai nephelines exhibit slightly more potassic than other Thai nepheline except one blue Bo Phloi sapphire (sample *3BA3g*) that is quite similar. In general, however, all nephline inclusions in Thai and Lao sapphires yielded rather similar mineral chemistry. Moreover, total cations recalculated on basic of 32 oxygen atoms, of all analyses are lower than 24. This may indicate the appearence of vacancy in cation sites similar to explain those Bo Phloi nepheline inclusions in previous Chapter 2. However, the occurrences of nepheline inclusions in basaltic sapphires of Southeast Asia would suggest an environmental formation having silica-undersaturation with high alkali content.

Table 3-3 Representative EPMA analyses of **nepheline inclusions** in basaltic sapphires of Southeast Asia *(n.a. = not analyzed).*

Mineral phase	Thailand						Laos	
Analysis (wt%)	Bo Phloi			Chan	Phrea		Huai Sai	
	2A7ia	3LGC12f	3BA3g	TC6d	PA1f	PA1m1	HSA5b	HSA5d4
SiO_2	42.43	42.86	42.20	41.20	44.01	42.50	41.52	41.79
TiO_2	n.a.	0.08	0.05	0.09	0.05	0.05	0.36	0.20
Al_2O_3	35.80	36.06	35.94	34.01	32.59	34.56	34.06	34.86
FeO	0.00	0.15	0.43	0.66	0.14	0.27	0.37	0.26
MnO	0.04	0.00	0.00	0.05	0.08	0.02	0.16	0.06
MgO	0.02	0.00	0.04	0.01	0.00	0.02	0.01	0.02
CaO	2.58	0.30	0.52	0.29	0.04	0.11	0.12	0.89
Na_2O	15.66	17.88	14.17	17.64	18.68	16.86	15.05	15.45
K_2O	4.54	3.54	8.10	5.09	4.84	6.52	8.78	7.21
Total	101.06	100.88	101.44	99.06	100.42	100.91	100.42	100.72
32 (O)								
Si	8.032	8.085	8.044	8.043	8.427	8.141	8.074	8.040
Ti	-	0.012	0.034	0.054	0.011	0.022	0.030	0.021
Al	7.987	8.018	8.073	7.824	7.354	7.801	7.806	7.905
Fe^{2+}	0.000	0.024	0.068	0.108	0.023	0.044	0.060	0.042
Mn	0.006	0.000	0.001	0.009	0.013	0.003	0.026	0.010
Mg	0.006	0.000	0.011	0.004	0.000	0.005	0.002	0.005
Ca	0.523	0.060	0.106	0.061	0.008	0.023	0.024	0.183
Na	5.746	6.541	5.238	6.677	6.935	6.261	5.673	5.762
K	1.096	0.852	1.969	1.267	1.181	1.593	2.178	1.770
Total*	23.396	23.591	23.543	24.046	23.952	23.893	23.874	23.737
ΣR	7.888	7.512	7.419	8.066	8.132	7.901	7.899	7.897
Vacancy (□)	0.604	0.409	0.457	-	0.048	0.107	0.126	0.263

ΣR = (2Ca+Na+K)

Spinel: spinel inclusions were only found in sapphires from a few deposits, i.e., Bo Phloi and Phrae in Thailand and Huai Sai in Laos. A couple of BSI images of spinel inclusions are displayed in Figure 3-6.

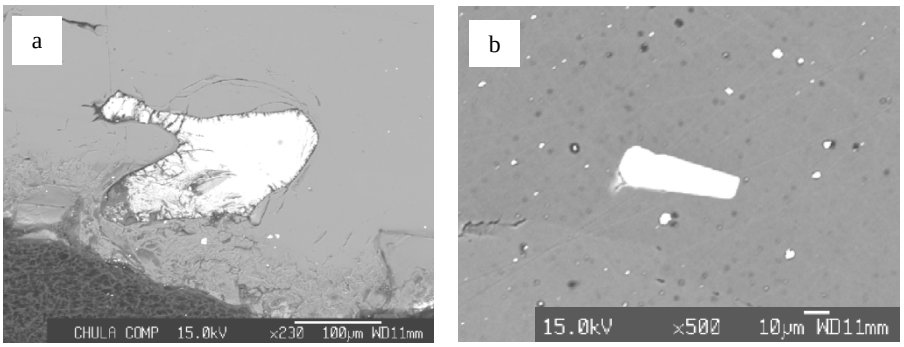

Figure 3-6 Back scattered electron images (BSI) of spinel inclusions found in (a) Phrae sapphire in Thailand and (b) Huai Sai sapphire in Laos.

The chemical compositions of these spinel inclusions (Table 3-4) exhibited significant chemical variability as shown on the ternary atomic plots of Al-Fe^{2+}-Mg and (Mn+Zn)-Fe^{2+}-Mg (see Figure 3-7)**.** Such variability may be due to the difference of the original sources or separated geographic localities. However, they clearly show that all spinel analyses fall within the area of Fe-rich side of hercynite. Phrae spinel inclusions show significantly higher Zn content (1.32-1.60 Zn p.f.u.) with the chemical compositions about 56-57% Al_2O_3, 29-30% FeO, 7-9% ZnO, ~3% MnO. These compositions are rather similar to the gahnospinel compositions reported by Deer *et al.* (1992) and consistent with the Zn-bearing spinel inclusions (2.86 Zn p.f.u.) in corundum from New England, Australia (Sutherland *et al.*, 1998b). The presence of Zn-spinel inclusion indicates that the Phrae sapphires might have input from a source compatible with a high Zn mantle during crystallization (Stoddard, 1979). On the other hand, spinel inclusions in Huai Sai sapphires give rather high Fe contents (e.g., 53-58% Al_2O_3, 42-48% FeO, ~0.3% MgO) which belong to the hercynite-magnetite series.

Although, chemical composition of spinel inclusions seem to differ from place to place; they are mostly hercynitic in composition rich in alumina and iron similar to those in Bo Phloi spinels. In general, hercynitic spinel is found commonly in metamorphosed argillaceous sediments richer in iron also in basic and ultrabasic igneous rocks as well as some granitic granulites (Deer *et al.*, 1992).

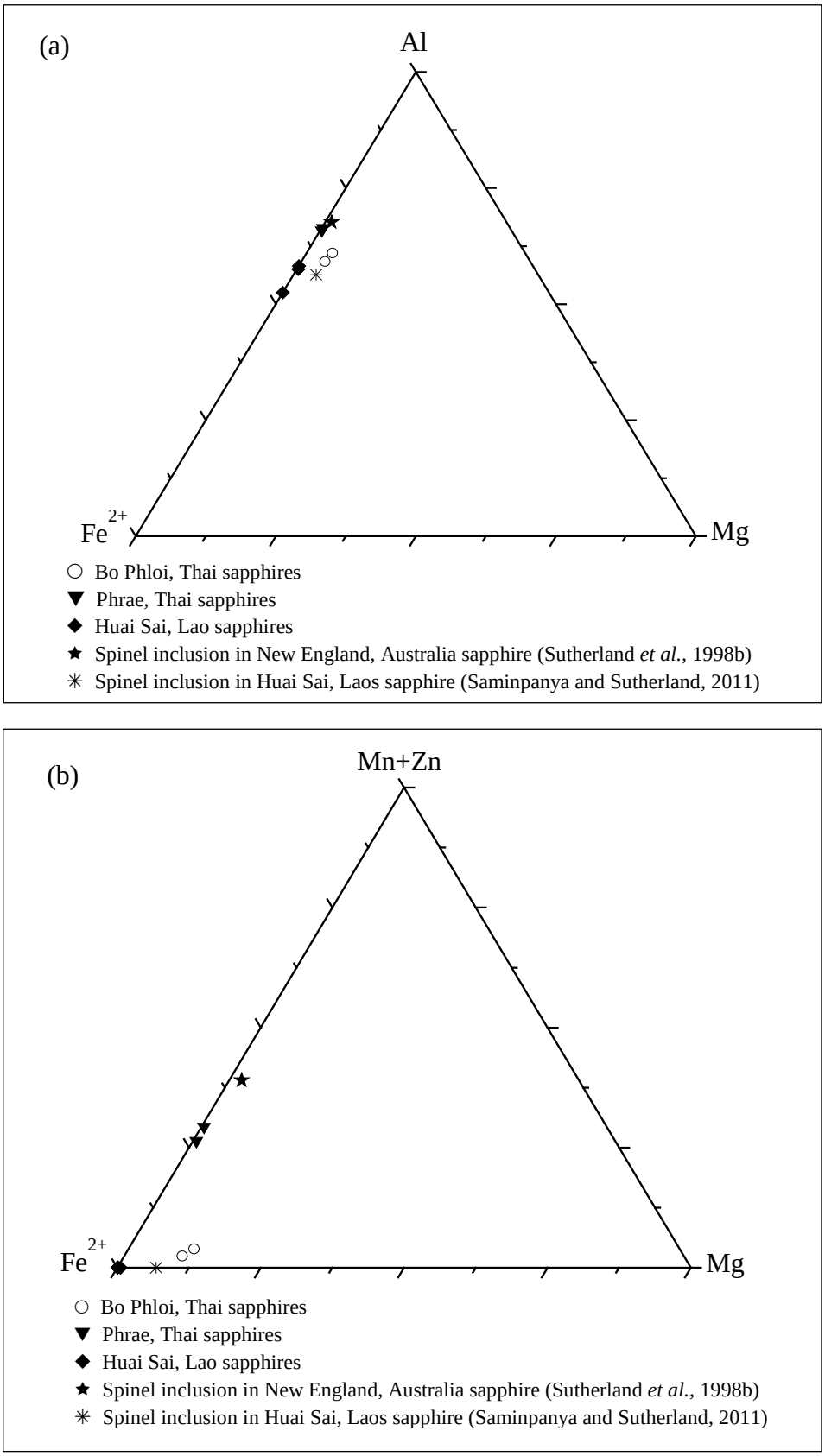

Figure 3-7 (a) Ternary Al-Fe^{2+}-Mg plots and (b) (Mn+Zn)-Fe^{2+}-Mg plots of compositions of spinel inclusions found in basaltic sapphires of Southeast Asia.

Table 3-4 Representative EPMA analyses of **spinel inclusions** in Southeast Asia sapphires *(n.a. = not analyzed).*

Mineral phase	Thailand				Laos			Australia	Laos
Analysis (wt%)	Bo Phloi		Phrea		Huai Sai			New England	Huai Sai
	2DGB 5b-1	3LGD 4b	PA1a	PA1a1	HSB2i	HSB 2i3	HSB 2e	Sutherland *et al.*, 1998	(Saminpanya and Sutherland, 2011)
SiO_2	0.09	0.00	0.00	0.00	0.21	0.10	0.36	0.00	n.a.
TiO_2	0.09	0.17	0.00	0.02	0.22	0.24	0.23	0.00	0.20
Al_2O_3	60.08	58.34	56.97	57.34	58.04	53.05	58.15	56.12	55.30
Cr_2O_3	0.00	0.02	0.02	0.00	0.03	0.00	0.00	0.00	n.a.
FeO	33.88	36.14	29.26	28.77	42.63	48.00	41.75	25.94	38.90
MnO	1.39	0.98	3.12	2.98	0.00	0.01	0.03	0.84	4.00
MgO	4.56	4.19	0.23	0.19	0.25	0.02	0.03	0.96	n.a.
ZnO	0.18	0.02	7.47	9.07	0.00	0.00	0.00	16.36	n.a.
CaO	0.01	0.00	0.00	0.00	0.06	0.00	0.00	0.00	n.a.
Total	100.28	99.85	97.07	98.36	101.43	101.42	100.56	100.22	98.40
32 (O)									
Si	0.020	0.000	0.000	0.000	0.048	0.024	0.084	0.000	-
Ti	0.016	0.029	0.000	0.003	0.037	0.044	0.040	0.000	0.036
Al	15.848	15.635	16.069	16.024	15.695	14.872	15.793	15.663	15.566
Cr	0.000	0.004	0.004	0.000	0.005	0.000	0.000	0.000	-
Fe^{2+}	6.233	6.471	5.955	5.747	8.009	8.252	8.101	4.691	7.291
Fe^{3+}	0.107	0.401	0.000	0.000	0.171	1.296	0.000	0.000	1.000
Mn	0.264	0.189	0.632	0.598	0.000	0.002	0.006	0.168	0.809
Mg	1.522	1.419	0.081	0.066	0.085	0.006	0.010	0.339	-
Zn	0.029	0.003	1.320	1.587	0.000	0.000	0.000	2.860	-
Ca	0.001	0.000	0.000	0.000	0.014	0.000	0.000	0.000	-
Total*	24.040	24.151	24.061	24.026	24.064	24.496	24.034	23.723	24.702
$\sum R^{2+}$	8.050	8.082	7.988	7.998	8.107	8.260	8.117	8.059	8.100
$\sum R^{3+}$	15.991	16.070	16.073	16.027	15.957	16.236	15.917	15.663	16.602

$\sum R^{2+} = Fe^{2+}+Mn+Mg+Zn+Ca$, $\sum R^{3+} = Si+Ti+Al+Cr+Fe^{3+}$

Pyroxene: is a commom inclusion found in all localities of Southeast Asian sapphires studied here. Representative BSI image of these inclusions is demonstrated in Figures 3-8.

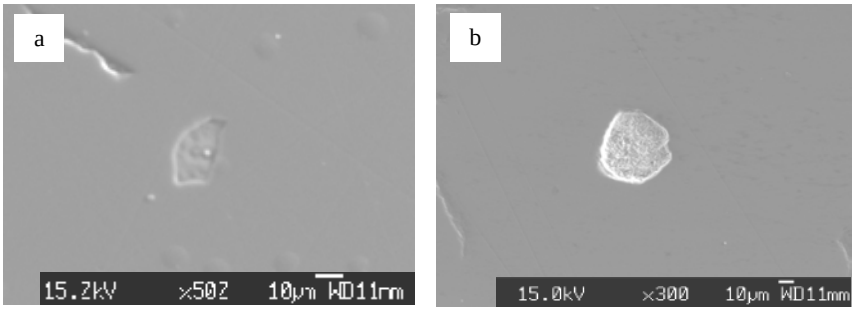

Figure 3-8 Back scattered electron images (BSI) of pyroxene inclusion found in (a) Pailin sapphire in Cambodia and (b) Gia Nghia sapphire in Vietnam.

All pyroxene analyses give approximately 57-65% SiO_2, 28-35% MgO, 0-8% Al_2O_3 and traces of FeO (Tables 3-5 and 3-6). Their compositions show relatively high Si and low Mg similar to those found in the Bo Phloi enstatite inclusion, except for the relatively low Si content of the sample *PA1k8* in Phrae sapphire. However, the variation of Al_2O_3 contents (up to about 8%) may be detected in these analyses. Pyroxene analyses in this study are categorized into two groups based on the A_2O_3 contents. The first group consists of lower Al_2O_3 content (less than 1 wt%, see Table 3-5) whereas the second one contains higher Al_2O_3 (see Table 3-6). However, the quadrilateral plots of pyroxene compositions (Figure 3-9) show very similar to one another and presumably have a similar formation. The chemical compositions of these inclusions are perfectly matched with enstatite end-member. Regarding to recalculated formula, total cations of all analyses are lower than the theoretical value of 4, based on 6 oxygen atoms. This may suggest the presence of vacancies in the cation sites. Excess of Si^{4+} may lead to charge compensation in cation sites which are mainly occupied by Mg with partly substitution of Al. Considering the chemical compositions in Table 3-5, the amount of Si_{excess} are equal to or nearby the vacancy occurred in the cation sites. This study demonstrates that the incorporation of Si_{excess} into cation sites in the enstatite structure is charge-balanced by Mg^{2+} vacancies. In contrast, when more amounts of Al_2O_3 contents are detected in enstatite analyses (see Table 3-6), the ambiguous correlation between the excess of Si^{4+} and vacancy within

cation sites are illustrated. This higher Al_2O_3 contents may obtain from the host of sapphires during analytical process because the small grains of these inclusions.

The appearance of these Si-rich enstatites in the study may be a result from contaminated melts of mafic and felsic contents at contact zone of crustral materials; richer in both Si and Al, and mantle-derived basaltic magma as previous described for the Bo Phloi enstatite inclusions as described in Chapter 2.

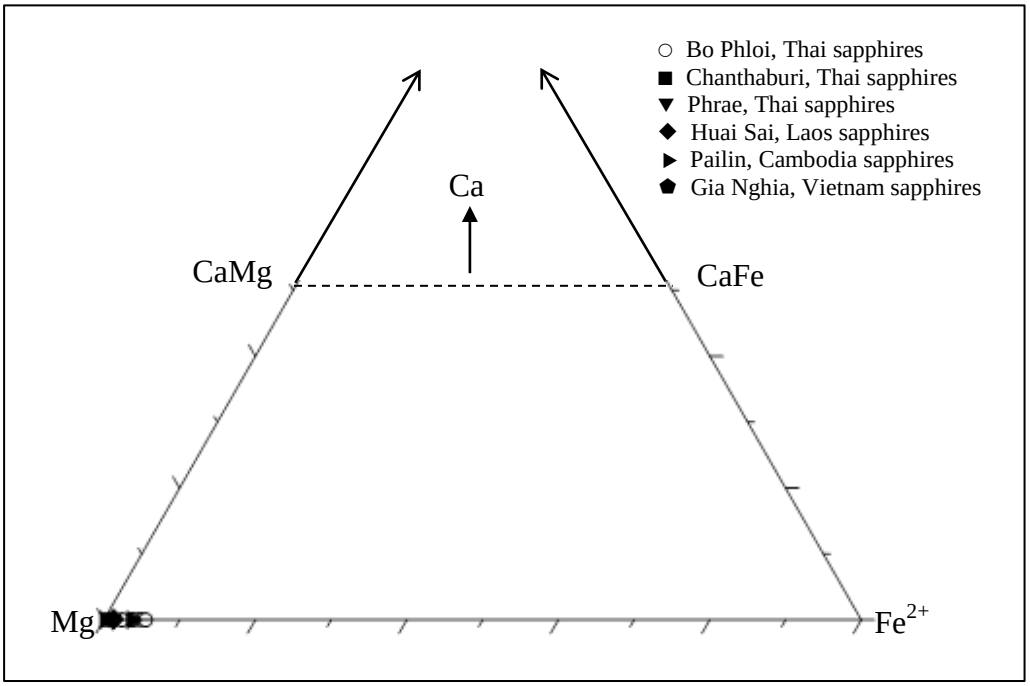

Figure 3-9 Pyroxene quadrilateral plots of Ca-Mg-Fe^{2+} compositions of pyroxene inclusions found in basaltic sapphires of Southeast Asia (modified after Lindsley, 1983).

Table 3-5 Representative EPMA analyses of **pyroxene inclusions** in Southeast Asia sapphires *(n.a. = not analyzed).*

Mineral phase	Thai			
Analysis (wt%)	Bo Phloi			Chan
	2DGB2a-2	3LGC8b-2	3BC2a	TC10g-1
SiO_2	60.30	64.77	64.73	65.78
TiO_2	0.03	0.02	0.02	0.00
Al_2O_3	0.09	0.40	0.15	0.46
Cr_2O_3	0.04	0.01	0.00	0.01
FeO	3.26	0.50	2.30	0.63
MnO	0.00	0.02	0.03	0.00
MgO	35.69	33.01	31.75	34.04
NiO	0.01	n.a.	0.05	0.00
CaO	0.02	0.02	0.00	0.01
Na_2O	0.02	0.06	0.01	0.00
K_2O	0.01	0.03	0.00	0.00
Total	99.47	98.84	99.05	100.92
6 (O)				
Si	2.046	2.159	2.169	2.149
Ti	0.001	0.000	0.000	0.000
Al	0.003	0.016	0.006	0.018
Cr	0.001	0.000	0.000	0.000
Fe	0.092	0.014	0.065	0.017
Mn	0.000	0.001	0.001	0.000
Mg	1.805	1.640	1.586	1.658
Ni	0.000	-	0.001	0.000
Ca	0.001	0.001	0.000	0.000
Na	0.001	0.004	0.000	0.000
K	0.001	0.001	0.000	0.000
Total*	3.952	3.835	3.828	3.842
ΣVacancy (□)	0.048	0.165	0.172	0.158
Si_{excess}	0.046	0.159	0.169	0.149
Charge balanced	3.990	3.990	3.993	3.999

Enstatite formula = (Mg, Fe, Al, Si_{excess})$_2Si_2O_6$ = (M2)$_2Si_2O_6$
*Charge balanced = (Mg*2+Fe*2+Al*3+Si_{excess}*4)*

Table 3-6 Representative EPMA analyses of **pyroxene inclusions** in Southeast Asia sapphires *(n.a. = not analyzed).*

Mineral phase	Thailand				Laos	Cambodia		Viet Nam	
Analysis (wt%)	Bo Phloi			Phrea	Huai Sai	Pailin		Gia Nghia	
	2DGA 7b-1	3LGD6c	3BA9b	PA1k8	HSB1c2	TPA3c	TPA 1b	GNB 4b-7	GNB 4c-4
SiO_2	60.69	60.10	60.28	58.30	57.79	60.96	60.30	61.41	58.89
TiO_2	0.00	0.00	0.04	0.01	0.02	0.00	0.00	0.02	0.03
Al_2O_3	2.15	3.86	2.92	7.05	8.00	2.93	5.51	2.51	5.51
Cr_2O_3	0.02	0.00	0.15	0.00	0.00	0.28	0.08	0.07	0.09
FeO	2.39	1.47	3.50	0.72	0.48	2.28	0.08	0.74	0.61
MnO	0.00	0.01	0.00	0.06	0.00	0.00	0.00	0.01	0.01
MgO	35.20	33.73	33.69	34.06	28.62	33.59	33.13	30.41	29.66
NiO	n.a.	n.a.	0.00	0.71	0.00	0.00	0.00	n.a.	n.a.
CaO	0.03	0.01	0.00	0.01	0.01	0.01	0.01	0.00	0.12
Na_2O	0.02	0.02	0.03	0.02	0.04	0.02	0.01	0.00	0.04
K_2O	0.03	0.00	0.06	0.00	0.03	0.00	0.02	0.00	0.00
Total	100.53	99.21	100.66	100.93	94.99	100.06	99.14	95.17	94.97
6 (O)									
Si	2.026	2.019	2.019	1.932	2.006	2.038	2.011	2.126	2.047
Ti	0.000	0.000	0.001	0.000	0.000	0.000	0.000	0.000	0.001
Al	0.085	0.153	0.115	0.275	0.327	0.115	0.216	0.103	0.226
Cr	0.000	0.000	0.004	0.000	0.000	0.007	0.002	0.002	0.002
Fe	0.067	0.041	0.098	0.020	0.014	0.064	0.002	0.021	0.018
Mn	0.000	0.000	0.000	0.002	0.000	0.000	0.000	0.000	0.000
Mg	1.751	1.689	1.682	1.682	1.481	1.674	1.647	1.569	1.537
Ni	-	-	0.000	0.019	0.000	0.000	0.000	-	-
Ca	0.001	0.000	0.000	0.000	0.000	0.000	0.000	0.000	0.004
Na	0.001	0.001	0.002	0.001	0.003	0.001	0.001	0.000	0.003
K	0.001	0.000	0.002	0.000	0.001	0.000	0.001	0.000	0.000
Total*	3.933	3.905	3.923	3.931	3.832	3.901	3.881	3.822	3.839
ΣVacancy (□)	0.067	0.095	0.077	0.069	0.168	0.099	0.119	0.178	0.161
Si_{excess}	0.026	0.019	0.019	0.000	0.006	0.038	0.011	0.126	0.047
Charge balanced	3.994	3.997	3.980	4.024	3.993	3.976	3.991	3.992	3.977

Enstatite formula = $(Mg, Fe, Al, Si_{excess})_2Si_2O_6 = (M2)_2Si_2O_6$
Charge balanced = $(Mg*2+Fe*2+Al*3+Si_{excess}*4)$

Garnet: is one of the significant inclusions recognized in many localities of Southeast Asian sapphires such as Thailand (i.e., Bo Phloi and Phrae deposits), Laos and Cambodia. Photomicrograph and BSI images of garnet inclusions found in these sapphires are displayed in Figures 3-10 and 3-11, respectively.

Figure 3-10 Garnet inclusion found in a Pailin sapphire from Cambodia.

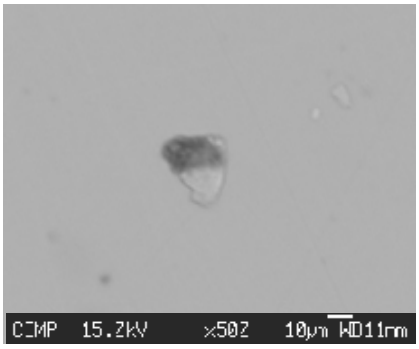

Figure 3-11 A back scattered electron image (BSI) of garnet inclusion found in Pailin sapphire in Cambodia.

Acceptable analyses of garnet inclusions are summarized in Table 3-7 and more result are collected in Appendix C. Their compositions were recalculated to cation formula on the basic of 24 oxygens, from which the atomic proportions of Mg, Fe, Ca and Mn end-members were obtained. In general, the compositions give approximately 40-46% SiO_2, 22-28% Al_2O_3 with quite variable ranges of FeO and MgO. Normalized atomic proportions of $Mg/(Mg+Fe^{2+})$ ratios vary widely, mainly > 90%, sometimes 70-90% and lesser < 70%. In addition, the ternary Ca-Fe^{2+}-Mg diagram of garnet inclusions in this study; including alluvial Bo Phloi garnet (Sutthirat, 2001) and garnet xenocryst in Nong Bon, Chanthaburi-Trat (Sutthirat *et al.*, 2001) shows the different compositions (Figure 3-12) not only the amount of Mg but also Fe^{2+} contents. This suggests that these garnets may genetically unrelate to each other. However, the $Mg/(Mg+Fe^{2+})$ ratio of Bo Phloi garnet inclusions are similar to those of alluvial Bo Phloi garnet as reported by Sutthirat (2001), which consist of 72-76 per cent of pyrope end-member. However, the alluvial Bo Phloi garnets contain higher Ca contents than that of the Bo Phloi garnet inclusion. On the other hand, Phrae garnet inclusions have a $Mg/(Mg+Fe^{2+})$ ratio of about 0.481 (Table 3-7), which

falls within the almandine-dominated garnet. While the garnet inclusions in Pailin sapphires have the $Mg/(Mg+Fe^{2+})$ ratios of 0.863-0.891 that fall into pyrope-dominated composition which are slightly different from one anothers. Huai Sai garnet inclusions are Mg-rich and vary slightly in composition of about 43-45% SiO_2, 24-26% Al_2O_3 and 28-30% MgO which have the $Mg/(Mg+Fe^{2+})$ ratios of 0.99-1.00. These Huai Sai garnets display the pyrope-rich components similar to garnet xenocrysts found in Nong Bon, Chanthaburi-Trat corundum reported by Sutthirat *et al.* (2001).

Even though there are quite diversity of chemical contents of garnet inclusions in Southeast Asia sapphires, their mineral chemistries are more towards pyrope-rich and Ca-poor end-members. These results imply that all these garnets could be crystallized from a similar provenance within mafic/ultramafic composition since their compositions are similar, except one from Phrae, but lower in Ca, slightly lower in Fe and higher in Mg, than the garnets in the alluvial Bo Phloi garnet and in garnet-peridotite xenolith in kimbolite (Deer *et al.*, 1992). This may suggest that the garnets and their host sapphires in this region have similar origins and closely relate to mafic environment.

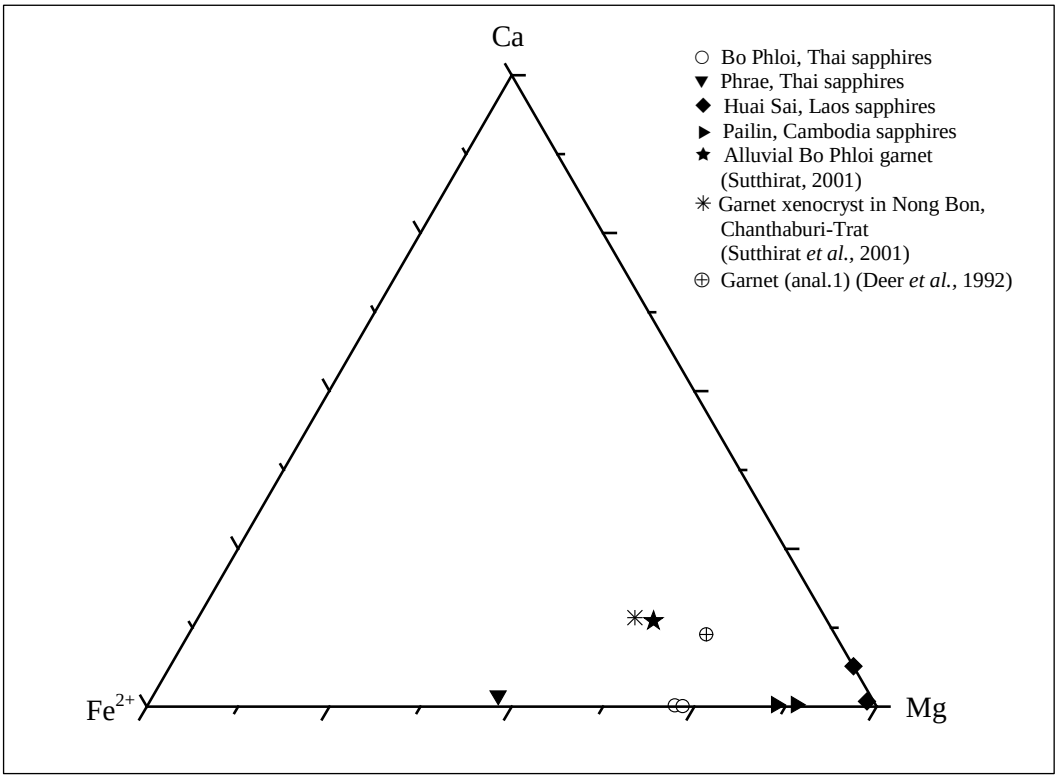

Figure 3-12 Ternary Ca-Fe^{2+}-Mg plot of compositions of garnet inclusions found in Southeast Asia sapphires.

Table 3-7 Representative EPMA analyses of **garnet inclusions** in Southeast Asia sapphires *(n.a. = not analyzed).*

Mineral phase	Thailand			Laos			Cambodia		Alluvial Bo Phloi (Sutthirat, 2001)	Nong Bon xenocryst (Sutthirat *et al.*, 2001)	Pyrope (Deer *et al.*, 1992)
Analysis (wt%)	Bo Phloi		Phrea	Huai Sai			Pailin				
	2DGB1a	3LGD6c-3	PA1j4	HSA5f7	HSC1d3	HSC3d	TPA1a1	TPA4m4	TKPG1	NB-5A	(anal.1)**
SiO_2	42.07	42.80	40.39	45.85	44.07	43.83	43.16	43.54	40.64	40.62	41.33
TiO_2	0.01	0.01	1.34	0.03	0.03	0.11	0.40	0.15	0.50	0.52	0.28
Al_2O_3	25.14	23.88	23.03	26.17	24.00	24.53	28.17	26.28	22.46	22.48	21.83
Cr_2O_3	0.04	0.04	0.01	0.04	0.06	0.00	0.00	0.00	0.00	0.05	1.73
FeO	13.58	13.32	22.28	0.45	0.48	0.55	6.35	5.40	13.87	14.08	10.44
MnO	0.01	0.02	0.62	0.00	0.01	0.02	0.00	0.00	0.50	0.37	0.44
MgO	20.00	20.68	11.58	27.88	28.75	30.48	22.47	24.63	16.67	16.34	19.60
CaO	0.07	0.03	0.60	0.34	2.73	0.12	0.11	0.13	5.03	5.35	4.40
Na_2O	n.a.	n.a.	0.17	0.03	0.04	0.04	0.03	0.04	0.21	n.a.	n.a.
K_2O	n.a.	n.a.	0.33	0.06	0.06	0.05	0.07	0.13	0.05	n.a.	n.a.
Total	100.94	100.78	100.34	100.85	100.22	99.73	100.75	100.30	99.93	99.81	100.05
24 (O)											
Si	5.942	6.046	6.022	6.098	5.978	5.933	5.895	5.963	5.939	5.944	5.948
Ti	0.001	0.001	0.150	0.003	0.003	0.011	0.041	0.015	0.055	0.057	0.030
Al	4.185	3.975	4.047	4.102	3.836	3.914	4.535	4.241	3.868	3.877	3.703
Cr	0.005	0.004	0.001	0.005	0.007	0.000	0.000	0.000	0.000	0.006	0.197
Fe^{2+}	1.604	1.573	2.778	0.050	0.000	0.000	0.725	0.618	1.377	1.553	1.042
Fe^{3+}	0.000	0.000	0.000	0.000	0.054	0.062	0.000	0.000	0.318	0.170	0.214
Mn	0.002	0.003	0.078	0.000	0.001	0.003	0.000	0.000	0.062	0.046	0.054
Mg	4.212	4.356	2.575	5.529	5.814	6.150	4.575	5.029	3.632	3.565	4.205
Ca	0.010	0.005	0.096	0.048	0.396	0.017	0.016	0.018	0.787	0.839	0.678
Na	-	-	0.049	0.009	0.010	0.011	0.007	0.011	0.059	-	-
K	-	-	0.063	0.011	0.010	0.008	0.011	0.023	0.009	-	-
Total*	15.962	15.963	15.859	15.855	16.108	16.109	15.806	15.919	16.107	16.057	16.072
$\sum R^{2+}$	5.828	5.936	5.527	5.627	6.211	6.170	5.316	5.665	5.858	6.002	5.979
$\sum R^{3+}$	4.191	3.980	4.198	4.110	3.900	3.986	4.575	4.256	4.241	4.110	4.144
$Mg/(Mg+Fe^{2+})$	0.724	0.735	0.481	0.991	1.000	1.000	0.863	0.891	0.725	0.697	0.801

$\sum R^{2+} = Fe^{2+}+Mn+Mg+Ni+Ca$, $\sum R^{3+} = Ti+Al+Cr$

***garnet-peridotite xenolith in kimbolite.*

Sapphirine: sapphirine inclusion was found only in Huai Sai sapphires from Laos. The acceptable compositions of Huai Sai sapphirine inclusions give approximately 13-14% SiO_2, 65-67% Al_2O_3, 17-20% MgO with minor amounts of about 0-2% FeO, and traces of CaO and alkali oxides (Table 3-8). In general, chemical contents of sapphirine inclusions in Huai Sai sapphires are similar to those of the Bo Phloi sapphirines although there are some minor differences. Huai Sai sapphirines are poorer in Si content (~1.60 p.f.u.) and some analyses are richer in Al content (8.862-9.028 p.f.u.), Fe (0.047-0.242 p.f.u.) than those of the Bo Phloi sapphirines. However, their formula of both occurrences correspond closely to sapphirine stoichiometry (Deer *et al*., 1992) and they also display high values of $Mg/(Mg+Fe^{2+})$ ratio (~92-99%). The $Mg/(Mg+Fe^{2+})$ ratios of sapphirines in Southeast Asia sapphires are similar to that of the sapphirine in Chanthaburi ruby reported by Sutthirat (2001). In general, the appearance of sapphirine is typically linked to high-pressure and high-temperature conditions. These results could indicate that the onset of crystallization of these sapphirines together with their host sapphires may have been under a relatively high temperature and pressure condition, probably regional/contact metamorphic environment.

Table 3-8 Representative EPMA analyses of **sapphirine inclusions** in Southeast Asia sapphires *(n.a. = not analyzed).*

Mineral phase	Thailand		Laos			Bo Na Wong (Sutthirat *et al.*, 2001)
Analysis (wt%)	Bo Phloi		Huai Sai			
	3LGD6d-2	3BB8b-1	HSA7h6	HSB1a5	HSC3a3	NWEP-9
SiO_2	20.87	18.32	14.19	13.67	13.39	13.79
TiO_2	0.06	0.04	0.03	0.02	0.16	0.00
Al_2O_3	56.50	67.94	65.92	66.76	65.46	62.91
Cr_2O_3	0.00	0.00	0.02	0.00	0.10	0.24
FeO	0.38	0.47	1.08	0.50	2.47	3.07
MnO	0.01	0.00	0.00	0.00	0.00	0.21
MgO	20.95	13.30	19.32	20.20	17.34	18.99
CaO	0.02	0.05	0.13	0.05	0.09	0.11
Na_2O	0.06	0.00	0.17	0.06	0.01	n.a.
K_2O	0.04	0.00	0.53	0.01	0.03	n.a.
Total	98.89	100.12	101.38	101.26	99.05	99.32
20 (O)						
Si	2.407	2.069	1.619	1.553	1.567	1.620
Ti	0.005	0.004	0.003	0.001	0.014	0.000
Al	7.682	9.043	8.862	8.940	9.028	8.710
Cr	0.000	0.000	0.002	0.000	0.009	0.022
Fe	0.036	0.044	0.103	0.047	0.242	0.302
Mn	0.001	0.000	0.000	0.000	0.000	0.021
Mg	3.604	2.239	3.286	3.421	3.026	3.326
Ca	0.003	0.006	0.016	0.006	0.012	0.014
Na	0.012	0.000	0.038	0.013	0.002	-
K	0.006	0.000	0.076	0.001	0.004	-
Total*	13.757	13.406	14.004	13.982	13.904	14.014
$\sum R^{2+}$	3.644	2.289	3.405	3.474	3.279	3.662
$Mg/(Mg+Fe^{2+})$	0.990	0.981	0.970	0.986	0.926	0.917

$\sum R^{2+} = Fe^{2+}+Mn+Mg+Ni+Ca$

Staurolite: strurolite inclusion was rarely found in basaltic sapphires of Southeast Asia (including Bo Phloi sapphires). In this work, only one analysis is acceptable as composition of staurolite inclusion in Gia Nghia sapphire from Vietnam (Table 3-9). Recalculated atomic cations, based on 48 oxygens, of Gia Nghia staurolite (GNA4d-1) is quite similar to that of the Bo Phloi staurolite (3LGC9b-1). Although, the Bo Phloi staurolite is slightly lower in MgO content, both comprise similar composition of 28-30% SiO_2, 52-59% Al_2O_3 and 12-15% MgO with traces of FeO. Even though the vaiability of chemical compositions is generally found in

staurolite structure, staurolite usually occurs at high temperature condition. Hence, the presence of staurolite inclusions in these sapphires may imply a high temperature condition of their host sapphire crystallization.

Table 3-9 Representative EPMA analyses of **staurolite inclusions** in Southeast Asia sapphires *(n.a. = not analyzed).*

Mineral phase	Thai	Viet Nam	Staurolite
Analysis (wt%)	Bo Phloi	Gia Nghia	(Deer *et al.*, 1992)
	3LGC9b-1	GNA4d-1	(anal.2)**
SiO_2	28.67	29.41	26.62
TiO_2	0.00	0.02	1.67
Al_2O_3	58.92	52.36	55.15
Cr_2O_3	0.03	0.00	n.a.
FeO	0.31	1.17	9.75
MnO	0.00	0.00	0.03
MgO	12.04	15.36	5.31
ZnO	n.a.	0.00	n.a.
CaO	n.a.	0.09	0.00
Total	99.97	98.40	98.53
48 (O)			
Si	7.657	8.049	7.546
Ti	0.000	0.003	0.356
Al	18.544	16.890	18.423
Cr	0.005	0.000	-
Fe^{2+}	0.069	0.267	2.311
Mn	4.793	6.269	2.244
Mg	0.000	0.000	0.000
Zn	-	0.026	-
Ca	-	0.026	0.000
Total*	31.068	31.529	30.880
$\sum R^{2+}$	4.862	6.587	4.555
$\sum R^{3+}$	26.206	24.942	26.325

$\Sigma R^{2+} = Fe^{2+}+Mn+Mg+Zn+Ca$

$\Sigma R^{3+} = Si+Ti+Al+Cr$

***Staurolite, sapphirine-garnet-gedrite-spinel-corundum-phlogospite rock.*

Zircon: zircon inclusions are found in only Thai sapphires from Kanchanaburi and Phrae. This may be due to the limited numbers of sapphires from other localitites. Some BSI images of these mineral inclusions are displayed in Figures 3-13.

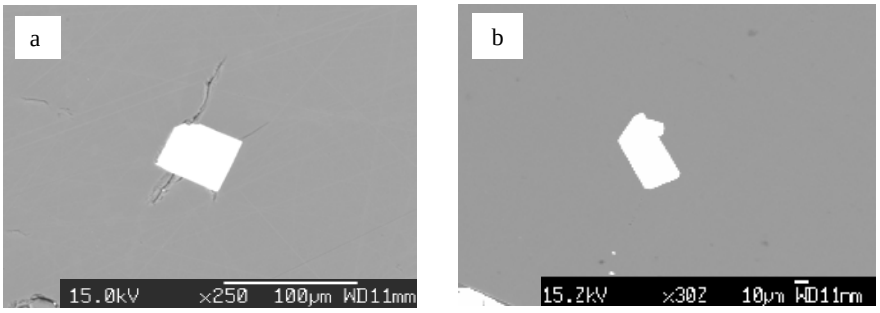

Figure 3-13 Back scattered electron images (BSI) of zircon inclusions found in (a) trapiche Kanchanaburi sapphire in Thailand (b) Phrae sapphire in Thailand.

The chemical compositions of zircon inclusions in Thai sapphires (Table 3-10) show very consistent contents of approximately 32-34% SiO_2, 61-66% ZrO_2 and 1.37-3.50% HfO_2. A zircon inclusion observed in trapiche Kanchanaburi sapphire has relatively higher HfO_2 content (3.47%) which is similar to a zircon inclusion of blue Bo Phloi sapphire (sample *3BC9a-1*). However, the ranges of Hf content (including the other elemental compositions) in all zircon inclusions studied here, also illustrate the chemical composition confirming zircon-corundum co-crystallization series (e.g., Guo *et al.*, 1996b, Sutherland *et al.*, 1998b; 2002). In addition, the Zr-Hf-Si ternary diagram of zircon inclusions from all localities display very close to one another (Figure 3-14). This result indicates that the zircon inclusions in Southeast Asia sapphires may have been originated from a similar provenance.

Table 3-10 Representative EPMA analyses of **zircon inclusions** in Southeast Asia sapphires.

Mineral phase	Thailand					
Analysis (wt%)	Bo Phloi				Trapiche Kanchanaburi	Phrea
	2DGC6a-REE2	3LGC1c-1	3BC9a-1	3LBC9a	TK1a-1	PB4a4
SiO_2	32.49	34.22	34.14	33.83	32.85	32.96
ZrO_2	65.57	64.04	62.40	65.13	61.68	63.47
HfO_2	1.75	1.37	3.50	2.33	3.47	1.20
Al_2O_3	0.01	0.00	0.17	0.02	1.10	2.23
CaO	0.00	0.02	0.00	0.00	0.07	0.00
FeO	0.06	0.03	0.04	0.05	0.31	0.07
Total	99.87	99.68	100.25	101.35	99.48	99.93
4 (O)						
Si	0.998	1.038	1.036	1.019	1.007	0.994
Zr	0.982	0.947	0.923	0.956	0.922	0.933
Hf	0.018	0.014	0.036	0.024	0.036	0.012
Al	0.000	0.000	0.006	0.001	0.040	0.079
Ca	0.000	0.001	0.000	0.000	0.002	0.000
Fe	0.001	0.001	0.001	0.001	0.008	0.002
Total*	2.001	2.001	2.002	2.001	2.015	2.021
Atomic%						
Si	49.9	51.9	51.9	51.0	51.2	51.2
Zr	49.1	47.4	46.3	47.8	46.9	48.1
Hf	0.9	0.7	1.8	1.2	1.8	0.6
Total**	100.0	100.0	100.0	100.0	100.0	100.0

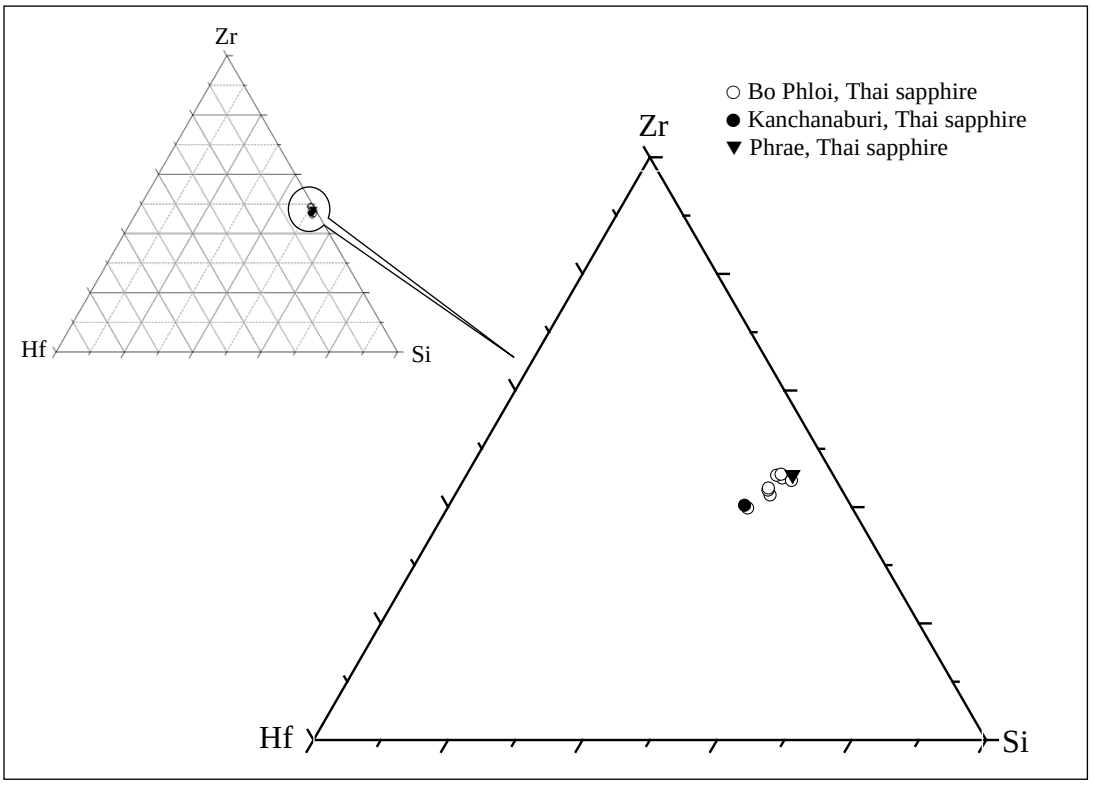

Figure 3-14 The Zr-Hf-Si ternary plots of compositions of zircon inclusions found in basaltic sapphires of Southeast Asia, mostly from Thailand.

Columbite: columbite inclusions were rarely found in Chanthaburi sapphires (only acceptable one analysis) and more commonly discovered in Pailin sapphires. Their major and some trace elements compositions are depicted in Table 3-11. Among the micro-sized mineral inclusions found in Southeast Asia basaltic sapphires, columbite inclusions exhibited the largest size crystals (up to 100 μm across; Figure 3-15). Some BSI images of columbite inclusions are displayed in Figure 3-15 and more data are collected in Appendix C.

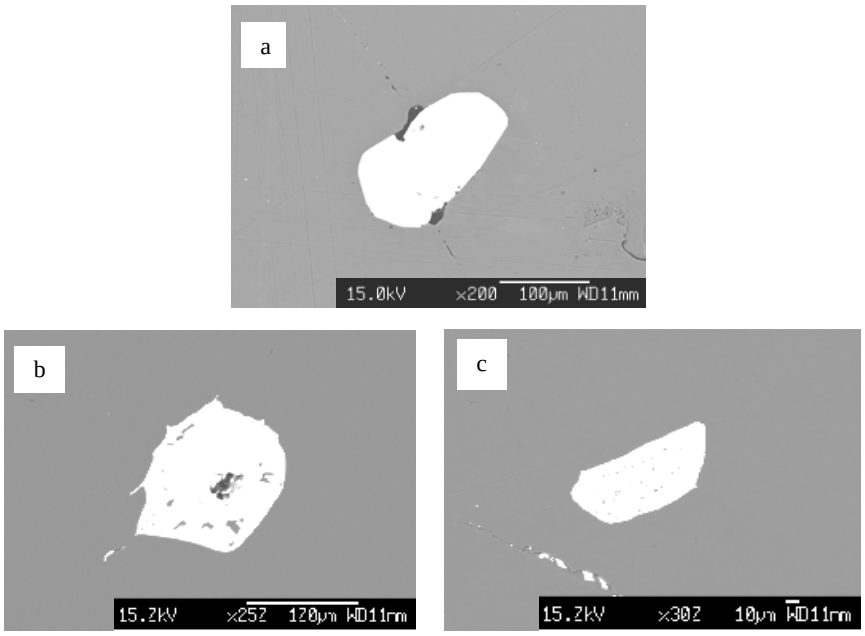

Figure 3-15 Back scattered electron images (BSI) of columbite inclusions found in (a) Chanthaburi sapphire in Thailand and (b, c) Pailin sapphires in Cambodia.

As seen in Table 3-11, all columbite analyses show quite similar chemistry which is close to ferrocolumbite composition. They comprise approximately 13.05-14.35% FeO, 5.77-7.35% MnO and low (1.00-2.23%) Ta_2O_5 contents. The chemical formula of Chantaburi and Pailin columbites can be expressed as $(Fe_{0.66}Mn_{0.28}Mg_{0.12}Ti_{0.07})$ $(Nb_{1.87}Ta_{0.02}Th_{0.01})O_6$ and $(Fe_{0.61\text{-}0.68}Mn_{0.32\text{-}0.35}Mg_{0.00\text{-}0.02}Ti_{0.03\text{-}0.05})(Nb_{1.84\text{-}1.89}Ta_{0.01\text{-}0.03}Th_{0.00\text{-}0.07})O_6$, respectively. In addition, the previous analyses of columbite inclusions in some Australian sapphires are also reported in Table 3-11 for comparison; including HN13 from Wenchang (Guo *et al.*, 1996a), LP32 from Lava Plains (Guo *et al.*, 1996a) and one from New England (Sutherland *et al.*, 1998b). The chemical composition of Southeast Asia columbite inclusions studied here, exhibit closely similar trace element patterns (see Figure 3-16) to the Australian columbite inclusions reported by Guo *et al.* (1996a) and Sutherland *et al.* (1998b). In addition, both Southeast Asia and Australia columbites are still enriched in Nb and depleted in Ta, suggesting similar environment of crystallization.

Columbite is usually abundance in Nb-Ta oxide. The high Nb concentration in these columbite inclusions therefore indicates that they should have formed in a Nb-rich environment. Although, columbite inclusion relationship favors growth from silicate melt (Sutherland *et al.*, 1998b), Guo *et al.* (1996a) earlier proposed that this inclusion relationship could also favor growth from carbonatite liquid. Therefore,

from such arguments, columbite inclusions could possibly be related to either silicate melt or carbonatite condition or both environments.

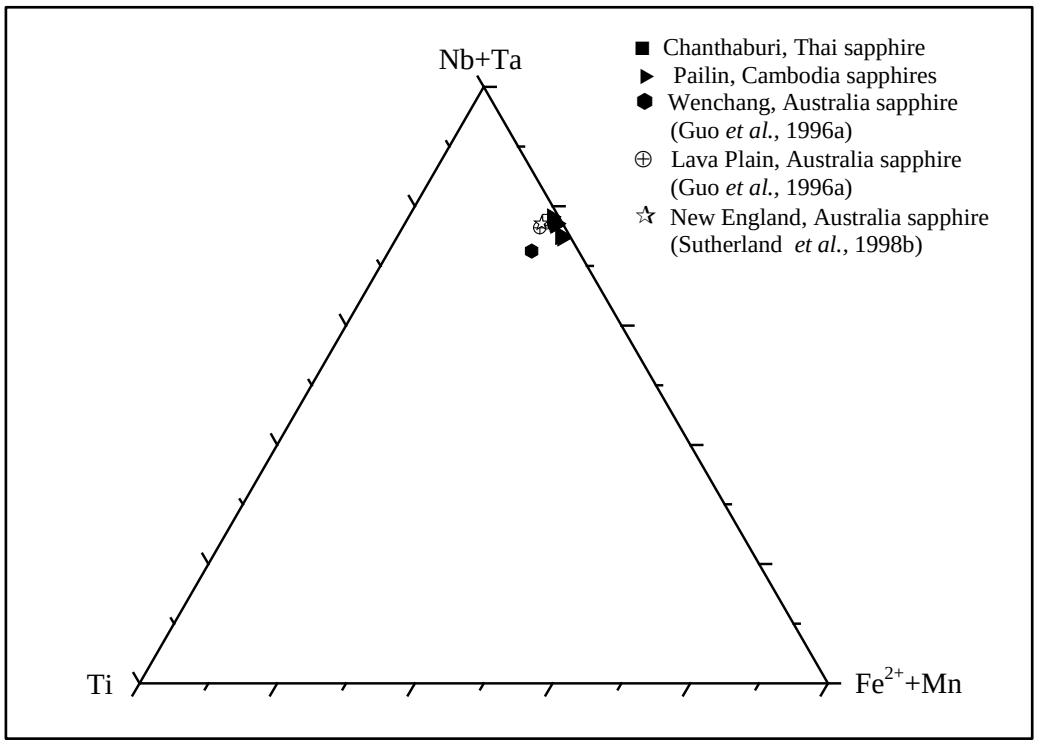

Figure 3-16 The (Nb+Ta)-Ti-(Fe^{2+}+Mn) ternary plots of compositions of columbite inclusions found in basaltic sapphires of Southeast Asia.

Table 3-11 Representative EPMA analyses of **columbite inclusions** in Southeast Asia sapphires *(n.a. = not analyzed).*

Mineral phase	Thailand	Cambodia				Australia		
Analysis (wt%)	Chan	Pailin				Wenchang (Guo *et al.*, 1996a)	Lava Plains (Guo *et al.*, 1996a)	New England (Sutherland *et al.*, 1998b)
	TC1a3	TPA4a1	TPA4e1	TPA4g1	TPA4h	HN13	LP32	(Nb-rich)
SiO_2	0.19	0.12	0.08	0.08	0.11	n.a.	0.01	0.00
TiO_2	1.72	1.10	0.81	1.22	1.17	6.62	3.57	3.03
Al_2O_3	0.05	2.22	0.67	0.62	1.09	n.a.	0.07	0.33
Cr_2O_3	0.00	0.01	0.02	0.02	0.00	n.a.	n.a.	0.00
FeO	13.96	13.05	13.92	14.30	14.35	15.89	16.59	17.44
MnO	5.77	7.34	7.35	7.17	6.69	4.32	2.99	2.19
MgO	1.41	0.21	0.13	0.25	0.13	0.34	1.18	0.54
CaO	0.09	0.02	0.09	0.05	0.06	0.01	0.03	0.00
ZnO	0.01	0.03	0.11	0.15	0.00	n.a.	n.a.	0.00
Nb_2O_5	73.34	72.41	73.40	72.59	72.40	66.50	71.98	73.95
Ta_2O_5	1.36	1.30	1.00	2.23	2.13	4.10	2.98	2.38
ThO_2	0.77	0.00	0.00	0.00	0.52	0.00	0.01	n.a.
UO_2	0.00	0.92	0.91	0.00	0.10	0.17	0.12	n.a.
ZrO_2	0.43	0.54	0.21	0.65	0.71	2.51	0.40	0.52
HfO_2	0.00	0.01	0.15	0.00	0.00	n.a.	n.a.	n.a.
P_2O_5	0.00	0.00	0.00	0.00	0.00	n.a.	n.a.	n.a.
Y_2O_3	0.00	0.00	0.00	0.00	0.00	0.08	0.01	n.a.
La_2O_3	0.00	0.00	0.00	0.00	0.00	n.a.	n.a.	n.a.
Ce_2O_3	0.14	0.06	0.06	0.10	0.00	n.a.	n.a.	n.a.
Nd_2O_3	0.00	0.05	0.07	0.03	0.04	0.04	n.a.	n.a.
Sm_2O_3	0.00	0.04	0.03	0.13	0.00	0.17	n.a.	n.a.
Total	99.24	99.41	99.01	99.58	99.50	100.75	99.94	100.38
6 (O)								
Si	0.011	0.007	0.005	0.005	0.006	-	0.001	0.000
Ti	0.073	0.046	0.035	0.052	0.050	0.280	0.150	0.127
Al	0.003	0.147	0.045	0.041	0.073	-	0.005	0.022
Cr	0.000	0.001	0.001	0.001	0.000	-	-	0.000
Fe	0.659	0.613	0.664	0.679	0.681	0.747	0.776	0.812
Mn	0.276	0.350	0.355	0.345	0.322	0.206	0.142	0.103
Mg	0.119	0.017	0.011	0.021	0.011	0.028	0.098	0.045
Ca	0.006	0.001	0.006	0.003	0.003	0.001	0.002	0.000
Zn	0.001	0.001	0.005	0.006	0.000	-	-	0.000
Nb	1.872	1.840	1.894	1.863	1.858	1.690	1.819	1.860
Ta	0.021	0.020	0.015	0.034	0.033	0.063	0.045	0.036
Th	0.010	0.000	0.000	0.000	0.007	0.000	0.000	-
U	0.000	0.011	0.012	0.000	0.001	0.002	0.001	-
Zr	0.005	0.007	0.003	0.008	0.009	0.031	0.005	0.006
Hf	0.000	0.000	0.002	0.000	0.000	-	-	-
P	0.000	0.000	0.000	0.000	0.000	-	-	-
Y	0.000	0.000	0.000	0.000	0.000	0.004	0.000	-
La	0.000	0.000	0.000	0.000	0.000	-	-	-
Ce	0.003	0.001	0.001	0.002	0.000	-	-	-
Nd	0.000	0.000	0.001	0.000	0.000	0.000	-	-
Sm	0.000	0.000	0.000	0.001	0.000	0.002	-	-
Total*	3.058	3.063	3.054	3.063	3.054	3.054	3.044	3.011

Apatite: some acceptable analyses of apatite inclusions in Chanthaburi sapphires are found herein. A BSI image of apatite inclusion is showed in Figure 3-17. Due to a certain limitation of EPMA technique applied in this study, the partial chemical analyses give unsatisfied results are displayed in Appendix C. The major

element contents of these analyses are approximately 45-54% CaO, 20-28% P_2O_5, 0.8% MnO, 0.1-0.5% FeO, which fall within a reasonable range of apatite (Deer *et al*., 1992), although, they show relatively too low P_2O_5 contents (probably due to poor polished surface). Generally, apatite is a common accessory mineral in many rock types, particularly, granitic pegmatite.

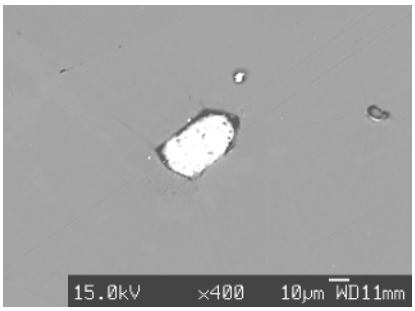

Figure 3-17 Back scattered electron image (BSI) of apatite inclusion found in a Chanthaburi sapphire from Thailand.

Pyrochlore: in this work, pyrochlore inclusions were only found in Pailin sapphires from Cambodia. Some micro-sized pyrochlore crystals are displayed in Figures 3-18; moreover, a BSI image is illustrated in Figures 3-19. Raman spectrum of pyrochlore inclusion is representatively shown in Figures 3-20.

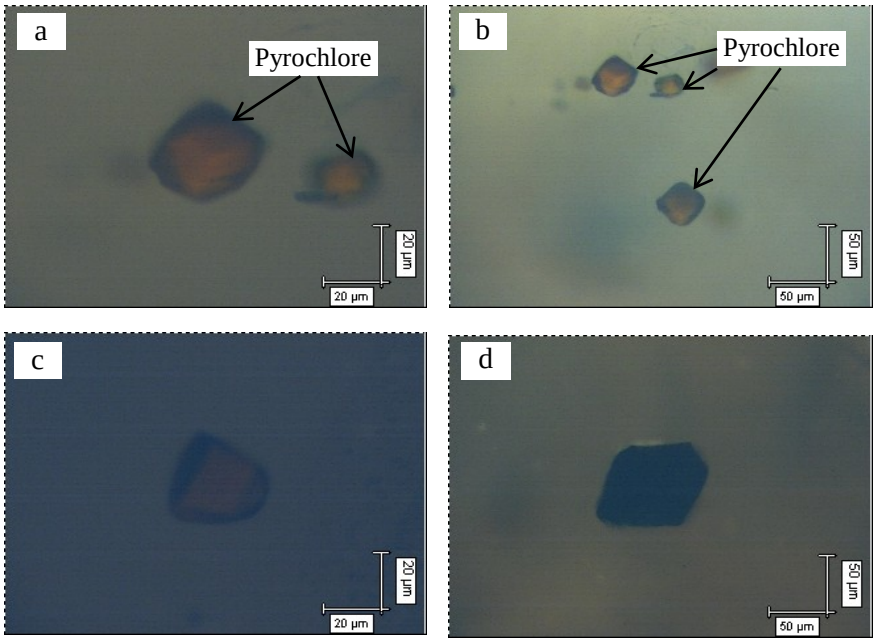

Figure 3-18 Pyrochlore inclusions (a-d) found in Pailin sapphires from Cambodia.

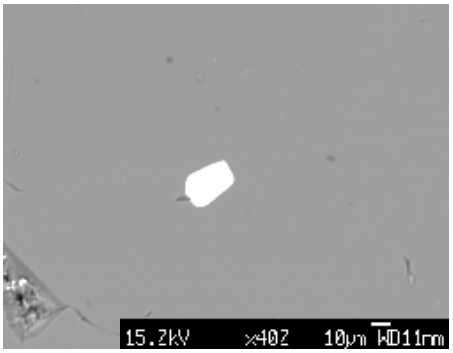

Figure 3-19 Back scattered electron image (BSI) of pyrochlore inclusion found in a Pailin sapphire from Cambodia.

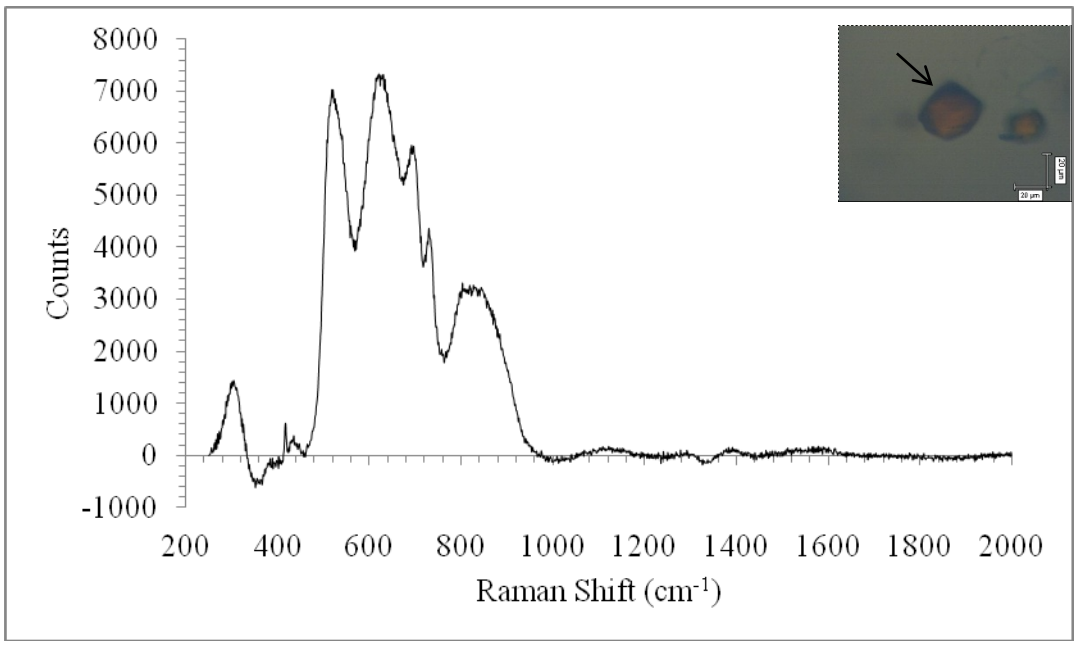

Figure 3-20 Raman spectrum of a pyrochlore inclusion observed in the sample *TPA7a* of Pailin sapphire in Cambodia.

The representative EPMA results of pyrochlore inclusions are shown in Table 3-12. The pyrochore analyses in these samples yielded very low total contents, probably due to the uncertainty in elemental peak overlaps as well as poor polished surface. In general the chemical formula of pyrochlore is rather variable; that can be simplified into $A_{1-2}B_2O_6(O,OH,F).nH_2O$ (where A represents Na, Ca, Mn, Fe, Mg etc. and B represents Nb, Ta, Ti, etc.). However, the presence of pyrochlore inclusions in Pailin sapphires was initially confirmed by Raman spectra (Figure 3-20), these pyrochlore analyses could be their approximated compositions that may contain

somewhat too high Nb contents. Most Pailin pyrochlore inclusions display Nb-rich with significant Ta substitution that indicate their host sapphires may related with the Nb-rich environment.

Table 3-12 Representative EPMA analyses of **pyrochlore inclusions** in Southeast Asia sapphires.

Mineral phase Analysis (wt%)	Cambodia		
	Pailin		
	TPA7a	TPA7g	TPA7b
SiO2	0.18	0.25	0.10
TiO2	4.63	4.77	1.14
Al2O3	0.75	0.64	0.09
FeO	1.06	0.79	0.12
MnO	0.06	0.15	0.82
MgO	0.00	0.01	0.17
ZnO	0.00	0.00	0.00
Na2O	7.15	6.21	6.76
K2O	0.16	0.00	0.76
CaO	7.34	7.34	7.45
Nb2O5	70.63	68.63	70.96
Ta2O5	5.85	2.12	1.02
UO2	0.20	1.23	2.01
ThO2	0.02	0.30	0.49
Ga2O3	0.00	0.00	0.00
Total	98.01	92.43	91.89
6 (O)			
Si	0.010	0.015	0.006
Ti	0.193	0.209	0.051
Al	0.049	0.044	0.006
Fe	0.049	0.038	0.006
Mn	0.003	0.008	0.042
Mg	0.000	0.001	0.015
Zn	0.000	0.000	0.000
Na	0.767	0.700	0.785
K	0.000	0.000	0.000
Ca	0.435	0.457	0.478
Nb	1.768	1.804	1.922
Ta	0.088	0.034	0.017
U	0.002	0.016	0.027
Th	0.000	0.004	0.007
Ga	0.000	0.000	0.000
Total*	3.364	3.328	3.362

CHAPTER 4
TRACE ELEMENT GEOCHEMISTRY AND DATING OF MINERAL INCLUSIONS

4.1 Introduction

Zircon is a common mineral inclusion found in most corundum deposits associated with alkali basalts in Southeast Asia and elsewhere; it normally assumes to be cogenetic with its host corundum (e.g., Coenraads *et al.*, 1995; Guo *et al.*, 1996a; 1996b). Hence the trace element geochemistry of zircon inclusions observed in sapphire is able to provide the fingerprints and important information for the genetic model of its host mineral. In addition, a zircon inclusion is often used for U-Pb geochronology by which the measured date could represent the age of its host sapphire crystallization and hence the parental melt.

Many models existing for sapphire formation at depth under basaltic fields were used to constrain by information obtained from the REE geochemistry and dating of zircon inclusions (e.g., Sutherland and Fanning, 2001; Sutherland *et al.*, 2002; 2008; Graham *et al.*, 2008). From previously published data, many U-Pb isotopic dating techniques including Sensitive High Resolution Ion Microprobe (SHRIMP), Laser Ablation Inductively Coupled Plasma Mass Spectrometry (LA-ICP-MS), Secondary Ion Mass Spectrometry (SIMS), and evaporation method were used for measuring the zircon ages (*e.g.*, Compston, 1999; Zhao *et al.*, 2002; Black *et al.*, 2003; Kusiak *et al.*, 2008). Among those techniques, LA-ICP-MS is the one widely used for age determination as well as trace element analysis due to its high sensitivity (e.g., Fryer *et al.*, 1993; Norman *et al.*, 1998; Kosler and Sylvester, 2003; Black *et al.*, 2004; Jackson *et al.*, 2004; Xia *et al.*, 2004; Chang *et al.*, 2006). It is also a robust and cost effective technique. This technique is however difficult to obtain the growth record of a zircon grain, because the spatial resolution of LA-ICP-MS method is usually greater than 25 μm; hence, the reliable ages of thin growth rims are difficult to determine. Furthermore, this method is also destructive technique during sample analysis.

Currently, the Th-U-Pb dating using Electron Probe Micro Analyzer (EPMA), a non-destructive analysis, is widely established and becoming an efficient tool for dating method (*e.g.*, Suzuki and Adachi, 1991; Montel *et al.*, 1996; Cocherie *et al.*,

1998; Cocherie and Albarede, 2001; Suzuki and Kata, 2008). The Th-U-Pb dating has been developed into an alternative, accurate, and truly *in-situ* means of geochronology which could provide valuable constraints on the timing at a μm scale (Williams and Jercinovic, 2002; Cocherie and Legendre, 2007). This ability to provide ages for very small areas has made it possible to illustrate the lack of significant diffusion process of elements in samples. This technique can be applied to measure the ages of zircon and monazite in particular. Because monazite usually contains rather high contents of Th and U and negligible amount of common Pb, this mineral is a suitable geochronometer for studying magmatic and polymetamorphic events (Parrish, 1990; Zhu and O'Nions, 1999; Liu *et al.*, 2007; Li *et al.*, 2008; Vlach, 2010). Also monazite is a LREE-bearing phosphate mineral that is present in a wide variety of rock types, has an extremely variable composition reflecting host rock conditions, and is a robust geochronometer that can preserve crystallization ages through a long history of geological events. The recognition that diffusion rates of many element in monazite is very slow, particular diffusion of Pb in monazite is negligible (Cherniak *et al.*, 2004), and thus monazite can retain a record of previous geologic conditions. Although, monazite has been isotropically dated for decades, the electron microprobe can now provide age constraints on the generally small and irregular domains that have been linked to geologic processes. However, the application of Th-U-Pb dating by EPMA technique on zircon and monazite inclusions in sapphires host has not been reported in previous literatures yet.

4.2 Sample and Methodology

In this study, a distinctive zircon inclusion (sample *1B3ib2*) observed in dark grayish brown Bo Phloi sapphire was selected as a suitable inclusion for analyses of trace element and rare earth element (REE) contents and U-Pb isotropic dating. This is because the inclusion has a good oval shape, large size (~ 200 μm) and lack of fracture (see in Figure 4-1). The LA-ICP-MS technique was employed for the trace element analysis and U-Pb dating of the zircon inclusion in this work. This technique was performed using a Perkin-Elmer ELAN 6000 ICPMS model coupled to a laser ablation microscope, based at GEMOC, Macquarie University, Australia. Detailed descriptions of instrumentation and analytical and calibration procedures are refered to Belousova *et al.* (2002). The laser-ablation system is a Continuum Surelite I-20 Q-

switched Nd: YAG laser with a fundamental infrared (IR) wavelength at 1,064 nm and a pulse width of 5-7 ns. Two frequency doubling crystals provide second and fourth harmonics in the visible (VIS, 532 nm) and ultraviolet (UV, 266 nm), respectively. The 266-nm beam was used for the trace element analyses reported here. Most of the analyses have been done with a pulse rate of 4 Hz (pulses per second) and beam energy of 1 mJ per pulse, producing a spatial resolution of 30-50 μm. This instrument is able to measure in sub-ppb level from Li up to Pb elements. It also requires the standard elements to calculate a concentration conversion factor which can then be used to convert the raw data from unknown samples into quantitative analyses. The NIST-610 standard glass was used as the external calibration standard. Quantitative results for all elements were obtained through calibration of relative element sensitivities using the NIST-610 standard glass, and normalisation of each analysis to the electron-probe data for Hf as an internal standard. The reference data for the NIST-610 calibration standard glass are given in Norman *et al.* (1996; 1998). The NIST-610 standard glass was analyzed as an unknown at least once for each 15 mineral analyses to assess the data quality. The precision and accuracy of these NIST-610 analyses are 2–5% for REE, Y, Sr, Nb, Ta, Hf, Th and U at the ppm concentration level, and from 8 to 10% for Mn, P, Fe, Ga, Sn and Pb.

Apart from U-Pb dating by LA-ICP-MS, the preliminary study of Th-U-Pb dating on zircon and monazite inclusions was also carried out using EPMA. Altogether ten mineral inclusions (six zircons and four monazites) were selected for initial investigation by this Th-U-Pb dating technique. These inclusions are variable in sizes from ten μm to several hundreds of μm across. Back Scattered Electron (BSE) images of zircon and monazite inclusions are illustrated in Figures 4-1 and 4-2, respectively. Chemical compositions of both mineral inclusions were quantitatively analyzed using an EPMA, JEOL model JXA-8100, based at Department of Geology, Chulalongkorn University (as shown in Figure 1-2, Chapter 1). For this dating technique, most of the standards used for calibration were pure oxides and mineral standards similar to those described in Chapter 1. Except for Th, U and REEs analyses, they were calibrated using external standards prepared by Miss Sopit Poompeang. In addition, to compare and select a better result, the measurement was performed at two accelerating voltage conditions of 15.0 and 20.0 kV. The others operating condition was set about 100 nA sample current, with focused beam smaller

than 1 μm. Measuring times of general elements were set at 30 seconds and 10 seconds for peak and background counts, respectively, for each element using suitable analytical crystals, while the counting time on peak and background of Pb, Th and U used for dating were set at 270, 120 and 180 seconds, respectively. The X-ray lines are $M\alpha$ for Pb, Th and U. Subsequently, the Th-U-Pb age of both zircon and monazite inclusions were calculated using "EPMA dating" program provided by Pommier *et al.* (2002) under the calculated detection limit (2σ) of are 60 ppm for Th, U and Pb in zircon samples and 150 ppm for those in monazite samples.

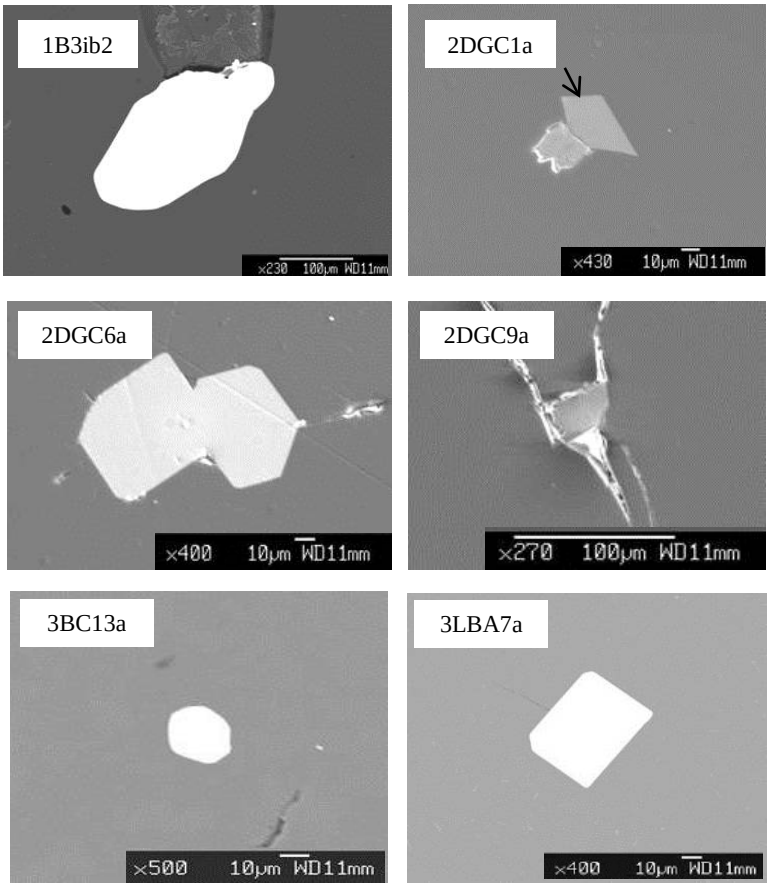

Figure 4-1 BSE images of zircon inclusions in Bo Phloi sapphires selected for Th-U-Pb dating by EPMA. The largest inclusion (sample *1B3ib2*; top left photo) found in a dark grayish brown sapphire was also selected for trace analysis and U-Pb dating by LA-ICP-MS.

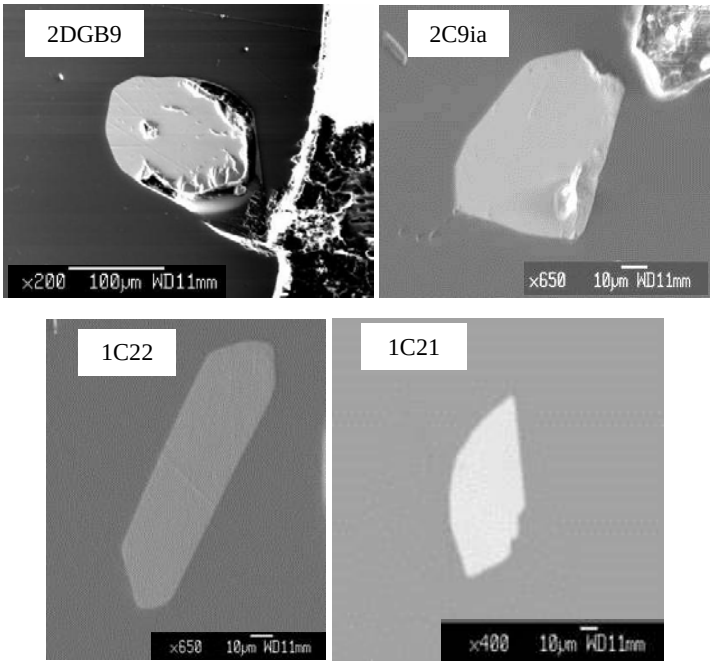

Figure 4-2 BSE images of monazite inclusions in Bo Phloi sapphires selected for Th-U-Pb dating by EPMA.

4.3 Trace Element Geochemistry of Bo Phloi Zircons

The trace element contents of Bo Phloi zircon inclusion (sample *1B3ib2*) are depicted in Table 4-1. In addition, the mean values of trace element compositions of zircons from different rocks; namely syenite, syenite pegmatite, nepheline-syenite pegmatite, carbonatite and granitoid rocks reported by Belousova *et al.* (2002) and zircon inclusion in Huai Sai sapphire (Sutherland *et al.,* 2002) are also displayed for comparison in this table. Trace element contents of Bo Phloi zircon inclusion exhibit closely similar to those of zircons from some rocks, particularly syenite, syenite pegmatite, nepheline-syenite pegmatite. Moreover, the Hf content in Bo Phloi zircon inclusion is rather high (1.32 wt%) which is close to those found in zircon grains from granitoid and nepheline-syenite pegmatites. The concentration of Y in Bo Phloi zircon inclusion falls in thousands of ppm which consistent with the isostructural relationship of xenotime (YPO_4) and zircon (Deer *et al.*, 1992). The total REE contents of Bo Phloi zircon (2507.27 ppm) are quite enriched and close to those of zircons from syenite-pegmatite rock (see Table 4-1). In general, the REEs substitute preferentially for Zr in the zircon structure because of their ionic radii are similar to Zr^{4+} and a coupled substitution mechanism is available ($REE^{3+} + P^{5+} = Zr^{4+} + Si^{4+}$). The highest Hf, Y, P REEs as well as Nb, Ta occur in Bo Phloi zircon inclusion

suggests coupled substitution of these elements within the zircon structure. For example, $(REE, Y)^{3+} + P^{5+} = Zr^{4+} + Si^{4+}$, $(REE, Y)^{3+} + (Nb, Ta)^{5+} => 2Zr^{4+}$ and $(REE, Fe)^{3+} + (Nb, Ta)^{5+} => 2Zr^{4+}$ coupled substitutions (as suggested by Belousova *et al.*, 2002).

Heaman *et al.* (1990) reported that the trace element contents in zircon mineral observed in different rock types such as carbonatite, kimberlite, alkali basalt, nepheline syenite, and granite could be applied as geochemical fingerprints and then used to differentiate their parent magma. In this study, the level of substitution of such elements for Zr in this zircon inclusion is exceptionally high, suggesting enrichments of Hf, Y, P and REEs in their parental environment. This indicates that the zircon inclusion together with its host sapphire may originate from very evolved magma. Also shown in Table 4-1, the Th/U ratio of Bo Phloi zircon inclusion is less than 1 (0.33), which is close to those of magmatic zircons (Hoskin and Schaltegger, 2003), to that of Huai Sai zircon inclusion (0.43) and to that of zircon inclusion found in basaltic sapphires (Guo *et al.*, 1996b). U^{4+} is preferentially substituted into the zircon structure relative to Th^{4+}, because its ionic radius is closer to that of Zr^{4+} (Ahrens *et al.*, 1967; Shannon, 1976). Therefore the low Th/U ratios may be due to such fact and/or U enrichment of the parent rocks. Moreover, the value of Nb/Ta ratio of Bo Phloi zircon inclusion is 1.75 similar to those of zircon from other rocks except for such value of zircons from nepheline-syenite pegmatites (about 13.33). In fact, both Nb and Ta have the same ionic radius with Zr (Zr^{4+} = 0.72 Å, Nb^{5+} = 0.64 Å and Ta^{5+} = 0.64 Å) (Shannon, 1976). The low Nb/Ta ratio in Bo Phloi zircon inclusion could be explained by the fact that the Ta might have been oxidised easily to 5+ valencies, while some Nb remains in the 4+ valence state (Belousova *et al.*, 2002). In this case, the ionic radius of Ta^{5+} is smaller than that of Nb^{4+}. As such Ta^{5+} would go preferentially into the Zr (Hf) lattice site in the case of Bo Phloi zircon inclusion which might have been formed in a relatively oxidizing environment.

In addition, the contents of Hf and Y of Bo Phloi zircon inclusion (Table 4-1) are plotted with the discriminant framework designed by Shnukov *et al.* (1997) as shown in Figure 4-3. Moreover, the Hf and Y contents of zircon in a zircon + sapphire + nepheline + hercynitic spinel assemblage and of zircon in the ‘Corsilzirspite’ gravel (an unusual rock comprising corundum, sillimanite, zircon and spinel) found in alluvial Bo Phloi gem-bearing layer, unpublished data of Pisutha-Arnond are also plotted for comparison in this figure. As shown in the figure, the Bo Phloi zircon

inclusion, and the zircons in the assemblage and the ‘Corsilzirspite’ gravel mostly fall within the III field (quartz-bearing intermediate and felsic rocks) except some are at the boundaries of II & III and III & IV. This plot suggests that all Bo Phloi zircons and probably its host sapphire are rather related to (non-quartz-bearing) intermediate and felsic rocks.

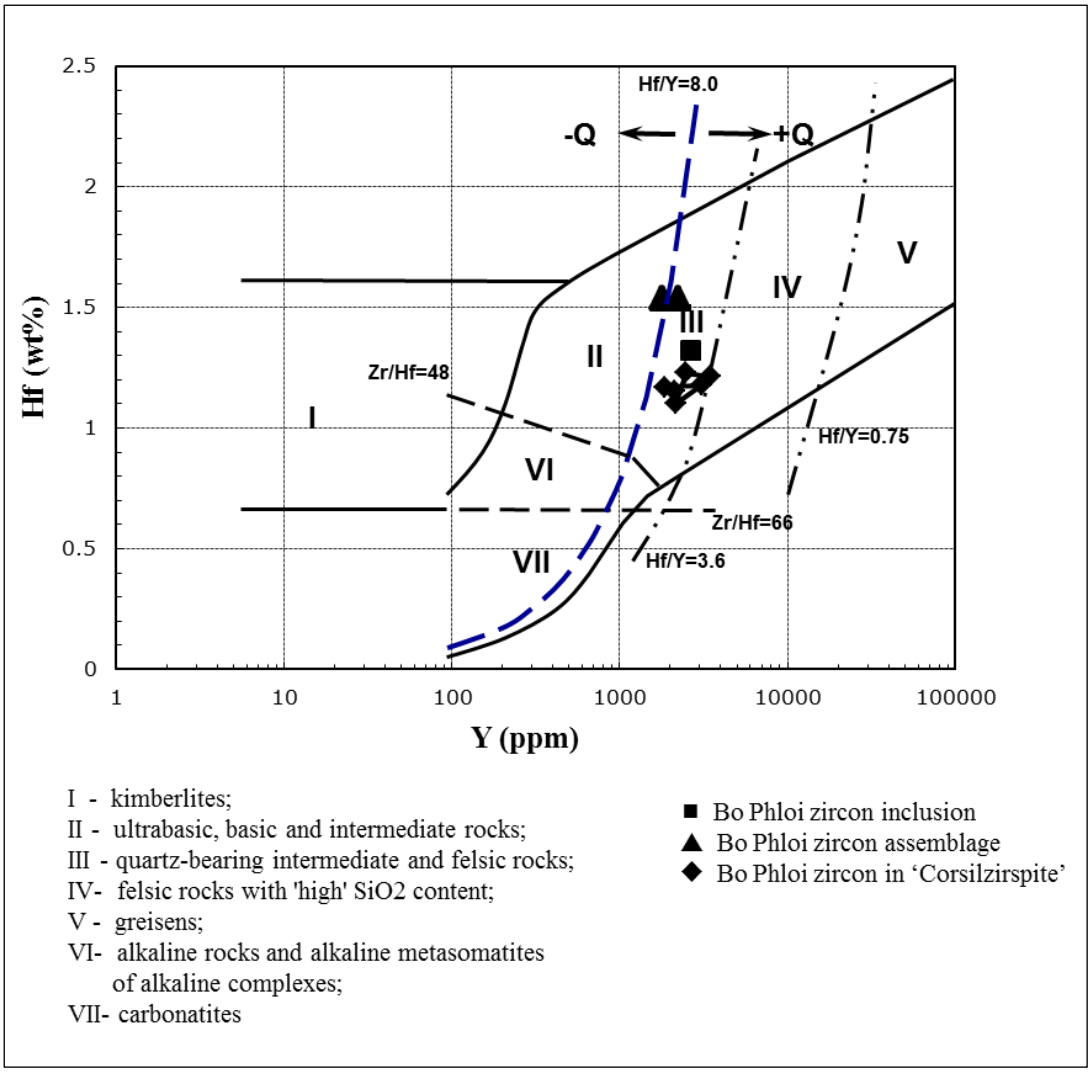

Figure 4-3 Hf and Y concentrations of a zircon inclusion (solid square), zircon assemblage (solid triangle) and zircon in ‘Corsilzirspite’ gravel (solid diamond) (both from unpublished data of Pisutha-Arnond), relative to the fields of zircon composition defined by Shnukov *et al.* (1997).

Some trace elements of Bo Phloi zircon inclusion as well as zircon from the Bo Phloi assemblage and Bo Phloi zircon in the ‘Corsilzirspite’ gravel (unpublished data of Pisutha-Arnond) are compared with those of other zircons in different rocks reported by Belousova *et al.* (2002) in Figures 4-4 to 4-7. Even though there are large

overlapping areas among those trace element cross-plots of zircons from different rock types reported by Belousova *et al.* (2002), some trace elements of Bo Phloi zircon inclusion and both Bo Phloi zircons in assemblage and Bo Phloi zircons in 'Corsilzirspite' gravel seem to fall most frequently in the area of syenite pegmatite (though it often overlaps with granitoids, lavikites, basic rocks and lamproites). These results seem to suggest that the occurrence of all Bo Phloi zircons could have been originated from syenite pegmatite.

Table 4-1 Trace elements data (ppm) of zircon inclusion (sample *1B3ib2*) in Bo Phloi sapphire *(n.a. = not analyzed).*

Analysis (ppm)	Bo Phloi Zircon inclusion (sample *1B3ib2*)	Huai Sai Zircon inclusion *(Sutherland et al., 2002)*	Zircons from different rocks (Belousova *et al.*, 2002)*				
			Syenite	Syenite pegmatite	Nepheline-syenite pegmatite	Carbonatite	Granitoid
Al	5352.71	n.a.	n.a.	n.a.	n.a.	n.a.	n.a.
P	1315.57	1070.00	n.a.	233.00	192.00	52.00	763.00
Ca	<154.73	n.a.	n.a.	n.a.	n.a.	n.a.	n.a.
Ti	8.52	n.a.	659.00	64.30	12.00	-	44.00
Mn	0.82	n.a.	n.a.	-	< 1.3	-	23.00
Fe	39.90	n.a.	n.a.	-	-	-	868.00
Co	<0.032	n.a.	n.a.	n.a.	n.a.	n.a.	n.a.
Ni	<0.49	n.a.	n.a.	n.a.	n.a.	n.a.	n.a.
Cu	<0.25	n.a.	n.a.	n.a.	n.a.	n.a.	n.a.
Zn	0.30	n.a.	n.a.	n.a.	n.a.	n.a.	n.a.
Ga	1.10	n.a.	-	-	-	-	< 4.6
Sr	0.78	n.a.	< 0.08	-	1.20	0.14	4.70
Y	2631.36	6275.00	148.00	3062.00	13036.00	379.00	2515.00
Zr	442873.50	n.a.	n.a.	n.a.	n.a.	n.a.	n.a.
Nb	11.21	n.a.	0.89	16.80	48.00	10.00	4.30
Sn	2.42	n.a.	n.a.	2.10	3.80	< 0.66	< 3.7
Ba	<0.00	n.a.	-	0.16	0.64	-	5.10
La	<0.0049	8.90	-	0.15	0.18	0.17	12.00
Ce	0.84	47.00	2.40	34.00	175.00	4.50	61.00
Pr	0.06	2.20	< 0.03	0.60	0.71	0.54	8.00
Nd	0.92	7.60	0.33	9.20	9.60	6.20	44.70
Sm	2.85	8.10	0.36	14.00	23.00	6.60	21.50
Eu	0.19	0.35	0.34	2.60	5.00	4.00	2.10
Gd	22.58	45.00	2.10	73.00	117.00	20.00	58.00
Dy	182.86	382.00	12.00	318.00	874.00	56.00	224.00
Ho	81.63	170.00	5.00	110.00	396.00	15.00	85.00
Er	467.28	1014.00	26.00	482.00	2231.00	53.00	378.00
Yb	1458.97	3045.00	67.00	836.00	4428.00	64.00	769.00
Lu	289.09	741.00	14.00	164.00	723.00	11.00	150.00
Hf (wt%)	1.32	3.03	0.59	0.95	1.46	1.04	1.28
Ta	6.42	n.a.	0.40	5.20	3.60	6.10	2.30
Pb206	2.31	n.a.	2.40	11.00	47.00	7.70	8.80
Pb207	<0.076	n.a.	n.a.	n.a.	n.a.	n.a.	n.a.
Pb208	0.11	n.a.	n.a.	n.a.	n.a.	n.a.	n.a.
Th	131.73	1580.00	31.00	647.00	2497.00	212.00	368.00
U	402.86	3635.00	88.00	356.00	9.00	0.29	764.00
Total REE	2507.27	5471.15	129.53	2043.55	8982.49	241.01	1813.30
Th/U	0.33	0.43	0.35	1.82	277.44	731.03	0.48
Nb/Ta	1.75	-	2.23	3.23	13.33	1.64	1.87

**mean values for zircons from each rock type*

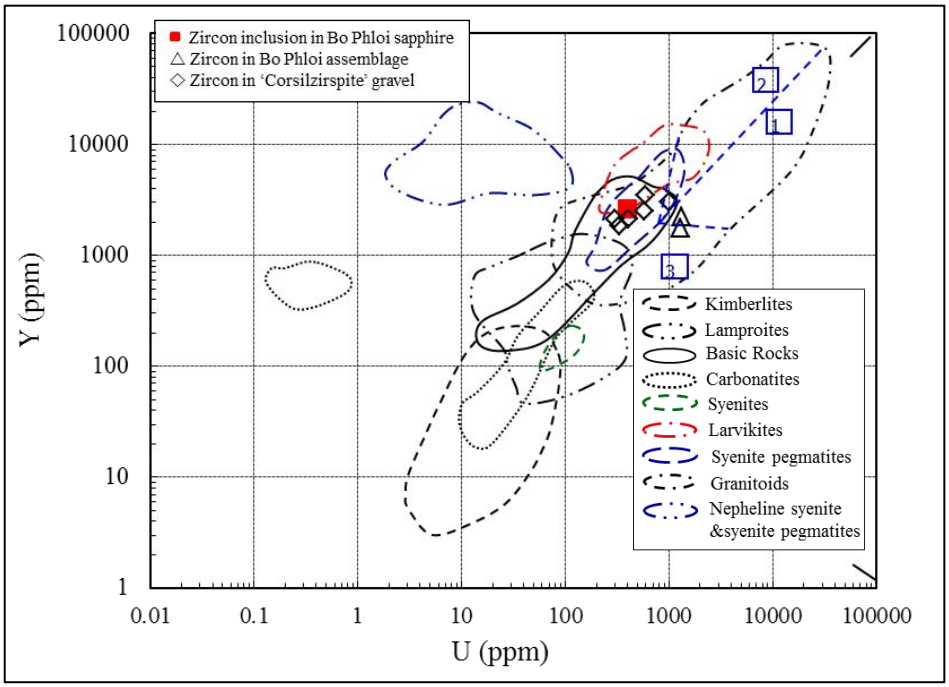

Figure 4-4 The Y-U plots of Bo Phloi zircon inclusion (red square), Bo Phloi zircon in assemblage (open triangle) and Bo Phloi zircon in 'Corsilzirspite' gravel (open diamond) compared with those values of zircons from different rock types reported by Belousova *et al.* (2002).

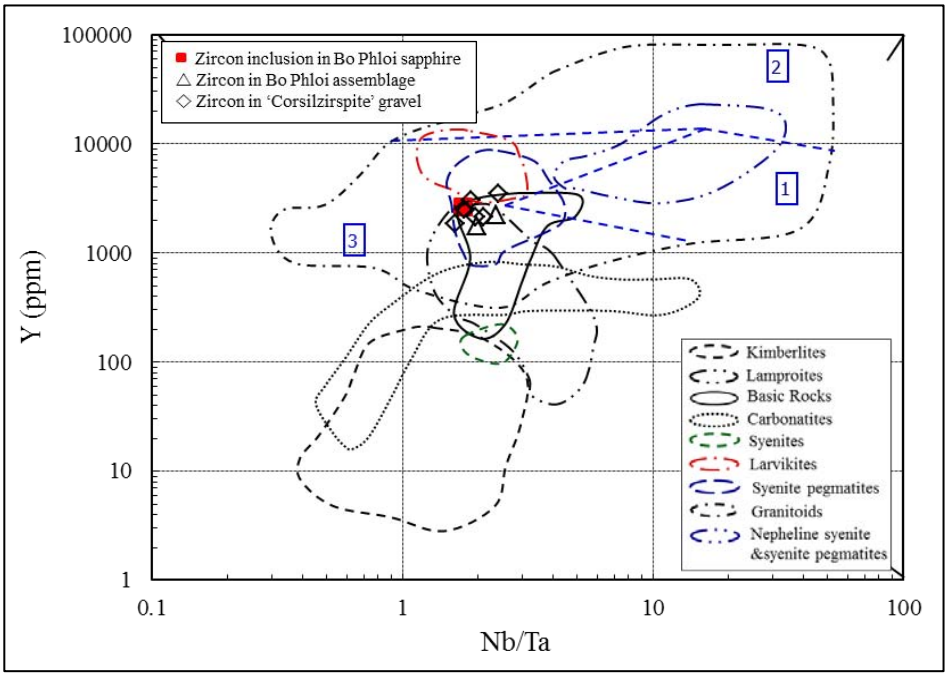

Figure 4-5 The Y-Nb/Ta plots of Bo Phloi zircon inclusion (red square), Bo Phloi zircon in assemblage (open triangle) and Bo Phloi zircon in 'Corsilzirspite' gravel (open diamond) compared with those values of zircons from different rock types reported by Belousova *et al.* (2002).

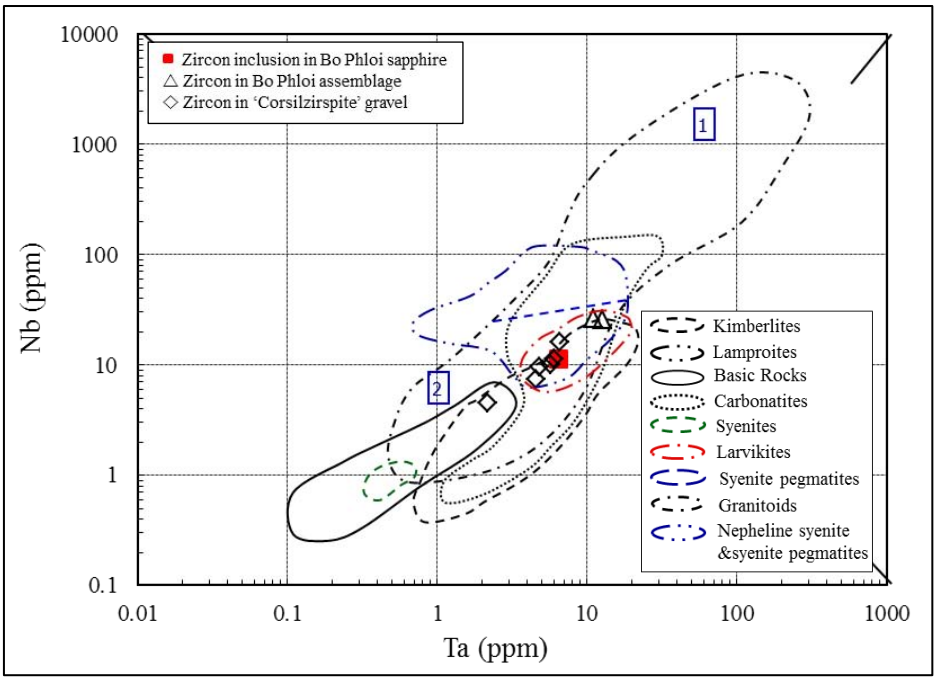

Figure 4-6 The Nb-Ta plots of Bo Phloi zircon inclusion (red square), Bo Phloi zircon in assemblage (open triangle) and Bo Phloi zircon in 'Corsilzirspite' gravel (open diamond) compared with those values of zircons from different rock types reported by Belousova *et al.* (2002).

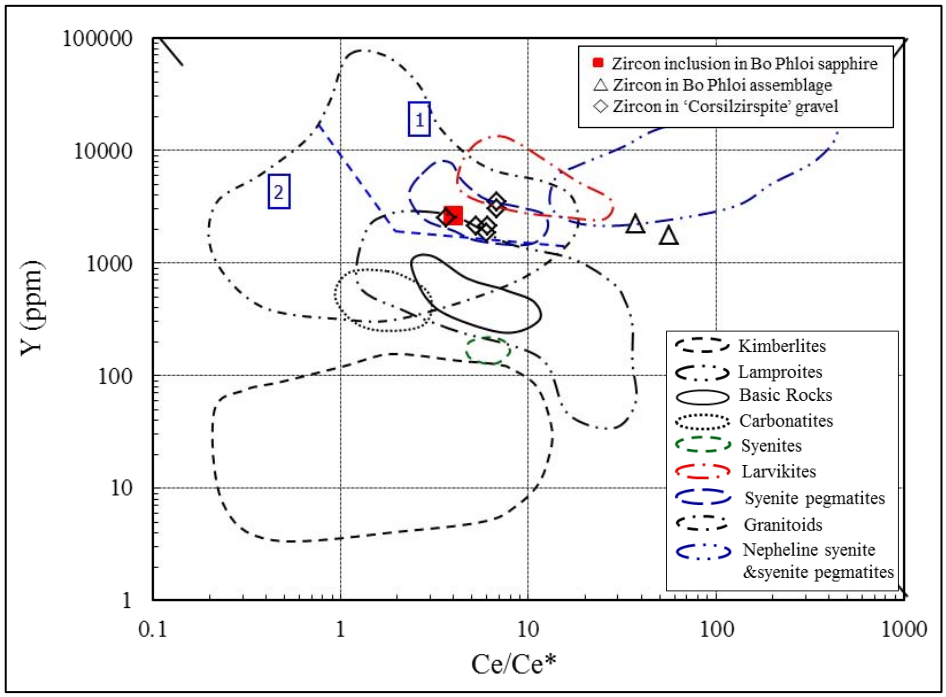

Figure 4-7 The Y-Ce/Ce* plots of Bo Phloi zircon inclusion (red square), Bo Phloi zircon in assemblage (open triangle) and Bo Phloi zircon in 'Corsilzirspite' gravel (open diamond) compared with those values of zircons from different rock types reported by Belousova *et al.* (2002).

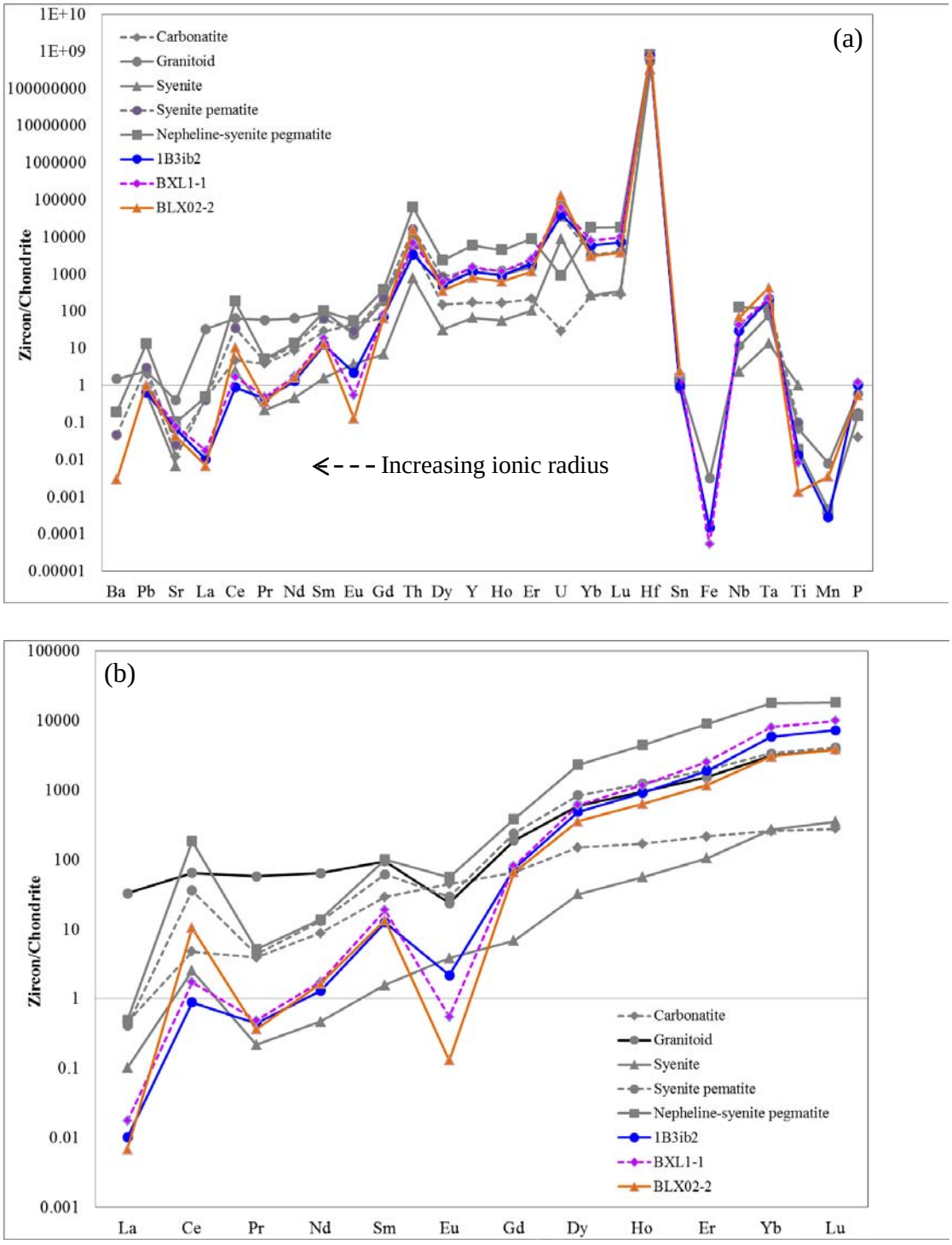

Figure 4-8 (a) Chondrite-normalized patterns of trace elements (b) chondrite-normalized REE patterns, of Bo Phloi zircon inclusion (sample *1B3ib2, blue line*) as well as zircon in Bo Phloi assemblage (sample *BLX02-2, orange line*) and zircon in 'Corsilzirspite' gravel (sample *BXL1-1, purple dashed line*) compared with patterns of zircons from various rocks (data from Belousova *et al.*, 2002).

The trace elements and REE contents of the zircon inclusion and the zircons in the assemblage and the ‘Corsilzirspite’ gravel from Bo Phloi were normalized to chondrites using the chondrite-normalized values from Taylor and McLennan (1985) are plotted together with zircons in various rock types from previous literatures in Figure 4-8. The chondrite-normalized pattern of Bo Phloi zircon inclusion appears to be similar to those of Bo Phloi zircon from assemblage and zircon from ‘Corsilzirspite’ gravel (unpublished data of Pisutha-Arnond). In addition, all three patterns are in good agreement with patterns of zircons from syenite pegmatites and nepheline syenite pegmatites. The chondrite-normalized trace elements of Bo Phloi zircons are typically enriched in Ce, Sm, Th, Y, U, Hf and Ta which are similar to those elements of zircon from syenite pegmatite rocks (Figure 4-8a). Moreover, the patterns are typically enriched in heavy REE and depleting in light REE with La/Lu ratios of Bo Phloi zircon inclusion about 1.69×10^{-5} (see Figure 4-8b). Because the ionic radii of the REEs decrease from La^{3+} to Lu^{3+}, the substitution into the zircon lattice becomes progressively easier for the REE with higher atomic number (Nagasawa, 1970; Watson, 1980; Fujimaki, 1986; Heaman *et al.,* 1990; Hanchar *et al.*, 2001). The overall shape of the REE patterns reflects interplay between magma chemistry and the crystal chemistry of the zircon. Moreover, the chondrite-normalized REE pattern of Bo Phloi zircons shows positive Ce anomaly with negative Eu anomaly and rapidly rising towards heavy REE that is concordant with the patterns of zircon from syenite pegmatites and nepheline-syenite pegmatite rocks. The strongest Eu depletion are found in U, Th, REE-enriched zircon that crystallized from the late magma indicating more fractionated and evolved melts (Belousova *et al.*, 2002). This suggests the Bo Phloi zircons may have crystallized from evolved with relatively oxidized melts such as granitoid or syenite pegmatite, where most Eu would be expected to be divalent. This anomaly largely reflect partitioning of Eu^{2+} into plagioclase during magmatic evolution, either resulting from plagioclase or pronounced alkali feldspar fractionation before it was trapped in host sapphire and later transported by basalt magma rising onto the surface. In contrast, the Ce enrichment relative to neighbouring REEs may due to the presence of Ce^{4+} which fits into the zircon structure. This can be explained by the fact that when Ce^{3+} is oxidized to Ce^{4+}, it behaves more like Zr or Hf, and thus is preferred by zircon over the LREE. This behavior may indicate a high oxidation state of the parental magma (Shnukov *et al.*, 1989). Several published data reported that the Ce anomaly was not a common

feature in zircon REE patterns, but positive Ce anomaly in zircon REE patterns was described by Murali *et al.* (1983) in the study of syenite zircon from the Indian Peninsula. Although, the typical positive Ce anomalies appear in these patterns, it is generally more oxidized nature of the Earth's crust that makes the terrestrial zircons different from those of meteorites and lunar rocks (Hinton and Meyer, 1991). Based on the previous literature of Hinton and Upton (1991), however, they demonstrated that the presence of positive Ce anomaly did not indicate a strongly oxidized environment because when the Ce anomalies are large the Ce^{4+}/Ce^{3+} ratios are very small. Therefore, the typical pattern of both negative Eu and positive Ce anomalies in Bo Phloi zircon should indicate a terrestrial condition less reducing environment. In addition, this Bo Phloi chondrite-normalized REE pattern also matches well with the REE pattern Type-4 zircon published by Nemchin *et al.* (2010) who reported such zircon may associate with some felsic and granitic source representing very late differentiation of primitive mafic magmas. Combination between results of chondrite-normalized trace element and REE patterns suggest that Bo Phloi zircon inclusion is similar to zircon from low-SiO_2 syenite pegmatite rocks representing terrestrial continental crust.

4.4 Dating Results

The great advance in understanding genesis of sapphires is the age dating of their zircon inclusions because geochronology of zircon inclusions may provide age of the host sapphires. Besides, detailed study of U-Pb of zircon inclusion may also provide a clearer picture of suitable sources of the zircon and thermal histories which may be possibly related to basaltic activity. Therefore, the U-Pb dating of Bo Phloi zircon inclusion and preliminary Th-U-Pb dating of zircon and monazite inclusions were carried out. These results are reported below.

4.4.1 U-Pb Dating of Zircon Inclusion

The largest zircon inclusion found in Bo Phloi sapphire (sample *1B3ib2*) was selected for U-Pb dating technique using LA-ICP-MS because its size is large enough (200 μm) to cover the spatial resolution of Laser beam and its large grain size without fracture may also minimize the amout of Pb diffusion out of the grain (Sutherland *et al.*, 2002). According to the previously experimental study on the diffusion time of Pb

in Thai alluvial zircon reported by Sutthirat (2001), he gave a diffusion time of about 1,650 years to reset totally the Pb in alluvial zircon (assuming the isotopic diffusion at a distance of 0.5 mm in all diffusion directions and the zircon carried by a basalts with temperature of about 1,200 °C). Based on the olivine speedometry studied by Sutthirat (2001) and application of Stokes' Law, Thai corundum-related basaltic magmas appeared to travel quickly to the surface, perhaps in less than one year. As such, it is highly unlikely that the U-Pb dates of this zircon inclusion were completely or even partially reset. The obtained U-Pb date in this zircon inclusion should therefore reflect the ages of its initial formation rather than the reset ages.

Based on previous reports, the $^{207}Pb/^{206}Pb$ dating is most suitable for Precambrain zircons. Dating of young zircon using $^{207}Pb/^{206}Pb$ decay scheme remains a problem. This is because relatively small amounts of ^{207}Pb produced during those times render the $^{207}Pb/^{206}Pb$ method less effective (e.g., Xia *et al.,* 2004, Black *et al.,* 2004). As such dating of relatively young (less than about 1000 Ma) zircon has mostly relied on the $^{238}U/^{206}Pb$ decay scheme. Because of the young ages of these zircons, these analyses are depleted in ^{207}Pb, so the accurate of $^{207}Pb/^{235}U$ ages and also $^{208}Pb/^{232}Th$ ages of young minerals is very poor and the errors are large. Therefore, only the $^{238}U/^{206}Pb$ with $\pm 2\sigma$ are most suitable and used in this study. The U-Pb date of this zircon inclusion could also represent the age of formation of its host sapphire.

The U-Pb dating results of Bo Phloi zircon inclusion (sample *1B3ib2*) in this study as well as the measured data of the Bo Phloi zircon in assemblage and Bo Phloi zircon in the 'Corsilzirspite' gravel are displayed in Table 4-2. As shown in the table, only one dating result was determined for the Bo Phloi zircon inclusion, whereas several dating results were reported for the zircons in the Bo Phloi assemblage (sample *BLX02*) and the 'Corsilzirspite' gravel (sample *BXL*) (both from unpublished data of Pisutha-Arnond). The dated ages of three spots on a zircon grain in the assemblage and those of ten spots on six zircon grains in the 'Corsilzirspite' gravel are within or close to the analytical precision for each analysis suggesting a weighted average age of 4.4±0.4 Ma and 10.86±0.14 Ma; repectively, at 95% confidence level (see Table 4-2 and Figure 4-9).

Table 4-2 Summary of U-Pb dating result of the largest zircon inclusion (sample *1B3ib2*) in Bo Phloi sapphire compared with those ages of zircons found in Bo Phloi mine (Unpublised data of Pisutha-Arnond)*

Sample	Analysis No.	Th	U	Pb^{207}/Pb^{206}	±2 s	Pb^{207}/U^{235}	± 2 s	**Pb^{206}/U^{238}**	**±2 s**	Pb^{208}/Th^{232}	± 2 s
Zircon inclusion	*1B3ib2*	14.03	5547.98	1794	128	55.8	4	**24**	**0.9**	22.4	3
Zircons in assemblage*	BLX02-1A	18.79	38537.05	396.4	209.2	5.1	0.48	**4.3**	**0.16**	4.7	0.5
	BLX02-1B	12.82	23482.20	101.9	268.7	4.6	0.54	**4.4**	**0.16**	5.1	0.56
	BLX02-1C	11.50	22456.93	45.7	281.26	4.6	0.56	**4.6**	**0.16**	5	0.62
Zircons in 'Corsilzirspite'*	BXL-1	5.32	4939.25	0.1	221.98	9.7	2.06	**10.3**	**0.46**	10.2	1.82
	BXL-1A	10.39	7691.91	219.9	270.16	11.8	1.4	**10.8**	**0.4**	12.7	1.44
	BXL-2A	5.56	4211.69	0.1	475.24	10.4	3.08	**10.9**	**0.76**	10.8	3.6
	BXL-2B	10.02	8337.27	0.1	141.16	10.6	1.32	**11**	**0.38**	10.7	1.38
	BXL-3A	5.94	5738.34	47.4	445.34	11.1	2.16	**10.9**	**0.52**	10.2	1.94
	BXL-3B	7.91	6549.97	147.3	297.64	11.6	1.52	**11**	**0.38**	11.2	1.56
	BXL-4A	6.43	5048.69	421.3	305	12.8	1.8	**10.8**	**0.42**	11.8	1.8
	BXL-4C	7.79	6470.84	0.1	0	8.6	2.84	**10.6**	**0.8**	10	3.46
	BXL-5A	4.71	4178.37	142.6	364.34	11.8	1.9	**11.2**	**0.46**	10.6	1.82
	BXL-6A	8.22	7751.59	417.8	304.36	13	1.8	**10.9**	**0.48**	10.1	1.48

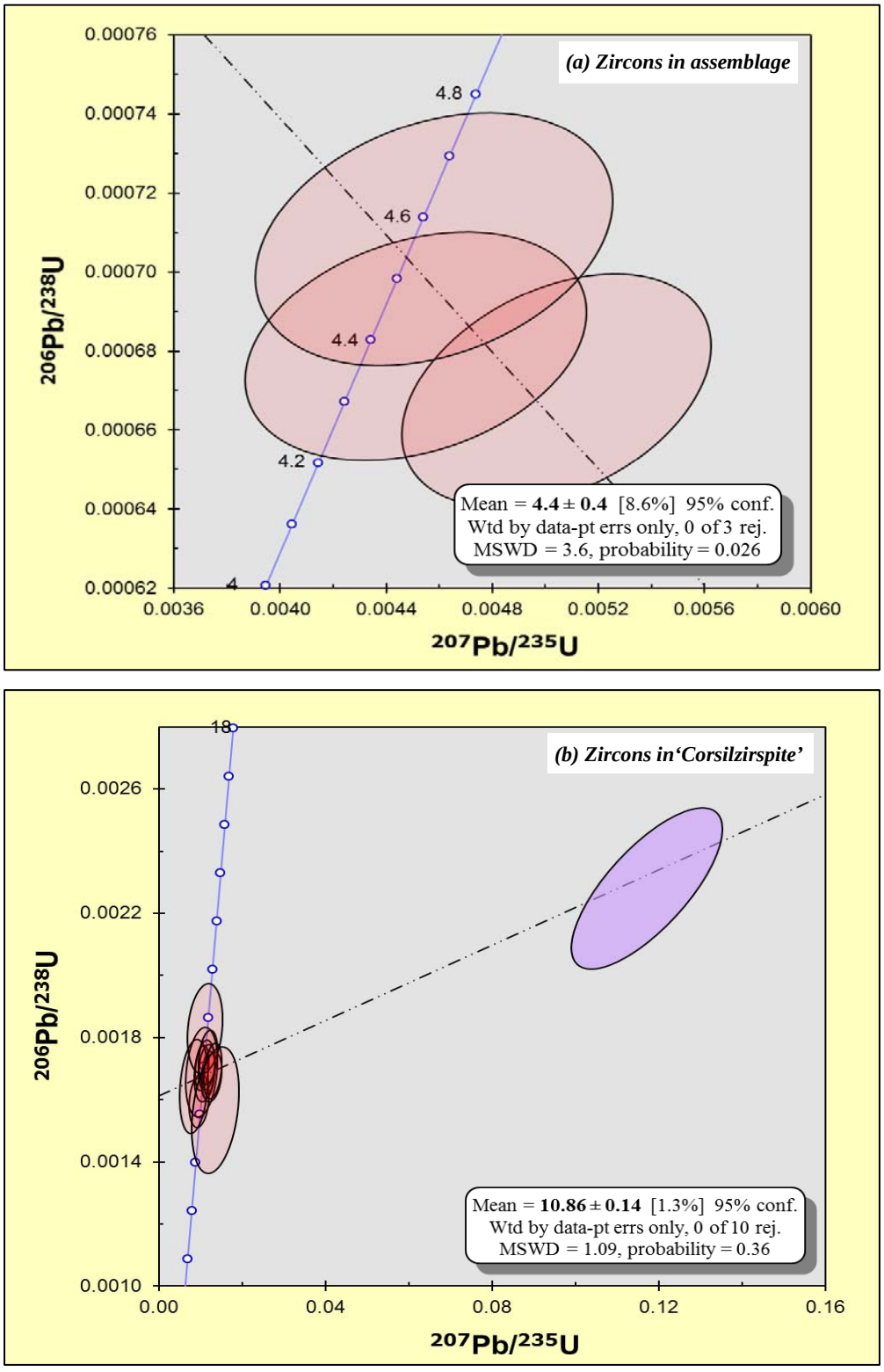

Figure 4-9 $^{206}Pb/^{238}U$ against $^{207}Pb/^{235}U$ Concordia diagram for dated zircon grains (a) in the zircon+sapphire+nepheline+hercynitic spinel assemblage and (b) in the 'Corsilzirspite' gravel, from Bo Phloi mine (Unpublised data of Pisutha-Arnond), error ellipses are 2σ.

As shown in Table 4-2, the Bo Phloi zircon inclusion gives an U-Pb age of 24.0±0.9 Ma; additionally, both Bo Phloi zircons in the assemblage and in the 'Corsilzirspite' gravel give U-Pb ages of 4.4±0.4 Ma and 10.86±0.14 Ma, respectively. The ages of these Bo Phloi zircons are older than the age of Huai Sai zircon inclusion (~1.2 Ma) found in a basaltic sapphire from Laos (Sutherland *et al.*, 2002). Based on $^{40}Ar/^{39}Ar$ geochronological data previously published by Sutthirat *et al*. (1994), they divided basaltic activities in Thailand into six major episodes, namely 22-24 Ma (late Oligocene), 18-20 Ma (early Miocene), 8-14 Ma (middle to late Miocene), 4-5.3 Ma (early Pliocene), 1.6-3.6 Ma (late Pliocene), and <1.6 Ma (Quaternary), while the ages of corundum-related basaltic eruptions were suggested to occur between 8-14 Ma, 4-5.3 Ma and 1.6-3.6 Ma periods. As such, the crystallization of the zircon inclusion and its host sapphire could have taken place during the same time as early basaltic volcanism in late Oligocene (~22-24 Ma). In addition, the age of both zircons in the Bo Phloi assemblage and in the 'Corsilzirspite' gravel fall in the range of basaltic activity and corundum-related basaltic eruption which they may associate with the Bo Phloi sapphire formation.

4.4.2 Th-U-Pb Dating of Zircon and Monazite Inclusions

This is the first study of the Th-U-Pb dating using Electron Probe Micro Analyzer (EPMA) technique applied to mineral inclusions in sapphire. Although, there are many advantages of this technique as described above, the effective limitation of the EPMA method concerns its precision regarding to U, Th and Pb determination. Therefore, the finding of the optimum condition used in this analytical process is necessary. Under experimental condition in this study, the analytical uncertainties of chemical compositions of inclusions were detected particularly on the PbO content, some date values were impossible to calculate. Some error ages of this data is possibly a result of Pb loss. Assuming that common Pb is negligible (Cherniak *et al.*, 2004), and that partial loss of Pb has not occurred, the simultaneous measurement of U, Th and Pb allow to obtain a geological age from a single electron probe analysis (Montel *et al.*, 1996). Although there are significant uncertainties inherent in this study, the Th-U-Pb dating by EPMA technique still has meaningful applications where certain uncertainty was acceptable as shown in Tables 4-3 and 4-4. Elemental compositions together with calculated dates of both zircon and monazite

inclusions are also depicted in Tables 4-5 and 4-6, respectively. In addition, details of analytical data of both zircon and monazite inclusions are also shown in Tables 4-7 to 4-9.

Table 4-3 Summary of Th-U-Pb measurments and ages of **zircon inclusions** found in Bo Phloi sapphires *(n.c. = not calculated)*.

Sample	Calculated Th-U-Pb ages (Ma) of zircon inclusions measured at	
	15 kV	20 kV
3LGC1c-D20k9	n.c.	18±11
2DGC6b-D20k1	n.c.	68±28

Table 4-4 Summary of Th-U-Pb measurement and ages of **monazite inclusions** found in Bo Phloi sapphires *(n.c. = not calculated)*.

Calculated Th-U-Pb dates (Ma) of monazite inclusions measured at			
Sample	15 kV	sample	20 kV
2DGB9a-dating1-3	54±2	2DGB9a-D20k1	30±4
2DGB9a-dating2-3	66±3	2DGB9a-D20k4	45±3
2DGB9a-dating1-4 (internal std.)	925±35	2DGB9a-D20k5	28±2
2DGB9a-dating2-4 (internal std.)	1006±38	2DGB9a-D20k6	25±2
		2DGB9a-D20k7	42±2

Tables 4-3 and 4-4 display the calculated ages of zircon and monazite inclusions measured at 15.0 and 20.0 kV accelerating voltage conditions. At 15.0 kV, the content of PbO in zircon grains can not analyse (see Table 4-5) which cause the age of zircon inclusions unable to be calculated whereas it is possible to do so for the monazite inclusions. At 20.0 kV, the PbO contents of both zircon and monazite inclusions could be detected. The calculated ages of both zircon and monazite inclusions show relatively large uncertainties due to the young age of the sapphires, its low Pb content and the small numbers of inclusion available for analysis.

Based on this study, it is clear that the 20.0 kV accelerating voltage gives a better result. At 20 kV, the monazite inclusions gave two ranges of ages at ~25-30 Ma and ~42-45 Ma, whereas the zircon incluions gave ages at 18±11 Ma and 68±28 Ma. The monazite ages of ~25-30 Ma are concordant with the U-Pb ages (24±0.9 Ma) of the Bo Phloi zircon inclusion studied here and U-Pb ages of alluvial Bo Phloi zircon (25, 30 Ma reported by Sutthirat, 2001). The apparent ages obtained by U-Pb zircon

and Th-U-Pb monazite inclusions studied here are somewhat older than the ages of Bo Phloi basalt reported by previous investigators; a K/Ar age of 3.14±0.17 Ma (Barr and Macdonald, 1981) and a $^{40}Ar/^{39}Ar$ age of 4.17±0.11 Ma (Sutthirat *et al.*, 1994).

Table 4-5 Representative analyses of **zircon inclusions** in Bo Phloi sapphires *(n.a. = not analyzed)*.

Mineral phase	Accelerating Voltage = 15 kV		Accelerating Voltage = 20 kV		
Analysis (wt%)	1B3ib-dating-3	1B3ib-dating-3	2DGC6b-D20k1	1B3ib-D20k5	3LGC1c-D20k9
P_2O_5	0.00	0.00	0.06	0.00	2.36
SiO_2	33.31	34.36	14.89	27.51	31.37
ThO_2	0.00	0.10	0.18	0.49	2.14
UO_2	0.51	0.56	1.52	0.34	3.37
Y_2O_3	0.16	0.26	0.00	0.00	0.00
La_2O_3	0.00	0.00	0.00	0.00	0.00
Ce_2O_3	0.05	0.06	0.06	0.02	0.01
Pr_2O_3	0.00	0.00	0.00	0.03	0.00
Nd_2O_3	0.00	0.00	0.01	0.02	0.00
Sm_2O_3	0.02	0.00	0.01	0.06	0.01
Eu_2O_3	0.00	0.00	0.01	0.04	0.00
Gd_2O_3	0.02	0.00	0.00	0.01	0.01
Dy_2O_3	0.02	0.02	0.00	0.01	0.09
Ho_2O_3	n.a.	n.a.	0.00	0.00	0.00
Er_2O_3	0.03	0.00	0.09	0.07	0.23
Yb_2O_3	0.09	0.08	0.16	0.17	0.51
Lu_2O_3	n.a.	n.a.	0.05	0.05	0.09
CaO	0.00	0.04	0.04	0.00	0.00
PbO	0.00	0.00	0.02	0.02	0.01
Al_2O_3	0.02	0.08	0.80	0.03	0.00
ZrO_2	66.37	64.14	61.00	57.89	59.98
HfO_2	1.85	1.48	1.26	0.38	1.54
MgO	n.a.	n.a.	0.01	0.00	0.02
FeO	n.a.	n.a.	0.02	0.16	0.01
MnO	n.a.	n.a.	0.00	0.01	0.01
Total	102.43	101.18	80.19	87.30	101.76
4 (O)					
P	0.000	0.000	0.002	0.000	0.061
Si	1.003	1.034	0.644	0.978	0.965
Th	0.000	0.001	0.002	0.004	0.015
U	0.003	0.004	0.015	0.003	0.023
Y	0.003	0.004	0.000	0.000	0.000
La	0.000	0.000	0.000	0.000	0.000
Ce	0.001	0.001	0.001	0.000	0.000
Pr	0.000	0.000	0.000	0.000	0.000
Nd	0.000	0.000	0.000	0.000	0.000
Sm	0.000	0.000	0.000	0.001	0.000
Eu	0.000	0.000	0.000	0.000	0.000
Gd	0.000	0.000	0.000	0.000	0.000
Dy	0.000	0.000	0.000	0.000	0.001
Ho	-	-	0.000	0.000	0.000
Er	0.000	0.000	0.001	0.001	0.002
Yb	0.001	0.001	0.002	0.002	0.005
Lu	-	-	0.001	0.001	0.001
Ca	0.000	0.001	0.002	0.000	0.000
Pb	0.000	0.000	0.000	0.000	0.000
Al	0.001	0.003	0.041	0.001	0.000
Zr	0.974	0.941	1.285	1.004	0.899
Hf	0.016	0.013	0.016	0.004	0.014
Mg	-	-	0.001	0.000	0.001
Fe	-	-	0.001	0.005	0.000
Mn	-	-	0.000	0.000	0.000
Total*	2.001	2.003	2.013	2.004	1.988
Th, U and Pb concentration (ppm), points age and standard errors (2%)					
Th	0	1000	1760	4940	21410
Error	0	200	60	99	428
U	5060	5600	15210	3410	33690
Error	101	112	304	68	674
Pb	0	0	150	210	100
Error	#####	#####	60	60	60
Age (Ma)	#####	#####	68	296	18
Error	#####	#####	28	88	11

Table 4-6 Representative analyses of **monazite inclusions** in Bo Phloi sapphires *(n.a. = not analyzed).*

Mineral phase	Accelerating Voltage= 15 kV				Accelerating Voltage= 20 kV				
Analysis (wt%)	2DGB9a-dating1-3	2DGB9a-dating2-3	2DGB9a-dating1-4	2DGB9a-dating2-4	2DGB9a-D20k1	2DGB9a-D20k4	2DGB9a-D20k5	2DGB9a-D20k6	2DGB9a-D20k7
P_2O_5	30.84	2.99	31.56	31.58	12.07	53.79	48.36	37.70	43.48
SiO_2	1.13	0.96	1.03	0.99	1.09	0.00	1.30	1.06	0.54
ThO_2	66.47	53.95	4.06	3.67	36.35	16.94	63.30	48.35	40.98
UO_2	18.50	14.82	1.25	1.16	2.50	20.08	17.60	13.29	14.19
Y_2O_3	27.57	28.26	30.86	31.73	0.00	0.00	0.00	0.00	0.00
La_2O_3	0.00	0.01	0.05	0.00	0.00	0.03	0.03	0.04	0.00
Ce_2O_3	0.17	0.19	0.23	0.15	0.42	0.00	0.18	0.13	0.09
Pr_2O_3	0.05	0.02	0.06	0.08	0.04	0.10	0.07	0.13	0.13
Nd_2O_3	0.66	0.68	0.74	0.79	0.52	0.10	0.65	0.41	0.39
Sm_2O_3	0.83	0.82	0.88	0.92	0.25	0.04	0.72	0.41	0.38
Eu_2O_3	0.00	0.00	0.00	0.00	0.00	0.00	0.00	0.00	0.00
Gd_2O_3	0.23	0.22	0.29	0.30	0.00	0.20	0.17	0.12	0.07
Dy_2O_3	5.24	4.96	5.82	5.76	3.34	2.49	3.97	2.67	1.55
Ho_2O_3	n.a.	n.a.	n.a.	n.a.	0.00	0.00	0.00	0.00	0.00
Er_2O_3	3.47	3.27	3.77	3.96	0.60	2.96	2.61	1.49	1.21
Yb_2O_3	3.44	3.17	3.90	3.93	0.91	0.20	2.75	0.96	1.02
Lu_2O_3	n.a.	n.a.	n.a.	n.a.	0.24	0.72	0.61	0.23	0.43
CaO	0.00	0.00	0.11	0.07	0.00	0.09	0.09	0.05	0.07
PbO	0.30	0.30	0.35	0.35	0.06	0.16	0.15	0.10	0.16
Al_2O_3	0.00	0.00	0.00	0.00	30.06	0.38	0.00	0.00	0.00
ZrO_2	0.00	0.00	0.00	0.00	0.00	0.00	0.00	0.00	0.00
HfO_2	0.16	0.08	0.37	0.18	0.03	0.17	0.09	0.03	0.04
TiO_2	n.a.	n.a.	n.a.	n.a.	0.00	0.60	0.00	0.00	0.00
MgO	n.a.	n.a.	n.a.	n.a.	0.00	0.11	0.00	0.00	0.00
FeO	n.a.	n.a.	n.a.	n.a.	0.19	0.01	0.00	0.00	0.01
MnO	n.a.	n.a.	n.a.	n.a.	0.00	0.01	0.00	0.01	0.01
Total	159.06	114.68	85.33	85.61	88.66	99.16	142.63	107.15	104.77
4 (O)									
P	0.774	0.148	1.029	1.026	0.402	1.342	1.111	1.129	1.219
Si	0.034	0.056	0.040	0.038	0.043	0.000	0.035	0.037	0.018
Th	0.448	0.717	0.036	0.032	0.325	0.114	0.391	0.389	0.309
U	0.122	0.193	0.011	0.010	0.022	0.132	0.106	0.105	0.105
Y	0.435	0.878	0.632	0.648	0.000	0.000	0.000	0.000	0.000
La	0.000	0.000	0.001	0.000	0.000	0.000	0.000	0.000	0.000
Ce	0.002	0.004	0.003	0.002	0.006	0.000	0.002	0.002	0.001
Pr	0.001	0.001	0.001	0.001	0.001	0.001	0.001	0.002	0.002
Nd	0.007	0.014	0.010	0.011	0.007	0.001	0.006	0.005	0.005
Sm	0.008	0.016	0.012	0.012	0.003	0.000	0.007	0.005	0.004
Eu	0.000	0.000	0.000	0.000	0.000	0.000	0.000	0.000	0.000
Gd	0.002	0.004	0.004	0.004	0.000	0.002	0.002	0.001	0.001
Dy	0.050	0.093	0.072	0.071	0.042	0.024	0.035	0.030	0.017
Ho	-	-	-	-	0.000	0.000	0.000	0.000	0.000
Er	0.032	0.060	0.046	0.048	0.007	0.027	0.022	0.017	0.013
Yb	0.031	0.056	0.046	0.046	0.011	0.002	0.023	0.010	0.010
Lu	-	-	-	-	0.003	0.006	0.005	0.002	0.004
Ca	0.000	0.000	0.005	0.003	0.000	0.003	0.003	0.002	0.003
Pb	0.002	0.005	0.004	0.004	0.001	0.001	0.001	0.001	0.001
Al	0.000	0.000	0.000	0.000	1.392	0.013	0.000	0.000	0.000
Zr	0.000	0.000	0.000	0.000	0.000	0.000	0.000	0.000	0.000
Hf	0.001	0.001	0.004	0.002	0.000	0.001	0.001	0.000	0.000
Ti	-	-	-	-	0.000	0.013	0.000	0.000	0.000
Mg	-	-	-	-	0.000	0.005	0.000	0.000	0.000
Fe	-	-	-	-	0.006	0.000	0.000	0.000	0.000
Mn	-	-	-	-	0.000	0.000	0.000	0.000	0.000
Total*	1.950	2.247	1.953	1.957	2.271	1.688	1.750	1.738	1.712
Th, U and Pb concentration (ppm), points age and standard errors (2%)									
Th	664720	539480	40620	36660	363500	169380	632960	483450	409840
Error	13294	10790	812	733	7270	3388	12659	9669	8197
U	184990	148230	12500	11580	25020	200770	175960	132870	141880
Error	3700	2965	250	232	500	4015	3519	2657	2838
Pb	2980	2960	3480	3480	580	1610	1450	1020	1610
Error	150	150	150	150	60	60	60	60	60
Age (Ma)	54	66	925	1006	30	45	28	25	42
Error	4	5	55	59	4	3	2	2	2

Table 4-7 Analytical data of **zircon inclusions** in Bo Phloi sapphires *(Accelerating Voltage = 20 kV).*

Sample	Age Ma	Error Age Ma	UO_2 ppm	Error U %	ThO_2 ppm	Error Th %	PbO ppm	Error Pb %	Th*(U) ppm	Error Th* %	Error Th* ppm	U*(Th) ppm	Error U* %	Error U* ppm	U/Pb	Error U/Pb %	Th/Pb	Error Th/Pb %	Corr
2DGC6b-D20k1	68	28	15210	2.00	1760	3.41	150	40.00	50298	2.05	1031	15762	2.05	323	101.400	40.05	11.733	40.15	0.995
2DGC6b-D20k2	1655	685	180	33.33	1700	3.53	180	33.33	2359	11.86	280	644	11.86	76	1.000	47.14	9.444	33.52	0.703
1B3ib-D20k5	296	88	3410	2.00	4940	2.00	210	28.57	16006	2.00	320	4932	2.00	99	16.238	28.64	23.524	28.64	0.995
3LGC1c-D20k9	18	11	33690	2.00	21410	2.00	100	60.00	128535	2.00	2571	40423	2.00	808	336.900	60.03	214.100	60.03	0.999

Table 4-8 Analytical data of **monazite inclusions** in Bo Phloi sapphires *(Accelerating Voltage = 15 kV).*

Sample	Age Ma	Error Age Ma	UO_2 ppm	Error U %	ThO_2 ppm	Error Th %	PbO ppm	Error Pb %	Th*(U) ppm	Error Th* %	U*(Th) ppm	Error U* %	U/Pb	Error U/Pb %	Th/Pb	Error Th/Pb %	Corr
2DGB9a-dating1-3	54	4	184990	2.00	664720	2.00	2980	5.03	1254462	2.00	393499	2.00	62.077	5.42	223.060	5.42	0.864
2DGB9a-dating2-3	66	5	148230	2.00	539480	2.00	2960	5.07	1012454	2.00	317303	2.00	50.078	5.45	182.257	5.45	0.865
2DGB9a-dating1-4	925	55	12500	2.00	40620	2.00	3480	4.31	83299	2.00	24397	2.00	3.592	4.75	11.672	4.75	0.823
2DGB9a-dating2-4	1006	59	11580	2.00	36660	2.00	3480	4.31	76478	2.00	22242	2.00	3.328	4.75	10.534	4.75	0.823

Table 4-9 Analytical data of **monazite inclusions** in Bo Phloi sapphires *(Accelerating Voltage = 20 kV).*

Sample	Age Ma	Error Age Ma	UO_2 ppm	Error U %	ThO_2 ppm	Error Th %	PbO ppm	Error Pb %	Th*(U) ppm	Error Th* %	U*(Th) ppm	Error U* %	U/Pb	Error U/Pb %	Th/Pb	Error Th/Pb %	Corr
2DGB9a-D20k1	30	4	25020	2.00	363500	2.00	580	10.34	443124	2.00	139241	2.00	43.138	10.54	626.724	10.54	0.964
2DGB9a-D20k4	45	3	200770	2.00	169380	2.00	1610	3.73	809033	2.00	253934	2.00	124.702	4.23	105.205	4.23	0.776
2DGB9a-D20k5	28	2	175960	2.00	632960	2.00	1450	4.14	1192859	2.00	374881	2.00	121.352	4.60	436.524	4.60	0.811
2DGB9a-D20k6	25	2	132870	2.00	483450	2.00	1020	5.88	906176	2.00	284827	2.00	130.265	6.21	473.971	6.21	0.896
2DGB9a-D20k7	42	2	141880	2.00	409840	2.00	1610	3.73	861776	2.00	270544	2.00	88.124	4.23	254.559	4.23	0.776

CHAPTER 5
DISCUSSIONS AND CONCLUSIONS

5.1 Multiple Sources and Processes of Bo Phloi Sapphire Formation

A wide range of mineral inclusions in Bo Phloi sapphires were discovered in this study and their detailed mineral chemistries are reported in Chapter 2. These inclusions are alkali feldspar, nepheline, hercynitic spinel, zircon, manganiferous-ilmenite, silica-rich enstatite, pyrope-almandine garnet richer towards pyrope component, monazite, calcite, sapphirine, biotite-phlogopite and staurolite. Most of these inclusions appear to have been incorporated into their host sapphires during the time of their formation because they seem to have an equilibrium mutual grain contact with the host sapphires without reaction rim or resorbed outline. Hence, they should provide valuable information about the chemical environment, physical conditions and geological processes during the initial host sapphire crystallization before they were brought up to the surface via basaltic eruptions. Among these, alkali feldspar, zircon and nepheline are the most dominant inclusions while Si-rich enstatite, hercynitic spinel, manganiferous-ilmenite, monazite, pyr>alm garnet, sapphirine, biotite-phlogopite, staurolite, and calcite are occasionally found. Based on their geochemical affinities, such mineral inclusions can be categorized into two groups, namely, alkaline-related and metamorphic-related mineral suites. Each group of inclusion may give clues to the parent rocks which relate to the origin of their host sapphires.

The alkaline-related inclusion suite comprises alkali feldspars, nepheline, zircon, manganiferous-ilmenite, monazite and probably calcite, which are likely to be mineral phases crystallized from alkaline felsic magma. The composition of alkali feldspar inclusions appear to span from Na-rich (albitic) phase in the grayish brown variety towards a K-richer phase in the blue variety. This variation seems to be consistent with the composition of nepheline inclusions in which the Na-rich nepheline is found in grayish brown variety while K-rich nepheline occurs in the blue variety only. In fact, both minerals are known as typical constituents of felsic syenite (Deer *et al.,* 1992; Wilkinson and Hensel, 1994; Pin *et al.,* 2006).

Apart from alkali feldspar and nepheline inclusions, the chemical composition of zircon inclusions identified here also support the formation of Bo Phloi sapphire

related to highly evolved felsic melts. The high contents of Hf, U, Th and REEs in Bo Phloi zircon inclusions and cross-plots of those trace elements (this study and unpublished data of Pisutha-Arnond) suggest that the zircon inclusion together with its host sapphire may originate from highly evolved magma (Heaman *et al.*, 1990; Shnukov *et al.*, 1997; Belousova *et al.*, 2002). Moreover, the chondrite-normalized REE patterns of these zircon inclusions also illustrate the similar pattern with characteristic of positive Ce anomaly and Eu depletion to those patterns of zircon from syenite-pegmatite rocks (Belousova *et al.*, 2002). Similar results were also obtained on the trace element study of a zircon in the zircon+sapphire+nepheline+hercynite assemblage and zircons in the 'Corsilzirspite' gravel (unpublished data of Pisutha-Arnond). Furthermore, the manganiferous-ilmenite generally occurs in granitic igneous rocks, and also in some carbonatites which may contain anomalous niobium (Deer *et al.*, 1992). Hence the presence of manganiferous (without anomalous Nb) ilmenite inclusions in Bo Phloi sapphires particularly in the blue variety also favor a felsic melt origin. In addition, the existence of monazite (as well as Nb oxide; Pisutha-Arnond *et al.*, 1999) inclusions in these sapphires also support the highly evolved melt model as they are common accessory minerals in felsic rocks. Based on the occurrences of this mineral inclusion suite, the majority of Bo Phloi sapphires appear to have crystallized from a highly evolved, alkaline rich, silica poor melt such as syenitic magma.

The syenitic origin is agreed fairly well with genetic model of Bo Phloi sapphire and other basaltic sapphires proposed by previous investigators. For examples, Saminpanya (2000) proposed a nepheline-syenite origin of Bo Phloi sapphires based on the presence of nepheline inclusion. Moreover, Guo *et al.* (1996a) reported ilmenite inclusion together with feldspar, zircon, uraninite and Fe, Cu sulphide inclusions in general basaltic sapphires, and assigned an alkaline granitic or syenitic liquid origin. This also agrees well with the previous genetic models of general basaltic sapphires originally derived from felsic rather than mafic melts (Coenraads *et al.*, 1990; 1995; Sutherland and Schwarz, 2001), most likely syenitic melts within metasomatised mantle (*e.g.*, Aspen, 1990; Upton *et al.*, 1999; Saminpanya *et al.*, 2003).

The metamorphic-related inclusion suite found in the Bo Phloi sapphires comprises Si-rich enstatite, pyr>alm garnet, sapphirine, staurolite, biotite-phlogopite

and probably hercynitic spinel. Although metamorphic-related inclusions are comparatively rarer than the alkaline-related inclusions in Bo Phloi sapphires, the presence of these metamorphic-related inclusions are especially noteworthy as most of these phases (except hercynitic spinel) have never been recorded as inclusions in basaltic Bo Phloi sapphires before. These mineral inclusions will further provide strong evidences for the previously proposed genetic model of Bo Phloi sapphire related to the contact metamorphic reaction of basaltic magma and crustal rocks.

The presence of Si-rich enstatite inclusions in Bo Phloi sapphires may give a crucial evidence of a hybrid metasomatic reaction between basaltic magma with crustal materials (e.g., alkaline felsic rocks or other crustal rocks present there) as its composition is rather derived from both types of source material. In addition, this Si-rich enstatite also contains rather high Al probably contributed from the crustal source. The crystallization of Si-rich enstatite therefore may be a result of contamination reaction at a contact metamorphic zone of a mantle-derived mafic magma with crustal rocks that are rich in both silica and alumina. Furthermore, the occurrence of pyrope-almandine garnet with pyrope rich end-member also supports deep seated source, most likely mantle; whereas almandine member may involve a high grade metamorphism, probably in deep crust.

The presences of sapphirine, staurolite, biotite-phlogospite inclusions in Bo Phloi sapphire further reinforce the high temperature contact metamorphic environments of the host sapphire formation. Even though hercynitic spinel can occur in both metamorphic and magmatic rocks (Deer *et al.*, 1992), the occurrence of hercynitic spinel inclusions in Bo Phloi sapphire which their compositions are similar to those of the hercynitic spinels in the “Corsilzirspite” gravel (an unusual assemblage of corundum+sillimanite+zircon+hercynitic spinel) (Pisutha-Arnond *et al.*, 1999; 2005), has pointed, at least some of them, to a contact metamorphic origin of an alumina-rich crustal rock. These evidences suggest that the Bo Phloi sapphires could also crystallize from metasomatic reactions and contaminated melt of a raising basaltic magma from the mantle with crustal rocks. In such a contact metasomatic condition, desilification of the crustal materials could occur. As a result, sapphire along with those metamorphic mineral suites could crystallize from metasomatized rocks and contaminated melt at or near the contact zone. The metamorphic related origin of Bo Phloi sapphires is also agree fairly with contact

metamorphic/metasomatic/contaminated gabbroic model proposed earlier by Pisutha-Arnond *et al.* (1998; 1999; 2005) based on the discovery of the "Corsilzirspite" gravel in sapphire-bearing gravel bed in Bo Phloi gem field.

Referring to the above evidences and discussion, it is reasonable to propose bimodal genetic models of Bo Phloi sapphires as (1) syenitic melt-related model, by which the sapphires could crystallize from a highly evolved melts of alkali felsic composition derived from a low degree partial melting of crustal material, and (2) contact metamorphic-related model, by which the sapphire could originate from the metasomatized crustal rocks and contaminated melt at the contact zone of basaltic intrusion. Both processes could occur in the lower crust. This is in an agreement with Peucat *et al*. (2007) who found that the trace element signatures of Bo Phloi sapphires overlapped both magmatic and metamorphic fields.

5.2 Timing of Sapphire Crystallization and Eruption of Sapphire-related Basalt in the Bo Phloi Gem Field

In this study, Bo Phloi zircon inclusion gave the U-Pb age of 24±0.9 Ma using LA-ICP-MS technique. The preliminary Th-U-Pb dating, an application of EPMA, gave the age of Bo Phloi zircon inclusion at 18±11 Ma and the Th-U-Pb of monazite ages about 25-30 Ma and 42-45 Ma. In addition, the U-Pb age of zircon in 'Corsilzirspite' gravel from Bo Phloi sapphire mine gave 10.86±0.14 Ma and the U-Pb age of Bo Phloi zircon from zircon+sapphire+nepheline+hercynitic spinel assemblage at 4.4±0.4 Ma (both from unpublished data of Pisutha-Arnond).

A chronological summary of Bo Phloi zircon and monazite inclusions ages obtained in this and previous studies are compared with the ages of Cenozoic basaltic activities in Thailand in Table 5-1. As shown in table, both K-Ar and $^{40}Ar/^{39}Ar$ age of Bo Phloi basalts were previous reported by Barr and Macdonal (1981) and Sutthirat *et al.* (1994) have average age about 3-4 Ma. These dates mark the ages of deep seated alkaline basaltic activities that carried Bo Phloi sapphire up to the surface. These ages are much younger than the ages of zircon and monazite inclusions found in their host sapphire and the zircon in the 'Corsilzirspite' gravel. However, the U-Pb age of zircon in the zircon+sapphire+nepheline+hercynitic spinel assemblage found in Bo Phloi sapphire mine gave 4.4±0.4 Ma (unpublished data of Pisutha-Arnond) which almost coincides or slightly older than the ages of Bo Phloi basalts. The result of these dating

imply that the formation of sapphire-bearing protoliths by multiple sources and processes took place episodically several million years underneath this area before the eruption of deep seated Bo Phloi basalt during Late Oligocence to Early Pliocene and brought those sapphires along with other xenoliths and xenocrysts to the surface.

Even though the Th-U-Pb dates, using EPMA, of zircon and monazite inclusions in Bo Phloi sapphires are less reliable due to analytical uncertainties as mentioned in Chapter 4 and some of those dates are much older than the ages of the Bo Phloi basalts and U-Pb dated zircons, but some of those dates still fall within activity episodes of Thai Cenozoic basalt of the region spanning from late Oligocene (22-24 Ma) and almost synchronous with the age of plate reconstruction (at least 24 Ma) of Southeast Asia region (Lee and Lawver, 1995; Lovatt-Smith *et al.*, 1996). This indicates an episodic magmatic activity of the region.

The 25, 30 Ma U-Pb ages of alluvial Bo Phloi zircons (Sutthirat, 2001) suggest that these zircons were crystallized much earlier from unknown source underneath long before they were brought up along with sapphire to the surface by 3-4 Ma alkaline basalt. The 2-3.5 Ma and 4.5-5.5 Ma fission track dates of those zircons (Sutthirat, 2001) could also help mark the upper limit age (so far recorded) of basaltic eruption that carried sapphire to the surface in Bo Phloi area. This is because the fission track dates are likely to be the reset ages by hot basaltic magma while it brought those zircons and sapphires upwards.

The older ages of these Bo Phloi inclusions could however imply a protogenetic origin of such inclusions having been formed much earlier than their host sapphire formation. Nevertheless, the old U-Pb age (10.86±0.14 Ma) of zircon intimately intergrown with sapphire (suggesting a cogenetic occurrence) in the corundum+sillimanite+zircon+hercynitic spinel assemblage suggests that such protogenetic origin of those inclusions is less likely. Moreover, the age of Bo Phloi inclusions give the U-Pb zircon (24±0.9 Ma) and the Th-U-Pb monazite (25-30 Ma) matching with the age range of alluvial Bo Phloi large zircon single crystals (25, 30 Ma of U-Pb dates by Sutthirat, 2001) indicating such minerals may be crystallized at about the same time.

Table 5-1 Geochronological scale with respect to radiometric dating of basalts, alluvial zircon and mineral inclusions in sapphires from Bo Phloi gem field

Geological Time Scale				Age (Ma)	Cenozoic basaltic activity in Thailand[1] ($^{40}Ar/^{39}Ar$)	Corundum-related basalts[1] ($^{40}Ar/^{39}Ar$)	Bo Phloi basalt	Alluvial Bo Phloi zircon[3]	Age of Bo Phloi inclusion[4]			U-Pb Bo Phloi zircon[5]
									U-Pb zircon	Th-U-Pb zircon	Th-U-Pb monazite	
Cenozoic	Quaternary	Pleistocene	Upper	0.001	<1.6							
			Middle	0.125								
			Lower	0.7								
	Neogene	Pliocene	Upper	1.8		1.6-3.6						
				1.6	1.6-3.6			2-3.5 (Fission-track)				
				2.5								
			Lower	3.5	4-5.3	4-5.3	3.14±0.17[2]	4.5-5.5 (Fission-track)				
		Miocene		5			4.17±0.11[1]					4.4±0.4[a]
				6								
				7								
				8	8-14	8-14						
				9								
				10								10.86±0.14[b]
				11								
				12								
				13								
				14								
				15								
				16								
				17								
				18	18-20					18±11		
				19								
				20								
	Paleogene	Oligocene			22-24							
				25				25 (U-Pb)	24±0.9		~25-30	
				30				30 (U-Pb)				
		Eocene		35								
											~42-45	
		Paleo-cene		55								
				65								

[1]Sutthirat *et al.* (1994); [2]Barr and Macdonald, 1978; 1981; [3]Sutthirat, (2001); [4]**this study**; [5]Unpublished data of Pisutha-Arnond
(a = zircon in zircon+sapphire+nepheline+hercynitic spinel assemblage; and b= zircon in 'Corsilzirspite' gravel, from Bo Phloi sapphire mine).

5.3 Genetic Model of Bo Phloi Sapphire Formation

Based on the above information and age dating results, we can divide the timing of Bo Phloi sapphire formation and basaltic eruption into 3 intervals as shown in Figure 5-1.

The first stage (Figure 5-1❶) is signified by the early formation of 'syenitic melt-related sapphire' at the age of ~24 Ma. This period is based on the apparent U-Pb age of Bo Phloi zircon inclusion yielded 24±0.9 Ma. In this period, both basaltic melt and felsic alkali melt were generated as a result of decompressed stress. Rifting and thinning of lithosphere at the Bo Phloi area as well as Southeast Asian region have been developed and led to an enomous pressure release. Consequently, expansion of hot asthenosphere had been activated. Subsequently, basaltic magma may have formed by such upwelling asthenosphere in the upper mantle under this region during the crustal extension. At the same time the felsic alkali melt (i,e,, syenite) could also be formed by low degree partial melting of lower crustal rocks as a result of crustal thinning and/or mantle plume. Hence, Bo Phloi sapphires could firstly crystallize from such early-formed syenitic melts at ~24 Ma while the melts were slowly cooled down shortly afterwards.

The second interval (Figure 5-1❷) was the main events of sapphire formation which span from 24-4 Ma based on the U-Pb age of zircon inclusion (24±0.9 Ma), the U-Pb age of zircon in 'Corsilzirspite' gravel (10.86±0.14 Ma) and the U-Pb age of zircon in assemblage of zircon+sapphire+nepheline+hercynitic spinel (4.4±0.4 Ma) (both of unpublished data of Pisutha-Arnond). In this interval, the larger area of both felsic alkali melt and basaltic melt were formed extensively which then causing an uprising of basaltic melts from the upper mantle to form contact zones with lower crustal rocks above the mantle plume in this region. The majority of Bo Phloi sapphires might have been formed during this period. The syenitic melt-related sapphires were still crystallized episodically during this interval, while such basaltic intrusions from the upper mantle into the lower crust could provide an additional formation of the so-called 'contact metamorphic-related sapphire' from such contact zone and contaminated melts. This is strongly confirmed by the apparent U-Pb age of zircon in 'Corsilzirspite' gravel at 10.86±0.14 Ma that may represent the age of the main contact metamorphic sapphires.

Final interval (Figure 5-1❸) was the main eruption period (≤ 4 Ma) starting when alkaline basaltic magma had risen from deep mantle and carried mantle xenoliths (e.g., spinel lherzolite suggested by Sutthirat *et al.*, 1999; Sutthirat, 2001; Srithai, 2005), xenocrysts (e.g., pleonastic spinel, diopsidic pyroxene, Al-Ti-rich magnetite, zircon reported by Pisutha-Arnond *et al.*, 1999; Saminpanya and Sutherland, 2008), crustal rocks including sapphires crystallized from felsic alkali melts, and contact metamorphic zones formed earlier and during the time of eruption rising onto the surface. This interval is supported by a range of basaltic eruption ages (3.14±0.17 Ma; 4.17±0.11 Ma) and the youngest age of fission track ages of alluvial zircon (2-3.5 Ma). In addition, the formation of placer sapphire deposit in Quaternary basin after the eruption also occurred in this interval. During this period, weathering and erosion of sapphire-related basalt took place and deposited sapphire along with other heavy minerals in sapphire-bearing gravel beds of Lam Taphoen river basin.

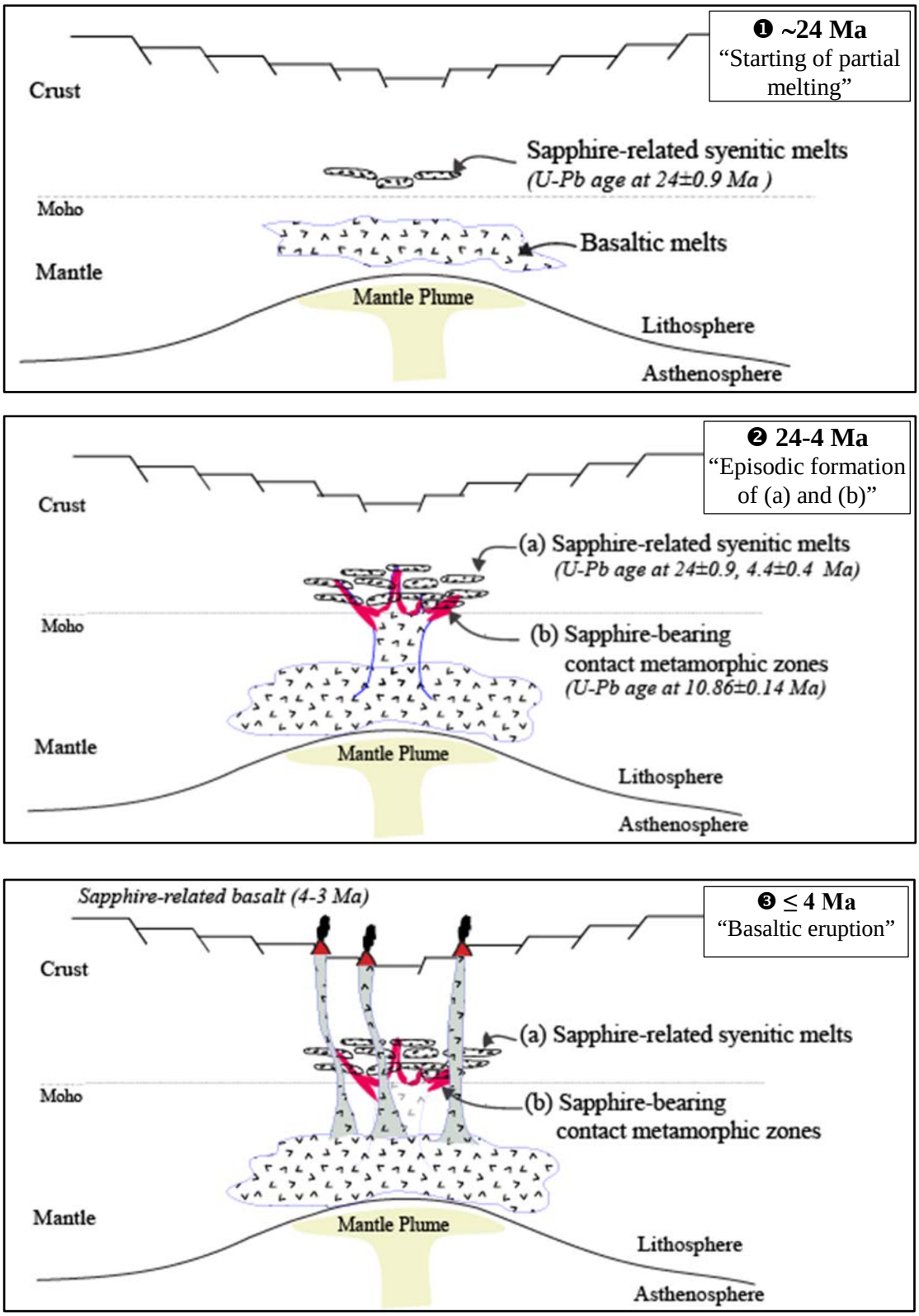

Figure 5-1 A bimodal genetic model of Bo Phloi sapphires including syenitic melt-related origin and contact metamorphic-related origin, based on chronological data described in the text.

5.4 Multiple Sources and Processes of Basaltic Sapphire Formation in Southeast Asia

Because the scope of this study is focused mainly on the inclusion study of Bo Phloi sapphires and extended to basaltic sapphires in the Southeast Asian region; therefore, the following discussion will be limited only to the formation of basaltic sapphire in Southeast Asia. The formation of basaltic ruby such as those occurred at Thai-Cambodia border (i.e., in Trat area of Thailand and extended to Pailin area of Cambodia) will only be mentioned briefly. This is because the basaltic ruby could have been formed under a different source provenance and condition (Sutthirat *et al.*, 2001; Saminpanya and Sutherland, 2011) which beyond the scope of this study.

The mineral inclusions in sapphires from Southeast Asia obtained in this study (i.e., from Kanchanaburi, Chanthaburi and Phrae in Thailand, Huai Sai in Laos, Pailin in Cambodia and Gia Nghia in Vietnam as described in details in Chapters 2 and 3) are compared with those from the previous studies in Table 5-2. As shown in the table, the Southeast Asia sapphires contain a wide range of mineral inclusions similar to those found in Bo Phloi sapphires. Among those the alkali feldspar and Si-rich enstatite are the most common inclusions found in sapphires from all localities in Southeast Asia by this study and previous researchers (except Si-rich enstatite); whereas, nepheline, zircon, garnet, spinel and ferrocolumbite inclusions also contained in some localities. In contrast, sapphirine, staurolite, apatite and pyrochlore inclusions are rarely observed in these sapphires.

Even though, some inclusions such as ilmenite, monazite, calcite and biotite-phlogopite were found in the Bo Phloi sapphire but have not yet been detected in other Southeast Asia sapphires; whereas more inclusions such as ferrocolumbite, pyrochlore and apatite were found in other Southeast Asia sapphires but so far have not encountered in the Bo Phloi sapphire yet. Nonetheless, the types of mineral inclusions observed in these Southeast Asia sapphires including those in Bo Phloi sapphires can still be classified, based on their geochemical affinities, into two main groups, namely felsic alkaline suite and contact metamorphic suites similar to those observed in Bo Phloi sapphires.

Table 5-2 Summary of mineral inclusions in basaltic sapphires from Southeast Asia found in this study and previous investigators.

Localities	Type of mineral inclusions			
	Silicates	Nb-Ta oxides	Other oxides	Others
Thailand				
Bo Phloi[1]	Zircon, alkali feldspar, nepheline, Si-rich enstatite, pyrope-almandine, biotite-phlogopite, sapphirine, staurolite		Hercynite, Manganiferous-ilmenite	Monazite, calcite
Bo Phloi[2]	Albite		Co-rich spinel	
Bo Phloi[3]	Zircon, feldspar, nepheline, biotite?,	Columbite?, pyrochlore?	Hercynite, Mn-ilmenite, thorite?	Monazite, calcite
Chanthaburi[1]	Nepheline, Si-rich enstatite	Ferrocolumbite	Apatite	
Chanthaburi[4]	Zircon, nepheline, feldspar	Columbite, pyrochlore	Magnetite	Monazite, calcite?
Phrae[1]	Alkali feldspar, nepheline, Si-rich enstatite, garnet, zircon		Zn-bearing spinel	
Laos				
Huai Sai[1]	Alkali feldspar, nepheline, Si-rich enstatite, garnet, sapphirine		Hercynite	
Huai Sai[5]	Zircon, albite	Columbite[7]	Cheralite, euxenite-Y	
Huai Sai[6]	Feldspar, Zircon	Ferrocolumbite, pyrochlore		Monazite
Cambodia				
Pailin[1]	Alkali feldspar, Si-rich enstatite, garnet	Ferrocolumbite, pyrochlore		
Pailin[7]	Plagioclase	Uranopyrochlore	Hercynite	
Vietnam				
Gia Nghia[1]	Alkali feldspar, Si-rich enstatite, staurolite			
Dak Nong[8]	Zircon, plagioclase	Columbite, pyrochlore	Apatite, ilmenite	

[1] **this study;** [2]Guo *et al.* (1996a); [3]Pisutha-Arnond *et al.* (1999; 2005); [4]Pumpang (2007); [5]Sutherland *et al.* (2002); [6]Singbamroong and Thanasuthipitak, (2004); [7]Sutherland *et al.* (1998b): [8]Pham Van *et al.* (2004).

The felsic alkaline-related mineral inclusions are exemplified by alkali feldspar, nepheline, zircon, manganiferous-ilmenite, monazite, ferrocolumbite, pyrochlore, probably Zn-bearing spinel and apatite. The alkali feldspar inclusions possess the chemical compositions similar to those inclusions from the other basaltic

sapphires in the world which were inferred to be related to the low-medium degrees of partial melting in the region (e.g., from Shandong in China sapphire, Guo *et al.,* 1992; from New England in Australia sapphire, Sutherland *et al.,* 1998b; from Huai Sai in Laos sapphire, Sutherland *et al.,* 2002). At such low degrees of partial melting occurred, a silica undersaturated melt could be produced then formed a nepheline syenite (Wilkinson and Hensel, 1994; Saminpanya, 2000; Saminpanya *et al.,* 2003). This could be verified by a common occurrence of nepheline inclusions in these sapphires.

Besides alkali feldspar and nepheline inclusions, the finding of zircon, monazite, maganiferous-ilmentite (as discussed in 5.1 above) as well as Nb-rich mineral inclusions (ferrocolumbite and pyrochlore) and apatite additionally supports the formation of Southeast Asia sapphires produced as a result of highly evolved felsic alkaline magma. For example, the existence of ferrocolumbite, pyrochlore including zircon, and alkali feldspar phases was used to indicate a melt-grown crystallization in an environment rich in high proportions of incompatible elements (e.g., U, Th, Nb, Ta, Zr and alkali) and volatiles related to late-stage crystallization from such melt (Coenraads *et al.,* 1995).

Even though, both ferrocolumbite and pyrochlore inclusions were assigned to a carbonatitic origin by Guo *et al.* (1996a), Sutherland *et al.* (1998b) later proposed a more syenitic source on the basic of high U, Nb and Ti contents. In fact, the chemical composition of ferrocolumbite and pyrochlore inclusions analyzed in this study contain higher Nb (up to 70 wt% Nb_2O_5), with traces of U and Ti contents which is somewhat differed from the composition of those inclusions analyzed by Guo *et al.* (1996a) and Sutherland *et al.* (1998b). As such our results agree fairly well with the proposal of Izokh *et al.* (2010) based on the presence of Nb-rich (ferrocolumbite) as well as zircon and plagioclase inclusions in Vietnam sapphires that the sapphire formation corresponded with the highly differentiated melt having a composition similar to phonolite (nepheline-syenite) or trachytes (syenite).

The Zn-bearing spinel inclusions in Phrae sapphires have the composition similar to gahno-spinel inclusion found in basaltic-type origin of Australia sapphires (Sutherland *et al.,* 1998b). The presence of these spinel inclusions reflects crystallizing of a typical alkaline igneous magma other than alkali basaltic magma (Frost and Lindsley, 1991) which confirms the magmatic origin of this mineral

inclusion. The presence of Zn-spinel inclusion indicates that the Phrae sapphires might have input from a source compatible with a high Zn mantle during crystallization (Stoddard, 1979).

This felsic alkaline mineral inclusion suite was earlier classified into the so-called ‘basaltic-magmatic-type’ or blue-green-yellow (BGY) sapphires (Sutherland *et al.,* 1998a) and those of magmatic sapphires linked to alkali basalts (e.g., Coenraads *et al.,* 1992a,b; Sutherland *et al.,* 1998a; Giuliani *et al.,* 2005; Graham *et al.,* 2008; Simonet *et al.,* 2008). Therefore, based on the data mentioned above, particularly those of Bo Phloi sapphires, it is likely that majority of Southeast Asia sapphires were crystallized from a highly evolved melt of alkaline syenitic/granitic composition. This data agrees well with the reports of some authors, *e.g.,* Aspen *et al.,* (1990) and Upton *et al.,* (1999), but differs from those of more complicated silicic-carbonatitic magma proposed by Guo *et al.* (1996a).

The metamorphic-related mineral inclusions are dominated by Si-rich enstatite, garnet (both alm>pyr and pyr>alm), sapphirine, staurolite and probably hercynitic spinel. Although this mineral inclusion suite is rarely found in Southeast Asia sapphires, the occurrence of these inclusions is a new evidence for more understanding of sapphires occurrence in this region. This inclusion suite indicates a growth from contact metasomatic reactions enriched in both mafic and felsic compositions rather than simple syenitic melts.

The Si-rich enstatite, sapphirine and sturolite inclusions are evidences to indicate the hybrid metasomatic reactions of basaltic magma and crustal rocks resembling earlier described in the Bo Phloi sapphire formation. Regarding garnet inclusions, garnets in Huai Sai sapphire have composition toward the pyrope member; garnet inclusions in Phrae sapphire have the composition richer toward almandine (alm>pyr) end-member and the Bo Phloi garnets have toward the pyrope-almandine (pyr>alm) end-member. The different end-members of such garnet inclusions recorded in each sample may also suggest the different environments in each locality during their crystallizations. The presence of pyrope-almandine garnet with the composition richer toward the pyrope end-member also support such metasomatic reactions as the pyrope member is likely to have occurred within lower crust-upper mantle; while almandine member reflects a high grade metamorphic rock of crustal material. In addition, hercynitic spinel can be both metamorphic and magmatic origins

(Deer *et al.,* 1992).The finding of hercynitic spinel inclusions in these sapphires that differ in composition from place to place may suggest that some may crystallize from alkaline felsic melts and perhaps others may be of metamorphic-related origin similar to those found in the “Corsilzirspite’ gravel from Bo Phloi mine. The presence of these mineral inclusions in other Southeast Asia sapphires (not just only occurred in Bo Phloi area) suggest that the contact metamorphic-related sapphires did occur and were a common origin among the Southeast Asia sapphire deposits as well.

This metamorphic mineral inclusion suite is however quite different from the ‘basaltic-metamorphic-type’ inclusion suites found in basaltic ruby at Thai-Cambodia border (i.e., high-Al diopside so called ‘fassaite’, pyrope garnet and sapphirine; Sutthirat *et al.,* 2001; Saminpanya and Sutherland, 2011), and probably at Barrington gem field in Australia previously proposed by Sutherland *et al.* (1998b) and Sutherland and Schwarz (2001). It is therefore likely that these two differing metamorphic inclusion suites could have been formed under entirely different sources provenance and condition with respect to such differing inclusion assemblages. The occurrence of this inclusion suite in basaltic sapphires has provided a strong argument to support another origin of metamorphic-related sapphire in Southeast Asia in addition to the magmatic origin of the basaltic sapphires as previous reported by many authors (e.g., Guo *et al.,* 1996a; Sutherland *et al.,* 1998a; Limtrakun *et al.,* 2001; Yui *et al.,* 2003; 2006). Hence, it is strongly suggested to include another contact metamorphic-related sapphire to the origin of Southeast Asia sapphires.

Referring to the results of mineral inclusions discussed above, it is reasonable to propose a generalized bimodal genetic model for Southeast Asia sapphire formation (resemble to that of the Bo Phloi sapphires) as (1) felsic alkaline origin, by which the sapphires could crystallize from a highly evolved melts of alkali felsic composition derived from a low degree partial melting of crustal material, and (2) contact metamorphic origin, by which the sapphires could originate from different basement sources such as the metasomatized crustal rocks and contaminated melt at the contact zone of basaltic intrusion.

5.5 Time Constraint on Sapphire Formation and Basaltic Eruption in Southeast Asia

Radiometric age dating results of basalts, alluvial zircons, mineral inclusions in sapphires and corundum-bearing assemblages from various localities in Southeast Asia are compiled in Table 5-3 and displayed as geochronological scale in Table 5-4. As shown in the tables, in general, the ages obtained by K-Ar method seem to give somewhat younger than those obtained by Ar-Ar technique; particularly, notifications of those were reported from the same areas, e.g. Bo Phloi, Nong Bon. The apparent younger K-Ar dates may be the partly-reset ages due to Ar lost.

Sapphire-related basalt in Wichianburi, Phetchabun province in Thailand gave the oldest age (11.03±0.03 Ma, Ar-Ar dating; Sutthirat *et al.*, 1994); whereas basalt from Khao Ploi Wean, Chanthaburi-Trat area gave the youngest age (0.44±0.11 Ma, K-Ar dating; Barr and Macdonald, 1979, 1981). This marks the oldest and youngest ages of corundum-related basalts so far recorded in Southeast Asia (most data from Thailand and some data from Laos, Vietnam and Cambodia). During this time interval, there were eruptions of such basalts episodically (e.g., ~9 Ma in Wichianburi, ~7-1 Ma in Dak Nong, Vietnam, ~5.6 Ma in Denchai, ~4-3 Ma in Bo Phloi, ~3.3 Ma in Ubon Ratchathani-Sri Saket, ~3 Ma in Khao Wua, ~2.4-1 Ma in Nong Bon, ~2.3 Ma in Sop Prab-Ko Kha, ~2 Ma in Nam Cho, ~1.7 Ma in Huai Sai, Laos, ~1 Ma in Pailin, Cambodia, and ~0.6 in Mae Tha; Barr and Macdonald, 1978; 1981; Sutthirat *et al.*, 1994; Sutthirat, 1995, 2001; Carbonnel *et al.*, 1973; Sasada *et al.*, 1987; Intasopa, 1993; Graham *et al.*, 2006). Eruptions of corundum-barren basalts were also took placed episodically from ~24 to <1 Ma (e.g., ~24, ~18 and ~11 Ma in Lam Narai, ~12.3, ~11.6, ~8.8 Ma in Djiring Plateau, Vietnam and ~0.92 Ma in Buriram; Barr and Macdonald, 1979, 1981; Intasopa, 1993). Furthermore, the fission track ages of alluvial zircons from some deposits span from 5.5 to 2.0 Ma (e.g., Carbonnel *et al.*, 1973; Sutthirat, 2001; Graham *et al.*, 2006) seem to match with the basalt ages in the areas suggesting that they are the reset ages by those hot basaltic magmas that carried them along with corundum from underneath.

Zircon inclusion in Bo Phloi sapphire gives the U-Pb age of 24±0.9 Ma using LA-ICP-MS; moreover, the Th-U-Pb ages of both zircon and monazite inclusions range, based on EPMA application, from 45-18 Ma (some of which match with

alluvial zircon ages). The U-Pb age of Bo Phloi zircon from zircon+sapphire+nepheline+hercynitic spinel assemblage is at 4.4±0.4 Ma, and the U-Pb age of zircon in 'Corsilzirspite' gravel from Bo Phloi sapphire mine gave 10.86±0.14 Ma (both from unpublished data of Pisutha-Arnond). The U-Pb ages of zircon inclusion in Huai Sai sapphire, Laos, give 1.2-1.3±0.3 Ma (Sutherland *et al.*, 2002). The U-Pb age of zircon in an unusual sapphire-zircon-magnetite xenolith in the alluvial at Khao Wua, Chanthaburi, Thailand, give 1-2(±<1) Ma (Coenraads *et al.*, 1995). These age data imply that the crystallization of sapphire occurred episodically at depth and had spanned continuously from as old as 45 Ma to as young as 1 Ma. However, more reliable data (U-Pb dating of zircon) appear to be those younger than 24 Ma. The eruption of corundum-barren basalts appear to have been taken place somewhat younger from ~ 24 to <1 Ma, and even younger for the corundum-related basalts from ~11 to <1 Ma. These scenarios seem to suggest that the eruption of deep-seated alkaline basalts and probably the formation of sapphire at depth could have been taken place and become increasingly more intensive towards the younger ages particularly those in the last 11 Ma in such a way that there were more chance of sapphire having been picked up by those basalts and carried them up to the surface more in the last episode.

Referring to the chronologic data discussed above, it is therefore proposed here that the generalized genetic model of Southeast Asia sapphires is divided into two-stages, each with distinctive chronologic signatures, at ≥ 11 Ma and ≤ 11 Ma. The older period represents the formation of early sapphires at depth while the younger period represents the time while they were still forming and starting to be picked up by deep seated basaltic magmas and carried to the surface. The 11 Ma is selected because it marks the oldest corundum-related basalt, so far dated, in this region.

Table 5-3 Compilation of radiometric age dating results of corundum-related basalts, alluvial zircon and mineral inclusions in sapphires from various localities from Southeast Asia.

Basaltic Localities	Age (Ma)						
	Basalts		Alluvial zircons		Zircon inclusions		Monazite inclusions
	K-Ar	Ar-Ar	Fission track	U-Pb	U-Pb	Th-U-Pb	Th-U-Pb
Thailand							
Bo Phloi❶	3.14±0.17[a]	4.17±0.11[b]	2-3.5, 4.5-5.5[c]	25,30[c]	24±0.9[M]	18±11[M]	~25–30[M], ~42–45[M]
Chanthaburi-Trat❶							
- Nong Bon	1.13±0.17[a]	2.38±0.16[b]					
- Khao Wua		3.0±0.19[b]	2.57±0.02[d]	1-2(±<1) [h] (X)			
- Khao Ploi Waen	0.44±0.11[a]						
Phrae-Sukothai (Denchai) ❶	5.64±0.28[a]						
Phetchabun (Wichianburi) ❶		8.82±0.09[b], 11.03±0.03[b] 9.08±0.29[f]					
Ubon Ratchathani-Sri Saket❶	3.28±0.48[a]						
Chiang Rai (Chiang Khong) ❶	1.74±0.12[a]						
Lampang❶							
- Mae Tha	0.8±0.3[e], 0.59 ±0.05[e]	0.59±0.05[b]					
- Nam Cho		2.02±0.10[g]					
- Sop Prap-Ko Kha		2.30±0.13[g]					
Lopburi (Lam Narai)❷	11.29±0.64[a], 18±0.7[f], 24.1±1.0[f]						
Buriram❷	0.92±0.3[a]						
Laos							
Huai Sai❶	1.74±0.18[a], 1-2[j]		2.4- 4.3[j]	3.3-4.09[j]	1.2-1.3±0.3[k]		
Cambodia							
Pailin❶	1.09±0.13[a]		2.27±0.15[a], 2.39±0.20[a], 2.60±0.2[a]				
Vietnam							
Dak Nong (Southern area)❶	1.1-7.1[j]			1.05[i], 6.5[i] (M)			
Djiring Plateau❷	8.8±0.3[a], 11.6±0.3[a], 12.3±1.1[a]						

M = Megacrysts; X = Xenolith, ❶= corundum related basalts, ❷ = corundum barren basalts

[a]Barr and Macdonald, (1978; 1981); [b]Sutthirat *et al.* (1994); [c]Sutthirat, (2001); [d]Carbonnel *et al.*, 1973; [e]Sasada *et al.*, 1987; [f]Intasopa, 1993; [g]Sutthirat *et al.*, 1995; [h]Coenraads *et al.*, 1995; [i]Garnier *et al.* (2005); [j]Graham *et al.* (2006), [k]Sutherland *et al.* (2002); [M]**this study**.

Table 5-4 Geochronological scales with respect to radiometric dating of basalts, alluvial zircon and mineral inclusions in sapphires from Southeast Asia.

Geological Time Scale			Age (Ma)	Cenozoic basaltic activity in Thailand ($^{40}Ar/^{39}Ar$)	Basaltic eruption (K-Ar, Ar-Ar, FT)	Alluvial zircon (U-Pb dating)	Mineral inclusion	
							U-Pb zircon dating	Th-U-Pb dating
Cenozoic	Quaternary	Holocene	0.001	<1.6[a]				
		Pleistocene	0.125					
			0.7		~0.4-11[a,b,c,d,e,f,g,j] (corundum-related basalts)			
			1.2			1-2(±<1)[h] (Khao Wua), 1.05[i] (Dak Nong)	1.2-1.3±0.3[k] (Huai Sai)	
	Neogene		1.6	1.6-3.6[a]				
		Pliocene	2.5					
			3.5	4-5.3[a]		3.3-4.1[j] (Huai Sai)		
			5			4.4±0.4[m] (in Bo Phloi assemblage)		
		Miocene	6			6.5[l] (Dak Nong)		
			7					
			8	8-14[a]				
			9					
			10					
			11			10.86±0.14[m] (in Bo Phloi 'Corsilzirspite')		
			12					
			13					
			14					
			15					
			16					
			17					
			18	18-20[a]				18±11[l] (Bo Phloi zircon)
			19					
			20					
	Paleogene		23	22-24[a]				
		Oligocene						
			25			25[c] (Bo Phloi)	24±0.9[l] (Bo Phloi)	~25-30[l] (Bo Phloi monazite)
			30			30[c] (Bo Phloi)		
		Eocene	35					
								~42-45[l] (Bo Phloi monazite)
		Paleo-cene	55					
			65					

[a]Sutthirat *et al.* (1994); [b]Barr and Macdonald, (1979, 1981);[c]Sutthirat, (2001); [d]Carbonnel *et al.*, 1973; [e]Sasada *et al.*, 1987; [f]Intasopa, 1993; [g]Sutthirat *et al.*, 1995; [h]Coenraads *et al.*, 1995; [i]Garnier *et al.* (2005); [j]Graham *et al.* (2006), [k]Sutherland *et al.* (2002); [l]**this study**; [m]Unpublished data of Pisutha-Arnond (zircon in Corsilzirspite gravel and zircon in assemblage from Bo Phloi sapphire mine).

5.6 A Generalized Genetic Model of Basaltic Sapphire Formation in Southeast Asia

The principal features for generalized model of Southeast Asia sapphire formation are present in Figure 5-4.

The first period (Figure 5-4,❶) was the main events of sapphire formation and eruptive period of sapphire-barren basalt range at ≥ 11 Ma. The existing ages of mineral inclusions (U-Pb zircon age at 24±0.9 Ma; Th-U-Pb zircon age at 18±11 Ma; Th-U-Pb ages of monazite inclusions at ~25-30 Ma and 42-45 Ma as well as alluvial zircons age at 25, 30 Ma recorded in this region) indicated that they are crystallized in this stage and appeared to at least ~11 Ma. The formation of sapphire during this interval may possibly relate to the India-Eurasia collision age (45-55 Ma; Klootwijk *et al.*, 1992; Fedorov and Koloskov, 2005) resulting in the development of Cenozoic basins in this region afterwards (e.g., McCabe *et al.*, 1988; Charusiri *et al.*, 1991). After plate collision, the decompressed stress was generated and then generating some localized melts in this region both in the upper mantle and lower crustal zones. In the upper mantle, pockets of basaltic magma may originate from partial melting of lithospheric upper mantle at a very great depth of over 100 km (Sutthirat *et al*., 2005). This process may be the result of heat transfer from the asthenosphere mantle plume. In the lower crust above, the plume allowed low degree partial melting of crustal protoliths leading to generation of small pockets of felsic alkaline or syenitic melts. Therefore, sapphires could be crystallized from such melt earlier (based on the dating ages of those mineral inclusions) so called ‘syenitic melt-related sapphire’. However, these small pockets of sapphire-bearing syenite still stayed at some particular depths as well as basaltic magma had be continuously derived from partial melting and resided in the mantle. In certain areas, however, basaltic eruptions could have taken place but there was less chance of picking these small sapphire-bearing pockets up to the surface. Hence, basaltic eruptions during this early period were mainly sapphire-barren basalts (based on the age dating of Southeast Asia basalts).

The second period (Figure 5-4,❷) was the main events of eruptive sapphire-related basalts at ≤ 11 Ma which are supported by the age dating of sapphire-related basaltic eruptions (11-0.4 Ma), the U-Pb age of zircon in ‘Corsilzirspite’ gravel (10.86±0.14 Ma), the U-Pb age of zircon in zircon+sapphire+nepheline+hercynitic spinel assemblage (4.4±0.4 Ma), (both from unpublished data of Pisutha-Arnond),

Huai Sai U-Pb zircon inclusion ages (1.2-1.3±0.3 Ma; Sutherland *et al.,* 2002), the U-Pb ages of zircon in an unusual sapphire-zircon-magnetite xenolith in the alluvial at Khao Wua (1-2 (±<1) Ma; Coenraads *et al.,* 1995) and the U-Pb ages of zircon megacryst in Dak Nong gem field (1.05, 6.5 Ma; Garnier, *et al.,* 2005). After 11 Ma, the syenitic melt-related sapphires could still be formed episodically. During this time interval, enormous basaltic melts could generated continuously from partial melting of upper mantle and rising up to the surface. During their ascending, this magma could be partly stored and contaminated with more felsic rocks resulting in the formation of sapphires at the contact metamorphic zone (supported by the presence of 'corsilzirspite' gravel in Bo Phloi gem field) so-called 'contact metamorphic-related sapphire'. However, main basaltic magmas could pick up sapphires from both origins (but mostly rather from syenitic origin) and other xenoliths and xenocrysts during their rising up to the surface with very fast rates as suggested by Sutthirat *et al.* (2005). Episodically, therefore sapphires from both origins, as well as xenoliths and xenocrysts from the different layers were picked up from various depths and carried to the earth surface via such basaltic eruptions in the region.

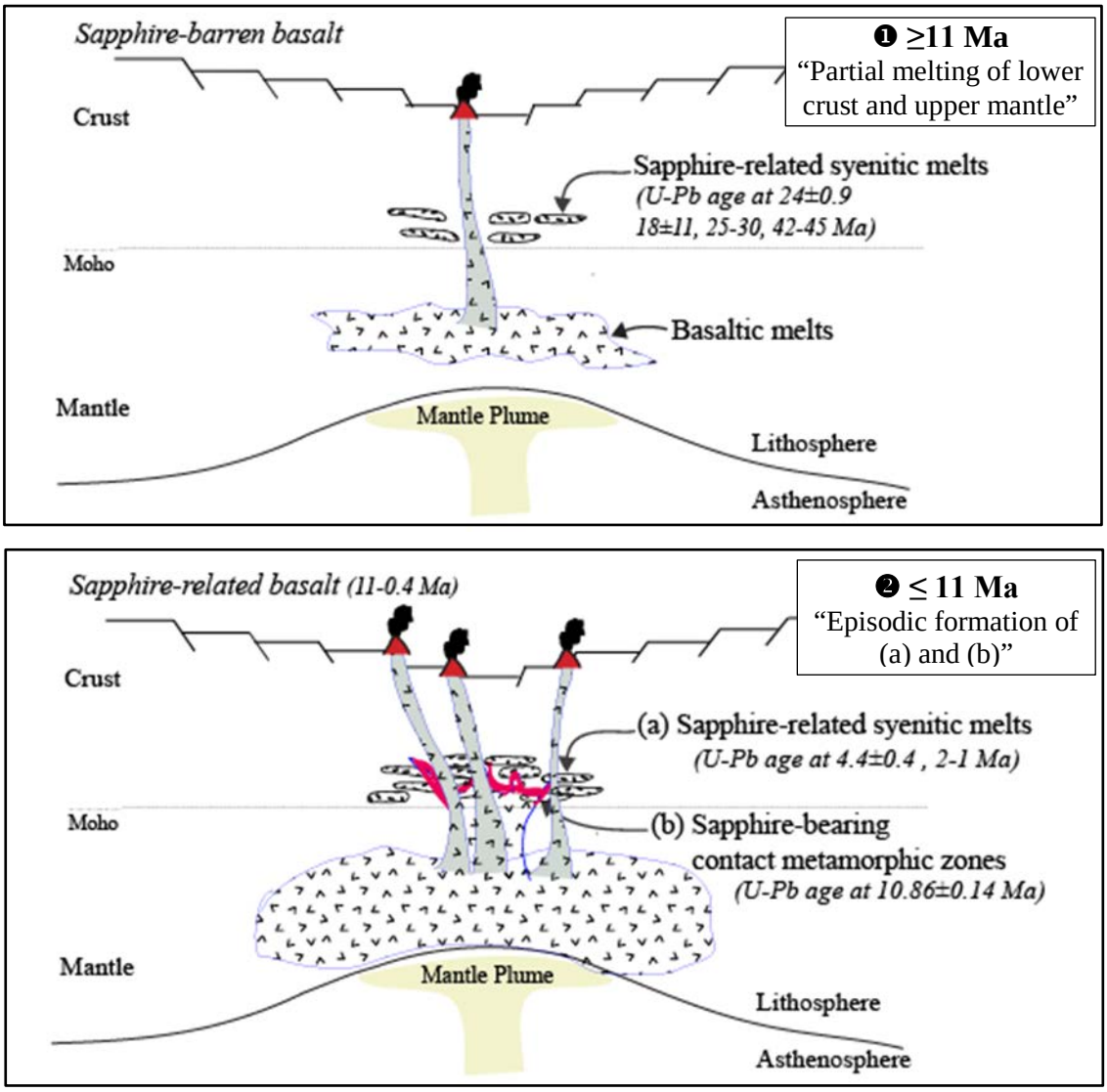

Figure 5-2 A generalized bimodal genetic model of Southeast Asia sapphires related to a syenitic melt-related origin and contact metamorphic-related origin based on chronological data described in the text.

5.7 Conclusions

The detailed mineral chemistry of inclusions in the basaltic Southeast Asia sapphires, particular those in the Bo Phloi sapphires, carried out by this study have given the unique mineral inclusion suites relevant to the origin of their host sapphires. The results of this study are summarized below.

1. The mineral inclusions found in the Bo Phloi sapphires illustrate a wide range of mineral phases which comprise alkali feldspar, nepheline, hercynitic spinel, zircon, manganiferous-ilmenite, silica-rich enstatite,

pyrope-almandine garnet richer towards pyrope component, monazite, calcite, sapphirine, biotite-phlogopite and staurolite.

2. The trace element study of representative zircon inclusion in Bo Phloi sapphire provide the typical characteristic positive Ce anomaly and Eu depletion of chondrite normalized REE patterns which conclusively demonstrate that this zircon inclusion was crystallized from a syenite-pegmatitic magma.
3. The mineral inclusions found in sapphires from Chanthaburi, Phrae in Thailand; Huai Sai in Laos; Pailin in Cambodia and Gia Nghia in Vietnam are similar to those found in the Bo Phloi sapphires, but lack ilmenite, monazite, calcite, biotite-phlogospite and additionally contain ferrocolumbite, pyrochlore and apatite.
4. The mineral chemistry of inclusions in sapphires from Southeast Asia sapphires (including Bo Phloi sapphire) appears to have at least two distinct mineral groups, namely felsic alkaline suite and contact metamorphic suite, which were likely to originate from different environments. A ‘bimodal genetic model’ is therefore proposed based on such strong evidences; one related to ‘a syenitic melt-related origin’ and the other to ‘a contact metamorphic-related origin’ for the Southeast Asia sapphire formation.
5. The U-Pb dating of a Bo Phloi zircon inclusion yields an age of 24±0.9 Ma, and the Th-U-Pb dating of Bo Phloi zircon and monazite inclusions give about 18±11 Ma and ~25-30 Ma, respectively, that are very close to the early volcanism (late Oligocene ~ 22-24 Ma) of Late Cenozoic basalts in Thailand. In addition, another Th-U-Pb dating of monazite inclusions give ages at ~42-45 Ma which may suggest that these alkali melt-related sapphire formation could possibly be formed first and closely linked to the early Cenozoic basaltic eruptions in the Southeast Asia region.

5.8 Recommendations for future works

Further study on the mineral inclusions in basaltic Southeast Asia corundums is recommended as follows:

1. More inclusions study should be carried out on sapphires from other localities except Bo Phloi sapphires as well as from basaltic rubies of the region in order to give a complete model of Southeast Asia basaltic corundum formation.
2. The detailed X-ray diffraction study on the crystallography of the Si-rich enstatite inclusions found in these sapphires should be investigated.
3. The REE and trace element analyses of monazite and pyrochlore inclusions should be performed by using the LA-ICP-MS technique. The information from such study should give a better understanding on their host sapphires.
4. The U-Pb dating of more zircon inclusions should be carried out to give a better constraint on the ages of their host sapphire crystallization in this region.
5. The Th-U-Pb dating of both zircon and monazite inclusions should be carried out in more details. The operating conditions of such analyses should be examined to obtain the optimal condition for measuring the mineral inclusions in sapphires.

REFERENCES

Abduriyim, A. and Kitawaki, H. 2006. Determination of the origin of blue sapphire using Laser Ablation Inductively Coupled Plasma Mass Spectroscopy (LA-ICP-MS). J. Gemmol. 30: 23-36.

Ahrens, L.H., Cherry, R.D. and Erlank, A.J. 1967. Observation on the Th–U relationship in zircons from granitic rocks and from kimberlites. Geochim. Cosmochim. Acta 31: 2379-2387.

Aspen, P., Upton, B.G.J. and Dickin, A.P. 1990. Anorthoclase, sanidine and associated megacrysts in Scottish alkali basalts: high-pressure syenitic debris from upper mantle sources. Eur. J. Mineral. 2: 503–517.

Barr, S.M. and Macdonald, A.S. 1978. Geochemistry and petrogenesis of Late Cenozoic alkaline basalts of Thailand. Geol. Soc. Malaysia Bull. 10: 21-48.

Barr, S.M. and Macdonald, A.S. 1981. Geochemistry and geochronology of Late Cenozoic basalts of Southeast Asia. Geol. Soc. Amer. Bull. 92: 1069-1142.

Belousova, E.A., Griffin, W.L., O'Reilly, S.Y. and Fisher, N.I. 2002. Igneous zircon: trace element composition as an indicator of source rock type. Contrib. Mineral. Petrol. 143: 602-622.

Belyanin, G.A., Rajesh, H.M., Van, R.D.D. and Mouri, H. 2010. Corundum+orthopyroxene±spinel intergrowths in an ultrahigh-temperature Al-Mg granulite from the Southern Marginal Zone, Limpopo Belt, South Africa. Am. Mineral. 95: 196–199.

Black, L.P., Kamo, S.L., Allen, C.M., Aleinikoff, J.N., Davis, D.W., Korsch, R.J. and Foudoulis, C. 2003. TEMORA 1: a new zircon standard for Phanerozoic U-Pb geochronology. Chem. Geol. 200 (1-2): 155-170.

Black, L.P., Kamo, S.L., Allen, C.M., Davis, D.W., Aleinikoff, J.N., Valley, J.W., Mundil, R., Campbell, I.H., Korsch, R.J., Williams, I.S. and Foudoulis, C. 2004. Improved $^{206}Pb/^{238}U$ microprobe geochronology by the monitoring of a trace-element-related matrix effect; SHRIMP, ID–TIMS, ELA–ICP–MS and oxygen isotope documentation for a series of zircon standards. Chem. Geol. 205: 115-140.

Bosshart, G. 1995. Sapphires and rubies from Laos. 25th International Gemmological Conference Program. Rayong, Thailand, pp. 23-26.

Carbonnel, J.P., Selo, M. and Poupeau, G. 1973. Fission track age of the gem deposits of Pailin (Cambodia) and recent tectonics in the Indochinan Province. Modern Geology 4: 61-64.

Chang, Z., Vervoort, J.D., McClelland, W.C. and Knaack, C. 2006. U-Pb dating of zircon by LA-ICP-MS. Geochem. Geophys. Geosyst. 7 (5): 1-14.

Charusiri, P., Clark, A.H. and Farrar, E., 1991. Miocene (Oligocene events in Thailand: Evidences from $^{40}Ar/^{39}Ar$ and K-Ar geochronology. Proceedings of the Annual Technical Meeting 1989 and IGCP-246. Chiang Mai, Thailand, pp. 245-262.

Cherniak, D.J., Bruce, W.E., Grove, M. and Mark, H.T. 2004. Pb diffusion in monazite: A combined RBS/SIMS study. Geochim. Cosmochim. Acta 68 (4): 829-840.

Chualaowanich, T., Sutthirat, C., Harzenberger, C. and Pisutha-Arnond, V. 2005. Another constraint on Thai-corundum genesis: new evidence from ruby-bearing xenoliths from the eastern gem field, Thailand. Proceedings of the International Conference on Geology, Geochronology and Mineral Resources of Indochina (GEOINDO 2005). Khon Kaen, Thailand, pp 345.

Cocherie, A., Legendre, O., Peaucat, J. J. and Kouamelan, A.N. 1998. Geochronology of polygenetic monazites constrained by in situ electron microprobe Th-U-total lead determination: Implications for lead behavior in monazite. Geochim. Cosmochim. Acta 62: 2475-2497.

Cocherie, A. and Albarede, F. 2001. An improved U-Th-Pb age calculation for electron microprobe dating of monazite. Geochim. Cosmochim. Acta 65 (24): 4509-4522.

Cocherie, A. and Legendre, O. 2007. Potential minerals for determining U-Th-Pb chemical age using electron microscope. Lithos 93: 288-309.

Coenraads, R.R., Sutherland, F.L. and Kinny, P.D. 1990. The origin of sapphires; U-Pb dating of zircon inclusions sheds new light. Mineral. Mag. 54: 113-122.

Coenraads, R.R. 1992a. Sapphires and rubies associated with volcanic provinces: inclusions and surface features shed new light on their origin. Austral. Gemmol. 54: 70-78.

Coenraads, R.R. 1992b. Surface features of natural rubies and sapphires associated with volcanic provinces. J. Gemmol. 23: 151-160.

Coenraads, R.R., Vichit, P. and Sutherland, F.L. 1995. An unusual sapphire-zircon magnetite xenolith from the Chanthaburi Gem Province, Thailand. Mineral. Mag. 59: 465-479.

Compston, W. 1999. Geological age by instrumental analysis: The 29th Hallimond lecture. Mineral. Mag. 63: 297-311.

Dao, N.Q. and Delaigue, L. 2000. Raman micro-spectrometry and its applications to the identification of inclusions in natural rubies. Analusis 28: 34-38.

Deer, W.A., Howie, R.A. and Zussman, J. 1992. An Introduction to the Rock-Forming Minerals. 2nd Edition, Longman, Essex, UK, 696 pp.

Droop, G.T.R. 1987. A general equation for estimating Fe^{3+} concentrations in ferromagnesian silicates and oxides from microprobe analyses, using stoichiometric criteria. Mineral. Mag. 51: 431-435.

Fedorov, P.I. and Koloskov, A.V. 2005. Cenozoic Volcanism of Southeast Asia. Petrology 13(4): 352-380.

Frost, B.R. and Lindsley, D.H. 1991. Occurrence of iron-titanium oxides in igneous rocks. Rev. Mineral. Geochem. 25: 433-468.

Fryer, B.J., Jackson, S.E. and Longerich, H.P. 1993. The application of laser ablation microprobe-inductively coupled plasma mass spectrometry (LAM-ICPMS) to in situ (U)-Pb geochronology. Chem. Geol. 109: 1-8.

Fujimaki, H. 1986. Partition coefficients of Hf, Zr, and REE between zircon, apatite, and liquid. Contrib. Mineral. Petrol. 94:42-45.

Garnier, V., Ohnenstetter, D., Giuliani, G., Fallick, A.E., Phan Trong, T., Hoàng Quang, V., Pham Van, L. and Schwarz, D. 2005. Basalt petrology, zircon ages and sapphire genesis from Dak Nong, southern Vietnam. Mineral. Mag. 69 (1): 21-38.

Giuliani, G., Fallick, A.E., Garnier, V., France-Lanord, C., Ohnenstetter, D. and Schwarz, D, 2005. Oxygen isotope composition as a tracer for the origins of rubies and sapphires. Geology 33: 249–252.

Graham, I.T, Sutherland, F.L. and Armstrong, R. 2006. Probing the 'Zircon Zip': Geochronology (FT and SHRIMP). Australian Earth Sciences Convention (AESC2006), Melbourne, Australia, pp. 1-2.

Graham, I.T, Sutherland, F.L, Zaw, K., Nechaev, V. and Khanchuk, A. 2008. Advances in our understanding of the gem corundum deposits of the West pacific continenetal margines intraplate basaltic fields. Ore Geol. Rev. 34: 200-215.

Gübelin, E.J. and Koivula, J.I. 2005. Photoatlas of Inclusions in Gemstones. Vol. 3. Basel: Opinio Publishers.

Guo, J., Wang, F. and Yakoumelos, G. 1992. Sapphires from Changle in Shandong Province, China. Gems Gemmol. 28 (4): 255-260.

Guo, J., Griffin, W.L. and O'Reilly, S.Y. 1994. A cobalt-rich spinel inclusion in a sapphire from Bo Ploi, Thailand. Mineral. Mag. 58: 247-258.

Guo, J., O'Reilly, S.Y. and Griffin, W.L. 1996a. Corundum from basaltic terrains: a mineral inclusion approach to the enigma. Contrib. Mineral. Petrol. 122: 358-386.

Guo, J., O'Reilly, S.Y. and Griffin, W.L. 1996b. Zircon inclusion in corundum megacrysts: I. Trace element geochemistry and clues to the origin of corundum megacrysts in alkali basalt. Geochim. Cosmochim. Acta. 60: 2347-2363.

Hanchar, J.M., Finch, R.J., Hoskin, P.W.O., Watson, E.B., Cherniak, D.J. and Mariano, A.N. 2001. Rare earth elements in synthetic zircon; part I. synthesis, and rare element and phosphorus doping. Am. Mineral. 86: 667-680.

Hansawek, R. and Pattamalai, K. 1997. Kanchanaburi sapphire deposits. Proceedings of the international conference on stratigraphy and tectonic evolution of Southeast Asia and the South Pacific. Bangkok, Thailand, pp. 717.

Heaman, L.M., Bowins, R. and Crocket, J. 1990. The chemical composition of igneous zircon suites: implications for geochemical tracer studies. Geochim. Cosmochim. Acta 54: 1597-1607.

Hinton, R.W. and Upton, B.G.J. 1991. The chemistry of zircon: variations within and between large crystals from syenite and alkali basalt xenoliths. Geochim. Cosmochim. Acta 55 (11): 3287-3302.

Hinton, R.W. and Meyer, C. 1991. Ion probe analysis of zircon and yttrobetatite in a lunar granite. Lunar Planet. Sci. XXII: 575-576.

Hoang, N. and Flower, M. 1998. Petrogenesis of Cenozoic Basalts from Vietnam: Implication for Origins of a 'Diffuse Igneous Province'. J. Petrology 39 (3): 369-395.

Hoskin, P.W.O. and Schaltegger, U. 2003. The composition of zircon and igneous and metamorphic petrogenesis. In: Hanchar, J.M. & Hoskin, P.W.O. (eds) Zircon. Rev. Mineral. Geochem. 53: 27–62.

Hughes, R.W. 1997. Ruby and Sapphire. RWH Publishing, Boulder, Colorado, 511 pp.

Intasopa, S. 1993. Petrology and geochronology of the volcanic rocks of the Central Thailand volcanic belt. Doctoral dissertation, The University of New Brunswick, Canada.

Intasopa, S., Atichat, W. and Pisutha-Arnond, V. 1998. Inclusions in Corundum: a New Approach to the Definition of Standards for Origin Determination, Science and Technology for Gem and Jewelry Industry, Thailand Research Fund, pp. 29-51 (in Thai).

Intasopa, S., Atichart, W., Pisutha-Arnond, V., Sriprasert, B., Narudeesombat, N. and Putharat, T. 1999. Inclusion in Chantaburi-Trat corundum: A clue to their genesis. (in Thai). Proceedings of the Symposium on Mineral, Energy, and Water Resources of Thailand: Towards the year 2000. Bangkok, Thailand, pp. 471-484.

Izokh, A.E., Smirnov, S.Z., Egorova, V.V., Anh, Tran Tuan, Kovyazin, S.V., Phuong, Ngo Thi. and Kalinina, V.V. 2010. The conditions of formation of sapphire and zircon in the areas of alkali-basaltoid volcanism in Central Vietnam. Russ. Geol. Geophys. 51: 719-733.

Jackson, S.E., Pearson, N.J., Griffin, W.L. and Belousova, E.A. 2004. The application of laser ablation-inductively coupled plasma-mass spectrometry to in situ U-Pb zircon geochronology. Chem. Geol. 211 (1-2): 47-69.

Jungyusuk, N. and Khositanont, S. 1992. Volcanic rocks and associated mineralization in Thailand. Proceedings of the National Conference on Geologic Resources of Thailand: Potential for future development. Bangkok, Thailand, pp. 528-532.

Klootwijk, C.T., Gee, J.S., Peirce, J.W., Smith, G.M. and McFadden, P.L. 1992. An early India-Asia contact: Paleomagnetic constraints from Ninetyeast Ridge, ODP Leg 121. Geology 20: 395-398.

Koivula, J.I. 1987. Sapphirine (not sapphire) in a ruby from Bo Rai, Thailand. J. Gemmol. 20: 369–370.

Kosler, J. and Sylvester, P.J. 2003. Present trends and the future of zircon in geochronology: laser ablation ICPMS. In: Hanchar JM and Hoskin PWO (eds), Zircon. Rev. Mineral. Geochem. 53: 243-275.

Krzemnicki, M.S., Hänni, H.A., Guggenheim, R. and Mathys, D. 1996. Investigations on sapphires from an alkali basalt, South West Rwanda. J. Gemmol. 25 (2): 90-106.

Kusiak, M.A., Dunkley, D.J., Słaby, E., Martin, H. and Budzyń, B. 2008. Sensitive high-resolution ion microprobe analysis of zircon reequilibrated by late magmatic fluids in a hybridized pluton. Geology 37 (12): 1063-1066.

Lee, T.Y and Lawver, L.A. 1995. Cenozoic plate reconstruction of South East Asia. Tectonophysics. 251: 85-138.

Levinson, A.A. and Cook, A. 1994. Gem corundum in alkali basalt: origin and occurrence. Gems Gemol. 30 (3): 253-262.

Lindsley, D. H. 1983. Pyroxene thermometry. Amer. Min. 68: 477-493.

Lovatt-Smith, P.F., Stokes, R.D., Bristow, C. and Carter, A. 1996. Mid-Cretaceous inversion in the Norththern Khoray Plateau of Lao PDR and Thailand. In: Hall, R., Blundell, D. (eds.). Tectonic Evolution of Southeast Asia, Geological Society Special Publication 106, pp. 233-247.

Li, Q., Liu, S., Wang, Z., Han, B., Shu, G. and Wang, T. 2008. Electron microprobe monazite geochronological constraints on the Late Palaeozoic tectonothermal evolution in the Chinese Tianshan. J. Geol. Soc. London 165: 511-522.

Limtrakun, P., Khin, Zaw, Ryan, C.G. and Mernagh, T.P. 2001. Formation of the Denchai gem sapphires, northern Thailand: evidence from mineral chemistry and fluid/melt inclusion characteristics. Mineral. Mag. 65: 725–735.

Liu, S., Liu, C., Li, Q., Lu, Y., Yu, S., Tian, W. and Feng, Y. 2007. EPMA Th-U-Pb Monazite Dating of Zhongtiao and Lüliang Precambrian Metamorphic Complexe. Earth Sci. Front. 14 (1): 64-74.

Maesschalck, A.A., and Oen, I.S. 1989. Fluid and mineral inclusions in corundum from gem gravels in Sri Lanka. Mineral. Mag. 53: 539-545.

McCabe, R., Celeya, M., Cole, J., Han, H.C., Ohnstadt, T., Paijitprapaporn, V. and Thitisawan, V. 1988. Extension tectonics; The Neogene opening of the N-S trend basin of central Thailand. J. Geophys. Res. 93: 11899-11910.

Montel, J.M., Foret, S., Veschambre, M., Nicollet, C. and Provost, A. 1996. Electron microprobe dating of monazite. Chem. Geol. 131: 37−53.

Murali, A.V., Parthasarathy, R., Mahadevan, T.M. and Sankar, D.M. 1983. Trace element characteristics, REE patterns and partition coefficients of zircons from different geological environments - a case study on Indian zircons. Geochim. Cosmochim. Acta 47: 2047-2052.

Nagasawa, H. 1970. Rare earth concentrations in zircon and apatite and their host dacites and granites. Earth Planet. Sci. Lett. 9: 359-364.

Nemchin, A.A., Grange, M.L. and Pidgeon, R.T. 2010. Distribution of rare earth elements in lunar zircon. Amer. Mineral. 95: 273-283.

Norman, M.D., Pearson, N.J., Sharma, A. and Griffin, W.L. 1996. Quantitative analysis of trace elements in geological materials by laser ablation ICP-MS: Instrumental operating conditions and calibration values of NIST glasses. Geostandard Newslett. 20: 247-261.

Norman, M.D., Griffina, W.L., Pearsona, N.J., Garciac, M.O. and O'Reillya, S.Y. 1998. Quantitative analysis of trace element abundances in glasses and minerals: a comparison of laser ablation inductively coupled plasma mass spectrometry, solution inductively coupled plasma mass spectrometry, proton microprobe and electron microprobe data. J. Anal. At. Spectrom. 13: 477-482.

Oakes, G.M., Barron, L.M. and Lishmund, S.R. 1996. Alkali basalts and associated volcaniclastic rocks as a source of sapphire in eastern Australia. Austral. J. Earth Sci. 43: 289-298.

Pakhomova, V., Zalishchak, B., Tishkina, V., Lapina, M., Karmanov, N., 2006. Mineral and melt inclusions in sapphires as an indicator of conditions of their formation and origin. Austral. Gemmol. 22: 508–511.

Palenza, V., Martino, D., Paleari, A., Spinolo, G. and Prosperi, L. 2008. Micro-Raman spectroscopy applied to the study of inclusions within sapphire. J. Raman Spectrosc. 39: 1007-1011.

Parrish, R.R. 1990. U-Pb dating of monazite and its application to geological problems. Can. J. Earth. Sci. 27: 1431-1450.

Peucat, J.J., Ruffault, P., Fritsch, E., Bouhnik-Le, M.C., Simonet, C. and Lasnier, B. 2007. Ga/Mg ratio as a new geochemical tool to differentiate magmatic from metamorphic blue sapphires. Lithos 98: 261-274.

Pham Van, L., Hoáng Quang, V., Garnier, V., Giuliani, G., Ohnensretter, D., Lhomme, T., Schwarz, D., Fallick, A., Dubessy, J. and Phan Trong, T. 2004. Gem corundum deposits in Vietnam. J. Gemmol. 29 (3): 129-147.

Pin, C., Monchoux, P., Paquette, J.L., Azambre, B., Wang, R.C. and Martin, R.F. 2006. Igneous albitite dikes in orogenic lherzolites, western Pyrénées, France: a possible source for corundum and alkali feldspar xenocrysts in basaltic terranes. II. Geochemical and petrogenetic considerations. Can. Mineral. 44: 837-850.

Pisutha-Arnond, V., Wathanakul, P., Intasopa, S. and Griffin, W.L. 1998. Corsilzirspite, a corundum-sillimanite-zircon-hercynite rock: New evidence on the origin of Kanchanaburi Sapphire, Thailand. Proceedings of International Conference on Nine Regional Congress on Geology, Mineral and Energy Resources of Southeast Asia-GEOSEA'98. Kuala Lumpur, Malaysia, pp. 95-96.

Pisutha-Arnond, V., Wathanakul, P. and Intasopa, S. 1999. New evidence on the origin of Kanchanaburi sapphire. Final Report Submitted to The Thailand Research Fund (TRF).

Pisutha-Arnond, V., Intasopa, S., Wathanakul, P., Griffin, W.L., Atichat, W. and Sutthirat, C. 2005. Sapphire xenocrysts in basalt from the Bo Phloi Gem Field, Western Thailand. Proceedings of the International Conference on GEOINDO 2005, Khon Kaen, Thailand, pp. 338-344.

Pommier, A., Cocherie, A. and Legendre, O. 2002. EPMA Dating User's Manual: Age calculation from electron probe microanalyzer measurements of U-Th-Pb. BRGM, Orléans, France, 9 pp.

Pownceby, M.I., MacRae, C.M. and Wilson, N.C. 2007. Mineral characterisation by EPMA Mapping. Miner. Eng. 20 (5): 444-451.

Pumpang, S. 2007. Trapiche sapphires from some deposits in Thailand and Vietnam. Master's Thesis. Department of Geology, Chulalongkorn University, Bangkok, Thailand.

Rankin, A.H. and Edwards, W. 2003. Some effects of extreme heat treatment on zircon inclusions in corundum. J. Gemmol. 28 (5): 257-264.

Sasada, M., Ratanasthien, B. and Soponpongpipat, R. 1987. New K/Ar ages from the Lampang basalt, Northern Thailand. Bull. Geol. Surv. Japan. 38 (1): 13-20.

Saminpanya, S. 2000. Mineralogy and origin of gem corundum associated with basalt in Thailand. Doctoral dissertation, Department of Earth Science, The University of Manchester, United Kingdom.

Saminpanya, S. 2001. Ti-Fe mineral inclusions in star sapphire from Thailand. Austral. Gemmol. 21: 125-128.

Saminpanya, S., Manning, D.A.C., Droop, G.T.R. and Henderson, C.M.B. 2003. Trace elements in Thai gem corundums. J. Gemmol. 28: 399-415.

Saminpanya, S. and Sutherland, F.L. 2008. Black opaque gem minerals associated with Corundum in the alluvial deposits of Thailand. Austral. Gemmol. 23: 242-253.

Saminpanya, S. and Sutherland, F.L. 2011. Different origins of Thai area sapphire and ruby, derived from mineral inclusions and co-existing minerals. Eur. J. Mineral. 23: 683-694.

Shannon, R.D. 1976. Revised effective ionic radii and systematic studies of interatomic distances in halides and chalcogenides. Acta. Crystallogr. A 32: 751-767.

Shnukov, S.E., Cheburkin, A.K. and Andreev, A.V. 1989. Geochemistry of wide-spread coexisting accessory minerals and their role in investigation of endogenetic and exogenetic processes (in Russian). Geol. J. 2: 107-114.

Shnukov, S.E., Andreev, A.V. and Savenok, S.P. 1997. Admixture elements in zircons and apatites: a tool for provenance studies of terrigenous sedimentary rocks. European Union of Geosciences (EUG 9), Strasbourg, Abstract 65/4P16: 597.

Simonet, C. Fritsch, E. and Lasnier, B. 2008. A classification of gem corundum deposits aimed towards gem exploration. Ore Geology Reviews 34 (1-2): 127-133.

Singbamroong, S. and Thanasuthipitak, T. 2004. Study of solid mineral inclusions in sapphires from Ban Huai Sai area, Laos by Raman Spectroscopy. Chiang Mai J. Sci. 31 (3): 251-263.

Smith, C.P., Kammerling, R.C., Keller, A.S., Peretti, A., Scarratt, K.V., Khoa, N.D. and Repetto, S. 1995. Sapphire from Southern Vietnam. Gems Gemol. 31 (3): 168-186.

Somwangsombat, N. and Sutthirat, C. 2009. Gemological Characteristics of Corundum from Gia Nghia, Southern Vietnam. BEST. 2 (1&2): 63-65.

Srithai, B. and Rankin, A.H. 1999. Fluid inclusion characteristics of sapphires from Thailand. In: Mineral deposits: Processes to Processing, Stanley, C. J., et. al. (Eds), Balkema Press, Rotterdam, pp. 107-110.

Srithai, B. 2005. Petrography and mineral chemistry of ultramafic xenoliths from Bo Ploi basalt, Kanchanaburi, Thailand. Proceedings of International Conference on Geology, Geotechnology and Mineral Resource of Indochina. Khon Kaen, Thailand, pp. 358-364.

Stoddard, E.F. 1979. Zinc-rich hercynite in high-grade metamorphic rocks: a product of the dehydration of staurolite. Am. Mineral. 64: 736-741.

Sutherland, F.L. 1996. Alkaline rocks and gemstones, Australia: a review and synthesis. Austral. J. Earth Sci. 43: 323-343.

Sutherland, F.L. and Coenraads, R.R. 1996. An ususual ruby-sapphire-sapphirine-spinel assemblage from the Teriary Barrington volcanic province, New South Wales, Australia. Mineral. Mag. 60: 623-638.

Sutherland, F.L., Schwarz, D., Jobbins, E.A., Coenraads, R.R. and Webb, G. 1998a. Distinctive gem corundum suites from discrete basalt fields: a comparative study of Barrington, Australia, and West Pailin, Cambodia, gemfields. J. Gemmol. 26 (2): 65-85.

Sutherland, F.L., Hoskin, P.W.O., Fanning, C.M. and Coenraads, R.R. 1998b. Models of corundum origin from alkali basaltic terrains: a reappraisal. Contrib. Mineral. Petrol. 133: 356-372.

Sutherland, F.L. and Fanning, C.M. 2001. Gem-bearing basaltic volcanism, Barrington, New South Wales: Cenozoic evolution, based on basalt K–Ar ages and zircon fission track and U–Pb isotope dating. Aust. J. Earth Sci. 48: 221-237.

Sutherland, F.L. and Schwarz, D. 2001. Origin of gem corundums from basaltic fields. Austral. Gemmol. 21: 30-33.

Sutherland, F.L., Bosshart, G., Fanning, C.M., Hoskin, P.W.O. and Coenraads, R.R. 2002. Sapphire crystallization, age and origin, Ban Huai Sai, Laos: age based on zircon inclusions. J. Asian Earth Sci. 20: 841-849.

Sutherland, F.L., Coenraads, R.R., Schwarz, D., Raynor, L.R., Barron, B.J. and Webb, G.B. 2003. Al-rich diopside in alluvial ruby and corundum-bearing xenoliths, Australian and SE Asian basalt fields. Mineral. Mag. 67 (4): 717-732.

Sutherland, F.L., Duroc-Danner, J.W. and Meffre, S. 2008. Age and origin of gem corundum and zircon megacrysts from the Mercaderes–Rio Mayo area, South-west Colombia, South America. Ore Geology Reviews 34, 155-168.

Sutthirat, C., Charusiri, P., Farrar, E. and Clark, A.H. 1994. New $^{40}Ar/^{39}Ar$ geochronology and characteristic of some Cenozoic Basalt in Thailand. Proceedings of International Symposiam on Stratigraphic Correlation of Southeast Asia. Bangkok, Thailand, pp. 306-321.

Sutthirat, C., Charusiri, P., Pongsapitch, W., Farrar, E. and Landgridge, R. 1995. A Late Pliocene Ko Kha - Sop Prap and Nam Cho Basaltic Eruption, Northern Thailand: Evidences from Geology and $^{40}Ar/^{39}Ar$ Geochronology. Proceeding of International Symposium Conference on Geology, Geotechnology and Mineral Resources of Indochina (Geo-Indo '95). Khon Kaen, Thailand, pp. 247-253.

Sutthirat, C., Droop, G.T.R., Henderson, C.M.B. and Manning D.A.C. 1999. Petrography and Mineral Chemistry of Xenoliths and Xenocrysts in Thai Corundum-Related Basalts: Implications for the Upper Mantle and Lower Crust beneath Thailand. Symposium on Mineral, Energy, and Water Resources of Thailand. Bangkok, Thailand, pp. 152-161.

Sutthirat, C. 2001. Petrogenesis of mantle and crustal xenoliths and xenocrystals in basaltic rocks associated with corundum deposits in Thailand. Doctoral dissertation, Department of Earth Science, The University of Manchester, United Kingdom.

Sutthirat, C., Saminpanya, S., Droop, G.T.R., Henderson, C.M.B. and Manning, D.A.C. 2001. Clinopyroxene-corundum assemblages from alkali basalt and alluvium, eastern Thailand: constraints on the origin of Thai rubies. Mineral. Mag. 65 (2): 277-295.

Sutthirat, C., Droop, G. and Henderson, M. 2005. Thermobarometry and Speedometry of Thai Corundum-Related Basalts: Evidences for their Petrogenesis. Proceeding of International Symposium Conference on Geology, Geotechnology and Mineral Resources of Indochina (Geo-Indo '95). Khon Kaen, Thailand, pp. 330-337.

Suzuki, K. and Adachi, M. 1991. The chemical Th-U-total Pb isochron ages of zircon and monazite from the Gray Granite of the Hida Terrane, Japan. J. Earth Sci. Nagoya Univ. 38: 11-38.

Suzuki, K. and Kato, T. 2008. CHIME dating of monazite, xenotime, zircon and polycrase: Protocol, pitfalls and chemical criterion of possibly discordant age data. Gondwana Res. 14 (4): 569‑586.

Taylor, S.R. and McLennan, S.M. 1985. The Continental Crust: Its Composition and Evolution. Blackwell, Oxford, 312 pp.

Upton, B.G.J., Hinton, R.W., Aspen, P., Finch, A. and Valley, J.W. 1999. Megacrysts and associated xenoliths: evidence for migration of geochemically enriched melts in the upper mantle beneath Scotland. J Petrol. 40: 935–956.

Vichit, P., Vudhichativanich, S. and Hansawek, R. 1978. The distribution and some characteristics of corundum-bearing basalts in Thailand. Jour. Geol. Soc. Thailand. Special Issue for III GEOSEA. 3: M4-1 – M4-38.

Vichit, P. 1992. Gemstone in Thailand. Proceedings of the National Conference on Geologic Resources of Thailand: Potential for future development. Bangkok, Thailand, pp.126-134.

Vlach, S.R.F. 2010. Th-U-Pb_T Dating by Electron Probe Microanalysis, Part I. Monazite: Analytical Procedures and Data Treatment. Geol. USP, Sér. cient. 10 (1): 61-85.

Wark, D.A. and Miller, C. F. 1993. Accessory mineral behavior during differentiation of a granite suite: monazite, xenotime and zircon in SweetwaterWash pluton, southeastern California, U.S.A. Chem. Geol. 110: 49–67.

Watson, E.B. 1980. Some experimentally determined zircon/liquid partition coefficients for the rare earth elements. Geochim. Cosmochim. Acta 44: 895-897.

Whitford-Stark, J.L. 1987. A survey of Cenozoic volcanism in mainland Asia. Geol. Soc. Spec. Publ. 213: 74 pp.

Wilkinson, J.F.G. and Hensel, H.D. 1994. Nephelines and analcimes in some alkaline igneous rocks. Contrib. Mineral. Petrol. 118: 79-91.

Williams, M.L. and Jercinovic, M.J. 2002. Microprobe monazite geochronology: putting absolute time into microstructural analysis, J. Struct. Geol. 24 (6-7): 1013-1028.

Xia, X., Sun, M., Zhao, G., Li, H. and Zhou, M. 2004. Spot zircon U-Pb isotope analysis by ICP-MS coupled with a frequency quintupled (213 nm) Nd-YAG laser system. Geochem. J. 38: 191-200.

Yaemniyom, N. and Pongsapich, W. 1982. Petrochemistry of the Bo Phloi basalt, Kanchanaburi Province. Proceedings of Annual Technical Meeting, Department of Geological Science, Chiang Mai University, pp.19-52.

Yui, T.F., Khin, Zaw and Limkatrun, P. 2003. Oxygen isotope composition of the Denchai sapphire, Thailand; a clue to its enigmatic origin. Lithos 67: 153-161.

Yui, T.F., Wu, C-M., Limkatrun, P., Sricharn, W. and Boonsoong, A. 2006. Oxygen isotope studies on placer sapphire and ruby in the Chanthaburi-Trat alkali basaltic gemfield, Thailand. Lithos 86: 197-211.

Zhao, G.C., Wilde, S.A., Cawood, P.A. and Sun, M. 2002. SHRIMP U-Pb zircon ages of the Fuping Complex: Implications for late Archean to Paleoproterozoic accreation and assembly of the North China Craton. Amer. J. Sci. 302: 191-226.

Zhu, X.K. and O'Nions, R.K. 1999. Monazite chemical composition: some implications for monazite geochronology. Contrib. Mineral. Petrol. 137: 351-363.

APPENDICES

APPENDIX A

INTERNAL FEATURES AND MINERAL INCLUSIONS IN SAPPHIRES

I. Internal features

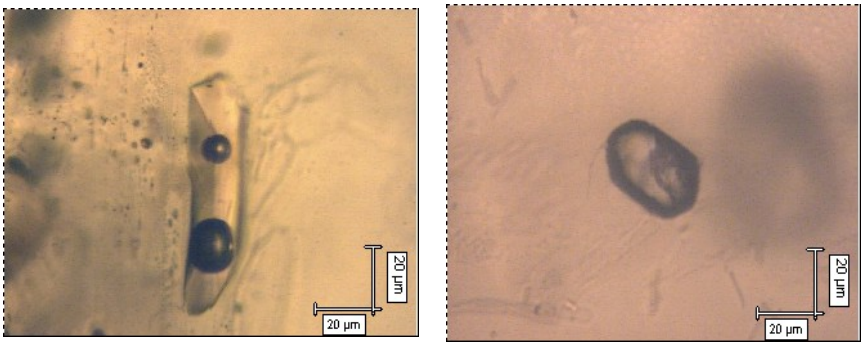

Figure A-1 Muti-phase inclusions (?) in the dark grayish brown Bo Phloi sapphires.

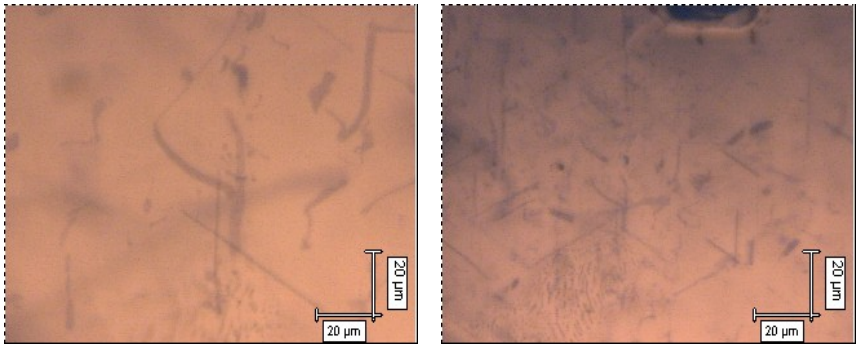

Figure A-2 Needle-like inclusions intersecting at 60°/120° along dark color zones of the dark grayish brown Bo Phloi sapphires.

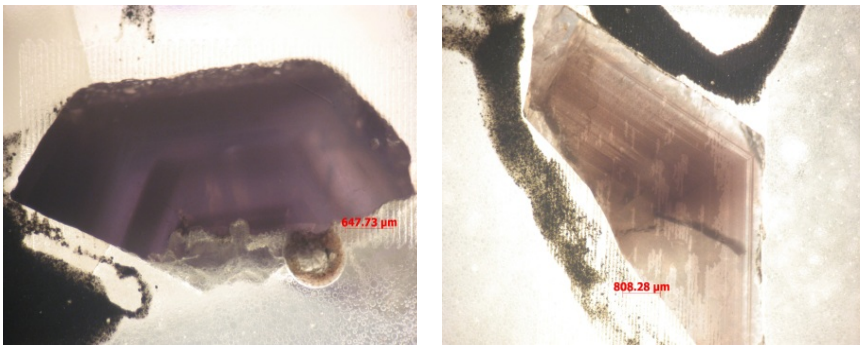

Figure A-3 Parts of the hexagonal color zoning found in the dark grayish brown Bo Phloi sapphires.

II. Photomicrographs of mineral inclusions

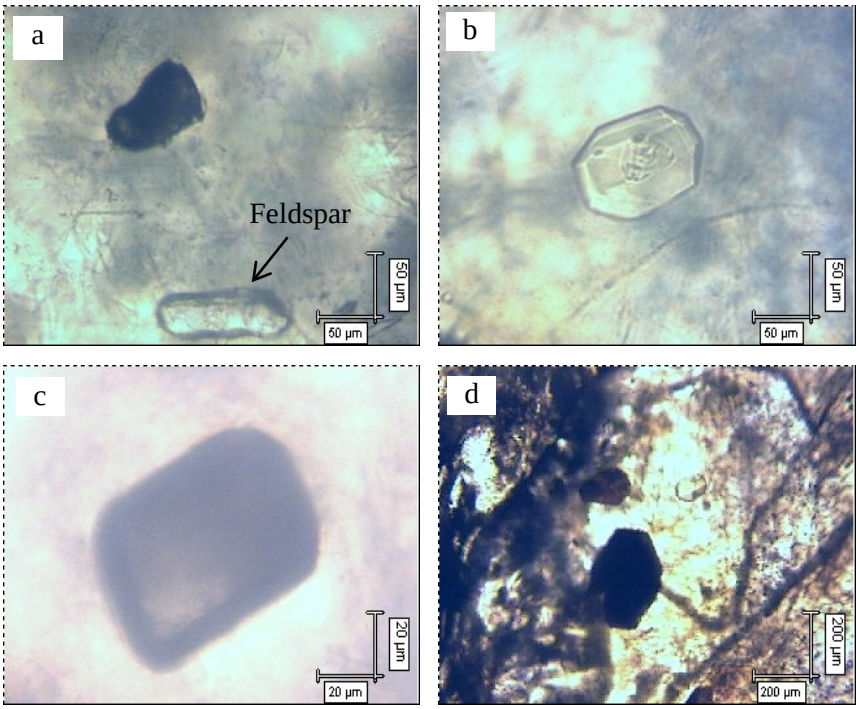

Figure A-4 Showing some mineral inclusions in the light grayish brown Bo Phloi sapphire; (a,b) feldspar inclusions; (c, d) spinel inclusions.

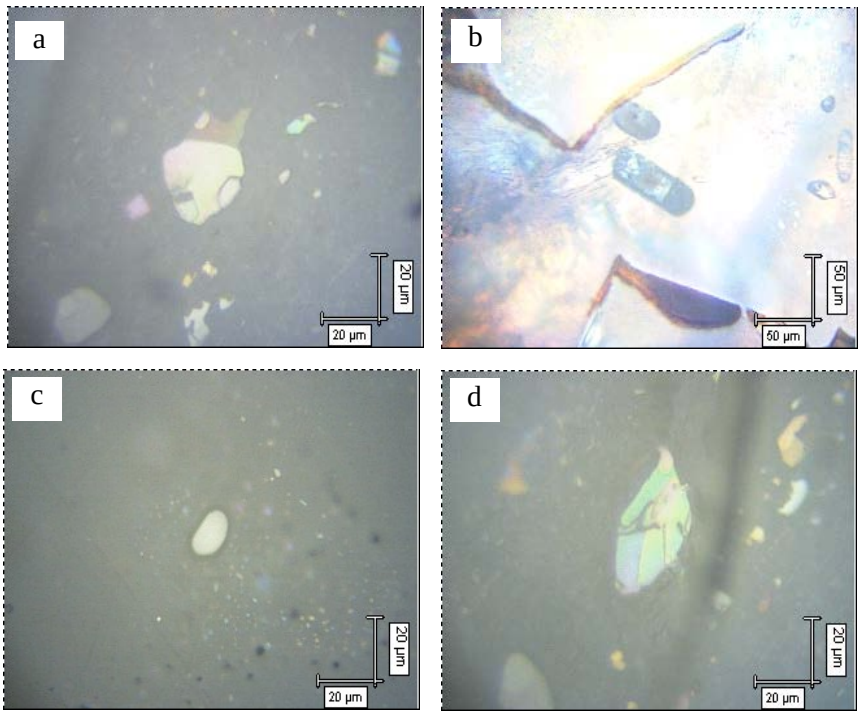

Figure A-5 Showing un-identified mineral inclusions in the blue Bo Phloi sapphires.

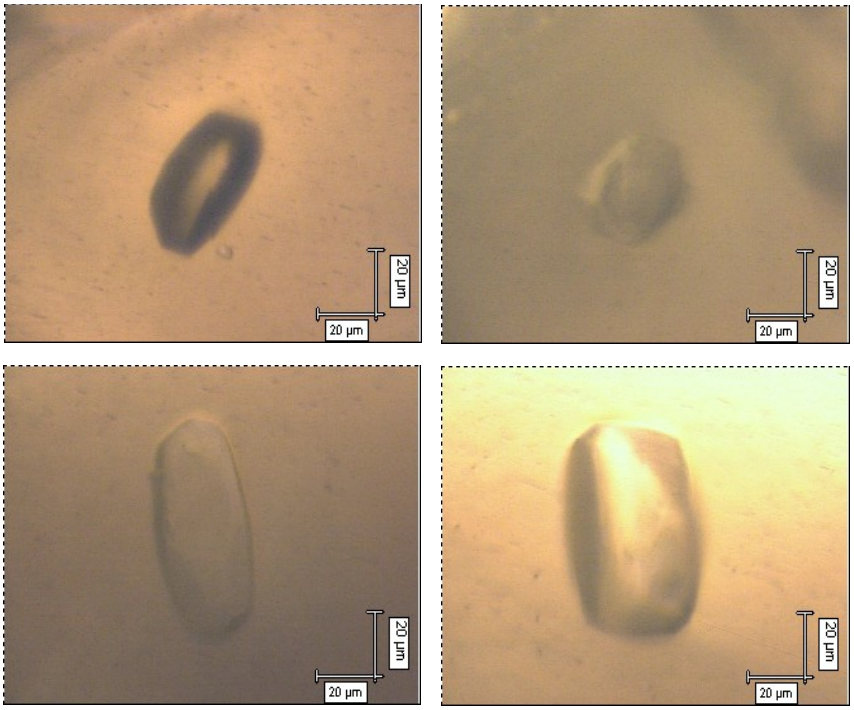

Figure A-6 Showing feldspar inclusions in the dark grayish brown Bo Phloi sapphires.

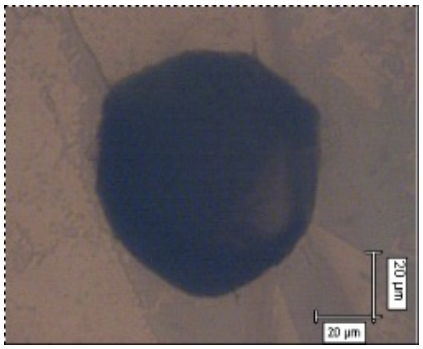

Figure A-7 Showing octahedral spinel inclusions in the dark grayish brown Bo Phloi sapphire.

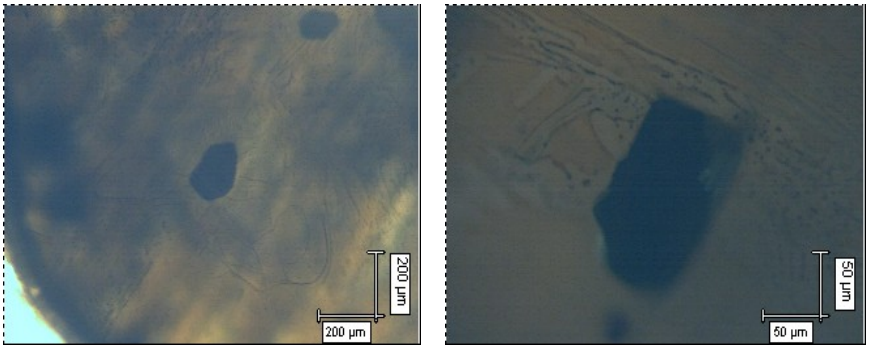

Figure A-8 Un-identified mineral inclusions found in the Pailin sapphires from Cambodia.

III. Back scattered electron (BSE) images of mineral inclusions

a) Bo Phloi sapphires in Thailand:

1) Dark grayish brown sapphires

Feldspar inclusions:

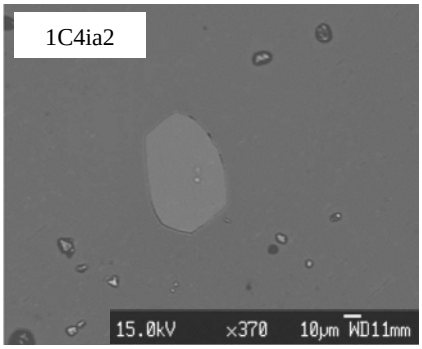

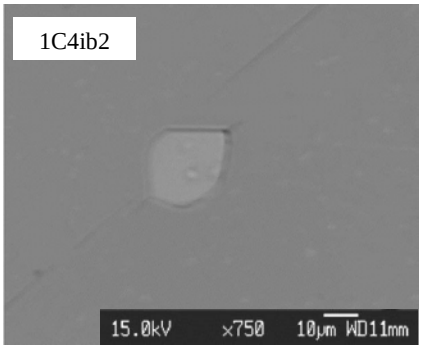

Nepheline inclusions:

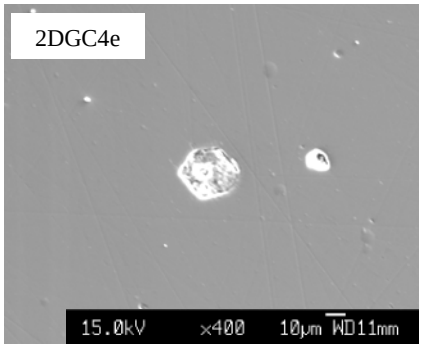

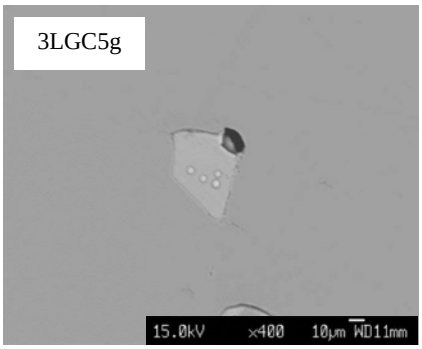

Spinel inclusions:

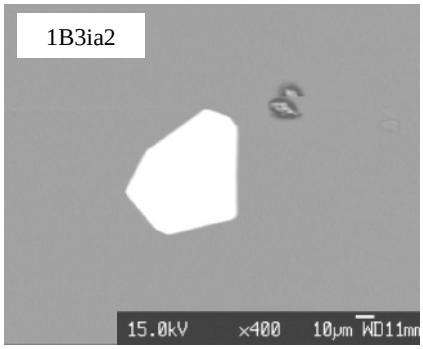

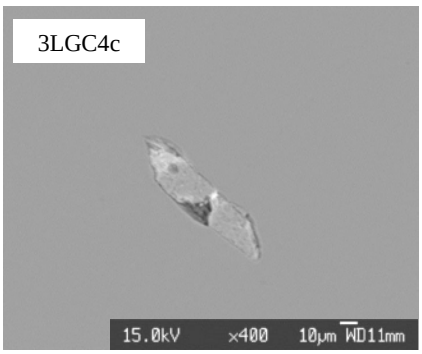

Pyroxene inclusions:

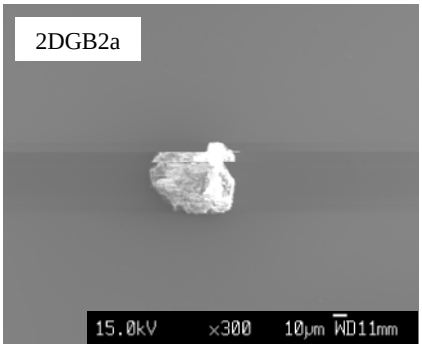

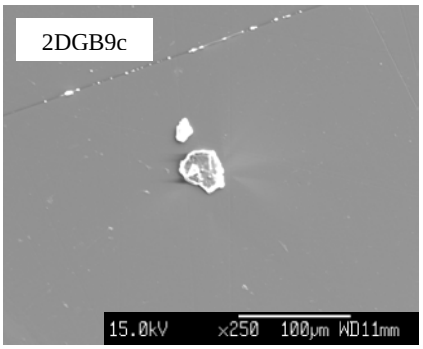

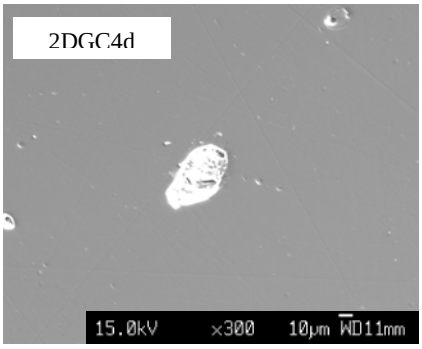

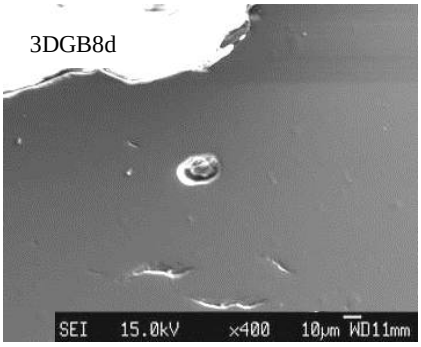

Garnet inclusions:

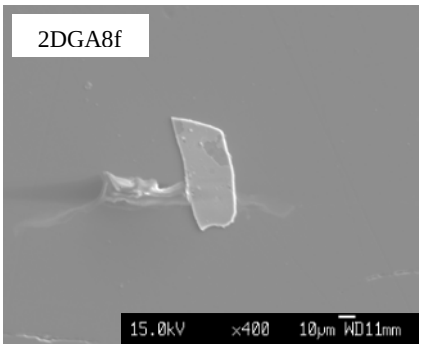

Mica inclusion:

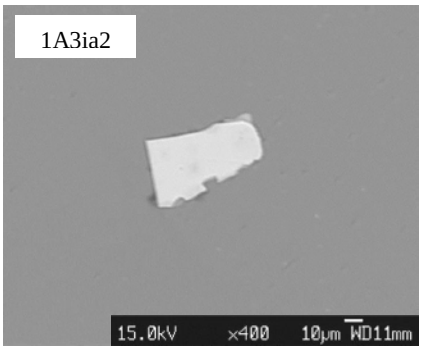

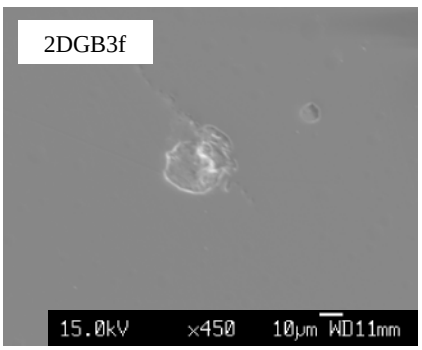

Zircon inclusions:

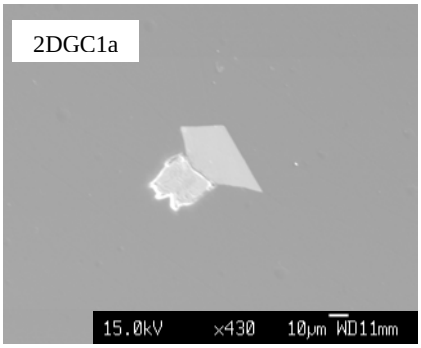

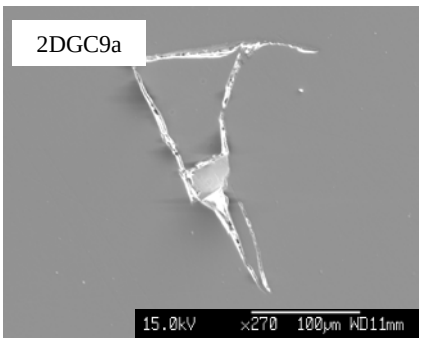

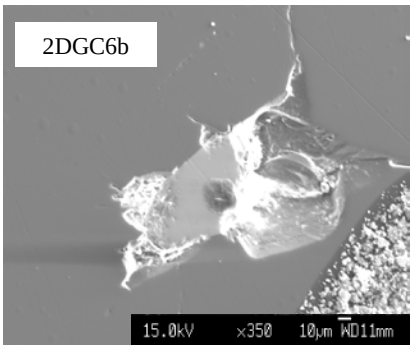

Monazite inclusions:

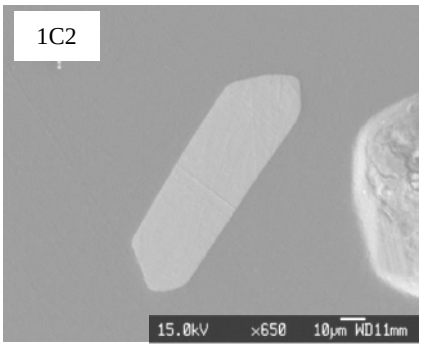

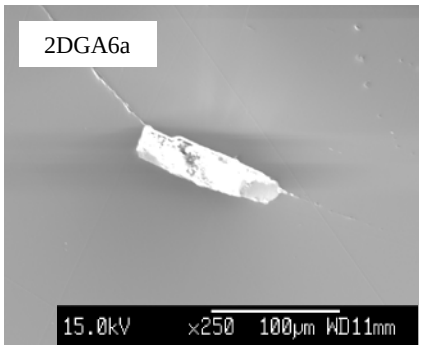

2) Light grayish brown sapphires

Feldspar inclusions:

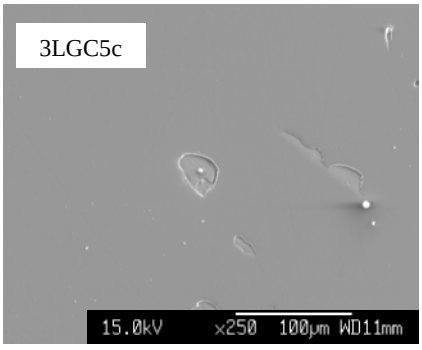

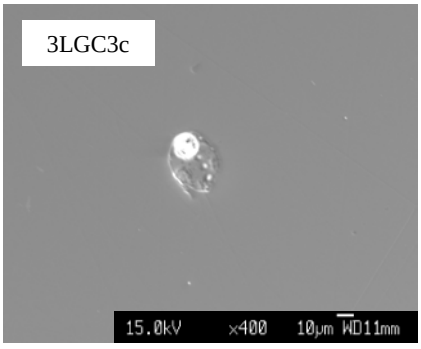

Spinel inclusions:

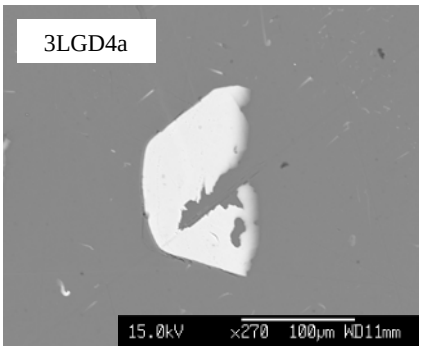

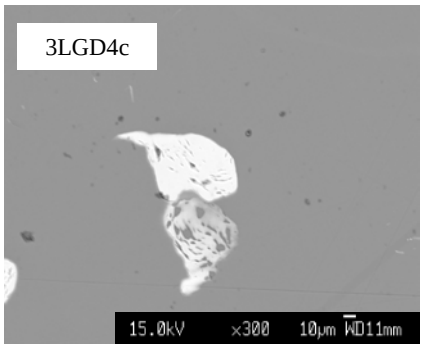

Pyroxene inclusions:

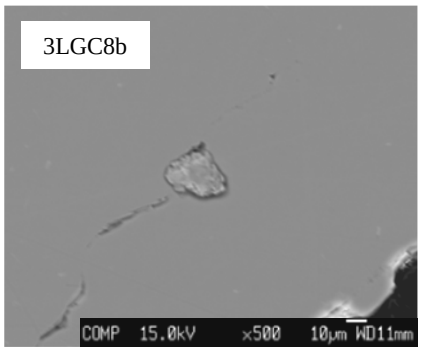

Garnet inclusions:

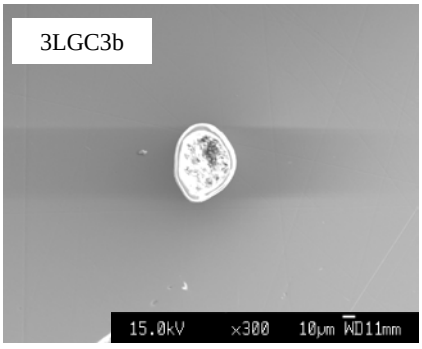

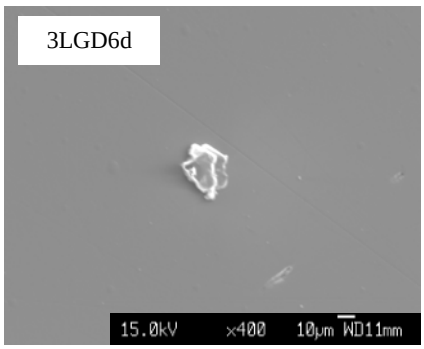

Zircon inclusions:

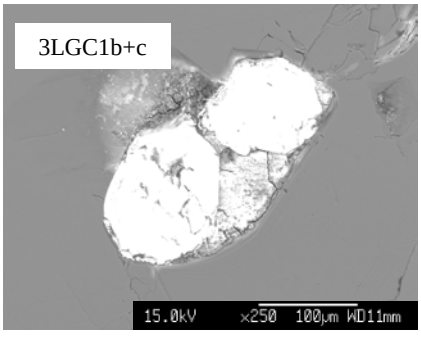

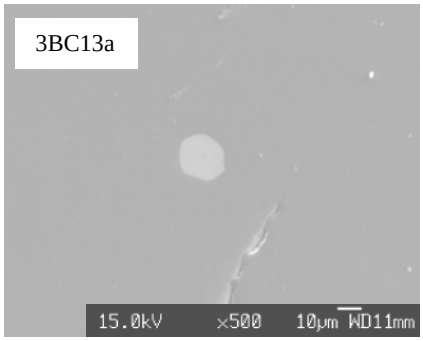

Fe-oxide inclusions:

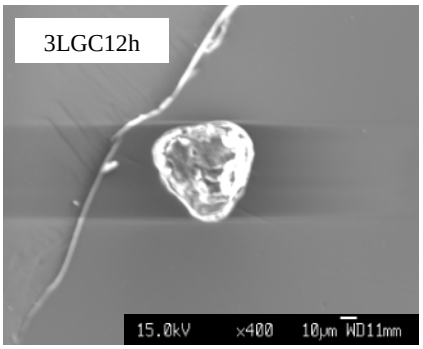

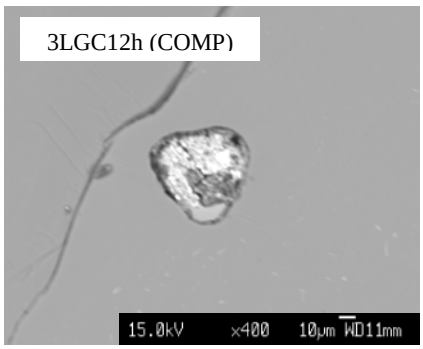

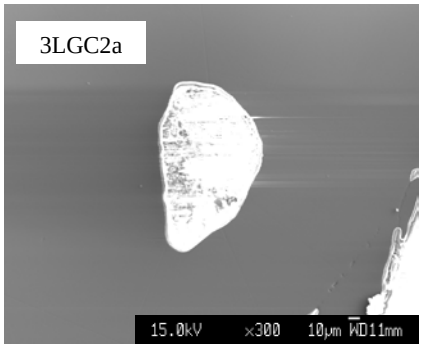

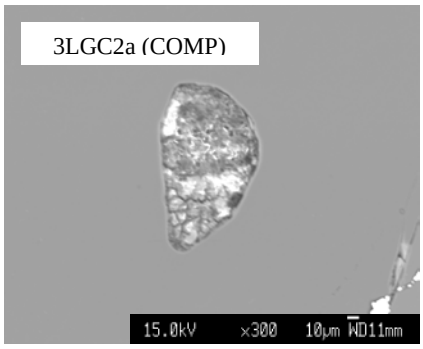

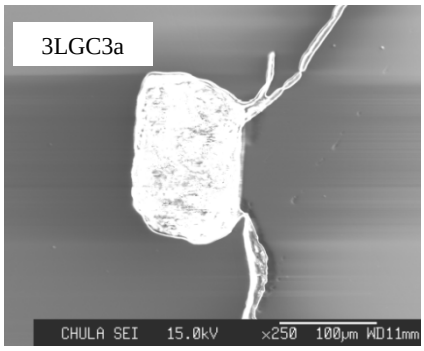

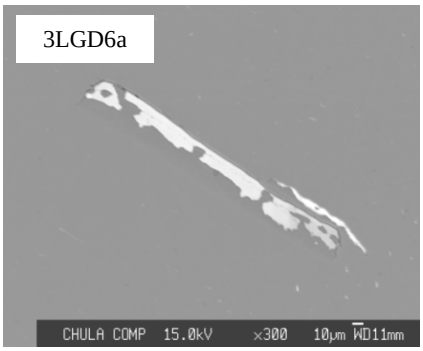

b) Chanthaburi sapphires in Thailand

Nepheline inclusion:

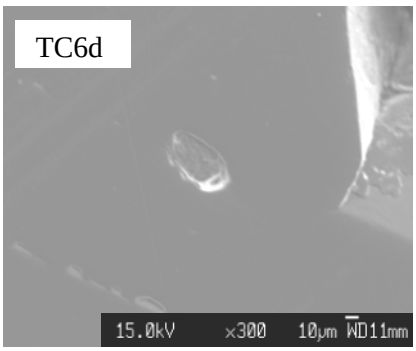

Magnetite (?) inclusion:

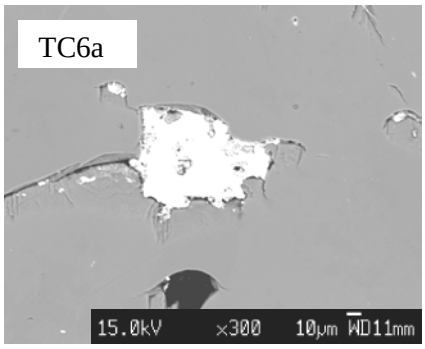

Columbite inclusion:

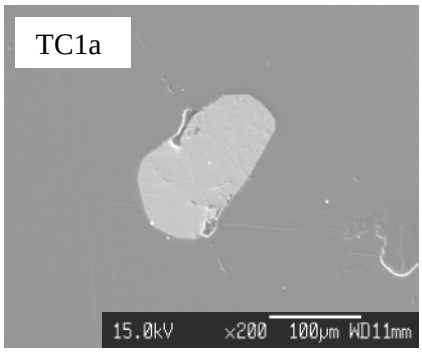

Fe-oxide inclusions:

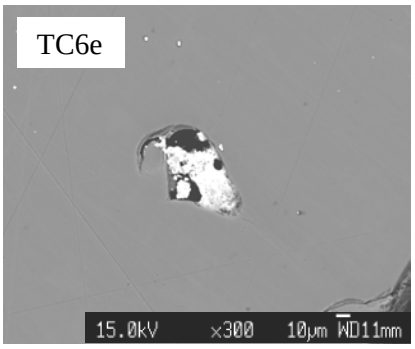

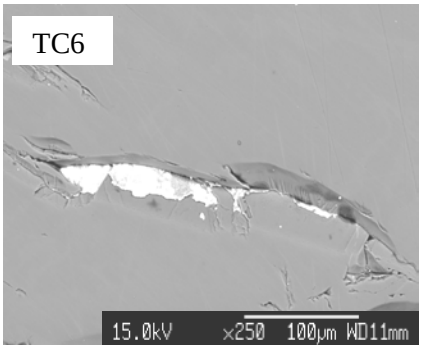

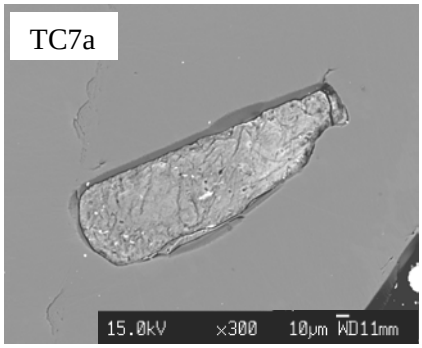

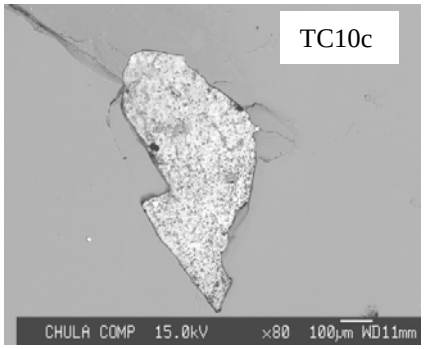

c) Other sapphires in Thailand

Nepheline inclusion in Phrae sapphire

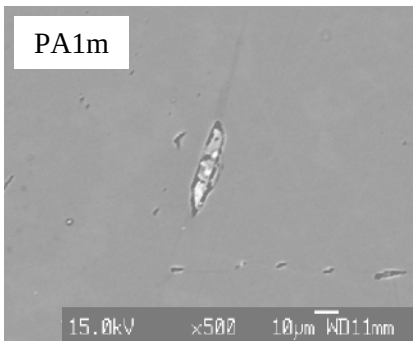

(Ti, Nb, Th)-oxide inclusion in trapiche Phrae sapphire

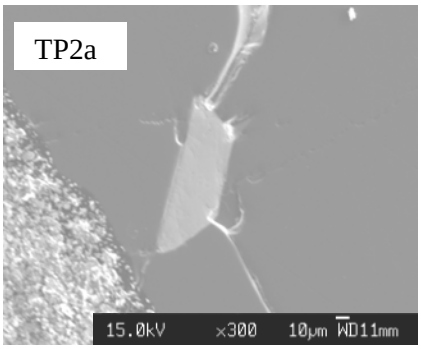

Zircon inclusion in trapiche Bo Phloi sapphire

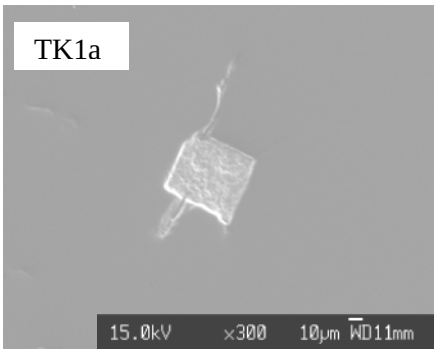

d) Huai Sai sapphires in Laos

Feldspar inclusion:

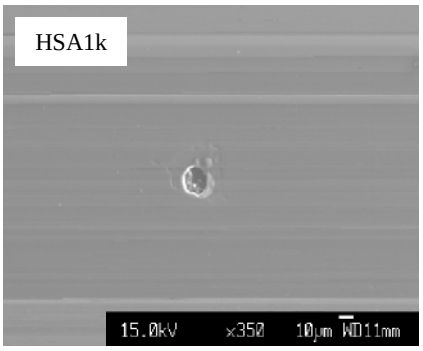

Garnet inclusion:

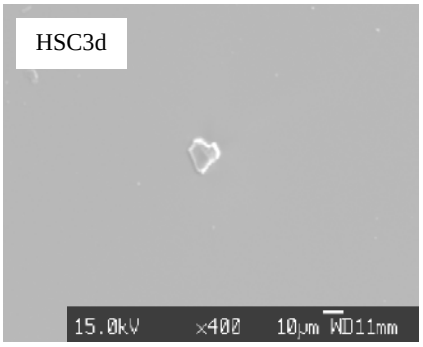

Pyroxene inclusions:

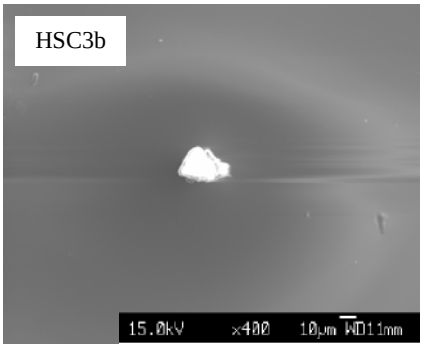

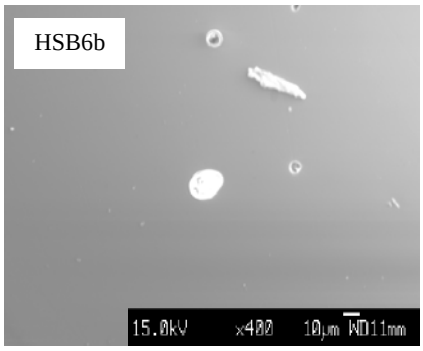

Euxenite (?) inclusions:

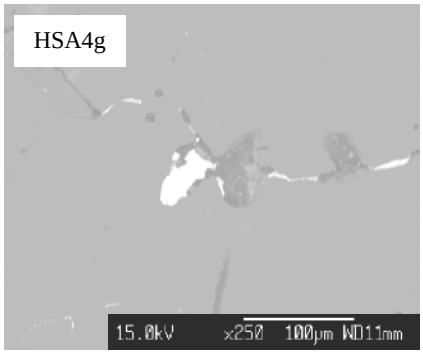

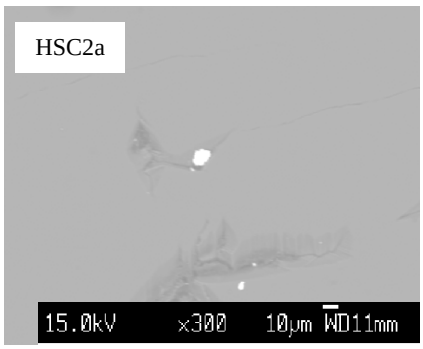

e) Pailin sapphires in Cambodia

Feldspar inclusions:

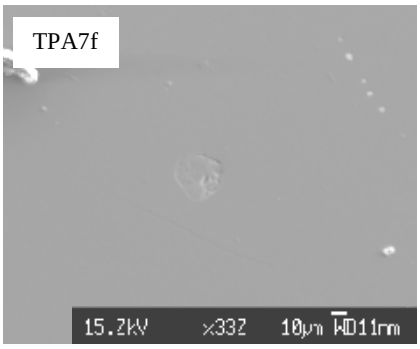

Columbite inclusions:

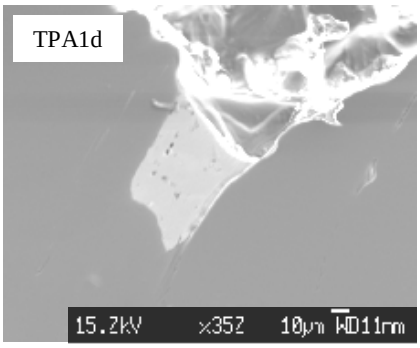

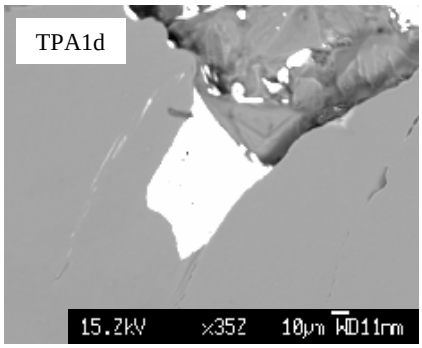

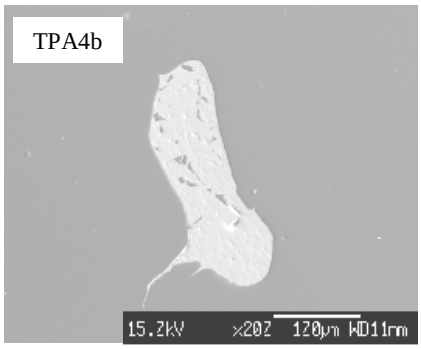

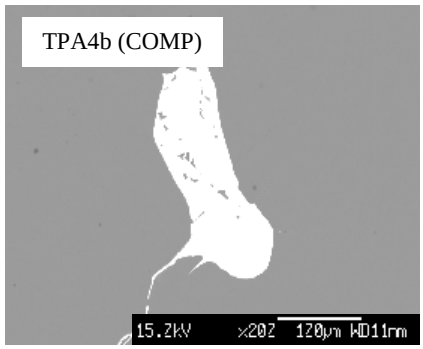

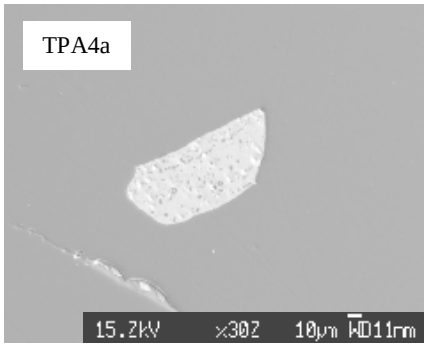

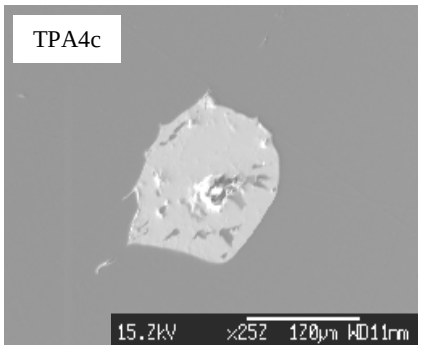

Columbite inclusions:

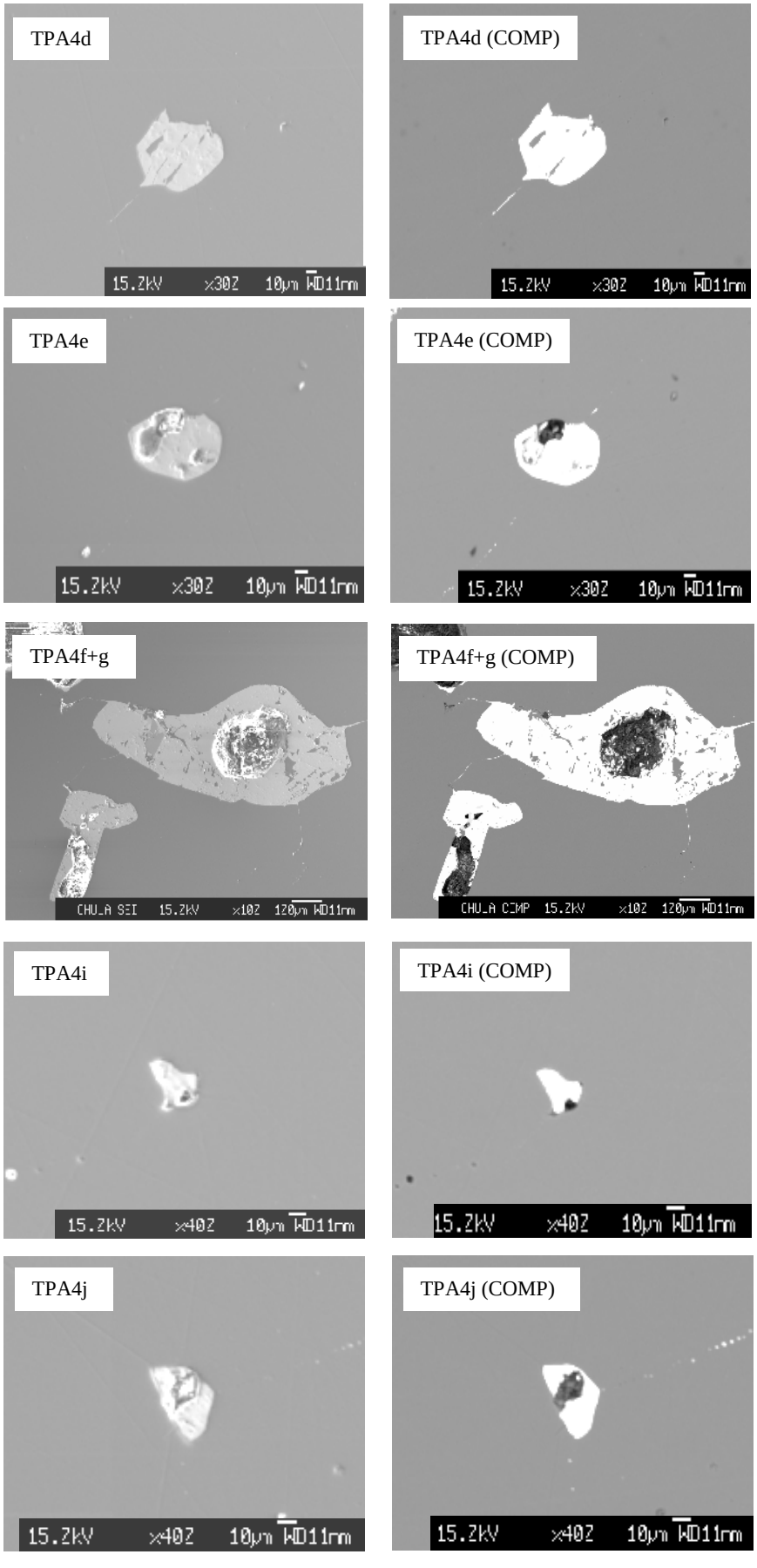

Columbite inclusions:

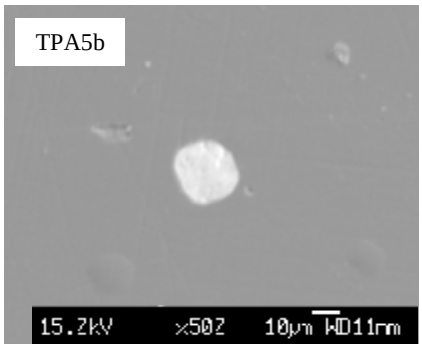

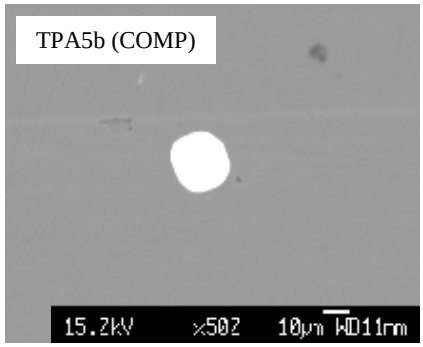

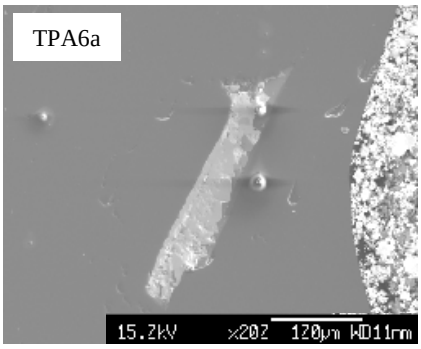

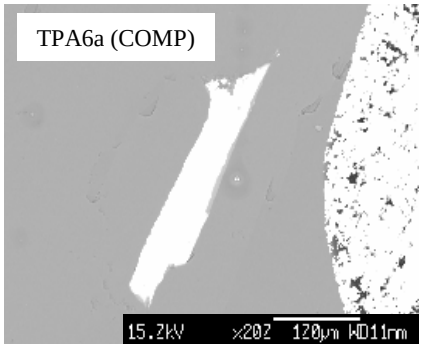

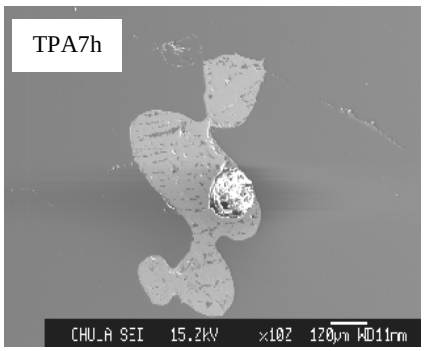

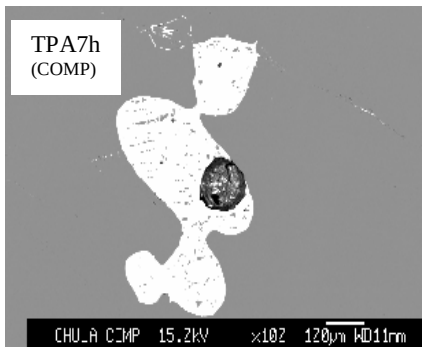

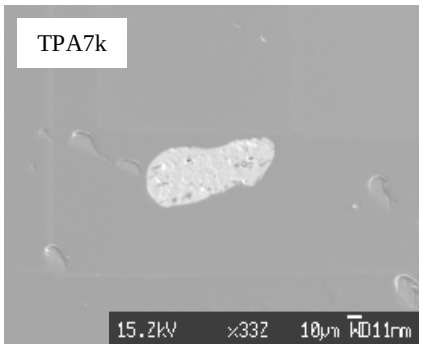

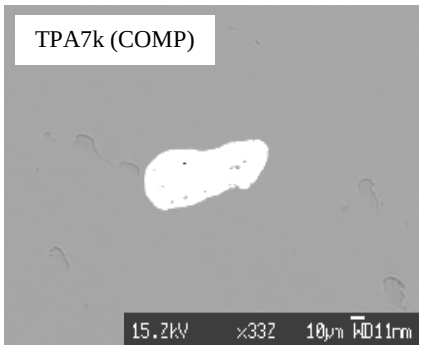

Pyrochlore inclusions:

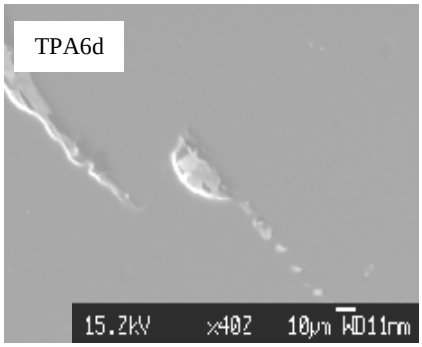

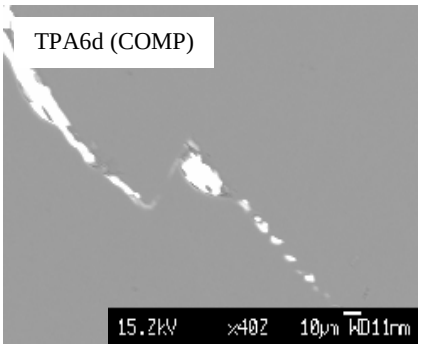

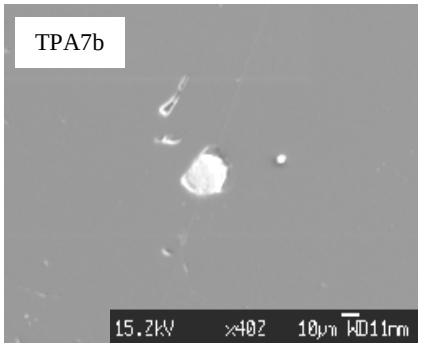

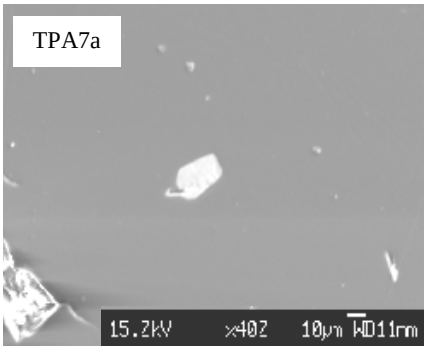

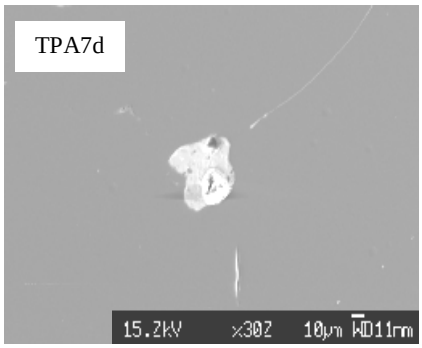

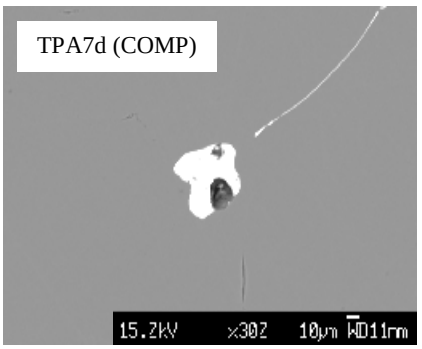

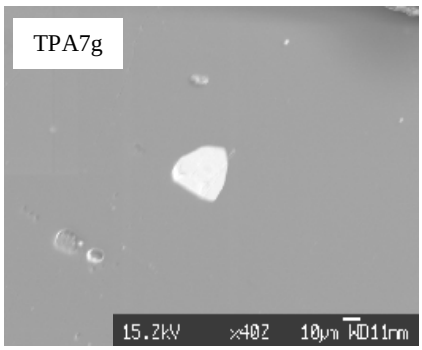

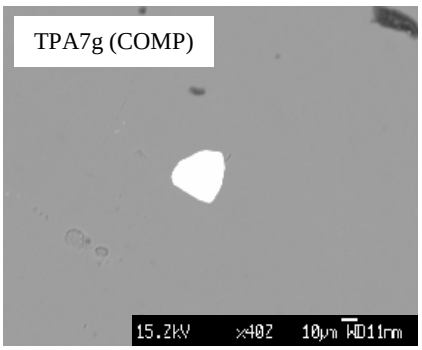

Pyrochlore inclusions:

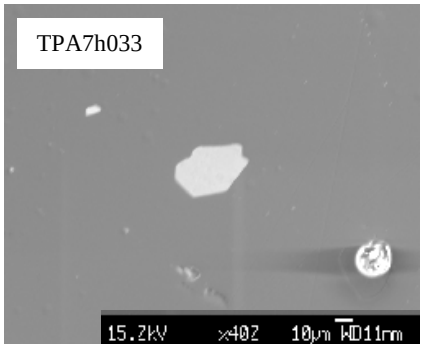

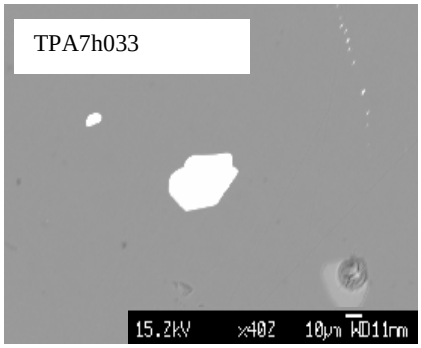

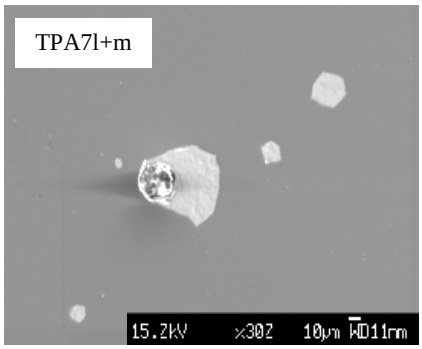

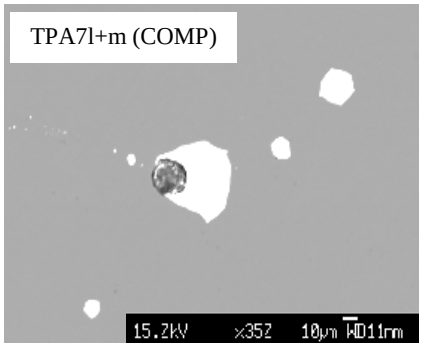

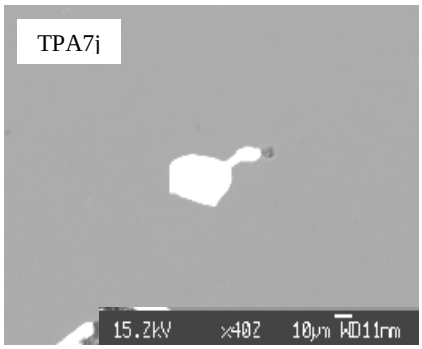

Fe-oxide inclusions

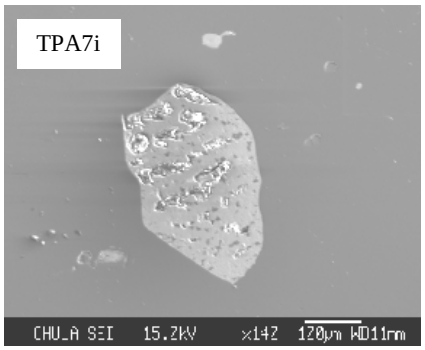

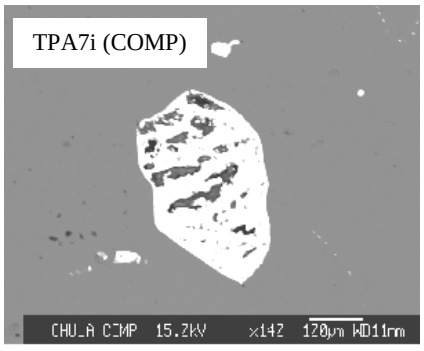

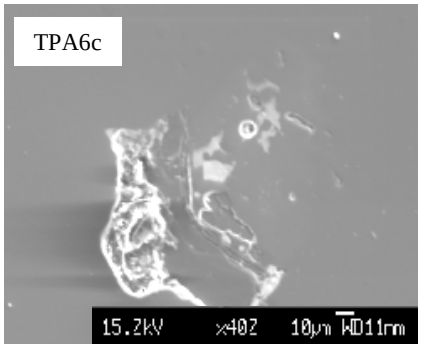

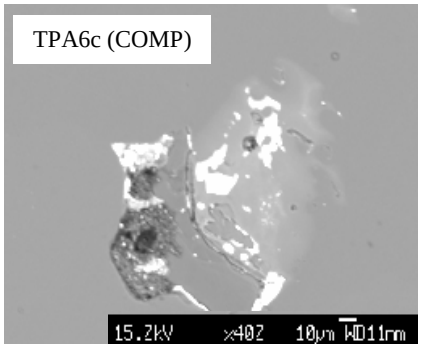

f) Gia Nghia sapphires in Vietnam

Feldspar inclusion:

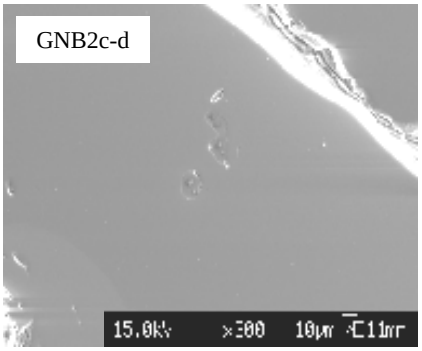

Pyroxene inclusions:

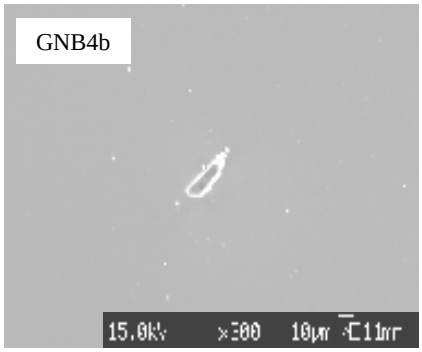

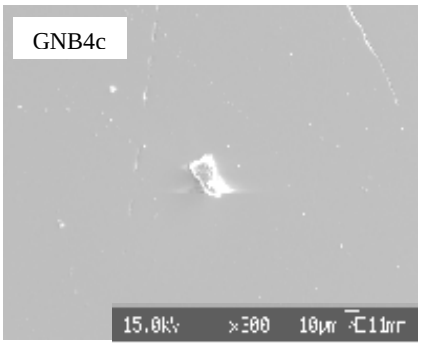

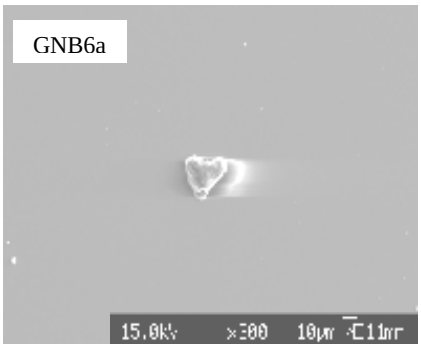

Titaniferous magnetite (?) inclusions:

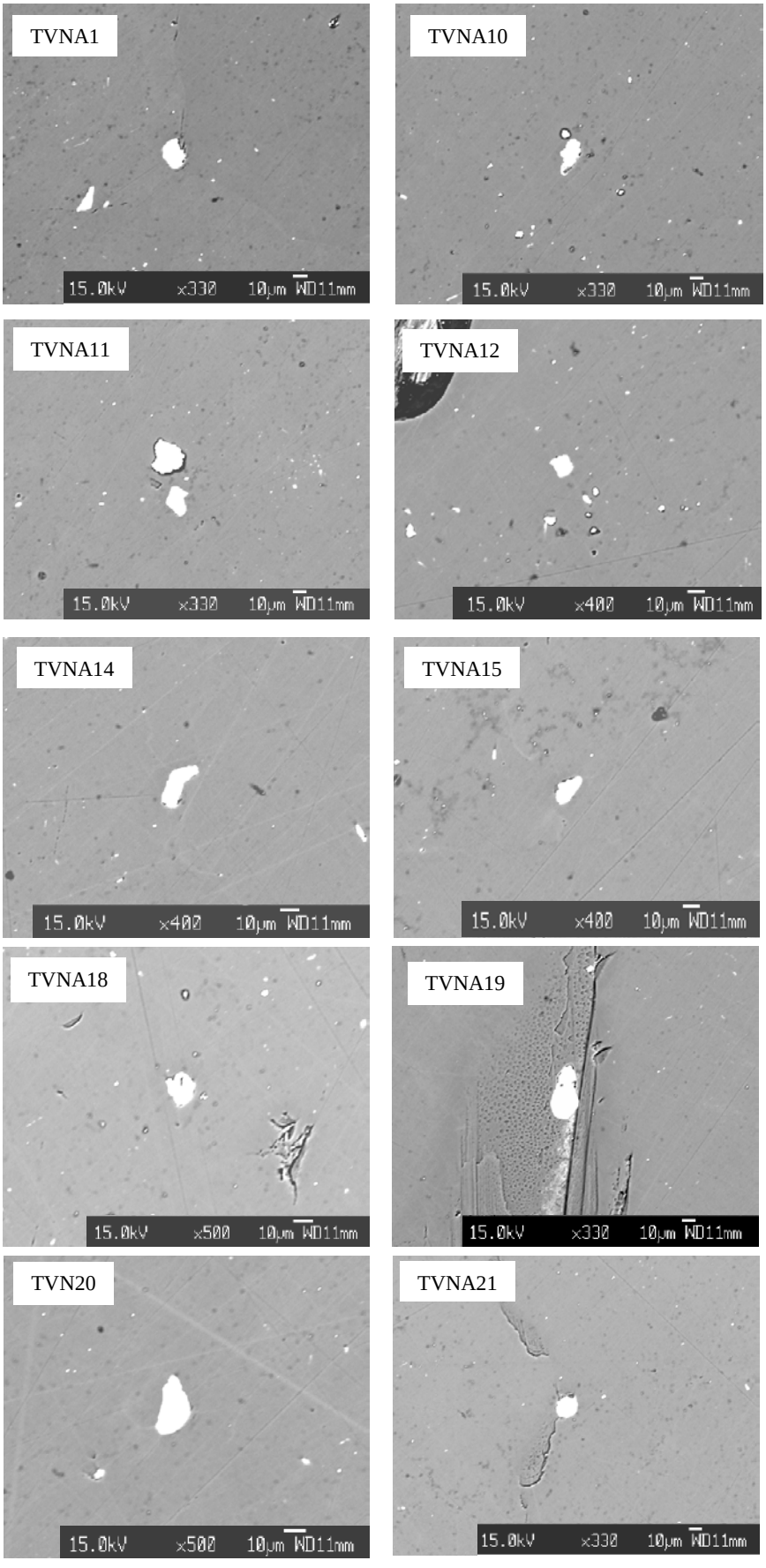

APPENDIX B

RAMAN SPECTRUMS OF MINERAL INCLUSIONS

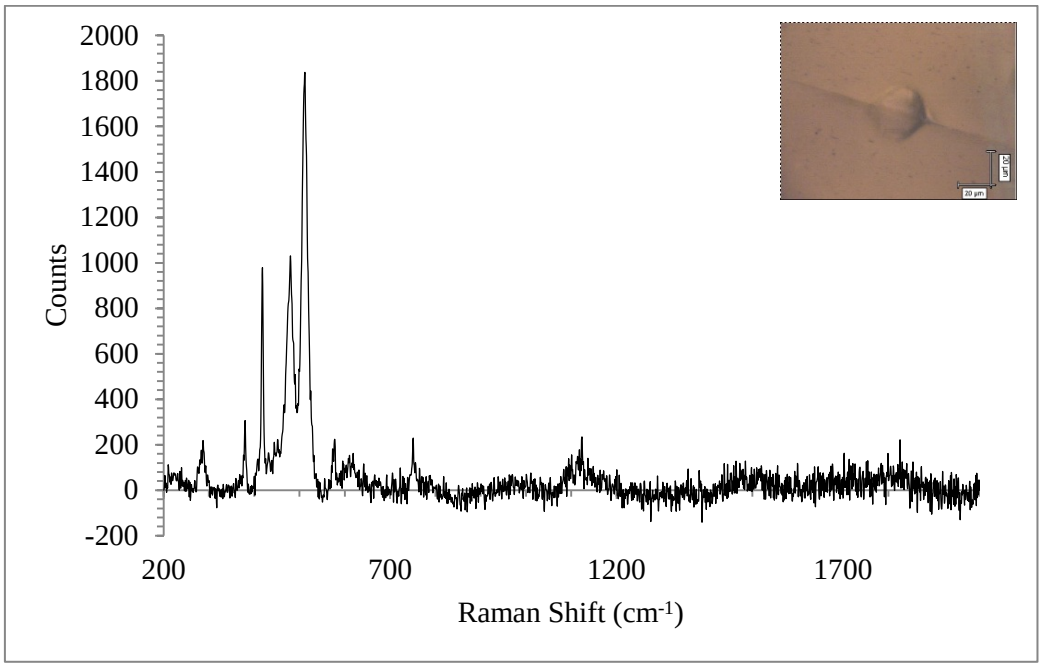

Figure B-1 Raman spectrum of a feldspar inclusion observed in the sample *1C4ih* of dark grayish brown Bo Phloi sapphire.

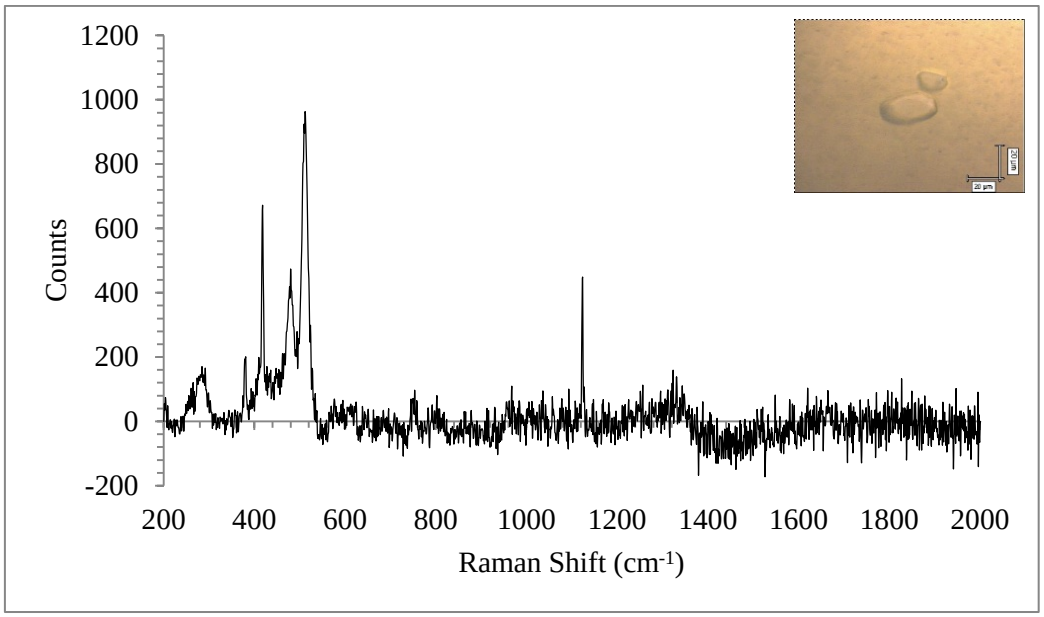

Figure B-2 Raman spectrum of a feldspar inclusion observed in the sample *1C4ij* of dark grayish brown Bo Phloi sapphire.

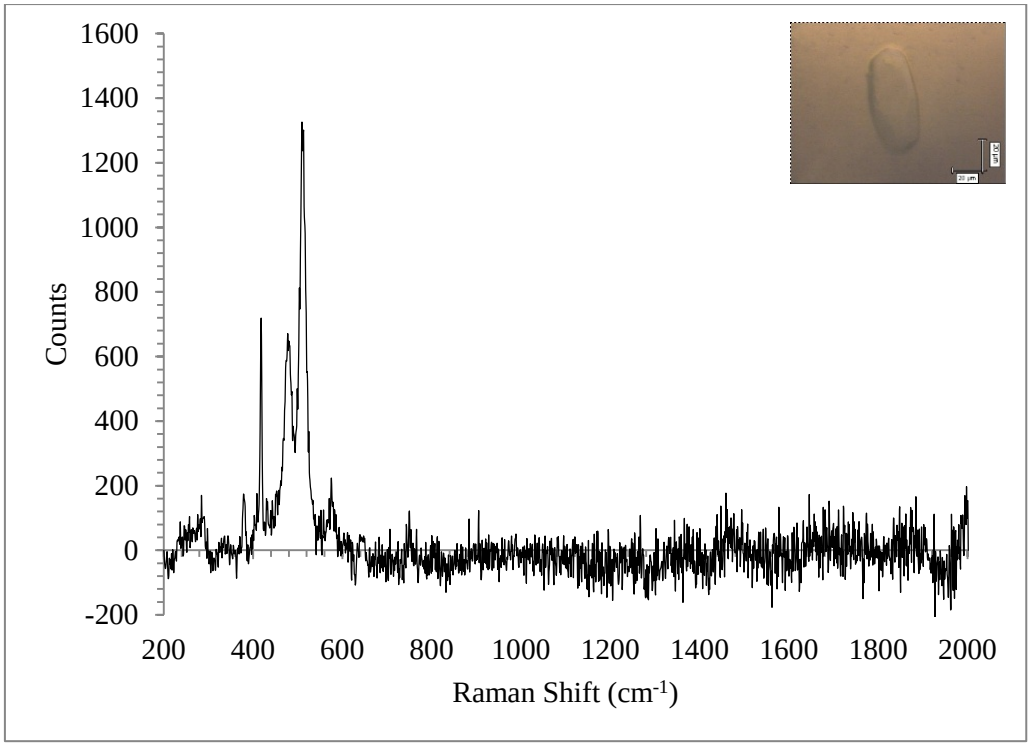

Figure B-3 Raman spectrum of a feldspar inclusion observed in the sample *1C4il* of dark grayish brown Bo Phloi sapphire.

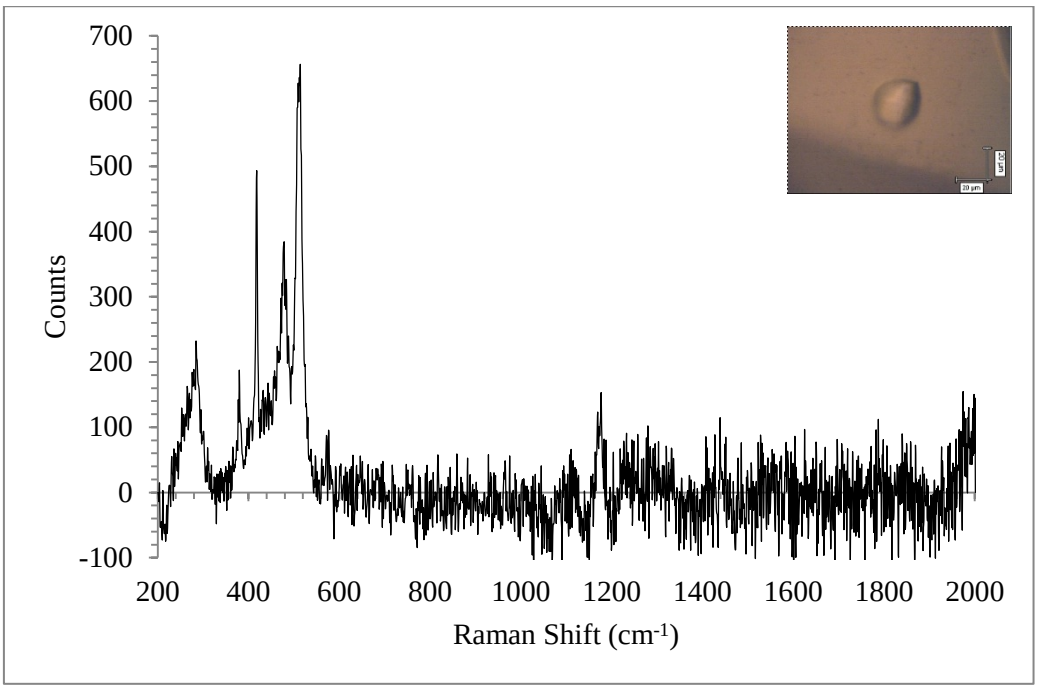

Figure B-4 Raman spectrum of a feldspar inclusion observed in the sample *1C4im* of dark grayish brown Bo Phloi sapphire.

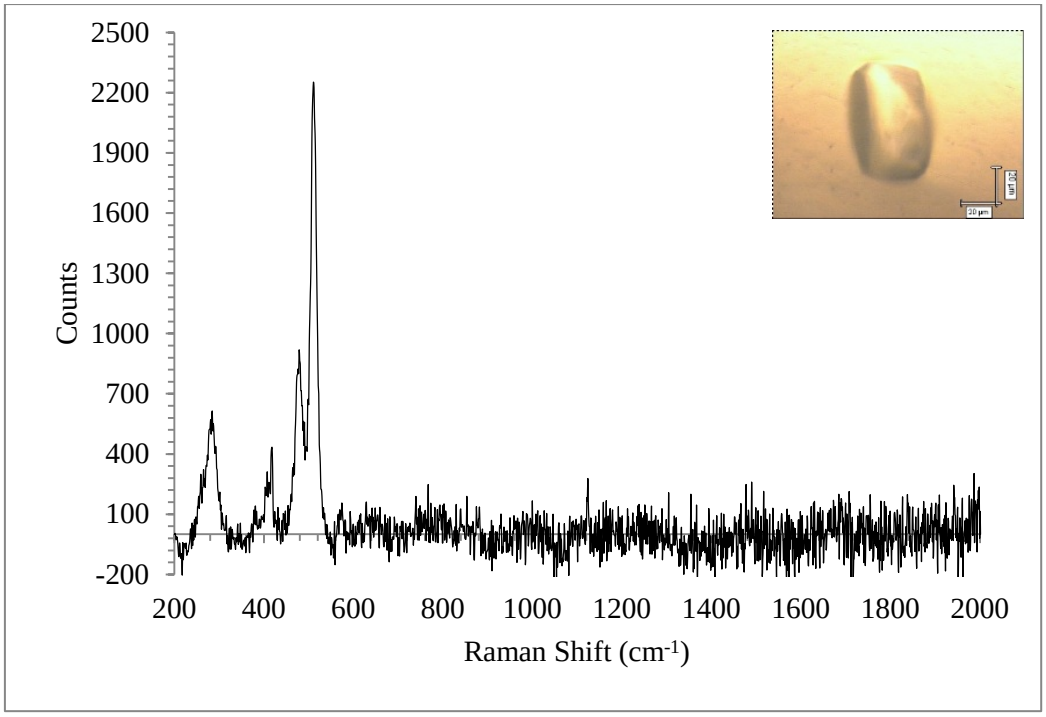

Figure B-5 Raman spectrum of a feldspar inclusion observed in the sample *1C4ik* of the dark grayish brown Bo Phloi sapphire.

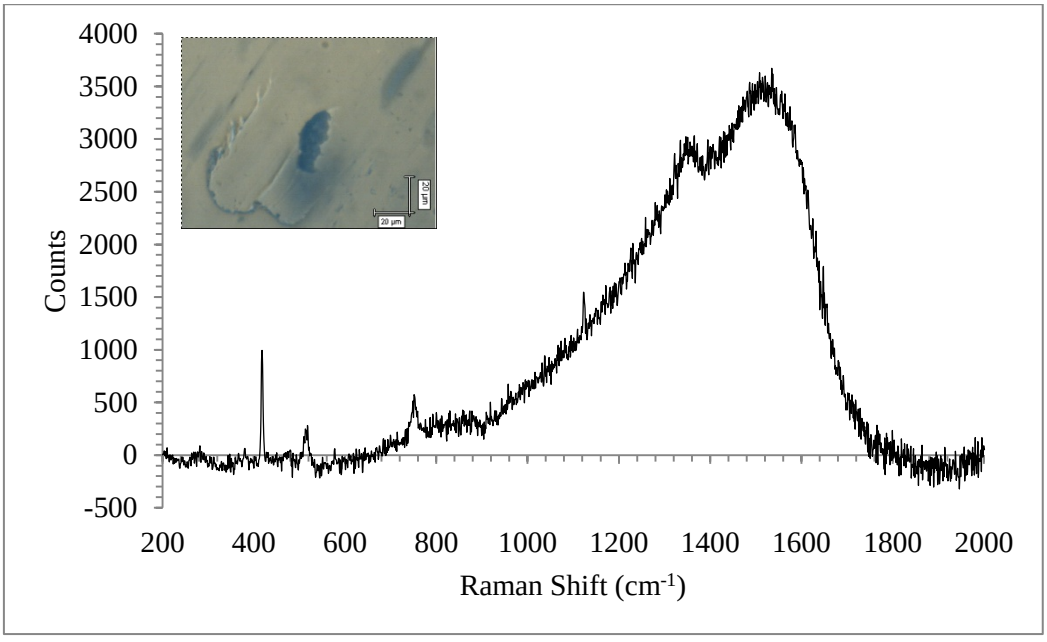

Figure B-6 Raman spectrum of a spinel inclusion observed in the sample *3DGB3* of the dark grayish brown Bo Phloi sapphire.

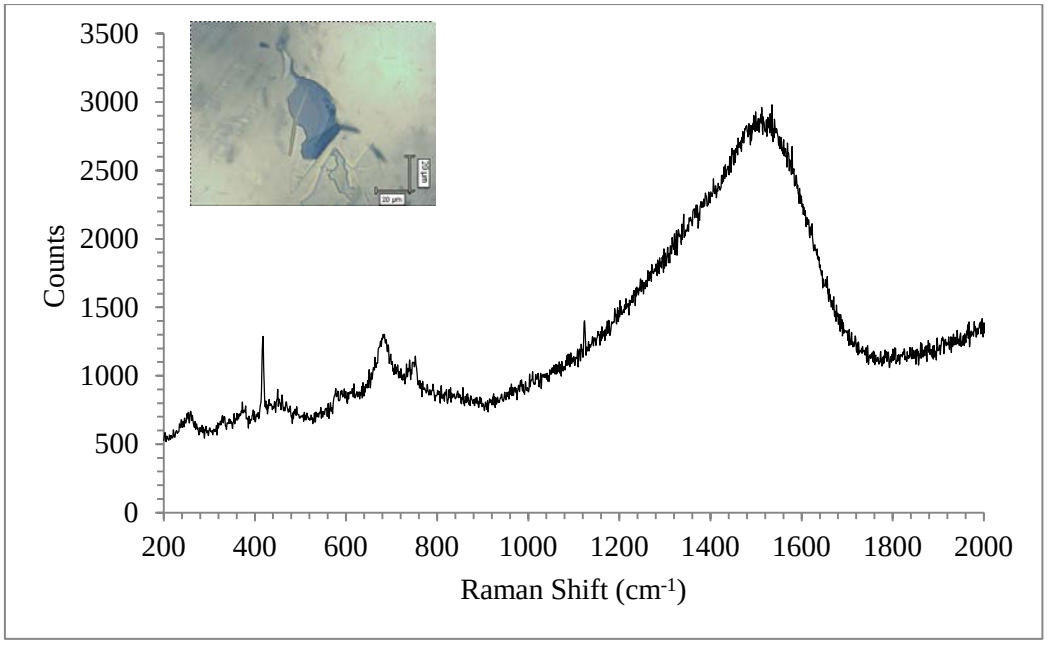

Figure B-7 Raman spectrum of a spinel inclusion observed in the sample *2DGA3* of dark grayish brown Bo Phloi sapphire.

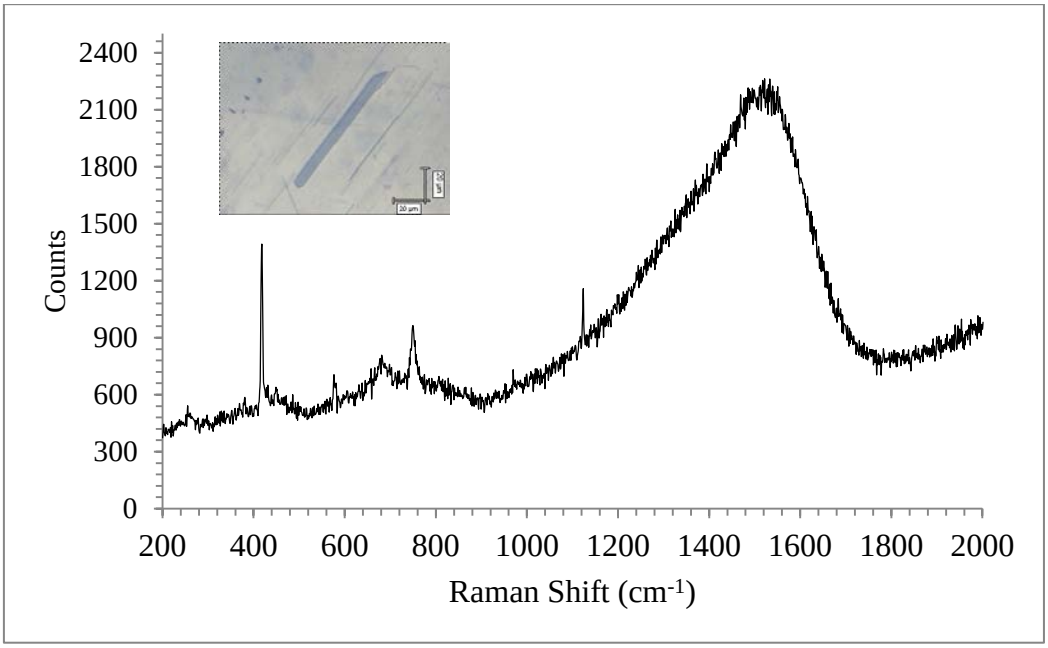

Figure B-8 Raman spectrum of a spinel inclusion observed in the sample *2DGA3* of dark grayish brown Bo Phloi sapphire.

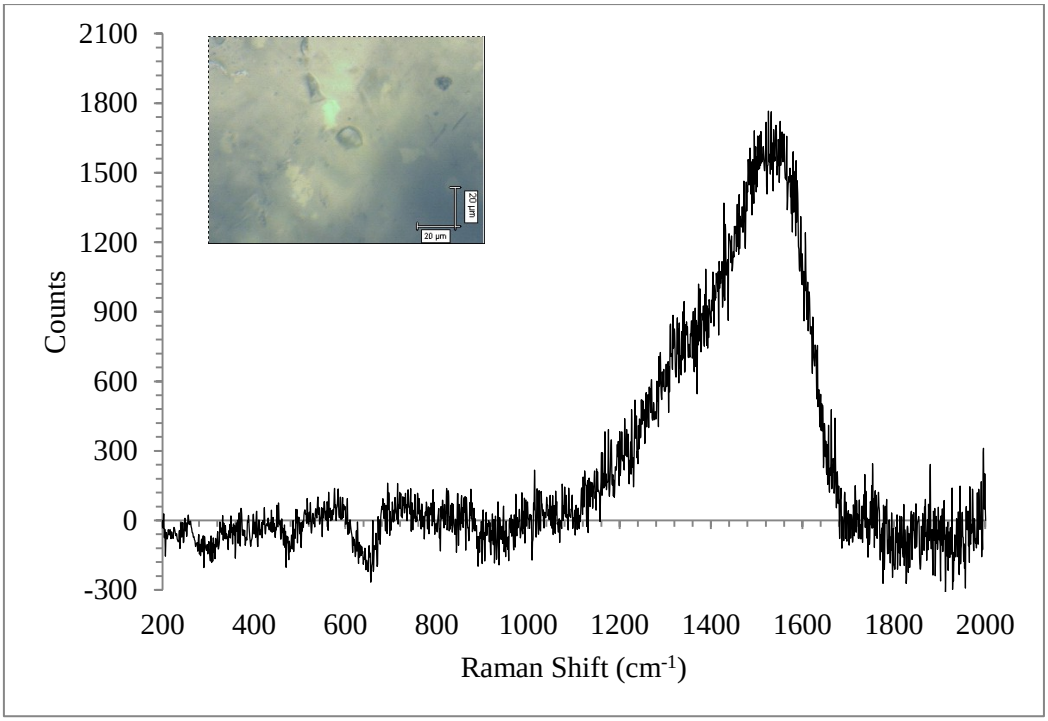

Figure B-9 Raman spectrum of a spinel inclusion observed in the sample *3DGA3* of dark grayish brown Bo Phloi sapphire.

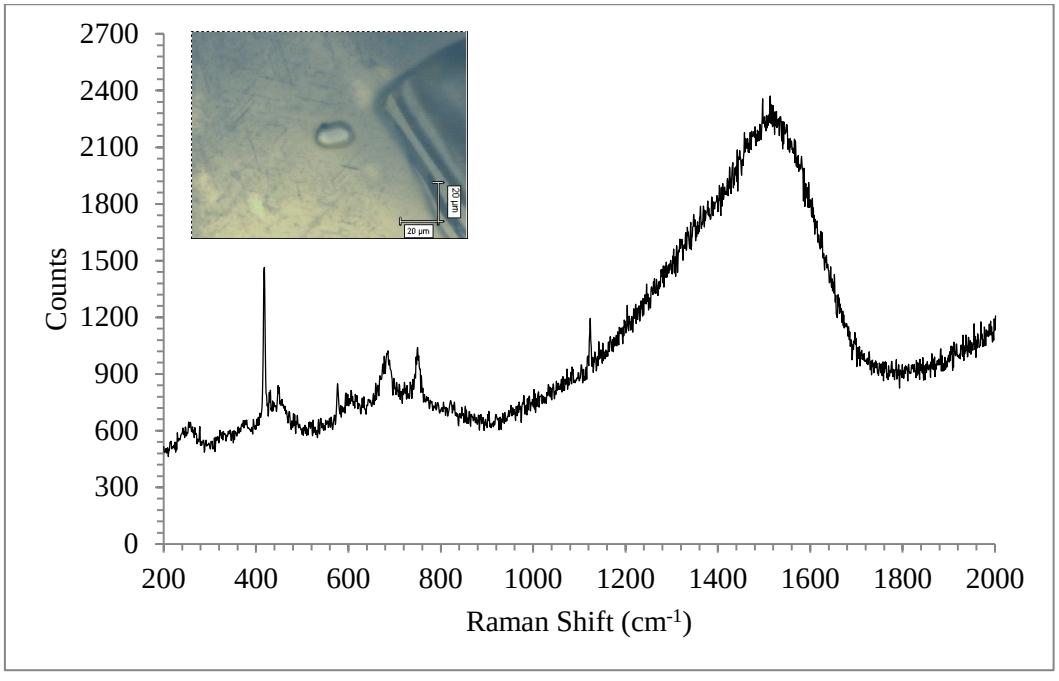

Figure B-10 Raman spectrum of a spinel inclusion observed in the sample *3DGB3* of dark grayish brown Bo Phloi sapphire.

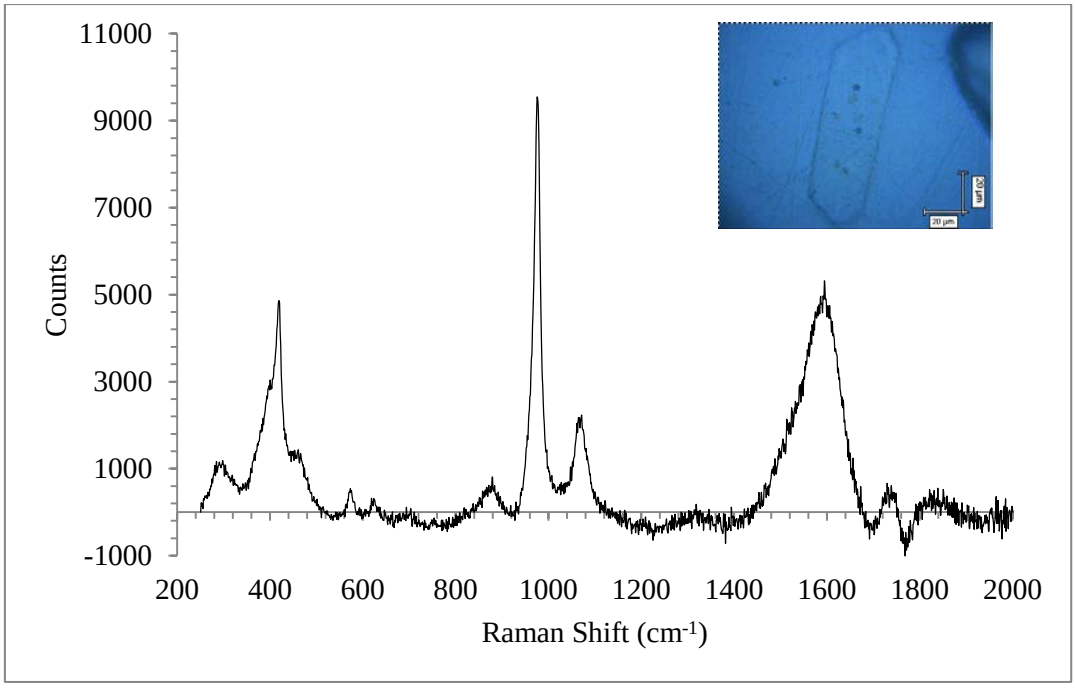

Figure B-11 Raman spectrum of a monazite inclusion observed in the sample *1C22* of dark grayish brown Bo Phloi sapphire.

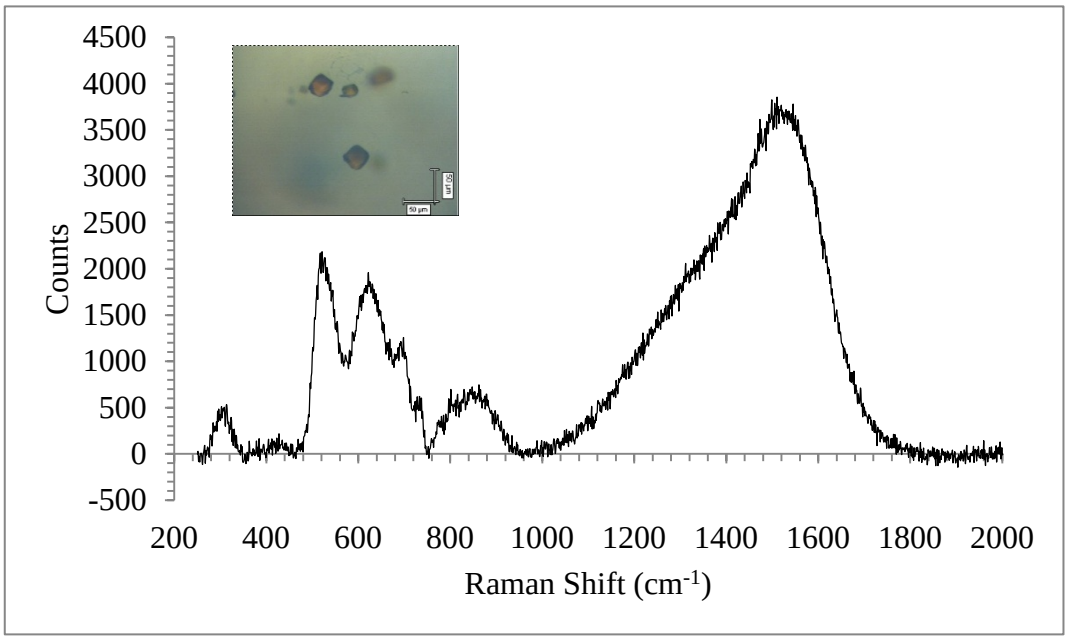

Figure B-12 Raman spectrum of a pyrochlore inclusion observed in the sample *TPA7a* of Pailin sapphire in Cambodia.

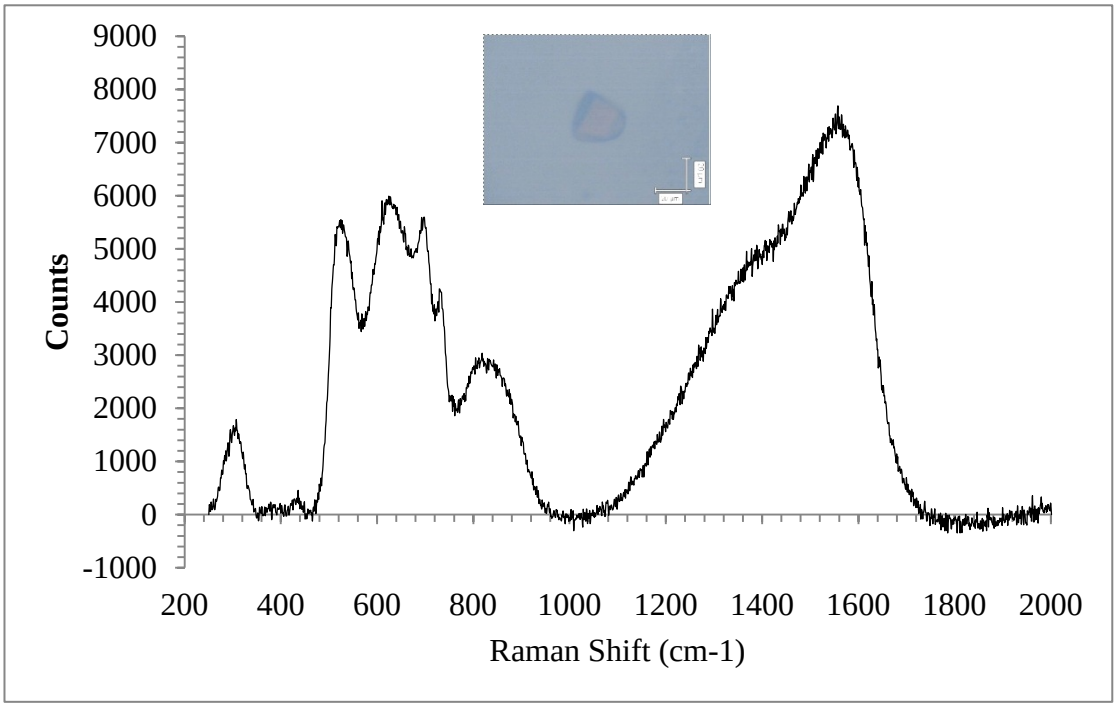

Figure B-13 Raman spectrum of a pyrochlore inclusion observed in the sample *TPA7m* of Pailin sapphire in Cambodia.

APPENDIX C

EPMA ANALYSIS OF MINERAL INCLUSIONS

A) Bo Phloi sapphires in Thailand:

Table C-1 EPMA analyses of **feldspar inclusions** in Bo Phloi sapphires *(n.a. = not analyzed).*

Mineral phase	Grayish brown sapphire							
Analysis (wt%)	Dark Gray					Light Gray		
	1C4ia2-3	1C4ia2-3	1C4ib2-1	1C4ib2-2	1C4ib2	3LGC1g	3LGC3c-2	3LGC3c-4
SiO_2	63.01	63.54	64.04	63.43	64.04	51.97	60.51	56.68
TiO_2	0.05	0.04	0.07	0.05	0.07	0.08	0.01	0.73
Al_2O_3	21.95	22.22	20.87	20.86	20.87	32.09	29.66	27.09
FeO	0.00	0.04	0.03	0.02	0.03	0.23	0.09	4.48
MnO	0.01	0.00	0.00	0.00	0.00	0.10	0.03	1.05
MgO	0.00	0.00	0.00	0.00	0.00	0.03	0.00	2.36
BaO	0.07	0.01	0.11	0.07	0.11	n.a.	n.a.	n.a.
CaO	2.88	2.73	1.77	1.75	1.77	1.16	0.04	0.04
Na_2O	7.81	8.45	7.22	7.31	7.22	3.66	4.39	2.27
K_2O	1.67	1.57	3.57	3.64	3.57	4.03	0.29	2.39
Total	97.44	98.59	97.65	97.13	97.65	93.33	95.01	97.09
8 (O)								
Si	2.854	2.847	2.906	2.897	2.906	2.468	2.719	2.602
Ti	0.002	0.001	0.002	0.002	0.002	0.003	0.000	0.025
Al	1.171	1.173	1.116	1.123	1.116	1.796	1.571	1.466
Fe	0.000	0.002	0.001	0.001	0.001	0.009	0.003	0.172
Mn	0.000	0.000	0.000	0.000	0.000	0.004	0.001	0.041
Mg	0.000	0.000	0.000	0.000	0.000	0.002	0.000	0.162
Ba	0.001	0.000	0.002	0.001	0.002	-	-	-
Ca	0.140	0.131	0.086	0.086	0.086	0.059	0.002	0.002
Na	0.686	0.734	0.635	0.648	0.635	0.337	0.382	0.202
K	0.096	0.089	0.206	0.212	0.206	0.244	0.017	0.140
Total*	4.950	4.977	4.954	4.970	4.954	4.922	4.695	4.811
Atomic%								
Na	74.37	76.90	68.47	68.51	68.47	52.64	95.42	58.64
Ca	15.17	13.72	9.26	9.05	9.26	9.23	0.42	0.59
K	10.46	9.37	22.27	22.44	22.27	38.13	4.16	40.78
Total**	100.00	100.00	100.00	100.00	100.00	100.00	100.00	100.00

Table C-1 (Cont.)

Mineral phase Analysis (wt%)	Blue sapphire					
	Blue					Light Blue
	3BB1b	3BB1b-1	3BB1b-3	3BB3b-1	3BB12a	3LBA2f-1
SiO_2	64.97	64.86	65.76	64.26	67.56	64.01
TiO_2	0.05	0.05	0.02	0.05	0.01	0.00
Al_2O_3	18.28	18.62	18.24	20.22	20.06	22.13
FeO	0.06	0.00	0.10	0.06	0.07	0.07
MnO	0.00	0.01	0.02	0.01	0.02	0.00
MgO	0.01	0.01	0.04	0.00	0.01	0.02
BaO	0.13	0.11	0.09	0.04	0.04	0.00
CaO	0.63	1.43	1.02	1.48	1.21	2.07
Na_2O	4.75	5.19	4.30	5.67	4.50	6.31
K_2O	5.66	4.64	4.60	3.04	5.36	4.39
Total	94.54	94.92	94.18	94.83	98.84	98.99
8 (O)						
Si	3.034	3.012	3.055	2.964	3.006	2.871
Ti	0.002	0.002	0.001	0.002	0.000	0.000
Al	1.006	1.019	0.999	1.099	1.052	1.170
Fe	0.002	0.000	0.004	0.002	0.003	0.002
Mn	0.000	0.000	0.001	0.000	0.001	0.000
Mg	0.000	0.001	0.003	0.000	0.001	0.001
Ba	0.002	0.002	0.002	0.001	0.001	0.000
Ca	0.032	0.071	0.051	0.073	0.058	0.099
Na	0.430	0.467	0.388	0.507	0.388	0.549
K	0.337	0.275	0.273	0.179	0.304	0.251
Total*	4.845	4.848	4.775	4.828	4.814	4.944
Atomic%						
Na	53.84	57.46	54.53	66.79	51.74	61.04
Ca	3.97	8.72	7.11	9.62	7.69	11.05
K	42.19	33.82	38.36	23.60	40.57	27.91
Total**	100.00	100.00	100.00	100.00	100.00	100.00

Table C-2 EPMA analyses of **nepheline inclusions** in Bo Phloi sapphires *(n.a. = not analyzed).*

Mineral phase	Grayish brown sapphire	Blue sapphire				
Analysis (wt%)	Light Gray	Blue				
	3LGC5c	3BA3j-3	3BA3j-5	3BC3a	3BA2i	3BA2i-2
SiO_2	41.74	42.20	47.12	44.05	44.902	47.733
TiO_2	0.03	0.05	0.05	n.a.	0.000	0.000
Al_2O_3	36.69	33.00	33.85	36.20	36.273	31.746
FeO	0.68	0.41	0.43	0.24	0.574	0.452
MnO	0.15	0.02	0.03	0.00	0.007	0.021
MgO	0.00	0.04	0.01	0.03	0.251	0.109
CaO	0.66	0.77	0.74	0.57	1.095	1.040
Na_2O	16.62	16.72	7.14	13.88	15.124	12.001
K_2O	1.53	5.75	4.93	5.31	2.058	5.110
Total	98.11	98.95	94.29	100.27	100.28	98.21
32 (O)						
Si	8.004	8.238	9.117	8.302	8.357	9.084
Ti	0.005	0.007	0.007	-	0.000	0.000
Al	8.291	7.592	7.718	8.041	7.956	7.120
Fe^{2+}	0.109	0.066	0.070	0.038	0.089	0.072
Mn	0.025	0.003	0.004	0.000	0.001	0.003
Mg	0.001	0.012	0.002	0.007	0.070	0.031
Ca	0.136	0.161	0.152	0.116	0.218	0.212
Na	6.176	6.329	2.678	5.070	5.457	4.428
K	0.375	1.431	1.217	1.277	0.489	1.240
Total**	23.121	23.839	20.965	22.851	22.638	22.190
∑R	6.822	8.081	4.200	6.579	6.382	6.092
Vacancy	1.178	0.000	3.800	1.421	1.618	1.908

Table C-3 EPMA analyses of **garnet inclusions** in Bo Phloi sapphires.

Mineral phase Analysis (wt%)	Grayish brown sapphire				
	Dark Gray		Light Gray		
	2DGA8f-4	2DGB2b-1	3LGC8c-1	3LGC8c-2	3LGC9b
SiO_2	46.653	45.313	43.562	42.483	46.150
TiO_2	0.029	0.113	0.002	0.037	0.017
Al_2O_3	21.395	18.888	18.280	29.441	24.537
Cr_2O_3	0.000	0.039	0.026	0.000	0.009
FeO	10.238	12.503	10.644	8.531	7.183
MnO	0.000	0.014	0.006	0.000	0.000
MgO	20.805	17.897	25.282	15.410	17.570
CaO	0.000	0.472	0.000	0.038	0.046
Total	99.120	95.239	97.802	95.940	95.512
24 (O)					
Si	6.557	6.718	6.296	6.098	6.594
Ti	0.003	0.013	0.000	0.004	0.002
Al	3.544	3.300	3.113	4.980	4.132
Cr	0.000	0.005	0.003	0.000	0.001
Fe^{2+}	1.203	1.550	1.286	1.024	0.858
Mn	0.000	0.002	0.001	0.000	0.000
Mg	4.360	3.956	5.447	3.297	3.743
Ca	0.000	0.075	0.000	0.006	0.007
Total*	15.667	15.617	16.146	15.409	15.337
$\sum R^{2+}$	5.563	5.582	6.734	4.327	4.608
$\sum R^{3+}$	3.547	3.317	3.117	4.984	4.135
$Mg/(Mg+Fe^{2+})$	0.784	0.718	0.809	0.763	0.813

$\sum R^{2+} = Fe^{2+}+Mn+Mg+Ni+Ca$, $\sum R^{3+} = Ti+Al+Cr$

Table C-4 EPMA analyses of **zircon inclusions** in Bo Phloi sapphires.

Mineral phase	Grayish brown sapphire							
Analysis (wt%)	Dark Gray							Light Gray
	1B3ib2-2	2DGC1a	2DGC6a	2DGC6b-REE1	2DGC6b-REE2	2DGC6b-REE4	2DGC9a-REE1	3LGC1b-2
SiO_2	33.473	32.657	32.47	32.08	32.24	32.32	31.97	31.90
ZrO_2	61.649	64.584	65.34	64.86	64.86	65.79	64.03	60.71
HfO_2	1.765	1.858	1.73	1.98	1.98	1.32	1.51	1.33
Al_2O_3	0.026	0.031	0.02	0.02	0.05	0.05	0.00	0.00
CaO	0.000	0.006	0.00	0.00	0.01	0.00	0.00	0.00
FeO	0.013	0.013	0.04	0.01	0.01	0.01	0.02	0.00
Total	97.253	99.149	99.59	98.95	99.15	99.50	97.53	93.94
4 (O)								
Si	1.043	1.008	1.000	0.996	0.998	0.996	1.004	1.030
Zr	0.937	0.972	0.981	0.982	0.979	0.989	0.980	0.956
Hf	0.019	0.019	0.018	0.021	0.021	0.014	0.016	0.015
Al	0.001	0.001	0.001	0.001	0.002	0.002	0.000	0.000
Ca	0.000	0.000	0.000	0.000	0.000	0.000	0.000	0.000
Fe	0.000	0.000	0.001	0.000	0.000	0.000	0.000	0.000
Total*	2.000	2.001	2.001	2.000	2.001	2.001	2.000	2.000
Atomic%								
Si	52.2	50.4	50.0	49.8	50.0	49.8	50.2	51.5
Zr	46.8	48.6	49.1	49.1	49.0	49.5	49.0	47.8
Hf	0.9	1.0	0.9	1.0	1.0	0.7	0.8	0.7
Total**	99.9	99.9	100.0	100.0	100.0	100.0	100.0	100.0

Table C-5 EPMA analyses of **monazite inclusions** in Bo Phloi sapphires *(n.a. = not analyzed).*

Mineral phase	Dark grayish brown sapphire					
Analysis (wt%)	2DGB9a	2DGA6a-REE2	2C9ia2	2C9ia2-4	1C21	1C22
P_2O_5	20.03	12.26	16.20	51.47	0.00	0.00
SiO_2	1.17	0.97	4.47	5.77	6.26	6.29
ThO_2	2.11	8.10	23.34	30.66	34.66	34.91
UO_2	1.19	0.33	0.00	0.00	0.00	0.00
Y_2O_3	22.34	1.27	0.00	0.00	0.00	0.00
La_2O_3	0.04	4.78	4.78	5.62	0.00	0.00
Ce_2O_3	0.00	5.13	20.74	20.97	0.00	0.00
Pr_2O_3	0.00	0.00	2.58	0.00	0.00	0.00
Nd_2O_3	0.00	0.00	4.02	0.00	0.00	0.00
Sm_2O_3	n.a.	n.a.	n.a.	n.a.	n.a.	n.a.
Eu_2O_3	n.a.	n.a.	n.a.	n.a.	n.a.	n.a.
Gd_2O_3	n.a.	n.a.	n.a.	n.a.	n.a.	n.a.
Dy_2O_3	1.74	0.20	0.00	0.00	0.00	0.00
Er_2O_3	n.a.	n.a.	n.a.	n.a.	n.a.	n.a.
Yb_2O_3	1.60	0.00	0.00	0.00	0.00	0.00
CaO	0.11	2.78	0.34	0.23	0.22	0.22
PbO	n.a.	n.a.	n.a.	n.a.	n.a.	n.a.
Al_2O_3	0.00	12.24	0.08	0.30	0.00	0.00
Total	50.33	35.81	76.46	114.72	41.14	41.42

Table C-6 EPMA analyses of **calcite inclusions** in Bo Phloi sapphires.

Mineral phase	Grayish brown sapphire					
Analysis (wt%)	Dark Gray					
	2DGB7a	2DGB7a-C	2DGB7a-C1	2DGB9b	2DGB9b-C	2DGB9b-2
SiO_2	0.00	0.05	0.01	6.21	4.02	0.66
TiO_2	0.03	0.00	0.02	0.01	0.06	0.18
Al_2O_3	5.08	5.27	1.92	1.29	2.54	2.03
FeO	0.00	0.01	0.05	0.05	0.65	0.46
MnO	0.00	0.06	0.01	0.00	0.00	0.01
MgO	0.00	0.02	0.27	0.14	0.17	0.00
CaO	51.69	54.62	61.96	34.27	42.84	32.98
Na_2O	0.00	0.00	0.00	0.04	0.09	0.00
K_2O	0.00	0.03	0.00	0.03	0.09	0.03
P_2O_5	0.02	0.03	0.09	0.03	0.03	0.01
F	0.04	0.07	0.14	0.06	0.19	0.00
Cl	0.00	0.02	0.02	0.04	0.00	0.02
SO_3	0.00	0.00	0.01	0.79	0.69	0.17
Total	56.88	60.17	64.48	42.95	51.36	36.56

B) Southeast Asia sapphires:

Table C-7 EPMA analyses of **feldspar inclusions** in Southeast Asia sapphires.

Mineral phase Analysis (wt%)	Laos							Vietnam	
	Huai Sai							Gia Nghia	
	HSA1c2	HSA1c5	HSA1d3	HSA1j5	HSB2a2	HSB7a2	HSB7a4	GNB2d	GNB2d-3
SiO_2	65.055	65.238	63.352	64.081	64.538	62.572	62.129	61.63	63.24
TiO_2	0.219	0.246	0.473	0.118	0.252	0.198	0.219	0.00	0.04
Al_2O_3	22.083	22.875	20.314	21.296	20.862	22.359	21.359	21.51	21.89
FeO	0.318	0.359	1.223	1.307	0.342	0.498	0.570	0.19	0.18
MnO	0.000	0.000	0.269	0.183	0.011	0.093	0.137	0.00	0.00
MgO	0.000	0.000	0.052	0.332	0.013	0.000	0.234	0.00	0.00
BaO	0.000	0.000	0.071	0.032	0.000	0.000	0.022	0.07	0.00
CaO	0.327	0.310	1.485	0.894	0.318	0.208	0.208	2.45	2.40
Na_2O	4.213	3.237	5.179	4.389	4.777	6.041	5.041	8.43	8.76
K_2O	5.849	5.877	6.377	6.827	7.976	5.365	9.365	4.97	2.17
Total	98.064	98.142	98.795	99.459	99.089	97.334	99.284	99.232	98.680
8 (O)									
Si	2.925	2.919	2.890	2.891	2.922	2.861	2.850	2.811	2.845
Ti	0.007	0.008	0.016	0.004	0.009	0.007	0.008	0.000	0.001
Al	1.170	1.206	1.092	1.132	1.113	1.205	1.155	1.156	1.161
Fe	0.012	0.013	0.047	0.049	0.013	0.019	0.022	0.007	0.007
Mn	0.000	0.000	0.010	0.007	0.000	0.004	0.005	0.000	0.000
Mg	0.000	0.000	0.004	0.022	0.001	0.000	0.016	0.000	0.000
Ba	0.000	0.000	0.001	0.001	0.000	0.000	0.000	0.001	0.000
Ca	0.016	0.015	0.073	0.043	0.015	0.010	0.010	0.120	0.116
Na	0.367	0.281	0.458	0.384	0.419	0.536	0.448	0.745	0.764
K	0.335	0.335	0.371	0.393	0.461	0.313	0.548	0.289	0.124
Total*	4.834	4.778	4.962	4.927	4.953	4.954	5.063	5.129	5.018
Atomic%									
Na	51.1	44.5	50.8	46.8	46.8	62.4	44.5	64.6	76.1
Ca	2.2	2.4	8.0	5.3	1.7	1.2	1.0	10.4	11.5
K	46.7	53.2	41.2	47.9	51.4	36.4	54.4	25.1	12.4
Total**	100.0	100.0	100.0	100.0	100.0	100.0	100.0	100.0	100.0

Table C-8 EPMA analyses of **nepheline inclusions** in Southeast Asia sapphires.

Mineral phase	Thailand	Laos			
Analysis (wt%)	Chanthaburi	Huai Sai			
	TC6d-1	HSA7b1	HSA1e1	HSA1j2	HSA5d1
SiO_2	40.87	42.00	49.87	45.04	41.788
TiO_2	0.06	0.00	0.04	0.00	0.190
Al_2O_3	34.84	34.03	33.50	35.18	34.808
FeO	0.84	0.06	0.16	0.32	0.226
MnO	0.26	0.02	0.00	0.00	0.059
MgO	0.03	0.00	0.00	0.00	0.000
CaO	0.62	0.05	0.08	0.04	0.818
Na_2O	17.03	17.45	15.83	14.99	14.396
K_2O	2.03	4.32	2.52	4.02	5.780
Total	96.575	97.934	101.983	99.594	98.065
32 (O)					
Si	8.031	8.198	9.058	8.495	8.146
Ti	0.069	0.005	0.012	0.025	0.018
Al	8.068	7.828	7.170	7.818	7.997
Fe^{2+}	0.138	0.010	0.024	0.051	0.037
Mn	0.043	0.003	0.000	0.000	0.010
Mg	0.010	0.000	0.000	0.000	0.000
Ca	0.130	0.010	0.015	0.008	0.171
Na	6.487	6.604	5.575	5.480	5.441
K	0.509	1.077	0.583	0.967	1.437
Total*	23.485	23.733	22.438	22.845	23.257
ΣR	7.257	7.700	6.188	6.463	7.220
Vacancy	0.515	0.267	1.562	1.155	0.743

ΣR = (2Ca+Na+K)

Table C-9 EPMA analyses of **pyroxene inclusions** in Southeast Asia sapphires *(n.a. = not analyzed).*

Mineral phase	Thailand			Vietnam	
Analysis (wt%)	Phrae			Gia Nghia	
	PA1k1	PA1k5	TPA1b1	GNB4c-2	GNB6a
SiO_2	59.444	61.967	58.360	60.56	60.01
TiO_2	0.025	0.006	0.000	0.03	0.02
Al_2O_3	4.691	5.285	9.754	5.51	1.85
Cr_2O_3	0.000	0.000	0.082	0.09	0.00
FeO	2.738	2.675	1.082	1.61	0.78
MnO	0.010	0.023	0.000	0.01	0.00
MgO	31.555	28.007	28.115	29.34	33.77
NiO	0.000	0.355	0.000	n.a.	n.a.
CaO	0.010	0.000	0.004	0.12	0.02
Na_2O	0.000	0.016	0.001	0.04	0.04
K_2O	0.004	0.000	0.011	0.00	0.02
Total	98.477	98.334	97.409	97.312	96.501
6 (O)					
Si	2.020	2.094	1.980	2.061	2.065
Ti	0.001	0.000	0.000	0.001	0.001
Al	0.188	0.210	0.390	0.221	0.075
Cr	0.000	0.000	0.002	0.002	0.000
Fe	0.078	0.076	0.031	0.046	0.022
Mn	0.000	0.001	0.000	0.000	0.000
Mg	1.599	1.411	1.422	1.489	1.732
Ni	0.000	0.010	0.000	-	-
Ca	0.000	0.000	0.000	0.004	0.001
Na	0.000	0.001	0.000	0.003	0.002
K	0.000	0.000	0.000	0.000	0.001
Total*	3.886	3.802	3.825	3.827	3.899
ΣVacancy	0.114	0.198	0.175	0.173	0.101
Si_{excess}	0.02	0.09	0.00	0.06	0.06
Charge balanced	3.996	3.978	4.074	3.978	3.993

Enstatite formula = $(Mg, Fe, Al, Si_{excess})_2Si_2O_6 = (M2)_2Si_2O_6$
Charge balanced = $(Mg*2+Fe*2+Al*3+Si_{excess}*4)$

Table C-10 EPMA analyses of **garnet inclusions** in Southeast Asia sapphires.

Mineral phase	Laos		Cambodia		
Analysis (wt%)	Huai Sai		Pailin		
	HSC1d 2	HSC3c2	TPA1a	TPA1a2	TPA4m1
SiO_2	44.07	48.83	45.62	46.27	43.02
TiO_2	0.00	0.05	0.08	0.10	0.32
Al_2O_3	22.00	24.53	24.37	28.43	24.22
Cr_2O_3	0.00	0.00	0.00	0.00	0.00
FeO	2.48	0.55	4.34	4.39	1.34
MnO	0.01	0.00	0.00	0.01	0.01
MgO	29.75	24.48	23.28	19.43	27.13
CaO	0.04	0.06	0.11	0.11	0.13
Na_2O	0.00	0.02	0.05	0.02	0.05
K_2O	0.06	0.01	0.05	0.58	0.12
Total	98.403	98.538	97.898	99.339	96.337
24 (O)					
Si	6.095	6.578	6.329	6.306	6.032
Ti	0.000	0.005	0.008	0.010	0.034
Al	3.586	3.895	3.985	4.566	4.003
Cr	0.000	0.000	0.000	0.000	0.000
Fe^{2+}	0.000	0.062	0.503	0.500	0.158
Fe^{3+}	0.349	0.000	0.000	0.000	0.000
Mn	0.001	0.000	0.000	0.002	0.001
Mg	6.134	4.916	4.816	3.948	5.670
Ca	0.006	0.009	0.016	0.016	0.019
Na	0.000	0.004	0.015	0.004	0.013
K	0.010	0.001	0.009	0.101	0.021
Total*	16.179	15.472	15.681	15.453	15.949
$\sum R^{2+}$	6.141	4.987	5.335	4.465	5.848
$\sum R^{3+}$	3.586	3.900	3.994	4.576	4.036
$Mg/(Mg+Fe^{2+})$	1.000	0.987	0.905	0.888	0.973

$\sum R^{2+} = Fe^{2+}+Mn+Mg+Ca$
$\sum R^{3+} = Ti+Al+Cr$

Table C-11 EPMA analyses of **sapphirine and staurolite inclusions** in Southeast Asia sapphires *(n.a. = not analyzed).*

Mineral phase	Sapphirine			Staurolite			
Analysis (wt%)	Laos			Vietnam			
	Huai Sai			Gia Nghia			
	HSB1a	HSB1a3	HSC3a1	GNB2e	GNB 2e-1	GNB 5c-1	GNC4a
SiO_2	18.67	23.60	17.60	37.37	37.13	28.20	22.93
TiO_2	0.02	0.00	0.14	0.02	0.02	0.05	0.03
Al_2O_3	63.40	57.39	61.93	41.95	41.98	45.96	54.80
Cr_2O_3	0.00	0.00	0.04	0.00	0.02	0.05	0.92
FeO	0.47	0.46	0.38	1.17	1.14	2.89	0.02
MnO	0.00	0.00	0.00	0.00	0.05	0.03	0.02
MgO	17.87	14.09	17.17	17.22	17.06	17.20	14.80
NiO	n.a.	n.a.	n.a.	0.00	0.00	0.00	0.00
CaO	0.02	0.03	0.08	0.04	0.00	0.02	0.00
Na_2O	0.03	0.02	0.00	n.a.	n.a.	n.a.	n.a.
K_2O	0.00	0.01	0.03	n.a.	n.a.	n.a.	n.a.
Total	100.48	95.60	97.37	97.76	97.39	94.39	93.52
20 (O)							
Si	2.115	2.775	2.059	10.214	10.187	8.160	6.630
Ti	0.001	0.000	0.013	0.004	0.005	0.010	0.007
Al	8.465	7.953	8.538	13.513	13.574	15.675	18.679
Cr	0.000	0.000	0.003	0.000	0.004	0.011	0.211
Fe^{2+}	0.044	0.046	0.037	0.268	0.262	0.698	0.005
Mn	0.000	0.000	0.000	7.016	6.977	7.418	6.381
Mg	3.019	2.469	2.995	0.000	0.000	0.000	0.000
Ni	-	-	-	0.011	0.000	0.005	0.000
Ca	0.003	0.004	0.010	0.011	0.000	0.005	0.000
Na	0.007	0.005	0.000	-	-	-	-
K	0.000	0.001	0.004	-	-	-	-
Total*	13.654	13.252	13.659	Total* 31.037	31.008	31.984	31.913
$\sum R^{2+}$	3.065	2.519	3.042	$\sum R^{2+}$ 7.306	7.238	8.127	6.386
$Mg/(Mg/Fe^{2+})$	0.986	0.982	0.988	$\sum R^{3+}$ 23.731	23.770	23.857	25.527

$\sum R^{2+} = Fe^{2+}+Mn+Mg+Ni+Ca$
$\sum R^{3+} = Ti+Al+Cr$

Table C-12 EPMA analyses of **columbite inclusions** in Southeast Asia sapphires.

Mineral phase	Cambodia															
Analysis (wt%)	Pailin															
	TPA4b	TPA4c	TPA4d	TPA4f	TPA4h1	TPA4i	TPA4j	TPA7d	TPA7i	TPA7i1	TPA7i2	TPA7j	TPA7j1	TPA7k	TPA7k1	TPA7m
SiO_2	0.06	0.14	0.23	0.08	0.07	0.23	0.10	0.07	0.11	0.06	0.07	0.05	0.06	0.03	0.06	0.09
TiO_2	1.01	1.12	1.29	1.15	0.87	1.05	1.14	1.20	0.99	1.60	1.31	1.21	1.13	1.15	1.16	1.27
Al_2O_3	0.70	2.18	2.30	0.13	1.00	0.66	5.42	0.46	0.88	0.17	0.19	0.04	0.02	6.24	3.01	0.05
FeO	13.64	12.76	13.21	15.85	13.32	13.31	13.24	14.11	15.89	15.89	15.65	14.46	14.64	13.40	13.38	14.53
MnO	7.00	7.17	6.26	6.04	7.39	7.82	5.97	6.82	6.56	6.14	5.28	6.03	6.14	6.29	6.43	6.11
MgO	0.11	0.16	0.19	0.35	0.15	0.19	0.13	0.16	0.27	0.16	0.07	0.19	0.16	0.16	0.18	0.15
CaO	0.03	0.00	0.00	0.30	0.01	0.14	0.11	0.06	0.03	0.30	0.26	0.13	0.10	0.02	0.01	0.09
Nb_2O_5	74.61	74.75	75.20	74.55	72.51	70.63	73.12	75.75	73.17	73.94	73.57	73.71	73.94	70.43	73.72	72.97
Ta_2O_5	0.91	1.26	1.30	0.84	1.15	0.95	1.00	0.81	1.09	0.97	0.62	1.00	0.97	0.88	1.10	4.08
Total	98.07	99.54	99.99	99.28	96.48	94.96	100.22	99.41	98.99	99.22	97.02	96.82	97.15	98.61	99.04	99.33
6 (O)																
Si	0.003	0.008	0.013	0.004	0.004	0.014	0.006	0.004	0.006	0.003	0.004	0.003	0.003	0.002	0.003	0.005
Ti	0.043	0.047	0.053	0.049	0.038	0.046	0.046	0.051	0.042	0.068	0.057	0.053	0.049	0.047	0.048	0.055
Al	0.047	0.142	0.149	0.009	0.068	0.046	0.345	0.030	0.059	0.011	0.013	0.003	0.001	0.402	0.197	0.003
Fe	0.650	0.592	0.608	0.749	0.645	0.656	0.597	0.663	0.752	0.751	0.756	0.700	0.707	0.612	0.621	0.694
Mn	0.338	0.337	0.292	0.289	0.363	0.390	0.273	0.325	0.314	0.294	0.258	0.296	0.301	0.291	0.302	0.295
Mg	0.009	0.014	0.015	0.029	0.013	0.017	0.010	0.013	0.022	0.014	0.006	0.016	0.014	0.013	0.015	0.013
Ca	0.002	0.000	0.000	0.018	0.000	0.009	0.006	0.003	0.002	0.018	0.016	0.008	0.006	0.001	0.000	0.006
Nb	1.921	1.875	1.872	1.905	1.899	1.881	1.783	1.924	1.873	1.890	1.920	1.930	1.931	1.740	1.849	1.884
Ta	0.014	0.019	0.020	0.013	0.018	0.015	0.015	0.012	0.017	0.015	0.010	0.016	0.015	0.013	0.017	0.063
Total*	3.027	3.033	3.022	3.066	3.049	3.073	3.080	3.025	3.088	3.065	3.038	3.024	3.028	3.121	3.052	3.018

Table C-13 EPMA analyses of **apatite inclusions** in Southeast Asia sapphires.

Mineral phase	Thailand		
Analysis (wt%)	Chanthaburi		
	TC1q	TC1q-1	TC1q-2
FeO	0.23	0.12	0.55
MnO	0.70	0.78	0.74
MgO	0.10	0.00	0.33
CaO	49.18	54.63	45.32
Na_2O	0.25	0.31	0.17
K_2O	0.00	0.03	0.00
P_2O_5	21.97	27.94	22.67
Total	72.43	83.81	69.79
25 (O)			
Fe	0.075	0.035	0.193
Mn	0.234	0.232	0.261
Mg	0.059	0.000	0.202
Ca	20.854	20.483	20.267
Na	0.194	0.210	0.141
K	0.000	0.013	0.000
P	1.472	1.655	1.602
Total*	22.889	22.629	22.667

BIOGRAPHY

Ms. Pornmanee Khamloet was born on the 9th July 1980 in Mueang District, Suphanburi Province, central part of Thailand. She acquired the Bachelor's degree in Chemistry from the Department of Chemistry, Faculty of Science, Chulalongkorn University in 2002. She continued her studied and also graduated the Master's degree in Analytical Chemistry at the same place in 2005. During the course study, she received the financial support from the Chulalongkorn University Graduate Scholarship Commemorate the 72nd Anniversary of H.M. King Rama IX. After graduation, she got a job at the Office of the Higher Education Commission, Ministry of Education. In 2007, she began her study in the Doctor of Philosophy Program in Geology, Faculty of Science, Chulalongkorn University. The research work has been focused on the mineral inclusions in basaltic Southeast Asia sapphires and their genetic model. She had completed her study in 2012.